UNIVERSIDADE FEDERAL DE PERNAMBUCO
DEPARTAMENTO DE FÍSICA – CCEN
PROGRAMA DE PÓS-GRADUAÇÃO EM FÍSICA

PAULO JOSÉ FONSECA CAVALCANTI

MULTIPLE-CONDENSATES EFFECTS IN NOVEL SUPERCONDUCTING MATERIALS

Recife
2020

PAULO JOSÉ FONSECA CAVALCANTI

MULTIPLE-CONDENSATES EFFECTS IN NOVEL SUPERCONDUCTING MATERIALS

Thesis presented to the Graduate Program in Physics at the Federal University of Pernambuco, as a partial requirement for obtaining the title of *Doctor Scientiae* in Physics.

Concentration Area: Condensed Matter and Materials Physics

Advisor: Prof. Arkady Shanenko

Co-Advisor: Alexei Vagov

Recife
2020

Catalogação na fonte
Bibliotecária Mariana de Souza Alves CRB4-2105

C376m Cavalcanti, Paulo José Fonseca
Multiple-Condensates effects in novel superconducting materials / Paulo José Fonseca Cavalcanti. – 2020.
149 f., il., fig.

Orientador: Arkady Shanenko.
Tese (Doutorado) – Universidade Federal de Pernambuco. CCEN, Física, Recife, 2020.
Inclui referências e apêndice.

1. Física da Matéria Condensada e de Materiais. 2. Supercondutividade. 3. Supercondutividade intertipo. 4. Formalismo estendido de Ginzburg-Landau. I. Shanenko, Arkady. (orientador) II. Título.

530.41 CDD (22. ed.) UFPE-CCEN 2021-08

PAULO JOSÉ FONSECA CAVALCANTI

MULTIPLE-CONDENSATES EFFECTS IN NOVEL SUPERCONDUCTING MATERIALS

Tese apresentada ao Programa de Pós-Graduação em Física da Universidade Federal de Pernambuco, como requisito parcial para a obtenção do título de Doutor em Física.

Aprovada em: 30/10/2020.

BANCA EXAMINADORA

Prof. Arkady Shanenko
Orientador
Universidade Federal de Pernambuco

Profa. Azadeh Mohammadi
Examinadora Interna
Universidade Federal de Pernambuco

Prof. Andrea Perali
Examinador Externo
University of Camerino

Prof. Andrey Chaves
Examinador Externo
Universidade Federal do Ceará

Prof. Mauro Melchiades Doria
Examinador Externo
Universidade Federal do Rio de Janeiro

Dedicatória In Memoriam de minha Mãe, Angela Fonseca Mesquita,

que me ensinou valores importantes para toda a vida.

Falecida por COVID-19 em 23/11/2020

AGRADECIMENTOS

Eu gostaria de primeiramente agradecer a pessoa que foi a figura mais importante para o desenvolvimento de minha tese, minha mãe *Angela Fonseca Mesquita*, sem ela nada disso seria possível. Queria agradecer a ela por todo suporte emocional, financeiro, além de todo encorajamento dado durante toda a minha vida. Que por infelicidade o destino veio a falar logo após minha defesa ao contrair COVID-19, foi uma pessoa que se dedicou completamente a família, onde até seus últimos dias, sacrificou sua vida em prol dos filhos e para poder dar a coisa mais importante que existe que é a educação. Eu realmente não tenho palavras para descrever o que minha mãe foi para mim, ela foi tudo, e sem ela eu não seria nada, e ela se foi, mas ficará eternamente na saudade e na minha memória. Espero do fundo do coração que justiça seja feita as milhares de vítimas dessa doença no Brasil, e que os responsáveis por esse genocídio por negligência cometido no Brasil pelo governo federal na figura do presidente da república assim como o ministro da saúde sejam responsabilizado e sejam presos.

Queria também fazer um agradecimento especial a minha avó, *Maria Ferreira Ramos*, que é como uma segunda mãe para mim que sempre quando precisei ela estava presente. Assim como familiares como meus tios *Josias Cavalcante* e *Val Moura* que mesmo de longe sempre me apoiaram e me ajudaram. E a todos os outros familiares que depositaram confiança em mim como meus primos, tios, minha irmã e meu pai.

Agradeço também aos inúmeros amigos do departamento de física da UFPE, que me acompanharam durante toda essa longa jornada desde a graduação, como *Wellington Moreira, Fillipe Cesar, Ricardo Batista*, assim como os vários amigos criados durante todo esse processo e a todos os outros que passaram pela minha vida no departamento mas pelo destino seguiram caminhos diferentes, como *Bruna Gabrielly*, e *Elizane Moraes*. Assim como os funcionários do departamento que foram grandes pessoas para mim.

E aos amigos brasileiros feitos durante a minha estadia na Alemanha, como *Liliane Lima*, *João Victor Dutra Gomes* e *Irene Beitelle*. Pessoas essas que se tornaram grandes amigos e que gostaria de cultivar a amizade para toda a minha vida.

I would also like to thank the Bayreuth university for all the support and hospitality during my stay in Germany, in particular I would like to thank Prof. *Martin Axt* for giving me the opportunity to be part of his group where I learned to have another worldview and how science is made in Germany, it was a unique experience, where I never felt like an outsider. I would also like to thank the countless friends made in the group, such as *Tim Seidelmann, Michael Cosacchi*, *Adam Mielnik-Pyszczorski, Luca Elia Nimmesgern*, and *Florian Ungar*, a group of people who made me feel like I was at home.

I thank my advisors *Arkady Shanenko* and *Alexei Vagov* for all the wisdom and opportunity to meet and be part of the Russian school of physics, which has contributed so much to the development of physics. And also for all the support given throughout my period as a student, I don't know how I would do this doctorate without these great people, who are not only great, they are two giants who helped me a lot, not just as a student-teacher relationship , but as friends.

”If I have seen further it is by standing on the shoulders of Giants.”

“Se eu vi mais longe, foi por estar sobre ombros de gigantes.”

Isaac Newton

(NEWTON, *1675, n. p).*

ABSTRACT

Coupled condensates with diverse coherence length scales interfere (interact) constructively or destructively, which leads to unconventional non-single-condensate physics. In the Thesis we investigate two phenomena governed by multiple condensates: the dependence of the superconducting magnetic response on the number of contributing bands and the multiband mechanism of screening the superconducting fluctuations. The first problem is related to the tacit assumption that multiband superconductors are essentially the same as multigap superconductors. More precisely, it is usually assumed that the number of excitation gaps in the energy spectrum determines the number of contributing bands in a relevant superconducting model capable to capture the essential physics. Here we demonstrate that contrary to this widely accepted perception, the superconducting magnetic properties are sensitive to the number of contributing bands even for degenerate excitation gaps. In particular, we find that the crossover between superconductivity types I and II and the related intertype physics are affected by difference between characteristic lengths of multiple contributing condensates. Coupled condensates interfere (interact), which results in non-single-condensate physics regardless of a particular structure of the excitation spectrum. The related formalism is based on the τ-expansion of the microscopic equations, with $\tau = 1 - T/T_c$ the proximity to the critical temperature, and goes to one order beyond the standard Ginzburg-Landau (GL) approach to capture a finite intertype crossover domain in the phase diagram of the superconducting magnetic response. Previously this extended GL formalism has been constructed for single- and two-band systems. In this work we generalize that formalism to the case of an arbitrary number of contributing bands. The second problem is focused on the superconducting fluctuations in systems with multiple coupled condensates. It is well known that superconductivity in quasi-one-dimensional (Q1D) materials is hindered by large fluctuations of the order parameter. They reduce the critical temperature and can even destroy the superconductivity altogether. Here we demonstrate that the situation changes dramatically when a Q1D pair condensate is coupled to a higher-dimensional stable one, as in recently discovered multiband superconductors with Q1D band(s). The fluctuations are suppressed even by vanishingly small pair-exchange coupling between different band condensates and the superconductor is well described by the mean field theory. In this case the low-dimensionality effects enhance the coherence of the system instead of suppressing it. As a result, the temperature of the multiband Q1D superconductor can increase by orders of magnitude when the system is tuned to the Lifshitz transition with the Fermi level close to the edge of the Q1D band.

Keywords: Superconductivity. Intertype Superconductivity. Extended Ginzburg-Landau Formalism. Multiband Systems. Superconducting Fluctuations. Quasi-One-Dimensional Condensates.

RESUMO

Condensados acoplados com diversas escalas de comprimento de coerência interferem (interagem) construtivamente ou destrutivamente, o que leva a uma física não convencional de condensado não único. Na Tese, investigamos dois fenômenos governados por condensados múltiplos: a dependência da resposta magnética supercondutora do número de bandas contribuintes e o mecanismo multibanda de blindagem das flutuações supercondutoras. O primeiro problema está relacionado à suposição tácita de que supercondutores multibandas são essencialmente os mesmos que supercondutores multigaps. Mais precisamente, geralmente é assumido que o número de gaps de excitação no espectro de energia determina o número de bandas contribuintes em um modelo supercondutor relevante capaz de capturar a essência física. Aqui, demonstramos que, ao contrário dessa percepção amplamente aceita, as propriedades magnéticas supercondutoras são sensíveis ao número de bandas contribuintes, mesmo para os gaps de excitação degenerados. Em particular, descobrimos que o cruzamento entre os tipos de supercondutividade I e II e a relacionada física intertipo são afetadas pela diferença entre os comprimentos característicos dos condensados múltiplos contribuintes. Os condensados acoplados interferem (interagem), o que resulta na física de condensado não único, independentemente de uma estrutura particular do espectro de excitação. O formalismo relacionado é baseado na expansão em τ das equações microscópicas, com $\tau = 1 - T/T_c$ na proximidade da temperatura crítica e vai para uma ordem além da abordagem padrão de Ginzburg-Landau (GL) afim de obter um domínio finito do cruzamento intertipo no diagrama de fase da resposta magnética supercondutora. Anteriormente, esse formalismo GL estendido foi construído para sistemas de banda única e banda dupla. Neste trabalho, generalizamos esse formalismo para o caso de um número arbitrário de bandas contribuintes. O segundo problema está focado nas flutuações supercondutoras em sistemas com condensados múltiplos acoplados. É bem conhecido que a supercondutividade em materiais quase unidimensionais (Q1D) é prejudicada por grandes flutuações do parâmetro de ordem. Eles reduzem a temperatura crítica e podem até destruir completamente a supercondutividade. Aqui, demonstramos que a situação muda drasticamente quando um par condensado Q1D é acoplado a um de dimensão superior estável, como nos supercondutores multibandas recentemente descobertos com banda(s) Q1D. As flutuações são suprimidas inclusive por um pequeno par de acoplamento de troca entre os diferentes condensados da banda e o supercondutor é bem descrito pela teoria do campo médio. Nesse caso, os efeitos de baixa dimensionalidade aumentam a coerência do sistema em vez de suprimi-la. Como resultado, a temperatura do supercondutor multibanda Q1D pode aumentar em ordens de magnitude quando o sistema é ajustado para a transição Lifshitz com o nível de Fermi próximo à borda da banda Q1D.

Palavras-chave: Supercondutividade. Supercondutividade intertipo. Formalismo estendido de Ginzburg-Landau. Sistemas multibandas. Flutuações Supercondutoras. Condensados quase unidimensionais

SUMMARY

1 INTRODUCTION

Concept of multiband superconductivity was introduced in 1959 [1], [2] as a possible explanation of a multigap fine structure observed in the frequency dependence of the real conductivity part of superconducting lead and mercury, extracted from the infrared absorption spectrum [3], [4]. Despite the long history of the problem, detailed and unambiguous results supporting this concept, were obtained only in 2000's after experiments with MgB_2, see, e.g., Ref. [5] and references therein. The observation of two well distinguished energy gaps in the excitation spectrum of MgB_2 [6], [7] have ignited a substantial interest in the problem and boosted further experiments focused on the multiband superconductivity. Now, after a decade of intensive investigations, it is clear that multiple overlapping bands are present in most of superconducting systems, ranging from iron-based materials [8] to high-T_c organic superconductors [9] and even topological superconductors [10], [11]. Recent calculations have indeed demonstrated that the Fermi surface of Pb is composed of two Fermi sheets, in agreement with the multiband interpretation [1] of the pioneering experiments reported in Refs. [3], [4].

By the historical reasons, the presence of the multiple energy gaps in the excitation spectrum of a superconductor is still considered as a key marker for the multiband superconductivity. For example, a standard expectation is that if the excitation spectrum does not exhibit the multigap structure, the system is single-band or effectively single-band (if there are several bands with degenerate excitation gaps) so that its superconducting properties are the same as those of single-band materials. More generally, it is usually assumed that the number of excitation gaps determines the number of contributing bands in a superconducting model designed to capture essential physics of interest. The well-known example is MgB_2 which exhibits two excitation gaps associated with π and σ states [5]-[7]. Consequently, superconducting models for MgB_2 include, as a rule, two contributing bands, see, e.g., Refs. [5], [12]-[15]. However, first principle calculations demonstrate [16], [17] that MgB_2 is in fact a four-band superconductor with two σ and two π bands, see also Ref. [5]. The two σ bands have different microscopic parameters (diverse Fermi sheets) but degenerate excitation gaps and the same holds for the π bands. Thus, a tacit common assumption is that multiband superconductivity manifests itself via multiple energy gaps in the excitation spectrum and, hence, multiband superconductors are essentially the same as multigap superconductors.

However, there is another possible view on a multiband superconductor as the system governed by a set of different and competing characteristic lengths. A fascinating consequence of such competition can be, e.g., spontaneous pattern formation. Examples of systems with such spontaneous patterns and textures are well-known in the literature and include magnetic films [18], [19], liquid crystals [20], multilayer soft tissues [19], [21], lipid monolayers [22], granular media [23], etc. Recently symmetry breaking patterns of vortices (labyrinths/stripes) caused by the competition of two significantly different π and σ coherence lengths have attracted interest in the context of unusual mixed-state configurations in MgB_2, see, e.g., Refs. [24], [25] and references therein. Coupled condensates with diverse coherence length scales in one system can interfere (interact) constructively or destructively, which leads to unusual non-single-condensate coherent phenomena. In addition to the labyrinths of vortices mentioned above, other effects can be listed, e.g., possible fractional vortices [26]-[31], chiral solitons [32], [33], a giant paramagnetic Meissner effect [34], enhancement of the intertype superconductivity [35], [36], hidden criticality [37], screening of superconducting fluctuations near the BCS-BEC crossover [38], etc. The set of diverse and competing coherence lengths and the multigap energy structure of the excitation spectrum in multiband superconductors are both consequences of a complex Fermi surface that exhibits multiple sheets associated with different contributing bands. However, a nontrivial interplay (interference) between band condensates is not directly related to the presence of multiple excitation gaps. Thus, we can expect that in principle, non-single-condensate physics can appear even when all such energy gaps are degenerate.

1.1 SUPERCONDUCTIVITY

For more than a century, the phenomenon of superconductivity has fascinated many scientists around the world, who despite the great discoveries there are still many problems open. First observed by Kamerlingh Onnes in Leiden in 1911 [39], when it was observed that a mercury sample abruptly loses its electrical resistivity when cooled below 4.2 Kelvin (K). As low temperatures were only possible because of the liquefaction of helium first obtained in 1908, by K. Onnes, and thus 1911 he observed superconductivity in mercury. The transition to the superconducting state was observed when at a sufficiently low temperature, called superconducting critical temperature T_c, the electrical resistivity fell to zero. after which the phenomena were observed in several other materials, cadmium (0.52 K), aluminum (1.18 K), titanium (2.38 K), tin (3.72 K), lead (7.20 K) and some alloys, etc. Since then, great progress has been made in understanding the phenomenon of superconductivity.

In 1933 physicists W. Meissner and R. Ochsenfeld [40], discovered an interesting property of superconductors, which was the property that a superconducting material has to exclude the magnetic field from its interior when it is subjected to an external magnetic field, as would happen with a perfect diamagnetic material, which became known as the Meissner-Ochsenfeld effect. In addition to the effect that occurs when a material is placed under an external magnetic field above a critical value (H_c), the superconductivity disappears regardless of the material's temperature. Thus, these and other properties of the superconductors aroused a great interest in the researchers to make a theory that explained the causes and the true description of the phenomenon.

In the first successful theory wrote by the London brothers, in 1935 [41], they proposed a phenomenological theory based on the Maxwell equations of the classical electrodynamics. The London equation describes the Meissner effect, i.e., the expulsion of the magnetic field from a superconductor. However, in this theory, superconductivity should exist even in the absence of an external magnetic field, so the London theory fails to attempt to explain the superconducting state when there is no magnetic field present, and a better theory was needed.

Then in 1950, L. Landau and V. Ginzburg published the famous paper of the theory of superconductivity [42], with the set of equations known as Ginzburg-Landau Equations. This is a phenomenological theory, based on experimental observations and some assumptions that could not be demonstrated from first principles at the time, but which brilliantly describes the properties presented at the time about the superconductors. The approach was based on the general theory of second-order phase transitions proposed by Landau in 1937 [43]. This theory was very successful in explaining several fundamental properties of superconductivity.

Although Ginzburg-Landau's theory has led to many experimentally confirmed predictions [44], but this theory was not developed on a microscopic basis and could not provide the true explanation for the phenomenon of superconductivity. Thus, it was reasonable to suppose that this phenomenon could not arise from classical physics, which is, it is a macroscopic manifestation of quantum mechanics.

Then a more fundamental theory was developed, capable of describing superconductivity from the first principles, and came about in 1957 when J. Bardeen, L. Cooper and J. Schrieffer [45] treated superconductivity as a purely quantum phenomenon, thus obtaining a complete description of the phenomenon and explaining its microscopic origin, which became known as the BCS theory of superconductivity.

Moreover, in 1959 [46], L. Gor'kov demonstrated a direct connection between the BCS approach and the GL Theory. When using the Hamiltonian formulation of the BCS model by Bogoliubov et al, Gor'kov derives from the quantum field theory the Ginzburg-Landau equations, that is, the Ginzburg-Landau equations can be obtained as a limiting case of microscopic theory.

1.2 INTERTYPE SUPERCONDUCTIVITY

The latest discoveries of new superconducting materials at high critical temperatures [47], [48] have led to a review of many of the field's longstanding problems. One is a classification of superconducting magnetic properties. As is well known, the Ginzburg-Landau (GL) theory distinguishes ideally type I and type II diamagnetic superconductors, where the field penetrates in the form of a regular Abrikosov lattice of a single quantum of vortices. These types are dependent on the parameter GL $\kappa = \lambda/\xi$, with λ and ξ being, respectively, the magnetic penetration depth and the coherence length GL. The change between types occurs abruptly when κ crosses the critical value κ_0.

Already in the 1970s, it was shown that the reality is more complex than that of the GL theory (see [51]-[55] and references therein): the table of superconductivity types separated by the single point κ is applied only at the limit $T \to T_c$. Below T_c, the intertype regime occupies a finite interval of κ, forming the inter-type domain between types II and I in the (κ, T) plane [51]. This domain exhibits an unconventional field dependence of magnetization, in particular the first-order phase transition between the Meissner and the mixed states [51], [52]. Subsequent works have revealed that the physics of the intertype domain is closely related to the self-duality Bogomolnyi [56], [57] that results in an infinite degeneration of the superconducting state at the point of Bogomolnyi (κ_0, T_c), see, e.g., [58]. This degeneracy results from the symmetry of the GL equations in κ_0 and implies that the mixed state comprises an infinite number of different spatial patterns of the magnetic (condensed) flux, including the very exotic ones. By lowering the temperature, degeneration is lifted and the Bogomolnyi point unfolds into a finite domain on the phase diagram between types II and I. In this case, nonstandard flow patterns model the internal structure of the intertype domain.

A comprehensive investigation of possible condensed flow states in this domain has not been presented so far. Theoretically, for bulk materials such research requires a greater approach than the GL theory, which is technically very demanding, see, e.g., [53]. The experimental study is also quite nontrivial because κ should be changed by appropriate doping to cross the intertype domain in the plane (κ, T) [51], [52]. To date, only one long-range attraction between the vortices of Abrikosov is well established in the intertype regime, bearing the name of "type II / 1" superconductivity [51] as opposed to the standard type II, referred to instead as "type II / 2", where the formation of giant vortices (multi-quantum) was considered for superconductors with $\kappa \sim 1$. However, the results were contradictory. Therefore, the state of the flux configurations in the bulk domain of superconductors remains unclear and requires extensive further investigation.

1.3 EXTENDED GINZBURG-LANDAU THEORY

In conventional single-band superconductors, the intertype domain is insignificantly small and therefore largely ignored in textbooks. However, it has recently been demonstrated that this domain is increased in superconductors of two bands and this enlargement can be attributed to the disparity between the microscopic parameters of the contributing bands [35]. It has also been argued that the effect is a generic phenomenon independent of the details of the model for band states. Its origin is the nonlocality of interactions in the aggregate condensate due to the appearance of multiple bands.

Thus, it is of importance to check this expectation and generalize the consideration of the intertype domain in two-band superconductors to the case of multiband superconducting materials with more than two contribution bands. In this project, the main purpose of our investigation is to study how the enlargement of the intertype domain is sensitive to increasing the number of contributing bands.

Multiband superconductors are materials in which more than one carrier band contributes to the formation of condensates. Since the discovery of superconductivity, multiband superconductivity has been also expected in some materials, e.g., in conventional Pb, but with the evolution of technology an infinity of multiband superconductors has been discovered, such as metal borides and boron carbides such as MgB_2 [69] and OsB_2 are observed, iron silicides such as $LiFe_3Si_5$ [71], chalcogenides such as $FeSe_{1-x}$, and pnictides of iron [72]. Unconventional characteristics and significantly elevated transition temperature have led to the general interest of such compounds as well as to the phenomenon of multiband superconductivity.

The distinction between the types diamagnetic type-I materials and type-II superconductors is routinely explained by the Ginzburg-Landau (GL), and occurs when the GL parameter $\kappa = \lambda/\xi$ crosses the critical value $\kappa_0 = 1/\sqrt{2}$ [44], where the type of interaction between the vortices is altered, being in the type-I attractive and repulsive in the type-II superconductors. And, at $\kappa = \kappa_0$, Bogomolnyi point, these vortices do not interact, due to the of the fact that the GL theory at this point reduces to a pair of the first-order self-dual Bogomolnyi equations. The self-duality, first discussed in the context of cosmological strings, leads to an infinite degeneracy of different flux configurations, from which the absence of the vortex-vortex interactions follows [35].

Beyond the GL theory, EGL theory, shows that the GL dichotomy of the superconductivity types is achieved only in the limit $T \to T_c$ (T_c is the critical temperature). At $T < T_c$ the Bogomolnyi point unfolds into a finite temperature-dependent interval of κ's (intertype domain), where the physics of this domain is not captured by the standard GL theory. The physics of the transitional domain is commonly restricted to the long-range vortex-vortex attraction. This, however, contradicts to the observation that other critical parameters exist inside this domain with the corresponding changes of admissible intertype flux patterns. Moreover, the number of such internal critical parameters is infinite due to the infinite degeneracy of the Bogomolnyi point. The intertype domain has a complex structure with different possible variants of the mixed state, structure that appears as a result of the removal of the infinite degeneracy of the Bogomolnyi point when lowering temperature [35].

The EGL theory offers a powerful and yet relatively simpler formalism for studies of the mixed state in both single and multiband superconductors. While the GL theory predicts a sharp interchange between type-I and II at $\kappa = \kappa_0$, the microscopic calculations and experimental results demonstrated that the border between types I and II broadens at $T < T_c$ into the finite interval of κ's, i.e., the intertype domain between types I and II in the (κ, T)-plane. Where the physics in this domain is not explained by the GL theory, the EGL theory can reproduce the boundaries of the intertype domain in full agreement with the experiments.

The analysis revealed that when the GL parameter κ is situated in the interval $[\kappa_2^*, \kappa_{li}^*]$ defined by the onset of the long-range vortex attraction (κ_{li}^*) and the appearance of the mixed state (κ_2^*), the system may demonstrate a great variety of unconventional magnetic states and properties. This rich diversity is closely related to the infinite degeneracy of the Bogomolnyi point, $\kappa = \kappa_0$ and $T = T_c$. When the temperature is lowered below T_c this degeneracy is gradually lifted, and the Bogomolnyi point projects itself onto the finite critical interval (critical domain). Its appearance defines a new separate type of superconductivity that can be tentatively called "critical superconductors". In particular, the preliminary analysis revealed the sub-domain in the critical domain, where the elementary entities are those twinning Abelian Higgs multi-quanta vortices. Remarkably, the structure of the critical domain is universal for single-band materials. Its boundaries are independent of the material parameters, as long as the system is in the clean limit.

Analysis of two-band superconductors have shown a very interesting property that the interplay between the bands leads to a systematic enlargement of the critical domain. A physical interpretation of this enlargement relates it with the increased non-locality in multiband systems, which is also responsible for the long-range vortex attraction. The previous results also brought the following conclusions, that in the absence of an additional symmetry, the GL order parameter in a multiband superconductor is single-component and defined by the standard single-component GL theory, however, the coefficients in the relevant equations have contributions of different bands. That, the difference between spatial profiles of different band condensates can be correctly described only within an approach that goes beyond the standard GL model, e.g., in the EGL formalism. The structure of the type-I/type-II border (near-Bogomolnyi regime) has been calculated for the single and two-band systems and exhibit a wealth of nonstandard spatial flux distributions, found neither in type I nor in type II. With patterns that far exceeds the complexity of these standard types, which were previously discussed in the literature in the context of the long-range interaction of vortices. This distinctive complexity dictates introducing a separate type of superconductivity, which can be tentatively called the critical type. In addition, it has been established that exotic magnetic properties of single- and multiband superconductors are closely related: they have the same origin, i.e., lifting of the infinite topological degeneracy of the Bogomolnyi critical state.

For multiband materials, it is generally believed that they could be modeled by the standard BCS theory that accounts for the multiple-carrier band structure. The mean-field BCS theory is then formulated in the form of multiband Bogoliubov-de Gennes (BdG), Gor'kov or Ellenberger equations. In particular, the BdG equations with a chosen approximation for the pseudo-potential are a convenient tool of studying clean systems with man-sized dimensions. In principle, the BCS theory gives the most complete description of a multiband system; however, fully microscopic calculations are not an easy task for strongly inhomogeneous mixed states. Investigations of inhomogeneous superconducting state are notably simpler in the vicinity of T_c, where the GL theory is legitimate. Moreover, Gor'kov built the bridge between the microscopic BCS and the phenomenological GL theories by relating the order parameter with the anomalous microscopic Green function.

Recently was developed a consistent extension of the GL theory, EGL theory, which is based on using the proximity to the critical temperature $\tau = 1 - T/T_c$ as the unique small parameter in the system. Where the implementation of this mathematical formalism has been used in a series of preliminary works, for the single- as well as the two-band cases [35]. All relevant physical quantities in this formalism are represented as the series expansion in τ (the so-called τ - expansion). Equations for the order parameter and the magnetic field, also written as the series expansion in τ, and are obtained from the condition of the stationary free energy functional. With this approach, the standard GL theory follows from the two lowest orders in the expansion: the first term defines the critical temperature and the second one yields the GL theory. Corrections to it are provided by the higher orders terms. For a multi-band system, the difference between the condensates, appear only in the leading order corrections to the GL theory: one can describe the relevant phenomena only when they are retained.

Thus, it is important to verify the expected results and generalize the formalism obtained in the single and two-band superconductors to the case of multiband superconducting materials, with more than two contributing bands.

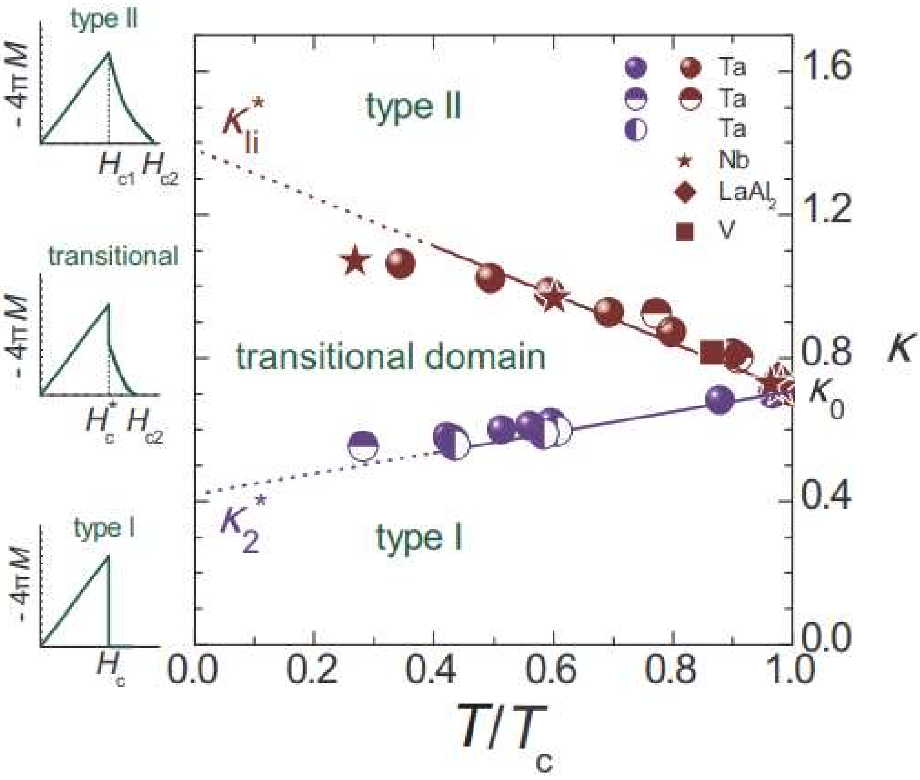

Figure 1.3-1 Phase diagram of superconductivity types in the (κ,T) plane derived from the EGL formalism and comparison with experimental data(symbols), where it is shown the boundaries of the intertype domain for single-band superconductors[35]

1.4 OBJECTIVES

In this doctoral thesis we address two remarkable phenomena directly related to multiple coupled condensates.

a) **Intertype magnetic response of multiband superconductors with degenerate excitation gaps.**

The concept of multiband superconductivity has been introduced in 1959 [1], [2] as a possible explanation of a multigap fine structure observed in frequency-dependent conductivity of superconducting Pb and Hg, extracted from the infrared absorption spectrum [4]. It has been confirmed only in 2000, after experiments with MgB_2 [5] by observations of two distinct energy gaps in the excitation spectrum [6], [7] [density of states (DOS) of superconducting electrons contains two peaks]. It is usually assumed that the number of excitation gaps in the single-particle energy spectrum of a uniform superconductor determines the number of contributing bands in the relevant superconducting model. So, if the spectrum doesn't show multigap structure, the expected superconducting properties are those of single band materials. A well-known example is MgB_2, which exhibits two spectral gaps associated with π and σ states [5]-[7] and, thus, theoretical models that explain this superconductivity consider only two contributing bands [5], [12]-[15], despite the fact that the first-principle calculations reveal [16], [17] four single particle bands [5]. The two π bands of MgB_2 have different microscopic parameters, but they exhibit degenerate excitation gaps. The same is true for the two σ bands.

However, there is another approach which is followed by this doctoral thesis and considers a multiband superconductor as a system governed by a set of competing characteristic lengths associated with different bands [37], [101]. The single-particle spectrum of superconducting electrons is usually measured for bulk superconductors to avoid problems with the interpretation of nonuniform measurements. When the corresponding tunnelling measurements reveal, for example, a single peak in the density of states, it does not mean that the position-dependent gap functions of different contributing condensates are always the same. Their characteristic spatial lengths can be different due to peculiarities of the Fermi surface.

The competition of different condensate length-scales can lead to non-trivial physical consequences due to interference/interaction of different contributing condensates. It is of importance that this competition can appear irrespective of the presence/absence of multiple spectral gaps in the uniform superconducting state. These features appear on different levels of the theory - the system can have multiple energy gaps in the excitation spectrum but a single characteristic length and, vice versa, a multiband superconductor can have multiple coherence lengths but a single excitation gap.

Here we demonstrate that the crossover between superconductivity types I and II—the intertype (IT) regime - is strongly affected by the difference between healing lengths of multiple contributing condensates even when the corresponding excitation gaps are degenerate and cannot be distinguished. Our analysis is done using the formalism of the extended Ginzburg-Landau (EGL) theory generalized to the case of an arbitrary number of contributing bands.

b) **Multiband material with a quasi-1D band as a robust high-temperature superconductor.**

It is well known that superconductivity in one-dimensional systems is suppressed due to large fluctuations of the order parameter, which reduce the critical temperature T_c and can even destroy the superconductivity completely. The superconducting state can still be achieved when several 1D structures (parallel chains of molecules or atoms) are coupled, thus creating a weakly coupled matrix. Theoretical studies demonstrated that such quasi-1D (Q1D) materials can superconduct [105]-[108] but the fluctuations still proliferate, reducing the critical temperature significantly [105]. This theoretical prediction was confirmed by the discovery of low temperature superconductivity in Bechgaard salts - organic Q1D superconductors [111], [112].

Later theoretical efforts were focused on finding the conditions under which the critical temperature of Q1D superconductors could be increased rather than reduced. In particular, it has been suggested that such increase can be achieved in the vicinity of the Lifshitz transition, at which the chemical potential approaches the edge of a Q1D single-particle energy band [119]-[122]. However, the fluctuations, which are already very large due to the Q1D effects, are increased due to the Bose-like character of the pairing near the Lifshitz point, tending to further deplete the condensate.

Recently the interest in Q1D superconductors has been boosted by the discovery of Cr_3As_3-chain based materials (such as $K_2Cr_3As_3$ and $KCr_3As_3H_x$). Such materials are multiband superconductors where Q1D bands coexist with conventional 3D bands. Previous investigations showed that the presence of the pair-exchange coupling between different bands can reduce fluctuations due to the multiband screening mechanism [91], [125]. The second part of this doctoral thesis is devoted to investigations of such screening mechanism in a multiband system comprising Q1D and 3D bands in the vicinity of the Lifshitz transition. We demonstrate that when a Q1D condensate is coupled to a 3D stable one, fluctuations are suppressed even by a vanishingly small pair-exchange coupling between different band condensates and the superconductor is well described by the mean-field theory. In this case, when approaching the Lifshitz transition (the chemical potential approaches the edge of the Q1D band), the low-dimensionality effects enhance the coherence of the system rather than suppress it. As a result, the critical temperature of the Q1D multiband superconductor can increase by orders of magnitude.

2 BASIC CONCEPTS

2.1 GINZBURG-LANDAU THEORY

London's theory had a serious flaw because it ignored the possibility of a positive surface energy, associated with a normal-superconducting interface [73]. Thus, to correct this shortcoming, Ginzburg and Landau proposed a different phenomenological description, which explains the surface energy in a natural way.

This theory was a great triumph of physical intuition, in which a pseudo wave function ψ was introduced as a parameter of complex order and $|\psi|^2$ represents the local density of the superconducting electron. The theory was developed by applying the variational method to a pre-defined expansion of the free energy density in powers of $|\psi|^2$ and $|\nabla\psi|^2$, resulting in a pair of differential equations coupled to ψ and the $\mathbf{A}$ vector potential. This result was a generalization of the London theory to deal with situations in which the density of the superconducting electron varied in space, and to deal with the nonlinear response to fields that are strong enough to change these electrons. The local approach to electrodynamics in London was remained.

The great value of this theory lies in the treatment of the macroscopic behavior of superconductors, in which free energy is more important than the spectrum of excitations. Thus, it will be quite reliable in predicting critical fields and the spatial structure ψ of non-uniform situations. In addition to also providing the qualitative structure helping to understand the behavior of the supercurrent because of quantum properties on a macroscopic scale.

The basic postulate of GL is that if ψ is small and varies slowly in space, the free energy f can be expanded in a series of the order parameter, where the odd terms are neglected in favor of the phase symmetry

$$f_s = f_n + \alpha|\psi|^2 + \frac{\beta}{2}|\psi|^4 + \cdots, \qquad 2.1\text{-}1$$

The free energy related to others thermodynamic variables is represented by the function f_n and will be treated as a constant independent of temperature, since it is assumed that the other quantities are well behaved close to the transition.

Then one must consider the superconducting case to happen when the part related to the transition is negative:

$$f = f_s - f_n < 0. \quad 2.1\text{-}2$$

Being superconducting state is energetically more favorable than normal state. The series should be truncated until the fourth in order to stay near the second-order phase transition at T_c where $|\psi|^2 \to 0$. The coefficient α represent the character of most phase transitions $\alpha(T) = a\tau$, where $\tau = 1 - T/T_c$, and $\beta = b$ must be positive otherwise the lowest free energy would occur for a arbitrarily large values of $|\psi|^2$. Two cases appear depending on if α is positive or negative. For a positive value of α, $T > T_c$, the minimum free energy occurs at $|\psi|^2 = 0$, which is the normal state. If α is a negative, $T < T_c$, value the minimum occurs when

$$\psi = \psi_\infty = \sqrt{\frac{|a|\tau}{b}}. \quad 2.1\text{-}3$$

where ψ_∞ is conventionally used because ψ approaches this value infinitely deep in the interior of the superconductor, where it is screened from any surface fields or currents. These behaviors are shown in the figure below.

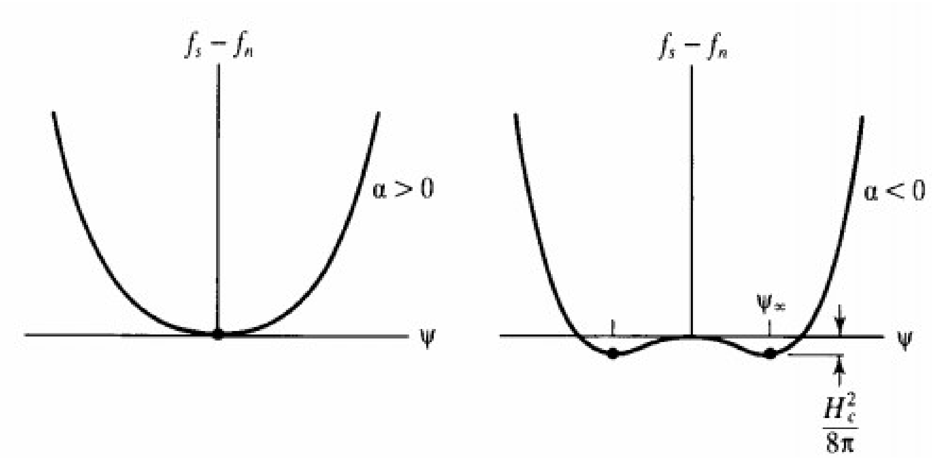

Figure 2.1-1 Ginzburg-Landau free energy functions for α positive and for α negative, the dots are the equilibrium positions, and for simplicity ψ has been taken to be real. Figure from [74].

In order to suppress spatial variations in ψ, and the order parameter is uniform in the absence of external fields, was added a term proportional to $|\nabla\psi|^2$, in analogy with the Schrödinger equation, and in presence of the magnetic field, the term is assumed to take the gauge-invariant form. So, the extra term added is given by, $\mathbf{D} = \nabla - i\frac{2e}{\hbar c}\mathbf{A}$, where the first term gives the extra energy associated with gradients in the magnitude of the order parameter and the second one gives the kinetic energy associated with supercurrents in a gauge-invariant form. And, we have also included a term to represents the energy density of the magnetic field. In this way, the free energy density becomes,

$$f[\psi, \psi^*, \mathbf{A}] = a\tau|\psi|^2 + \frac{b}{2}|\psi|^4 + K|\mathbf{D}\psi|^2 + \frac{1}{8\pi}(\nabla \times \mathbf{A})^2. \quad 2.1\text{-}4$$

So, with the free energy density is possible to calculate the Gibbs free energy difference and derive the thermodynamic critical field H_c, where is considered the energy necessary to take the system from the uniform solution $\left(|\psi_\infty|^2 = \frac{|a|\tau}{b}\right)$ at zero field to the normal state:

$$G = \int g d\mathbf{r}, \qquad \mathrm{g} = f + \frac{{H_c}^2}{8\pi} - \frac{H_c\mathbf{B}}{4\pi}, \quad 2.1\text{-}5$$

So,

$$H_c = \sqrt{\frac{4\pi a^2\tau^2}{b}}. \quad 2.1\text{-}6$$

This is the critical field of the Meissner state, where the magnetic field penetrates the superconductor only up to a typical length λ_L, London penetration depth. The parameters a, b and K are phenomenological and must be determined in order to match experimental results and within the framework of a microscopic theory where it was possible to derive analytic expressions for them in terms of microscopic parameters.

A stationary point of the functional given by Eq. 2.1-4 yields the main equations of the GL theory, the Ginzburg-Landau Equations. So, the condition of minimum energy allows the use of the Euler-Lagrange equations for the free energy density

$$\frac{\partial f}{\partial q} - \sum_i \frac{\partial f}{\partial(\partial_i q)} = 0, \quad 2.1\text{-}7$$

where for our case q is ψ or $\mathbf{A}$, then follow the GL equations

$$a\tau|\psi|^2 + b|\psi|^4 + K|\mathbf{D}\psi|^2 = 0, \qquad \nabla \times \nabla \times \mathbf{A} = 4\pi\mathrm{i}\frac{2e}{\hbar\mathrm{c}}K(\psi^*\mathbf{D}\psi - \psi\mathbf{D}^*\psi^*). \quad 2.1\text{-}8$$

Thus, the Ginzburg-Landau theory gives two coupled differential equations Eq. 2.1-8, involving the order parameter and vector potential, which can be analytically solved in some regimes of approximation to determine some properties of the superconducting state.

Characteristic lengths

In the two simple cases in which exact closed form, solution can be found, the GL equations provide us characteristic lengths.

First, we consider a case where in which no fields are present; then, we can take ψ to be real since the differential equation has only real coefficients. Moreover, introducing the normalized wave function $f = \frac{\psi}{\psi_\infty}$. In addition, we assume that, $x > 0$ is filled with a superconductor and, $x < 0$, is a vacuum or normal material, we obtain (in one dimension)

$$\xi^2 \frac{d^2 f}{dx^2} + f - f^3 = 0, \qquad \xi^2 = \frac{K}{|a|\tau}, \tag{2.1-9}$$

where the characteristic length ξ is called the coherence length, is one of the two fundamental length scale associated with superconductivity, which importance is shown graphically in the Figure 2.1-2. We see that ψ is close to ψ_∞ far inside the superconductor, is zero at the interface with the normal material, and has intermediate values in a transition layer near the interface with a width in the order of ξ.

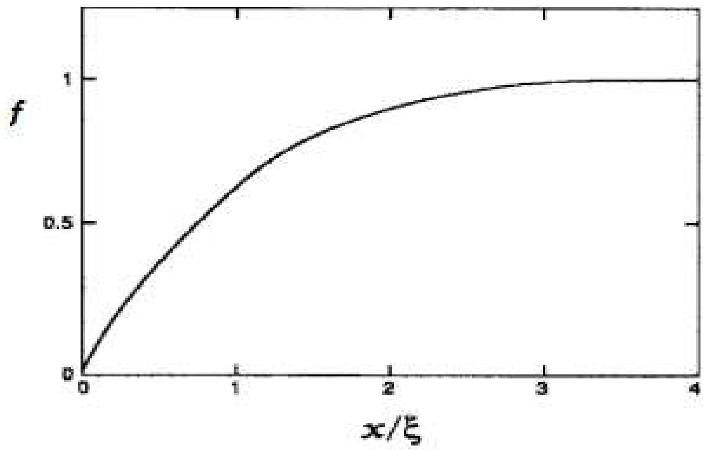

Figure 2.1-2 Dependence of the normalized order parameter on distance inside a superconductor with a material that prevents the formation of the superconducting condensate in the boundary in situations. The order parameter is larger for $x > \xi$. Figure from [74].

The second characteristic length come into play when we consider a system with an applied magnetic field with an essentially uniform order parameter $\psi = \psi_\infty$, spatial variations of the order parameter can be neglected. So, the GL equations, Eq. 2.1-8, are reduced to the London equation:

$$\frac{c}{4\pi}(\nabla \times \nabla \times \mathbf{A}) = -2\frac{(2e)^2}{\hbar^2 c}|\psi_\infty|^2 \mathbf{A}, \tag{2.1-10}$$

where can also be written as

$$\nabla \times \nabla \times \mathbf{A} = \frac{1}{\lambda_L^2}\mathbf{A}, \qquad \lambda_L^2 = \frac{\hbar^2 c^2}{e^2}\frac{b}{32\pi K|a|\tau}. \qquad 2.1\text{-}11$$

The second fundamental length of a superconductor is the λ_L, London penetration depth. Which measures how much field penetrates in the superconductor.

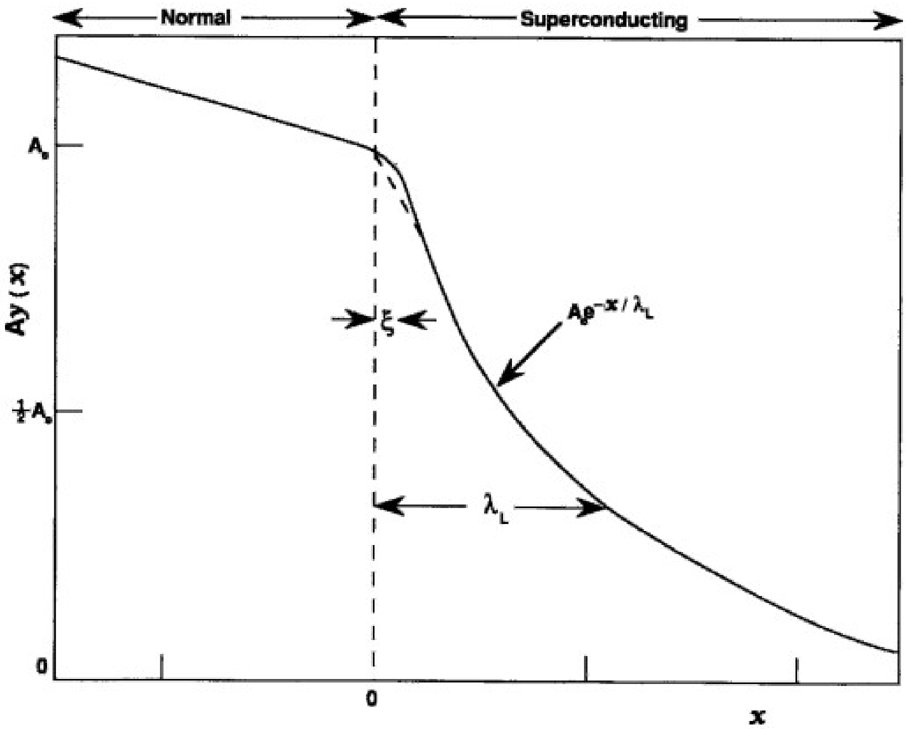

Figure 2.1-3 Dependence of the vector potential on distance x, where a constant applied magnetic field decays exponentially inside the superconductor, becoming very small for $x \gg \lambda_L$. Figure from [73].

As ψ is interpreted as a wave function, $|\psi|^2$ gives the local density of superconducting particles. Then, for the uniform solution, this density reads $n_s = |\psi_\infty|^2 = |a|\tau/b$. Also, $|\mathbf{D}\psi|^2$ works as a kinetic term, thus one can define $K = \hbar^2/2m$, where instead of K, the phenomenological quantity is the mass of the particles involved m. Therefore, with such assumptions the London theory is recovered. This is the so-called London limit of the GL equations.

We defined two characteristic lengths $\xi(T)$ and $\lambda_L(T)$, are phenomenological quantities which determine the behavior of superconductor near the transition point. They both diverge in $T \to T_c$, so it is conventional to introduce the Ginzburg-Landau parameter

$$\kappa = \frac{\lambda_L(T)}{\xi(T)}. \qquad 2.1\text{-}12$$

The cases studied before are limiting case of a more general picture where ξ and λ_L may be comparable. Thus, the importance of the parameter κ is better understood when is studied the energy associated with a surface separating normal and superconducting material.

The possibility of a surface energy arises from the occurrence of the two lengths. Now we will analyze the situation where the magnetic field is so strong that it destroys the superconducting state for $x \leq 0$ and, as the order parameter recovers from zero to its maximum value, the magnetic field tends to zero, for $x > 0$.

$$x \to -\infty: \qquad \psi = 0, \qquad B = H_c.$$

$$x \to \infty: \qquad \psi = \psi_\infty, \qquad B = 0. \qquad 2.1\text{-}13$$

Thus, we calculate the Gibbs free energy difference per unit area for this configuration, the so-called surface energy, done through a Legendre transformation, where one obtains the Gibbs free energy from the Helmholtz free energy by adding the term $-\mathbf{H}\cdot\mathbf{B}/4\pi$ to f_s related to the expulsion of the field.

$$\sigma_{sn} = \int_{-\infty}^{\infty} dx(g_s - g_n), \qquad g_{s(n)} = f_{s(n)} - \frac{\mathbf{H}\cdot\mathbf{B}}{4\pi}. \qquad 2.1\text{-}14$$

where f_s is given by Eqs. 2.1-4, 2.1-7and $g_n = f_{n(B=0)} + \frac{\mathbf{H}^2}{8\pi}$. The external magnetic field $\mathbf{H}$ is constant and its absolute value is equal to the thermodynamic critical field H_c. In the normal phase, $\mathbf{B} = \mathbf{H}$ and $H = B = H_c$, which results in $g_n = f_{n(B=0)} + \frac{{H_c}^2}{8\pi}$. (We changed the notation of B to h for a better understanding of the graphic in Figure 2.1-4)

$$\sigma_{sn} = \int_{-\infty}^{\infty} dx\left(a\tau|\psi|^2 + \frac{b}{2}|\psi|^4 + K|\mathbf{D}\psi|^2 + \frac{(h - H_c)^2}{8\pi}\right),$$

$$\sigma_{sn} = \int_{-\infty}^{\infty} dx\left(-\frac{b}{2}|\psi|^4 + \frac{(h - H_c)^2}{8\pi}\right). \qquad 2.1\text{-}15$$

where, after integrating by parts and neglecting the surface term, and using the Eq. 2.1-7 in order to obtain the concise form in the last line. This form clearly displays how σ_{sn} is determined by the balance between the positive diamagnetic energy and the negative condensation energy due to the superconductivity. By numerical solutions the GL equations demonstrates that if the GL parameter is larger than $\kappa_o = 1/\sqrt{2}$, then σ_{sn} becomes negative and, otherwise, positive.

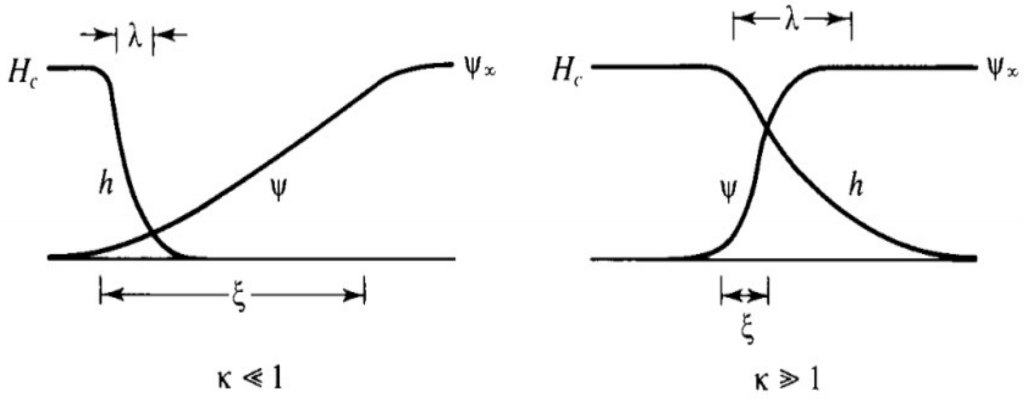

Figure 2.1-4 Diagram of the variation of the field (h) and ψ in a surface region between normal and superconductor state. $\kappa \ll 1$ *we have a positive wall energy, refers to type I,* $\kappa \gg 1$ *we have a negative wall energy, is a type II superconductor. Figure from [74].*

In other words, this parameter determines whether the domain-wall solution is energetically favorable. Materials are conventionally classified as type I or type II according if σ_{sn} is positive or negative.

2.2 MICROSCOPIC DERIVATION OF THE GINZBURG-LANDAU

As is known since the classical work by Gor'kov, the GL equations can be derived from the microscopic BCS theory in the most elegant way via the Green function formalism. So, in this topic we will present the Gorkov's microscopic derivation of the Ginzburg-Landau equations, which makes it possible to determine the phenomenological constants in terms of the microscopic parameters. The core of this derivation relies on the assumption that the excitation gap can be identified as the order parameter of the system[73], [74].

Our starting point is the Hamiltonian formulation of the BCS model by Bogoliubov et al[73][74]. This Hamiltonian includes the usual kinetic part absorbing the chemical potential in such a way that only the average number of particles is controlled (the grand canonical formalism). The interaction part is the second term, the last two terms in the equation below. Other terms related to the interaction between particles, the Hartree and Fock contributions, are accounted as constants and hidden in the chemical potential μ, once they do not have a specific reason to vary significantly when crossing T_c.

$$H_{BCS} = \int d^3\boldsymbol{x} \left[\sum_{\sigma} \psi_{\sigma}^{\dagger}(\boldsymbol{x})\mathcal{T}_x\psi_{\sigma}(\boldsymbol{x}) + \psi_{\uparrow}^{\dagger}(\boldsymbol{x})\psi_{\downarrow}^{\dagger}(\boldsymbol{x})\Delta(\boldsymbol{x}) + \psi_{\downarrow}(\boldsymbol{x})\psi_{\uparrow}(\boldsymbol{x})\Delta^{*}(\boldsymbol{x})\right], \qquad 2.2\text{-}1$$

$\mathcal{T}_x$ is the single-electron Hamiltonian, and the summation in the kinetic term is taken over the coinciding spin indices

$$\mathcal{T}_x = -\frac{\hbar^2}{2m_e}\left(\boldsymbol{\nabla} - \mathrm{i}\frac{e}{\hbar c}\mathbf{A}\right)^2 - \mu, \qquad 2.2\text{-}2$$

the energy gap (the convention by Gor'kov, de Gennes used a minus sign) is given by

$$\Delta(\boldsymbol{x}) = g\langle\psi_{\uparrow}(\boldsymbol{x})\psi_{\downarrow}(\boldsymbol{x})\rangle. \qquad 2.2\text{-}3$$

The Fermi field operators satisfy usual anticommutation relations:

$$\left\{\psi_{\sigma}(\boldsymbol{x}), \psi_{\sigma'}^{\dagger}(\boldsymbol{x}')\right\} = \delta_{\sigma\sigma'}\delta(\boldsymbol{x} - \boldsymbol{x}'),$$

$$\{\psi_{\sigma}(\boldsymbol{x}), \psi_{\sigma'}(\boldsymbol{x}')\} = 0. \qquad 2.2\text{-}4$$

Introducing the Heisenberg picture with imaginary time ($t \rightarrow$ real, imaginary time representation) to derive the equations of motion.

Then, the Heisenberg operators are defined as:

$$\psi_\uparrow(\boldsymbol{x},t) = \exp(H_{BCS}t/\hbar)\psi_\uparrow(\boldsymbol{x})\exp(-H_{BCS}t/\hbar),$$

$$\bar{\psi}_\downarrow(\boldsymbol{x},t) = \exp(H_{BCS}t/\hbar)\psi_\downarrow^\dagger(\boldsymbol{x})\exp(-H_{BCS}t/\hbar). \qquad 2.2\text{-}5$$

Then, we can find the equations of motion of the Heisenberg field operators in the imaginary-time representation:

$$\hbar\partial_t\psi_\uparrow(\boldsymbol{x},t) = -\mathcal{T}_x\psi_\uparrow(\boldsymbol{x},t) - \Delta(\boldsymbol{x})\bar{\psi}_\downarrow(\boldsymbol{x},t),$$

$$\hbar\partial_t\bar{\psi}_\downarrow(\boldsymbol{x},t) = -\Delta^*(\boldsymbol{x})\psi_\uparrow(\boldsymbol{x},t) + \mathcal{T}_x^*\bar{\psi}_\downarrow(\boldsymbol{x},t). \qquad 2.2\text{-}6$$

Introducing the temperature (Matsubara) Green's function:

$$\mathcal{G}(\boldsymbol{x}t,\boldsymbol{x}'t') = -\frac{1}{\hbar}\langle\mathcal{T}_t\left(\psi_\uparrow(\boldsymbol{x}t)\bar{\psi}_\uparrow(\boldsymbol{x}'t')\right)\rangle,$$

$$\mathcal{F}(\boldsymbol{x}t,\boldsymbol{x}'t') = -\frac{1}{\hbar}\langle\mathcal{T}_t\left(\bar{\psi}_\downarrow(\boldsymbol{x}t)\bar{\psi}_\uparrow(\boldsymbol{x}'t')\right)\rangle,$$

$$\bar{\mathcal{G}}(\boldsymbol{x}t,\boldsymbol{x}'t') = -\frac{1}{\hbar}\langle\mathcal{T}_t\left(\bar{\psi}_\downarrow(\boldsymbol{x}t)\psi_\downarrow(\boldsymbol{x}'t')\right)\rangle,$$

$$\bar{\mathcal{F}}(\boldsymbol{x}t,\boldsymbol{x}'t') = -\frac{1}{\hbar}\langle\mathcal{T}_t\left(\psi_\uparrow(\boldsymbol{x}t)\psi_\downarrow(\boldsymbol{x}'t')\right)\rangle, \qquad 2.2\text{-}7$$

And the generalized time-ordering procedure is given by:

$$\mathcal{T}_t\big(A(t)B(t')\big) = \theta(t-t')A(t)B(t') - \theta(t'-t)B(t')A(t),$$

So, the equations of motion for the temperature Green's functions is obtained as:

$$-\hbar\partial_t\mathcal{G}(\boldsymbol{x}t,\boldsymbol{x}'t') = \delta(\boldsymbol{x}-\boldsymbol{x}')\delta(t-t') + \mathcal{T}_x\mathcal{G}(\boldsymbol{x}t,\boldsymbol{x}'t') + \Delta(\boldsymbol{x})\bar{\mathcal{F}}(\boldsymbol{x}t,\boldsymbol{x}'t'),$$

$$-\hbar\partial_t\bar{\mathcal{F}}(\boldsymbol{x}t,\boldsymbol{x}'t') = \Delta^*(\boldsymbol{x})\mathcal{G}(\boldsymbol{x}t,\boldsymbol{x}'t') - \mathcal{T}_x^*\bar{\mathcal{F}}(\boldsymbol{x}t,\boldsymbol{x}'t'),$$

$$-\hbar\partial_t\bar{\mathcal{G}}(\boldsymbol{x}t,\boldsymbol{x}'t') = \delta(\boldsymbol{x}-\boldsymbol{x}')\delta(t-t') + \Delta^*(\boldsymbol{x})\mathcal{F}(\boldsymbol{x}t,\boldsymbol{x}'t') - \mathcal{T}_x^*\bar{\mathcal{G}}(\boldsymbol{x}t,\boldsymbol{x}'t'),$$

$$-\hbar\partial_t\mathcal{F}(\boldsymbol{x}t,\boldsymbol{x}'t') = -\mathcal{T}_x\mathcal{F}(\boldsymbol{x}t,\boldsymbol{x}'t') - \Delta(\boldsymbol{x})\bar{\mathcal{G}}(\boldsymbol{x}t,\boldsymbol{x}'t'). \qquad 2.2\text{-}8$$

So called the Gor'kov equations. Their original form was different because Gor'kov did not work with the anomalous averages first introduced by Bogoliubov.

In his work, Gor'kov derived and used the first two equations 2.2-8. Supplemented with the two additional relations, the Gor'kov equations can be rewritten as

$$\left\{\begin{pmatrix}\hbar\partial_t & 0\\ 0 & \hbar\partial_t\end{pmatrix}\begin{pmatrix}\mathcal{T}_x & \Delta(\vec{x})\\ \Delta^*(\vec{x}) & -\mathcal{T}_x^*\end{pmatrix}\right\}\begin{pmatrix}\mathcal{G} & \mathcal{F}\\ \bar{\mathcal{F}} & \bar{\mathcal{G}}\end{pmatrix} = -\delta(\vec{x}-\vec{x}')\delta(t-t')\begin{pmatrix}1 & 0\\ 0 & 1\end{pmatrix}. \qquad 2.2\text{-}9$$

It can also be written in a short notation

$$G(\boldsymbol{x}t,\boldsymbol{x}'t') = \begin{pmatrix} \mathcal{G}(\boldsymbol{x}t,\boldsymbol{x}'t') & \mathcal{F}(\boldsymbol{x}t,\boldsymbol{x}'t') \\ \bar{\mathcal{F}}(\boldsymbol{x}t,\boldsymbol{x}'t') & \bar{\mathcal{G}}(\boldsymbol{x}t,\boldsymbol{x}'t') \end{pmatrix},$$

$$H_{BdG} = \begin{pmatrix} \mathcal{T}_x & \Delta(\boldsymbol{x}) \\ \Delta^*(\boldsymbol{x}) & -\mathcal{T}_x^* \end{pmatrix}, \qquad \text{Bogoliubov-de Gennes Hamiltonian,}$$

$$\breve{1} = \begin{pmatrix} 1 & 0 \\ 0 & 1 \end{pmatrix},$$

so, we can write Eq. 2.2-9 in an elegant form that is usually called Gor'kov-Nambu equation.

$$\{\hbar\partial_t\breve{1} + H_{BdG}\}G(\boldsymbol{x}t,\boldsymbol{x}'t') = -\delta(\boldsymbol{x}-\boldsymbol{x}')\delta(t-t')\breve{1}, \qquad 2.2\text{-}10$$

Using the boundary condition:

$$A(\boldsymbol{x},\boldsymbol{x}',\Delta t) = -A(\boldsymbol{x},\boldsymbol{x}',\Delta t+\beta\hbar), \qquad [A = \mathcal{G},\tilde{\mathcal{G}},\mathcal{F},\tilde{\mathcal{F}}], \qquad 2.2\text{-}11$$

results in the expansion in terms of the Matsubara frequencies (ω_n):

$$A(\boldsymbol{x},\boldsymbol{x}',\Delta t) = \frac{1}{\beta\hbar}\sum_n e^{-in\omega_n\Delta t}A(\boldsymbol{x},\boldsymbol{x}',\omega_n), \qquad \omega_n = \frac{\pi(2n+1)}{\beta\hbar}. \qquad 2.2\text{-}12$$

And, being well-known that the temperature Green's functions are defined only for $-\beta\hbar < t-t' < \beta\hbar$, due to the antiperiodic boundary condition. Thus, we arrive at:

$$\delta(t-t') = \frac{1}{\beta\hbar}\sum_n e^{-in\omega_n(t-t')}. \qquad -\beta\hbar < t-t' < \beta\hbar. \qquad 2.2\text{-}13$$

And allow us to write the Gor'kov-Nambu in the following form:

$$\left\{\begin{pmatrix} i\hbar\omega_n & 0 \\ 0 & i\hbar\omega_n \end{pmatrix} - \begin{pmatrix} \mathcal{T}_x & \Delta(\boldsymbol{x}) \\ \Delta^*(\boldsymbol{x}) & -\mathcal{T}_x^* \end{pmatrix}\right\}\begin{pmatrix} \mathcal{G}_\omega(\boldsymbol{x},\boldsymbol{x}',\omega_n) & \mathcal{F}_\omega(\boldsymbol{x},\boldsymbol{x}',\omega_n) \\ \bar{\mathcal{F}}_\omega(\boldsymbol{x},\boldsymbol{x}',\omega_n) & \bar{\mathcal{G}}_\omega(\boldsymbol{x},\boldsymbol{x}',\omega_n) \end{pmatrix} = -\delta(\boldsymbol{x}-\boldsymbol{x}')\begin{pmatrix} 1 & 0 \\ 0 & 1 \end{pmatrix},$$

$$\{i\hbar\omega_n\breve{1} - H_{BdG}\}G_\omega(\boldsymbol{x},\boldsymbol{x}') = \delta(\boldsymbol{x}-\boldsymbol{x}')\breve{1},$$

$$G_\omega = \begin{pmatrix} \mathcal{G}_\omega(\boldsymbol{x},\boldsymbol{x}',\omega_n) & \mathcal{F}_\omega(\boldsymbol{x},\boldsymbol{x}',\omega_n) \\ \bar{\mathcal{F}}_\omega(\boldsymbol{x},\boldsymbol{x}',\omega_n) & \bar{\mathcal{G}}_\omega(\boldsymbol{x},\boldsymbol{x}',\omega_n) \end{pmatrix}. \qquad 2.2\text{-}14$$

To solve these equations, it is convenient to introduce new operators in the Hilbert space defined as:

$$\langle \boldsymbol{x}|\hat{A}_\omega|\boldsymbol{x}'\rangle = A_\omega(\boldsymbol{x},\boldsymbol{x}') \to \breve{G}_\omega = \begin{pmatrix} \hat{\mathcal{G}}_\omega & \hat{\mathcal{F}}_\omega \\ \hat{\bar{\mathcal{F}}}_\omega & \hat{\bar{\mathcal{G}}}_\omega \end{pmatrix}, \qquad 2.2\text{-}15$$

and

$$\langle \boldsymbol{x}|\hat{\mathcal{T}}|\boldsymbol{x}'\rangle = \delta(\boldsymbol{x}-\boldsymbol{x}')\mathcal{T}_x,$$

$$\langle \boldsymbol{x}|\hat{\Delta}|\boldsymbol{x}'\rangle = \delta(\boldsymbol{x}-\boldsymbol{x}')\Delta(\boldsymbol{x}'), \qquad 2.2\text{-}16$$

The H_{BdG} operator can be expressed as the sum of the kinetic and interaction (condensate) contributions:

$$\breve{\mathcal{T}} = \begin{pmatrix} \hat{\mathcal{T}} & 0 \\ 0 & -\hat{\mathcal{T}}^* \end{pmatrix}, \qquad \breve{\Delta} = \begin{pmatrix} 0 & \hat{\Delta} \\ \hat{\Delta}^* & 0 \end{pmatrix}. \qquad 2.2\text{-}17$$

Equation 2.2-14 become:

$$i\hbar\omega_n\langle \boldsymbol{x}|\breve{G}_\omega|\boldsymbol{x}'\rangle = \delta(\boldsymbol{x}-\boldsymbol{x}')\breve{1} + H_{BdG}G_\omega(\boldsymbol{x},\boldsymbol{x}'),$$

$$i\hbar\omega_n\langle \boldsymbol{x}|\breve{G}_\omega|\boldsymbol{x}'\rangle = \langle \boldsymbol{x}|\boldsymbol{x}'\rangle\breve{1} + \langle \boldsymbol{x}|(\breve{\mathcal{T}}+\breve{\Delta})|\boldsymbol{x}'\rangle. \qquad 2.2\text{-}18$$

With completeness relation of the Hilbert space, it is obtained the operator form of the Gor'kov-Nambu equations:

$$(i\hbar\omega_n - \breve{\mathcal{T}})\breve{G}_\omega = \breve{1} + \breve{\Delta}\breve{G}_\omega, \qquad 2.2\text{-}19$$

To the normal state $\hat{\Delta} = 0$, and we obtain the normal or unperturbed Green function operator

$$(i\hbar\omega_n - \breve{\mathcal{T}})\breve{G}_\omega^{(0)} = \breve{1}, \qquad 2.2\text{-}20$$

And using Eqs. 2.2-19 and 2.2-20 one obtains

$$\breve{G}_\omega = \breve{G}_\omega^{(0)} + \breve{G}_\omega^{(0)}\breve{\Delta}\breve{G}_\omega, \qquad 2.2\text{-}21$$

Which is the Gor'kov-Nambu formalism as Dyson equation for the Green function $\breve{G}_\omega$. And iterating

$$\breve{G}_\omega = \breve{G}_\omega^{(0)} + \breve{G}_\omega^{(0)}\breve{\Delta}\breve{G}_\omega^{(0)} + \breve{G}_\omega^{(0)}\breve{\Delta}\breve{G}_\omega^{(0)}\breve{\Delta}\breve{G}_\omega^{(0)} + \cdots. \qquad 2.2\text{-}22$$

Now, we need to extract the equation for the anomalous Green function in order to construct the self-consistency equation for the superconducting gap. So, from the Eq. 2.2-21

$$\begin{pmatrix} \hat{\mathcal{G}}_\omega & \hat{\mathcal{F}}_\omega \\ \hat{\bar{\mathcal{F}}}_\omega & \hat{\bar{\mathcal{G}}}_\omega \end{pmatrix} = \begin{pmatrix} \hat{\mathcal{G}}_\omega^{(0)} & 0 \\ 0 & \hat{\bar{\mathcal{G}}}_\omega^{(0)} \end{pmatrix} + \begin{pmatrix} \hat{\mathcal{G}}_\omega^{(0)} & 0 \\ 0 & \hat{\bar{\mathcal{G}}}_\omega^{(0)} \end{pmatrix}\begin{pmatrix} 0 & \hat{\Delta} \\ \hat{\Delta}^* & 0 \end{pmatrix}\begin{pmatrix} \hat{\mathcal{G}}_\omega & \hat{\mathcal{F}}_\omega \\ \hat{\bar{\mathcal{F}}}_\omega & \hat{\bar{\mathcal{G}}}_\omega \end{pmatrix}, \qquad 2.2\text{-}23$$

thus, we obtain

$$\hat{\hat{\mathcal{G}}}_\omega = \hat{\hat{\mathcal{G}}}_\omega^{(0)} + \hat{\hat{\mathcal{G}}}_\omega^{(0)} \hat{\Delta}^* \hat{\mathcal{F}}_\omega \,,$$

$$\hat{\mathcal{F}}_\omega = \hat{\mathcal{G}}_\omega^{(0)} \hat{\Delta} \hat{\hat{\mathcal{G}}}_\omega. \qquad 2.2\text{-}24$$

And we obtain the following after iteration:

$$\hat{\mathcal{F}}_\omega = \hat{\mathcal{G}}_\omega^{(0)} \hat{\Delta} \hat{\hat{\mathcal{G}}}_\omega^{(0)} + \hat{\mathcal{G}}_\omega^{(0)} \hat{\Delta} \hat{\hat{\mathcal{G}}}_\omega^{(0)} \hat{\Delta}^* \hat{\mathcal{G}}_\omega^{(0)} \hat{\Delta} \hat{\hat{\mathcal{G}}}_\omega^{(0)} + \cdots. \qquad 2.2\text{-}25$$

From Eq. 2.2-7 is obtained a relation between the energy gap and the anomalous Green function

$$\Delta(\boldsymbol{x}) = g\langle \psi_\uparrow(\boldsymbol{x}) \psi_\downarrow(\boldsymbol{x}') \rangle = -g\hbar \lim_{\boldsymbol{x}' \to \boldsymbol{x}} \lim_{\Delta t \to 0} \mathcal{F}(\boldsymbol{x}t, \boldsymbol{x}'t'),$$

$$\Delta(\boldsymbol{x}) = -g\hbar \lim_{\boldsymbol{x}' \to \boldsymbol{x}} \lim_{\Delta t \to 0} \frac{1}{\beta\hbar} \sum_\omega e^{-\mathrm{i}\omega\Delta t} \mathcal{F}_\omega(\boldsymbol{x}, \boldsymbol{x}'),$$

$$\Delta(\boldsymbol{x}) = -gT \lim_{\boldsymbol{x}' \to \boldsymbol{x}} \lim_{\Delta t \to 0} \sum_\omega e^{-\mathrm{i}\omega\Delta t} \mathcal{F}_\omega(\boldsymbol{x}, \boldsymbol{x}'), \qquad 2.2\text{-}26$$

with g the (Gor'kov) coupling constant, and from Eq. 2.2-25 obtains the self-consistency equation which is expanded in powers of the order parameter (gap function)

$$\Delta(\boldsymbol{x}) = \int d^3\boldsymbol{y}\, K_a(\boldsymbol{x}, \boldsymbol{y}) \Delta(\boldsymbol{y})$$
$$+ \int \left(\prod_{i=1}^3 d^3\boldsymbol{y}_i \right) K_b(\boldsymbol{x}, \boldsymbol{y}_1, \boldsymbol{y}_2, \boldsymbol{y}_3) \Delta(\boldsymbol{y}_1) \Delta^*(\boldsymbol{y}_2) \Delta(\boldsymbol{y}_3) \qquad 2.2\text{-}27$$
$$+ \int \left(\prod_{i=1}^5 d^3\boldsymbol{y}_i \right) K_c(\boldsymbol{x}, \boldsymbol{y}_1, \boldsymbol{y}_2, \boldsymbol{y}_3, \boldsymbol{y}_4, \boldsymbol{y}_5) \Delta(\boldsymbol{y}_1) \Delta^*(\boldsymbol{y}_2) \Delta(\boldsymbol{y}_3) \Delta^*(\boldsymbol{y}_4) \Delta(\boldsymbol{y}_5) + \cdots.$$

and the integral kernels are given

$$K_a(\boldsymbol{x}, \boldsymbol{y}) = -gT \lim_{\Delta t \to 0} \sum_\omega e^{-i\omega\Delta t} \mathcal{G}_\omega^{(0)}(\boldsymbol{x}, \boldsymbol{y}) \bar{\mathcal{G}}_\omega^{(0)}(\boldsymbol{y}, \boldsymbol{x}),$$

$$K_b(\boldsymbol{x}, \boldsymbol{y}_1, \boldsymbol{y}_2, \boldsymbol{y}_3) = -gT \lim_{\Delta t \to 0} \sum_\omega e^{-\mathrm{i}\omega\Delta t} \mathcal{G}_\omega^{(0)}(\boldsymbol{x}, \boldsymbol{y}_1) \bar{\mathcal{G}}_\omega^{(0)}(\boldsymbol{y}_1, \boldsymbol{y}_2) \mathcal{G}_\omega^{(0)}(\boldsymbol{y}_2, \boldsymbol{y}_3) \bar{\mathcal{G}}_\omega^{(0)}(\boldsymbol{y}_3, \boldsymbol{x}),$$

$$K_c(\boldsymbol{x}, \boldsymbol{y}_1, \dots, \boldsymbol{y}_5) = -gT \lim_{\Delta t \to 0} \sum_\omega e^{-\mathrm{i}\omega\Delta t} \mathcal{G}_\omega^{(0)}(\boldsymbol{x}, \boldsymbol{y}_1) \bar{\mathcal{G}}_\omega^{(0)}(\boldsymbol{y}_1, \boldsymbol{y}_2) \mathcal{G}_\omega^{(0)}(\boldsymbol{y}_2, \boldsymbol{y}_3) \bar{\mathcal{G}}_\omega^{(0)}(\boldsymbol{y}_3, \boldsymbol{y}_4) \mathcal{G}_\omega^{(0)}(\boldsymbol{y}_4, \boldsymbol{y}_5) \bar{\mathcal{G}}_\omega^{(0)}(\boldsymbol{y}_5, \boldsymbol{x}). \qquad 2.2\text{-}28$$

Equation 2.2-27 can be truncated to a desired order. To obtain the GL equations is necessary keep only the first and third powers (the Gor'kov truncation). To obtain the EGL formalism, it is of importance to include the fifth-power term.

For the normal-state temperature Green function $\mathcal{G}_{\omega}^{(0)}(\boldsymbol{x},\boldsymbol{y})$, we have (at zero magnetic field)

$$\mathcal{G}_{\omega}^{(0)}(\boldsymbol{x},\boldsymbol{y}) = \int \frac{d^3\boldsymbol{k}}{(2\pi)^3}\frac{e^{-\mathrm{i}\boldsymbol{k}(\boldsymbol{x}-\boldsymbol{y})}}{i\hbar\omega - \xi_k}. \qquad 2.2\text{-}29$$

for a spherically symmetric Fermi surface and in the parabolic band approximation the single-particle energy is given by $\xi_k = \frac{\hbar^2 k^2}{2m} - \mu$, measured from the chemical potential μ, and $\bar{\mathcal{G}}_{\omega}^{(0)}(\boldsymbol{x},\boldsymbol{y}) = -\mathcal{G}_{-\omega}^{(0)}(\boldsymbol{y},\boldsymbol{x})$.

The inclusion of the magnetic field in the formalism is made by the field-induced corrections through the field-dependent Peierls phase factor in the Green function obtained before

$$\mathcal{G}_{Gor}^{(0)}(\boldsymbol{x},\boldsymbol{x}') = e^{\mathrm{i}\Phi(\boldsymbol{x},\boldsymbol{x}')}\mathcal{G}_{\omega}^{(0)}(\boldsymbol{x},\boldsymbol{x}'), \qquad 2.2\text{-}30$$

From the equation for the normal Green function

$$\boldsymbol{\nabla}_x\Phi(\boldsymbol{x},\boldsymbol{x}') = \frac{e}{\hbar c}\mathbf{A}(\boldsymbol{x}), \qquad 2.2\text{-}31$$

in the semi-classical approximation is obtained

$$\Phi(\boldsymbol{x},\boldsymbol{x}') \approx \frac{e}{\hbar c}\mathbf{A}(\boldsymbol{x})\cdot(\boldsymbol{x}-\boldsymbol{x}'). \qquad 2.2\text{-}32$$

And considering that typical length of the spatial variations of the gap becomes much larger than the typical spatial length of the integral kernels, it is convenient to use the gradient expansion:

$$\Delta(\boldsymbol{y}) = \Delta(\boldsymbol{x}+\boldsymbol{z}) = \sum_{n=1}^{\infty}\frac{1}{n!}(\boldsymbol{z}\cdot\boldsymbol{\nabla})^n\Delta(\boldsymbol{x}) \qquad 2.2\text{-}33$$

And as the typical length of the spatial variations of the vector potential is much larger than the characteristic lengths of the integral kernels in the self-consistency equation:

$$e^{\mathrm{i}\Phi(\boldsymbol{z})} = 1 + \mathrm{i}\frac{e}{\hbar c}\boldsymbol{z}\mathbf{A}(\boldsymbol{x}). \qquad 2.2\text{-}34$$

Then finally, we can calculate Eq. 2.2-27, and in the presence of the magnetic field, in particular, the GL equation is obtained when keeping only the first two terms, including K_a and K_b:

$$\Delta(\boldsymbol{x}) = \int d^3\boldsymbol{z}\, K_a(\boldsymbol{z})\Delta(\boldsymbol{x}) + \frac{1}{6}\int d^3\boldsymbol{z}\, K_a(\boldsymbol{z}) \mathrm{z}^2 \mathbf{D}^2\Delta(\boldsymbol{x}) + \int \left(\prod_{i=1}^{3} d^3\boldsymbol{y}_i\right) K_b(\boldsymbol{x},\boldsymbol{y}_1,\boldsymbol{y}_2,\boldsymbol{y}_3)|\Delta(\boldsymbol{x})|^2\Delta(\boldsymbol{x}), \qquad 2.2\text{-}35$$

where $\mathbf{D} = \boldsymbol{\nabla} - \mathrm{i}\frac{2e}{\hbar c}\mathbf{A}$, the so-called gauge invariant derivative.

Expanding in terms of τ, collecting terms of the order $\tau^{1/2}$, gives the ordinary BCS expression for the critical temperature T_c:

$$T_c = \frac{2e^{\gamma}}{\pi}\hbar\omega_{\mathrm{c}} \exp[-1/gN(0)]. \qquad 2.2\text{-}36$$

Where T_c is expressed in terms of the microscopic parameters of the superconductor, ω_{c} denotes the Debye (cut-off) frequency used as regulator of the well-known ultraviolet divergence by introducing the cut-off energy, which is identified with the Debye energy when the superconductivity is mediated by phonons, g the coupling constant, $\gamma = 0.577$ the Euler constant, and $N(0)$ the density of the carrier state (DOS) at the Fermi surface.

In the order $\tau^{3/2}$, one recovers the standard GL equation:

$$a\tau\Delta + b|\Delta|^2\Delta - K\mathbf{D}^2\Delta = 0, \qquad 2.2\text{-}37$$

Where

$$a = gN(0), \qquad b = gN(0)\,\frac{7\zeta(3)}{8\pi^2 T_c^2}, \qquad K = \frac{b}{6}\hbar^2 v_F^2.$$

With v_F the Fermi velocity and $\zeta(\dots)$ the Riemann zeta function.

To find the GL equation for the current, Gor'kov has employed the linear response to the magnetic field

$$\boldsymbol{j}(\boldsymbol{x}) = \lim_{\Delta t\to 0}\lim_{x'\to x}\left[\frac{i\hbar e}{m}(\boldsymbol{\nabla}_x - \boldsymbol{\nabla}_{x'})\bar{\mathcal{G}}(\boldsymbol{x}t,\boldsymbol{x}'t') - \frac{2e^2}{mc}\mathbf{A}(\boldsymbol{x})\bar{\mathcal{G}}(\boldsymbol{x}t,\boldsymbol{x}'t')\right], \qquad 2.2\text{-}38$$

where the expression for $\bar{\mathcal{G}}$ must be accounted up to the leading correction $\delta\bar{\mathcal{G}}_\omega$

$$\bar{\mathcal{G}}_\omega(\boldsymbol{x},\boldsymbol{x}') = \bar{\mathcal{G}}^{(0)}_{Gor,\omega}(\boldsymbol{x},\boldsymbol{x}') + \delta\bar{\mathcal{G}}_\omega(\boldsymbol{x},\boldsymbol{x}'),$$

$$\delta\bar{\mathcal{G}}_\omega(\boldsymbol{x},\boldsymbol{x}') = \frac{1}{\hbar^2}\int d^3\boldsymbol{y}\, d^3\boldsymbol{z}\, \bar{\mathcal{G}}^{(0)}_{Gor,\omega}(\boldsymbol{x},\boldsymbol{y})\mathcal{G}^{(0)}_{Gor,\omega}(\boldsymbol{y},\boldsymbol{z})\bar{\mathcal{G}}^{(0)}_{Gor,\omega}(\boldsymbol{z},\boldsymbol{x}')\Delta^*(\boldsymbol{y})\Delta(\boldsymbol{z}). \quad 2.2\text{-}39$$

The contribution of $\bar{\mathcal{G}}^{(0)}_{Gor,\omega}(\boldsymbol{x},\boldsymbol{x}')$ to $\boldsymbol{j}(\boldsymbol{x})$ is zero, considering the linear expansion in the Peierls factor

$$\lim_{x'\to x}\frac{\mathrm{i}\hbar e}{m}(\boldsymbol{\nabla}_x - \boldsymbol{\nabla}_{x'})\bar{\mathcal{G}}(\boldsymbol{x},\boldsymbol{x}') = \lim_{x'\to x}\frac{2e^2}{mc}\mathbf{A}(\boldsymbol{x})\bar{\mathcal{G}}(\boldsymbol{x},\boldsymbol{x}'), \quad 2.2\text{-}40$$

So, Eq. 2.2-38 becomes

$$\boldsymbol{j}(\boldsymbol{x}) = \frac{\mathrm{i}eT}{m}\sum_n[(\boldsymbol{\nabla}_x - \boldsymbol{\nabla}_{x'})\delta\bar{\mathcal{G}}_\omega(\boldsymbol{x},\boldsymbol{x}')]_{x'\to x} - \frac{2e^2T}{m\hbar c}\mathbf{A}(\boldsymbol{x})\sum_n\delta\bar{\mathcal{G}}_\omega(\boldsymbol{x},\boldsymbol{x}'),$$

$$\boldsymbol{j}(\boldsymbol{x}) = \frac{\mathrm{i}eT}{m}\int d^3\boldsymbol{y}\, d^3\boldsymbol{z}\,\Delta(\boldsymbol{x})\Delta^*(\boldsymbol{z})e^{\mathrm{i}\Phi(y,z)}\mathcal{G}^{(0)}_\omega(\boldsymbol{y},\boldsymbol{z})\left\{e^{\mathrm{i}\Phi(z,x')}\mathcal{G}^{(0)}_{-\omega}(\boldsymbol{z},\boldsymbol{x}')\boldsymbol{\nabla}_x\left[e^{\mathrm{i}\Phi(y,x')}\mathcal{G}^{(0)}_{-\omega}(\boldsymbol{y},\boldsymbol{x})\right]\right.$$
$$\left. - e^{\mathrm{i}\Phi(y,x)}\mathcal{G}^{(0)}_{-\omega}(\boldsymbol{y},\boldsymbol{x})\boldsymbol{\nabla}_x\left[e^{\mathrm{i}\Phi(x',z)}\mathcal{G}^{(0)}_{-\omega}(\boldsymbol{x}',\boldsymbol{z})\right]\right\} - \frac{2e^2T}{m\hbar c}\mathbf{A}(\boldsymbol{x})\sum_n\delta\bar{\mathcal{G}}_{Gor,\omega}(\boldsymbol{x},\boldsymbol{x}'). \quad 2.2\text{-}41$$

By using Eq. 2.2-34, and due of the spherical symmetry, we obtain the second GL equation

$$\boldsymbol{j}(\boldsymbol{x}) = \frac{eT}{m\mathrm{i}\hbar^2}\int d^3\boldsymbol{y}\, d^3\boldsymbol{z}\,\mathcal{G}^{(0)}_\omega(\boldsymbol{y},\boldsymbol{z})\left[\mathcal{G}^{(0)}_\omega(\boldsymbol{x},\boldsymbol{z})\boldsymbol{\nabla}_x\mathcal{G}^{(0)}_\omega(\boldsymbol{y},\boldsymbol{x}) - \mathcal{G}^{(0)}_\omega(\boldsymbol{y},\boldsymbol{x})\boldsymbol{\nabla}_x\mathcal{G}^{(0)}_\omega(\boldsymbol{x},\boldsymbol{z})\right]$$
$$\times\left[-\frac{2\mathrm{i}e}{\hbar c}|\Delta(\boldsymbol{x})|^2\mathbf{A}(\boldsymbol{x})\cdot(\boldsymbol{z}-\boldsymbol{y}) + \Delta^*(\boldsymbol{x})\,\boldsymbol{y}\cdot\boldsymbol{\nabla}\Delta(\boldsymbol{x}) + \Delta^*(\boldsymbol{x})\,\boldsymbol{z}\cdot\boldsymbol{\nabla}\Delta^*(\boldsymbol{x})\right],$$

$$\boldsymbol{j}(\boldsymbol{x}) = gN(0)\,\frac{7\zeta(3)\hbar^2v_F^2}{16\pi^2T_c^2}[\Delta^*(\boldsymbol{x})\mathbf{D}\Delta(\boldsymbol{x}) - \Delta(\boldsymbol{x})\mathbf{D}\Delta^*(\boldsymbol{x})]. \quad 2.2\text{-}42$$

2.3 EXTENDED GINZBURG-LANDAU FORMALISM

Over time, several theorists wished to develop an extension to the GL theory, with the idea of improving the formalism and retaining some advantages of its original formulation. Thus, several GL-type theories have been proposed.

In the first developments, the so-called "local superconducting" formalism there appeared a complicated synthesis of the BCS and GL approaches. With a GL theory with nonlocal corrections, including higher order parameter gradients, where it was used in higher critical field anisotropy studies and the vortex structure in d-wave superconductors. In the previous examples, the extension of the GL theory was based on the expansion of the self-consistent gap equation, including higher powers of the order parameter and its spatial gradients phenomenologically. But the calculation of these terms is not so simple, where the fundamental problem is to correctly select all the relevant contributions of the same order of magnitude. This problem does not arise in the derivation of the original GL theory for a single-band superconductor, where only the first nonlinear term and the second order gradient of the condensed wave function are included. But for the GL theory of a two-band superconductor, it leads to the appearance of incomplete contributions of higher order. Such incomplete terms may lead to misleading conclusions and should be avoided.

Thus, it is necessary to use a single small parameter in the expansion. In the case, such a small parameter is the proximity to the critical temperature, i.e., $\tau = 1 - T/T_c$. In fact, the standard GL approach is the lowest order in the expansion τ of the self-consistent gap equation. However, the next orders in τ are also of great importance, for example, to capture physics of different healing lengths of different condensates in multiband superconductors. Higher orders in τ are also important in the case of single band, surprisingly improving the GL theory [65].

So, based on the formalism of the Gor'kov Green function, using the first three orders of the expansion τ of the gap equation, that is, $\tau^{n/2}$ with $n = 1,2,3$. We have, for the order $\tau^{1/2}$, we find the equation for the critical temperature. The terms proportional to $\tau^{3/2}$ give the standard GL theory, giving the lowest order contributions (in τ) to the superconducting condensate, that is, $\propto \tau^{1/2}$, and the magnetic field, that is, $\propto \tau$. Then, with the terms of the order $\tau^{5/2}$, is derived the equations for the next-to-leading corrections to the superconducting order parameter and magnetic field, $\propto \tau^{3/2}$ and $\propto \tau^2$, respectively. The equations that control the order parameter and the magnetic field up to the next-to-leading order in τ constitutes the extended GL formalism (EGL).

So, with these considerations, we use the Taylor expansion of the gaps up to the fourth order derivatives for the gaps inside the integrals (Eq. 2.2-27) involving K_a, up to the second order inside the integrals involving K_b and just the leading term inside the integral involving K_c. Due to the spherical symmetry of the kernels, some odd-order terms of these expansions can be neglected and a systematic expansion of the gap equation in τ can be facilitated by introducing the scaling transformation for the order parameter, the coordinates, and the spatial derivatives of the order parameter in the following form:

$$\Delta = \tau^{1/2}\overline{\Delta}, \qquad \boldsymbol{x} = \tau^{-1/2}\overline{\boldsymbol{x}}, \qquad \boldsymbol{\nabla}_{\vec{x}} = \tau^{1/2}\boldsymbol{\nabla}_{\overline{x}}$$

In further calculations we omit the bars unless it causes any confusion ($\boldsymbol{\nabla}_{\boldsymbol{x}} = \boldsymbol{\nabla}$). The result reads as

$$\begin{aligned}\frac{\tau^{1/2}}{g}\Delta = a_1\tau^{1/2}\Delta + a_2\tau^{3/2}\boldsymbol{\nabla}^2\Delta + a_3\tau^{5/2}\boldsymbol{\nabla}^2(\boldsymbol{\nabla}^2\Delta) - b_1\tau^{\frac{3}{2}}|\Delta|^2\Delta \\ - b_2\tau^{5/2}[2\Delta|\boldsymbol{\nabla}\Delta|^2 + 3\Delta^*(\boldsymbol{\nabla}\Delta)^2 + \Delta^2\boldsymbol{\nabla}^2\Delta^* + 4|\Delta|^2\boldsymbol{\nabla}^2\Delta] \\ + c_1\tau^{5/2}|\Delta|^4\Delta,\end{aligned} \tag{2.3-1}$$

the coefficients are given by

$$a_1 = \mathcal{A} - a\left[\tau + \frac{\tau^2}{2} + \mathcal{O}(\tau^3)\right], \qquad \mathcal{A} = N(0)\ln\left(\frac{2^\gamma\hbar\omega_c}{\pi T_c}\right), \qquad a = -N(0),$$

$$b_1 = b[1 + 2\tau + \mathcal{O}(\tau^2)], \qquad b = N(0)\,\frac{7\zeta(3)}{8\pi^2T_c^2},$$

$$a_2 = K[1 + 2\tau + \mathcal{O}(\tau^2)], \qquad K = \frac{b}{6}\hbar^2v_F^2,$$

$$c_1 = c[1 + \mathcal{O}(\tau)], \qquad c = N(0)\,\frac{93\zeta(5)}{1288\pi^4T_c^4},$$

$$a_3 = Q[1 + \mathcal{O}(\tau)], \qquad Q = \frac{c}{30}\hbar^4v_F^4,$$

$$b_2 = L[1 + \mathcal{O}(\tau)], \qquad L = \frac{c}{9}\hbar^2v_F^2.$$

The solution to the gap equation 2.3-1 must also be sought in the form of a series expansion in τ .

So, we can introduce the expansion in small deviation from the critical temperature

$$\Delta(\boldsymbol{x}) = \tau^{1/2} \sum_{n=0}^{\infty} \tau^n \, \Delta^{(n)}(\boldsymbol{x}), \qquad 2.3\text{-}2$$

Then, collecting terms of the same order, we obtain a set of equations for each $\Delta^{(n)}$

$$(\mathrm{g}^{-1} - \mathcal{A})\Delta^{(0)} = 0,$$

$$a\Delta^{(0)} + b\left|\Delta^{(0)}\right|^2 \Delta^{(0)} - K\boldsymbol{\nabla}^2\Delta^{(0)} = 0,$$

$$a\Delta^{(1)} + b\left(2\Delta^{(1)}\left|\Delta^{(0)}\right|^2 + \Delta^{(1)*}\Delta^{(0)2}\right) - K\boldsymbol{\nabla}^2\Delta^{(1)} = F, \qquad 2.3\text{-}3$$

And F is given by

$$F = -\frac{a}{2}\Delta^{(0)} + 2K\boldsymbol{\nabla}^2\Delta^{(0)} + Q\boldsymbol{\nabla}^2\left(\vec{\nabla}^2\Delta^{(0)}\right) - 2b\left|\Delta^{(0)}\right|^2\Delta^{(0)}$$
$$- L\left[2\Delta^{(0)}\left|\boldsymbol{\nabla}\Delta^{(0)}\right|^2 + 3\Delta^{(0)*}\left(\boldsymbol{\nabla}\Delta^{(0)}\right)^2 + \Delta^{(0)2}\boldsymbol{\nabla}^2\Delta^{(0)*}\right.$$
$$\left. + 4\left|\Delta^{(0)}\right|^2\boldsymbol{\nabla}^2\Delta^{(0)}\right] + c\left|\Delta^{(0)}\right|^4\Delta^{(0)}$$

The solution to first equation, i.e., $g\mathcal{A} = 1$, gives the ordinary BCS expression for the critical temperature, i.e., $T_c = \frac{2e^{\gamma}}{\pi}\hbar\omega_c \exp[-1/gN(0)]$.

The extended equation is a linear differential inhomogeneous equation to be solved after $\Delta^{(0)}$ is found from standard GL equation. Note that similar features in the τ expansion of the gap equation appear for a two-band superconductor as well. While the equation for $\Delta^{(0)}$ is nonlinear, the higher-order contributions to Δ will be controlled by inhomogeneous linear differential equations. Such a system of equations is solved recursively, starting from the lowest order, since solutions for previous orders will appear in the higher-order equations, but not vice versa.

The solution to the system will thus be uniquely defined (when the relevant boundary conditions are specified), ensuring consistency of the developed expansion. The structure of Eq. 2.3-3 makes it possible to conclude that the next-to-leading term $\Delta^{(1)}$ is not trivially proportional to $\Delta^{(0)}$. For that reason, the spatial profile of $\Delta^{(1)}$ is different compared to $\Delta^{(0)}$. This means that the characteristic length for the spatial variations of Δ in EGL differs from the standard GL coherence length. However, both lengths have the same dependence on τ , i.e., $\boldsymbol{\nabla}\Delta^{(1)} \propto \tau$.

2.4 INTERTYPE SUPERCONDUCTIVITY

The division of Abrikosov between types I and II of superconductivity was very important in order to establish a pattern of interpretation of very complex phenomena in superconductors, and the distinction between types of superconductivity for single-band materials were well explained by the Ginzburg-Landau theory that ideally distinguishes type I and type II superconducting materials. However, experimental investigations as well as theoretical calculations beyond GL theory have shown that this GL dichotomy of superconductivity types is achieved only at the limit $T \to T_c$.

With the study of unconventional vortex configurations in MgB_2, interest in other possible types of superconductivity in multiband superconductors has been aroused, where many carrier bands contribute to the state of condensation.

Vagov et al. considering single-band and two-band superconducting cases under the effect of magnetic fields applied in the vicinity of $\kappa_0 = 1/\sqrt{2}$, brought in another physical image for the unusual phenomena observed in multiband compounds, where they considered the Bogomolnyi self-duality in the EGL equations, in order to describe the so-called intertype domain between the standard types I and II in the plane (κ, T) which can be significantly increased to a two-band superconductor. Thus, it has been shown that the intertype domain cannot be captured by the standard GL theory because of non-local effects beyond the GL domain that must be considered [61].

In the presence of a magnetic field, the gap function $\vec{\Delta}$ and the magnetic field $\mathbf{B}$ (or the vector potential $\mathbf{A}$) must also be expanded in powers of τ, so they are represented in the form for a two-band system

$$\vec{\Delta} = \tau^{1/2}\left(\vec{\Delta}^{(0)} + \tau\vec{\Delta}^{(1)} + \cdots\right),$$

$$\mathbf{B} = \tau\left(\mathbf{B}^{(0)} + \tau\mathbf{B}^{(1)} + \cdots\right),$$

$$\mathbf{A} = \tau^{1/2}\left(\mathbf{A}^{(0)} + \tau\mathbf{A}^{(1)} + \cdots\right). \qquad 2.4\text{-}1$$

Matching the terms of the same order in τ the EGL free-energy density, following the analysis [35][61], we can write

$$f = \tau^2\left(\tau^{-1}f^{(-1)} + f^{(0)} + \tau f^{(1)} + \cdots\right), \qquad 2.4\text{-}2$$

where the lowest-order contribution reads

$$f^{(-1)} = \langle \vec{\Delta}^{(0)} | L | \vec{\Delta}^{(0)} \rangle, \qquad 2.4\text{-}3$$

with $\langle ... \rangle$ denoting the scalar product of vectors in the band space. Here L for a two-band system is a 2x2 matrix where the elements given by

$$L_{ij} = \gamma_{ij} - \mathcal{A}_i \delta_{ij},$$

being δ_{ij} the Kronecker symbol, and γ_{ij} the inverse of the coupling matrix, where each element is given by the term g_{ij}(elements of the coupling matrix) that are symmetric, the coupling constants. The gap vector must be proportional to the eigenvector associated with the zero eigenvalue $\vec{\Delta}^{(0)} = \psi(\boldsymbol{x})\vec{\eta}_1$.

The next-order contribution to the free energy density is the GL functional

$$f^{(0)} = \frac{\mathbf{B}^{(0)2}}{8\pi} + \left(\langle \vec{\Delta}^{(0)} | L | \vec{\Delta}^{(1)} \rangle + c.c. \right) + \sum_n a_n \left| \Delta_n^{(0)} \right|^2 + \frac{b_n}{2} \left| \Delta_n^{(0)} \right|^4 + K_n \left| \mathbf{D} \Delta_n^{(0)} \right|^2, \qquad 2.4\text{-}4$$

$\mathbf{D} = \boldsymbol{\nabla} - \mathrm{i} \frac{2e}{\hbar c} \mathbf{A}^{(0)}$ the gauge-invariant derivative with the leading order contribution of the vector potential and the coefficients are related to the band n.

The leading correction to the GL functional is obtained in the form

$$f^{(1)} = \frac{\left(\mathbf{B}^{(0)} \cdot \mathbf{B}^{(1)} \right)}{4\pi} + \left(\langle \vec{\Delta}^{(0)} | L | \vec{\Delta}^{(2)} \rangle + c.c. \right) + \langle \vec{\Delta}^{(1)} | L | \vec{\Delta}^{(1)} \rangle + \sum_n \left(f_{n,1}^{(1)} + f_{n,2}^{(1)} \right), \qquad 2.4\text{-}5$$

where $f_{n,1}^{(1)}$ contains only the lowest-order contributions to the band gap and the magnetic field,

$$\begin{aligned} f_{n,1}^{(1)} = {} & \frac{a_n}{2} \left| \Delta_n^{(0)} \right|^2 + 2K_n \left| \mathbf{D} \Delta_n^{(0)} \right|^2 + \frac{b_n}{36} \frac{e^2 \hbar^2}{m^2 c^2} \vec{B}^{(0)2} \left| \Delta_n^{(0)} \right|^2 + b_n \left| \Delta_n^{(0)} \right|^4 \\ & - Q_n \left\{ \left| \mathbf{D}^2 \Delta_n^{(0)} \right|^2 + \frac{1}{3} \left(\boldsymbol{i}_n \cdot \boldsymbol{i} \times \mathbf{B}^{(0)} \right) + \frac{4e^2}{\hbar^2 c^2} \mathbf{B}^{(0)2} \left| \Delta_n^{(0)} \right|^2 \right\} \\ & - \frac{L_n}{2} \left\{ 8 \left| \Delta_n^{(0)} \right|^2 \left| \mathbf{D} \Delta_n^{(0)} \right|^2 + \left[\Delta_n^{(0)2} \left(\mathbf{D}^* \Delta_n^{(0)*} \right)^2 + c.c. \right] \right\} - \frac{c_n}{3} \left| \Delta_n^{(0)} \right|^6, \end{aligned} \qquad 2.4\text{-}6$$

while $f_{n,2}^{(1)}$ includes also the leading corrections to the band gap and the field,

$$\begin{aligned} f_{n,2}^{(1)} = {} & \left(a_n + b_n \left| \Delta_n^{(0)} \right|^2 \right) \left(\Delta_n^{(0)*} \Delta_n^{(1)} + c.c. \right) \\ & + K_n \left[\left(\mathbf{D} \Delta_n^{(0)} \cdot \mathbf{D}^* \Delta_n^{*(1)} + c.c. \right) - \mathbf{A}^{(1)} \cdot \boldsymbol{i}_n \right], \end{aligned} \qquad 2.4\text{-}7$$

$\boldsymbol{i}_n = \mathrm{i}\frac{2e}{\hbar c}\left(\Delta_n^{(0)}\mathbf{D}^*\Delta_n^{*(0)} - \Delta_n^{*(0)}\mathbf{D}\Delta_n^{(0)}\right)$ is the supercurrent density contribution of band n, and Q_n, L_n, c_n are the coefficients each band. From this functional, it is possible to derive the Gibbs free energy that is used in the criterion of the interchange between types I and II.

Now, we will check the switching between types I and II for an isotropic single-band case, the criterion for such interchange utilizes the corresponding Gibbs free energy: when it becomes smaller than that of the Meissner state at the thermodynamic critical field H_c. The respective difference between the Gibbs free energies is written as

$$G = \int g d^3\boldsymbol{x}, \qquad \mathrm{g} = f + \frac{{H_c}^2}{8\pi} - \frac{H_c\mathbf{B}}{4\pi}. \qquad 2.4\text{-}8$$

Then, the nucleation of a non-uniform condensate/field configuration can be investigated based on the criterion $G(\kappa, T) = 0$. That yields the corresponding GL critical parameter $\kappa^*(T)$, hereafter referred to as simply a critical parameter. On the (κ, T) plane κ^* separates domains with and without the flux/condensate configuration of interest, called types II and I. Using this criterion for various nonuniform configurations (e.g., for the single vortex solution, the domain wall between the normal and superconducting state, etc.), it is possible to find the corresponding value of κ above which a non-uniform pattern (representing the well-known mixed state) becomes stable. In the following results it is convenient to use the dimensionless quantities

$$\boldsymbol{x} = \lambda\bar{\boldsymbol{x}}, \qquad \psi = \psi_\infty\bar{\psi}, \qquad \mathbf{B} = \frac{H_c^{(0)}\lambda}{\kappa\sqrt{2}}\bar{\mathbf{B}}, \qquad \mathbf{A} = \frac{H_c^{(0)}\lambda}{\kappa}\bar{\mathbf{A}},$$

$$\boldsymbol{i} = \frac{H_c^{(0)}}{4\pi K\lambda}\bar{\boldsymbol{i}}, \qquad f = \frac{H_c^{(0)2}}{4\pi}\bar{f}, \qquad g = \frac{H_c^{(0)2}}{4\pi}\bar{g}, \qquad G = \frac{H_c^{(0)2}\left(\lambda\sqrt{2}\right)^3}{4\pi}\bar{G}.$$

In the following we write the dimensionless quantities without bars unless it causes any confusion. The density of the Gibbs free energy difference is given by the expansion

$$g = \tau^2\left(g^{(0)} + \tau g^{(1)} + \cdots\right), \qquad 2.4\text{-}9$$

where in the lowest order we have the GL contribution

$$g^{(0)} = \frac{1}{2}\left(\frac{\left|\mathbf{B}^{(0)}\right|}{\kappa\sqrt{2}} - 1\right)^2 + \frac{1}{2\kappa^2}|\mathbf{D}\psi|^2 - |\psi|^2 + \frac{1}{2}|\psi|^4, \qquad 2.4\text{-}10$$

while the leading correction writes

$$g^{(1)} = \left(\frac{|\mathbf{B}^{(0)}|}{\kappa\sqrt{2}} - 1\right)\left(\frac{1}{2} + \frac{ac}{3b^2}\right) - \frac{|\psi|^2}{2} + |\psi|^4 - |\psi|^2 + \frac{|\mathbf{D}\psi|^2}{\kappa^2}$$
$$+ \frac{1}{4\kappa^4}\frac{aQ}{K^2}\left\{|\mathbf{D}^2\psi|^2 + \frac{1}{3}\left(\nabla \times \mathbf{B}^{(0)}\right)^2 + \mathbf{B}^{(0)2}|\psi|^2\right\} \qquad 2.4\text{-}11$$
$$+ \frac{1}{4\kappa^2}\frac{aL}{bK}\{8|\psi|^2|\mathbf{D}\psi|^2 + [\psi^2(\mathbf{D}^*\psi^*)^2 + c.c.]\} + \frac{ac}{3b^2}|\psi|^6,$$

As we are interested in the boundaries between types I and II in the (κ, T) plane it is useful to expand G around $\kappa_0 = 1/\sqrt{2}$. So, expanding with respect to $\delta\kappa$, $\delta\kappa = \kappa - \kappa_0$, we obtain

$$G = \tau^2\left(G^{(0)} + \left.\frac{dG^{(0)}}{d\kappa}\right|_{\kappa_0}\delta\kappa + \tau G^{(1)} + \cdots\right), \qquad 2.4\text{-}12$$

The derivative $dG^{(0)}/d\kappa$ contains the direct contribution coming from the explicit appearance of κ and the indirect one related to the derivatives $d\psi/d\kappa$ and $d\mathbf{A}/d\kappa$. However, one can immediately see that the indirect contribution is equal to zero because the corresponding terms in the integrand are proportional to $\delta G^{(0)}/\delta\psi$ and $\delta G^{(0)}/\delta\vec{A}$ which are zero in the equilibrium.

The expression for $\frac{dg^{(0)}}{d\kappa}$ reads

$$\frac{dg^{(0)}}{d\kappa} = -\frac{|\mathbf{B}^{(0)}|}{\kappa^2\sqrt{2}}\left(\frac{|\mathbf{B}^{(0)}|}{\kappa\sqrt{2}} - 1\right) - \frac{1}{\kappa^3}|\mathbf{D}\psi|^2, \qquad 2.4\text{-}13$$

At $\kappa = \kappa_0$ solutions to the GL equations are obtained using the Bogomolnyi self-duality equations

$$(\partial_y + i\partial_x)\psi = (\mathbf{A}_x - i\mathbf{A}_y)\psi,$$
$$|\mathbf{B}^{(0)}| = 1 - |\psi|^2, \qquad 2.4\text{-}14$$

that are useful to simplify the integrals in G, that can be written as

$$G = \tau^2\left\{-\sqrt{2}\mathcal{I}\delta\kappa + \tau\left[\left(1 - \frac{ac}{3b^2} + 2\frac{aQ}{K^2}\right)\mathcal{I} + \left(2\frac{aL}{bK} - \frac{ac}{3b^2} - \frac{5}{3}\frac{aQ}{K^2}\right)\mathcal{J}\right] + \cdots\right\}, \qquad 2.4\text{-}15$$

With

$$\mathcal{I} = \int |\psi|^2(1 - |\psi|^2)d^3x, \qquad \mathcal{J} = \int |\psi|^4(1 - |\psi|^2)d^3x, \qquad 2.4\text{-}16$$

It is important to notice that $G^{(0)}$ is zero for any solution of the GL equations at $\kappa = \kappa_0$, manifesting the degeneracy of the Bogomolnyi point, so G comprises only two contributions, $\propto \delta\kappa$ and $\propto \tau$.

Substituting Eq. 2.4-15 into $G(\kappa, T) = 0$ one obtains the general expression for critical parameters up to the leading correction in τ,

$$\kappa^* = \kappa_0 \left\{ 1 + \tau \left[1 - \frac{ac}{3b^2} + 2\frac{aQ}{K^2} + \frac{\mathcal{J}}{\mathcal{I}} \left(2\frac{aL}{bK} - \frac{ac}{3b^2} - \frac{5}{3}\frac{aQ}{K^2} \right) \right] + \cdots \right\}, \tag{2.4-17}$$

Where the constants are not dependent on the material parameters, which points to the robustness of the approach. Thus, we can calculate the critical parameter based on the criterion of interchange, which is dependent to the ratio of $\mathcal{J}/\mathcal{I}$.

The first criterion is based on the appearance of a flat Normal-Superconductor domain wall. The corresponding solution for this criterion is $\mathcal{J}/\mathcal{I} = 0.559$. So,

$$\kappa_s^* = \kappa_0(1 - 0.027\tau), \tag{2.4-18}$$

The thermodynamic stability of an isolated Abrikosov vortex, given by the condition $H_c = H_{c1}$ yields to $\mathcal{J}/\mathcal{I} = 0.735$. Thus

$$\kappa_1^* = \kappa_0(1 + 0.093\tau), \tag{2.4-19}$$

The condition of changing the sign of the long-range vortex-vortex interaction is calculated using G for the state with two single-quantum vortices separated by distance R. In the asymptotic case $\mathcal{J}/\mathcal{I} = 2$ $(R \to \infty)$

$$\kappa_{li}^* = \kappa_0(1 + 0.95\tau), \tag{2.4-20}$$

Finally, onset of the superconductivity nucleation is defined by the condition $H_{c2} = H_c$. To solve this equation, we can use Eq. 2.2-19 and utilize the fact that in the limit $B = H_{c2}$ and the order parameter vanishes. Thus, in this limit one obtains $\mathcal{J}/\mathcal{I} \to 0$ and the corresponding critical parameter writes

$$\kappa_2^* = \kappa_0(1 - 0.407\tau), \tag{2.4-21}$$

The boundaries between types I and II is given by the upper and lower limits κ_{li}^* and κ_2^* respectively, in the limit $T \to T_c$ the difference disappears and one arrives at the standard classification: type I is below κ_0 while type II is above κ_0. Below T_c is find the intertype domain between types I and II.

As we can see in the Figure 2.4-1:

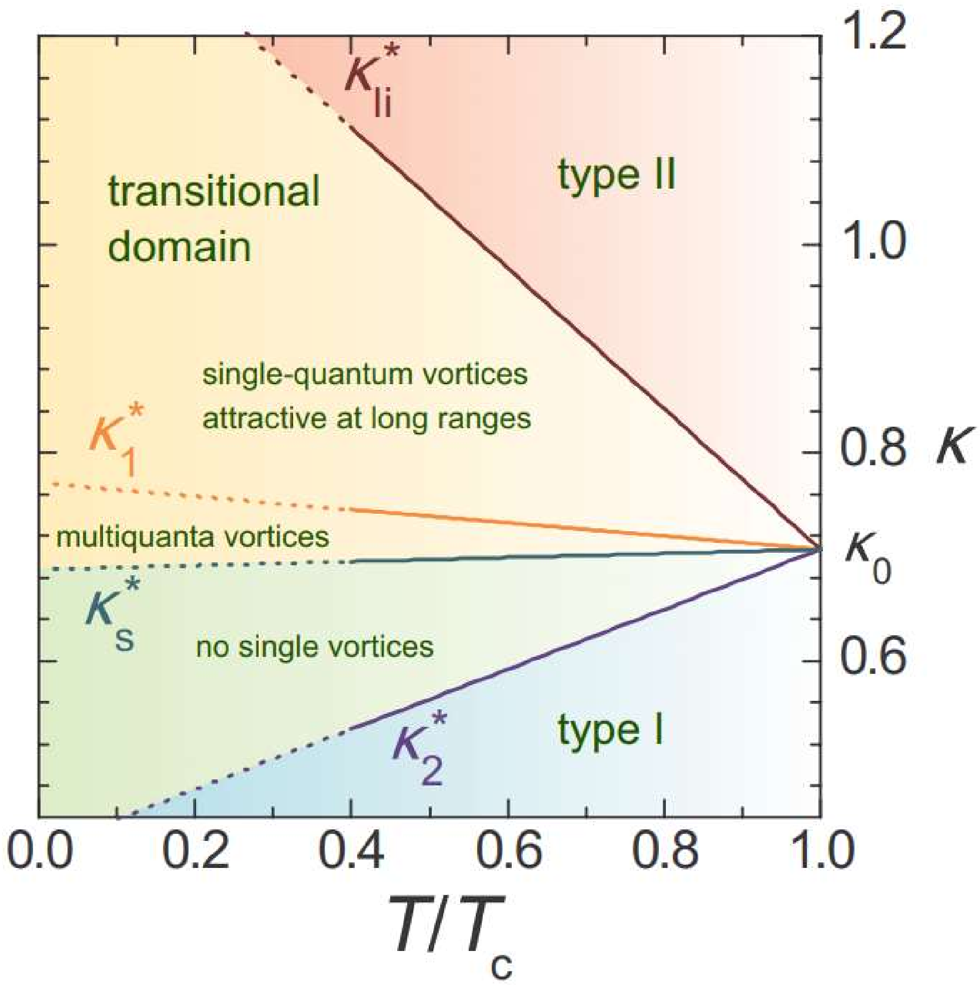

Figure 2.4-1 Internal structure of the transitional (intertype) domain $[\kappa_2^*(T), \kappa_{li}^*(T)]$ *as following from analysis of different isolated-vortex solutions. The subdivision in the three subdomains is dictated by the presence of critical parameters* $\kappa_{1,N}^*(T)$ *displaying stability of N-quantum vortices in the interval* $[\kappa_s^*(T), \kappa_1^*(T)]$*. Figure from [35]*

2.5 FLUCTUATION – DRIVEN SHIFT OF T_c

Introduced by Landau, the notion of quasiparticles has promoted great success in low temperature physics. Where, according to this hypothesis the properties of many body interacting systems at low temperatures are determined by the spectra of some low-energy, long-living excitations (quasiparticles). Phenomena which cannot be described by the quasiparticle method or by mean field approximation (MFA) are usually called fluctuations. A successful example of the use of both MFA and the quasiparticle description is, for example, the BCS theory, explained before. And due the fact that fluctuations give small corrections to the MFA results determined the success of the theory for traditional superconductors [104].

BCS Theory provides good results for the traditional superconductors, however in the vicinity of transition, fluctuations lead to small corrections in the physical characteristics in a wide range of temperatures. So, we can use the fluctuation theory to obtain the correction in the critical temperature.

2.5.1 Partition function and free energy

The complete description of thermodynamic properties can be done through the calculation of the partition function, in the vicinity of the superconducting transition, side by side with the fermionic electron excitations, fluctuation Cooper pairs of a bosonic nature appear in the system and they can be described by means of classical bosonic complex fields $\psi(\boldsymbol{r})$ which can be treated as "Cooper pair wave functions".

So, we need to find the free-energy functional with the fluctuation corrections, in D-dimensions, and j is related for each direction, we have for the anisotropic model:

$$\mathcal{F} = \int_{L^D} d^D\boldsymbol{r} \left\{ a|\psi(\boldsymbol{r})|^2 + \frac{b}{2}|\psi(\boldsymbol{r})|^4 + \sum_j K^{(j)} \left|\partial_j \psi(\boldsymbol{r})\right|^2 \right\}. \quad \textit{2.5.1-1}$$

In order to find the fluctuation contribution, we have to write the order parameter as the sum of the equilibrium, ψ_0, and fluctuation, $\eta(\boldsymbol{r})$, parts.

$$\psi(\boldsymbol{r}) = \psi_0 + \eta(\boldsymbol{r}). \quad \textit{2.5.1-2}$$

where $\psi_0 = \sqrt{-\frac{a}{b}}$.

So, the free energy can be written as

$$\mathcal{F} = \mathcal{F}_0 + \mathcal{H}. \tag{2.5.1-3}$$

Being, $\mathcal{F}_0$ the mean field contribution to the free energy, and, $\mathcal{H}$ is called the fluctuation Hamiltonian that is the fluctuation contribution to the free energy and has dependence on $\eta(\boldsymbol{r})$ and $\eta^*(\boldsymbol{r})$.

Therefore, we can calculate the partition function

$$\mathcal{Z} = \int \mathrm{D}\psi(\boldsymbol{r})\mathrm{D}\psi^*(\boldsymbol{r})\exp\left\{-\frac{\mathcal{F}}{T}\right\},$$

$$\mathcal{Z} = \exp\left\{-\frac{\mathcal{F}_0}{T}\right\}\int \mathrm{D}\eta(\boldsymbol{r})\mathrm{D}\eta^*(\boldsymbol{r})\exp\left\{-\frac{\mathcal{H}[\eta(\boldsymbol{r}),\eta^*(\boldsymbol{r})]}{T}\right\}. \tag{2.5.1-4}$$

Applying $\psi(\boldsymbol{r}) = \psi_0(\boldsymbol{r}) + \eta(\boldsymbol{r})$, into the equation of free energy Eq. 2.5.1-1, and considering only the quadratic terms ($|\eta|^2, \eta^2, \eta^{*2}$) in the fluctuation, odd terms do not contribute to Gaussian fluctuation. Then, we have:

1. $a|\psi(\boldsymbol{r})|^2 = a\big(\psi_0 + \eta(\boldsymbol{r})\big)\big(\psi_0 + \eta^*(\boldsymbol{r})\big) \rightarrow a|\psi_0|^2 + a|\eta|^2$;
2. $\frac{b}{2}|\psi(\boldsymbol{r})|^4 = \frac{b}{2}\big(\psi_0 + \eta(\boldsymbol{r})\big)^2\big(\psi_0 + \eta^*(\boldsymbol{r})\big)^2 = \frac{b}{2}(\psi_0^2 + \eta^2 + 2\psi_0\eta)(\psi_0^2 + \eta^{*2} + 2\psi_0\eta^*) \rightarrow \frac{b}{2}(\psi_0^4 + \psi_0^2\eta^2 + \psi_0^2\eta^{*2} + 4\psi_0^2|\eta|^2)$;
3. $K^{(j)}\left|\partial_j\psi(\boldsymbol{r})\right|^2 = K^{(j)}\left|\partial_j\big(\psi_0 + \eta(\boldsymbol{r})\big)\right|^2 \rightarrow K^{(j)}\left|\partial_j\eta\right|^2$.

Collecting the terms only with dependence in ψ_0, we can find

$$\mathcal{F}_0 = \int_{L^D} d^D\boldsymbol{r}\left\{a|\psi_0|^2 + \frac{b}{2}\psi_0^4\right\} = -\frac{a^2}{2b}L^D. \tag{2.5.1-5}$$

With the remaining terms we can obtain the fluctuation Hamiltonian

$$\mathcal{H} = \int_{L^D} d^D\boldsymbol{r}\left\{(a + 2b\psi_0^2)|\eta|^2 + \frac{b}{2}\psi_0^2\eta^2 + \frac{b}{2}\psi_0^2\eta^{*2} + \sum_j K^{(j)}\left|\partial_j\eta\right|^2\right\}. \tag{2.5.1-6}$$

2.5.2 Gaussian fluctuation Hamiltonian in terms of the Fourier components

The fluctuation contribution to the partition function is written as:

$$\mathcal{Z}_{Fluc} = \int \mathrm{D}\eta(\boldsymbol{r})\mathrm{D}\eta^*(\boldsymbol{r})\exp\left\{-\frac{\mathcal{H}[\eta(\boldsymbol{r}),\eta^*(\boldsymbol{r})]}{T}\right\}. \quad 2.5.2\text{-}1$$

To solve this functional integral we perform a Fourier transform from configuration space to the momentum space and separating into real and imaginary parts.

$$\eta(\boldsymbol{r}) = \frac{1}{L^{D/2}}\sum_{\mathbf{q}} e^{i\mathbf{q}\cdot\boldsymbol{r}}\eta_{\mathbf{q}}, \qquad \eta^*(\boldsymbol{r}) = \frac{1}{L^{D/2}}\sum_{\mathbf{q}} e^{-i\mathbf{q}\cdot\boldsymbol{r}}\eta^*_{\mathbf{q}}. \quad 2.5.2\text{-}2$$

Rewriting the Gaussian Hamiltonian and separating the terms

$$\begin{aligned}\mathcal{H} = (a + 2b\psi_0)\int_{L^D} d^D\boldsymbol{r}|\eta(\boldsymbol{r})|^2 + \frac{b}{2}\psi_0^2\int_{L^D} d^D\boldsymbol{r}[\eta^2(\boldsymbol{r})] \\ + \frac{b}{2}\psi_0^2\int_{L^D} d^D\boldsymbol{r}[\eta^{*2}(\boldsymbol{r})] + \sum_j K^{(j)}\int_{L^D} d^D\boldsymbol{r}\left|\partial_j\eta\right|^2.\end{aligned} \quad 2.5.2\text{-}3$$

So, performing the transformation for each integral

1. $\int_{L^D} d^D\boldsymbol{r}|\eta(\boldsymbol{r})|^2 = \int_{L^D} d^D\boldsymbol{r}\frac{1}{L^D}\sum_{\mathbf{q},\mathbf{q}'} e^{i(\mathbf{q}-\mathbf{q}')\cdot\boldsymbol{r}}\eta_{\mathbf{q}}\eta^*_{\mathbf{q}'} = \sum_{\mathbf{q},\mathbf{q}'}\eta_{\mathbf{q}}\eta^*_{\mathbf{q}'}\delta_{\mathbf{q},\mathbf{q}'} = \sum_{\mathbf{q}}\left|\eta_{\mathbf{q}}\right|^2;$
2. $\int_{L^D} d^D\boldsymbol{r}[\eta^2(\boldsymbol{r})] = \int_{L^D} d^D\boldsymbol{r}\frac{1}{L^D}\sum_{\mathbf{q},\mathbf{q}'} e^{i(\mathbf{q}+\mathbf{q}')\cdot\boldsymbol{r}}\eta_{\mathbf{q}}\eta_{\mathbf{q}'} = \sum_{\mathbf{q},\mathbf{q}'}\eta_{\mathbf{q}}\eta_{\mathbf{q}'}\delta_{\mathbf{q},-\mathbf{q}'} = \sum_{\mathbf{q}}\eta_{\mathbf{q}}\eta_{-\mathbf{q}},$

as all coefficients are symmetric under $\mathbf{q} \to -\mathbf{q}$, we assume $\eta_{\mathbf{q}} = \eta_{-\mathbf{q}}$;

3. $\int_{L^D} d^D\boldsymbol{r}[\eta^{*2}(\boldsymbol{r})] = \int_{L^D} d^D\boldsymbol{r}\frac{1}{L^D}\sum_{\mathbf{q},\mathbf{q}'} e^{-i(\mathbf{q}+\mathbf{q}')\cdot\boldsymbol{r}}\eta^*_{\mathbf{q}}\eta^*_{\mathbf{q}'} = \sum_{\mathbf{q}}\eta^*_{\mathbf{q}}\eta^*_{-\mathbf{q}};$
4. $\int_{L^D} d^D\boldsymbol{r}\left|\partial_j\eta(\boldsymbol{r})\right|^2 = \int_{L^D} d^D\boldsymbol{r}\frac{1}{L^D}\sum_{\mathbf{q},\mathbf{q}'}\partial_j\left(e^{i\mathbf{q}\cdot\boldsymbol{r}}\eta_{\mathbf{q}}\right)\cdot\partial_j\left(e^{-i\mathbf{q}\cdot\boldsymbol{r}}\eta^*_{\mathbf{q}}\right) =$
   $\int_{L^D} d^D\boldsymbol{r}\frac{1}{L^D}\sum_{\mathbf{q},\mathbf{q}'}\left[\left(i\mathrm{q}_j e^{i\mathbf{q}\cdot\boldsymbol{r}}\right)\cdot\left(-i\mathrm{q}'_j e^{-i\mathbf{q}'\cdot\boldsymbol{r}}\eta^*_{\mathbf{q}'}\right)\right] = \sum_{\mathbf{q}}\mathrm{q}_j^2\left|\eta_{\mathbf{q}}\right|^2.$

Collecting all these terms, we obtain

$$\mathcal{H} = \sum_{\mathbf{q}}\left[\left(a + 2b\psi_0^2 + \sum_j K^{(j)}\mathrm{q}_j^2\right)\left|\eta_{\mathbf{q}}\right|^2 + \frac{b}{2}\psi_0^2\left(\eta_{\mathbf{q}}\eta_{-\mathbf{q}} + \eta^*_{\mathbf{q}}\eta^*_{-\mathbf{q}}\right)\right]. \quad 2.5.2\text{-}4$$

The real and imaginary parts of the fluctuation field can be separated in the following form

$$\eta_{\mathbf{q}} = x_{\mathbf{q}} + iy_{\mathbf{q}}, \quad 2.5.2\text{-}5$$

where, $x_{\mathbf{q}} = \mathrm{Re}\{\eta_{\mathbf{q}}\}$, and $y_{\mathbf{q}} = \mathrm{Im}\{\eta_{\mathbf{q}}\}$.

And, the following term

$$\eta_{\mathbf{q}}\eta_{-\mathbf{q}} + \eta^*_{\mathbf{q}}\eta^*_{-\mathbf{q}} = (x_{\mathbf{q}} + iy_{\mathbf{q}})(x_{-\mathbf{q}} + iy_{-\mathbf{q}}) + (x_{\mathbf{q}} - iy_{\mathbf{q}})(x_{-\mathbf{q}} - iy_{-\mathbf{q}}) = 2x_{\mathbf{q}}x_{-\mathbf{q}} - 2y_{\mathbf{q}}y_{-\mathbf{q}}.$$

So, our Gaussian Hamiltonian becomes

$$\mathcal{H} = \sum_{\mathbf{q}} \left[\left(a + 2b\psi_0^2 + \sum_j K^{(j)}\, \mathrm{q}_j^2 \right)(x_{\mathbf{q}}^2 + y_{\mathbf{q}}^2) + b\psi_0^2 (x_{\mathbf{q}}x_{-\mathbf{q}} - y_{\mathbf{q}}y_{-\mathbf{q}}) \right],$$

That can be written as

$$\mathcal{H} = \sum_{\mathbf{q}} [A_{\mathbf{q}}(x_{\mathbf{q}}^2 + y_{\mathbf{q}}^2) + B(x_{\mathbf{q}}x_{-\mathbf{q}} - y_{\mathbf{q}}y_{-\mathbf{q}})], \qquad 2.5.2\text{-}6$$

with $A_{\mathbf{q}} = a + 2b\psi_0^2 + \sum_j K^{(j)}\, \mathrm{q}_j^2$ and $B = b\psi_0^2$.

2.5.3 Fluctuation part of free energy

Now, we have everything to our disposal to calculate the fluctuation part of free energy. First, we need to rearrange the fluctuation Hamiltonian and express it in a matrix form.

Taking into account that we have a summation over all momenta **q**, we can change its sign to express it in a more convenient form, in function of matrices.

$$\mathcal{H} = \sum_{\mathbf{q}} (A_{\mathbf{q}}x_{\mathbf{q}}^2 + Bx_{\mathbf{q}}x_{-\mathbf{q}} + A_{\mathbf{q}}y_{\mathbf{q}}^2 - By_{\mathbf{q}}y_{-\mathbf{q}}),$$

$$\mathcal{H} = \frac{1}{2}\sum_{\mathbf{q}} [(A_{\mathbf{q}}x_{\mathbf{q}}^2 + Bx_{\mathbf{q}}x_{-\mathbf{q}} + +Bx_{-\mathbf{q}}x_{\mathbf{q}} + A_{\mathbf{q}}x_{-\mathbf{q}}^2) + (A_{\mathbf{q}}y_{\mathbf{q}}^2 - By_{\mathbf{q}}y_{-\mathbf{q}} - By_{-\mathbf{q}}y_{\mathbf{q}} + A_{\mathbf{q}}y_{-\mathbf{q}}^2)].$$

$$\mathcal{H} = \frac{1}{2}\sum_{\mathbf{q}} \left[(x_{\mathbf{q}} \quad x_{-\mathbf{q}}) \begin{pmatrix} A_{\mathbf{q}} & B \\ B & A_{\mathbf{q}} \end{pmatrix} \begin{pmatrix} x_{\mathbf{q}} \\ x_{-\mathbf{q}} \end{pmatrix} + (y_{\mathbf{q}} \quad y_{-\mathbf{q}}) \begin{pmatrix} A_{\mathbf{q}} & -B \\ -B & A_{\mathbf{q}} \end{pmatrix} \begin{pmatrix} y_{\mathbf{q}} \\ y_{-\mathbf{q}} \end{pmatrix} \right],$$

$$\mathcal{H} = \sum_{\mathbf{q}, q_x \geq 0} \left[(x_{\mathbf{q}} \quad x_{-\mathbf{q}}) \begin{pmatrix} A_{\mathbf{q}} & B \\ B & A_{\mathbf{q}} \end{pmatrix} \begin{pmatrix} x_{\mathbf{q}} \\ x_{-\mathbf{q}} \end{pmatrix} + (y_{\mathbf{q}} \quad y_{-\mathbf{q}}) \begin{pmatrix} A_{\mathbf{q}} & -B \\ -B & A_{\mathbf{q}} \end{pmatrix} \begin{pmatrix} y_{\mathbf{q}} \\ y_{-\mathbf{q}} \end{pmatrix} \right], \qquad 2.5.3\text{-}1$$

where $q_x \geq 0$ assures that for each pair **q** and $-\mathbf{q}$ only one vector of the wavenumber is present in the sum.

In order to proceed, we need to get the diagonal representation for both x- and y-contributions, so we need to find the eigenvalues and eigenstates of the matrices

$$(x_{\mathbf{q}} \quad x_{-\mathbf{q}})\begin{pmatrix} A_{\mathbf{q}} & B \\ B & A_{\mathbf{q}} \end{pmatrix}\begin{pmatrix} x_{\mathbf{q}} \\ x_{-\mathbf{q}} \end{pmatrix} = (\alpha_{\mathbf{q}} \quad \beta_{\mathbf{q}})\begin{pmatrix} E_{\mathbf{q},+}^{(x)} & 0 \\ 0 & E_{\mathbf{q},-}^{(x)} \end{pmatrix}\begin{pmatrix} \alpha_{\mathbf{q}} \\ \beta_{\mathbf{q}} \end{pmatrix}, \qquad 2.5.3\text{-}2$$

And

$$(y_{\mathbf{q}} \quad y_{-\mathbf{q}})\begin{pmatrix} A_{\mathbf{q}} & -B \\ -B & A_{\mathbf{q}} \end{pmatrix}\begin{pmatrix} y_{\mathbf{q}} \\ y_{-\mathbf{q}} \end{pmatrix} = (\xi_{\mathbf{q}} \quad \zeta_{\mathbf{q}})\begin{pmatrix} E_{\mathbf{q},+}^{(y)} & 0 \\ 0 & E_{\mathbf{q},-}^{(y)} \end{pmatrix}\begin{pmatrix} \xi_{\mathbf{q}} \\ \zeta_{\mathbf{q}} \end{pmatrix}. \qquad 2.5.3\text{-}3$$

The unitary matrix $\mathcal{U}_x$ is made of eigenvectors of $\begin{pmatrix} A_q & B \\ B & A_q \end{pmatrix}$, then

$$\mathcal{U}_x^{\dagger}\begin{pmatrix} A_{\mathbf{q}} & B \\ B & A_{\mathbf{q}} \end{pmatrix}\mathcal{U}_x = \begin{pmatrix} E_{\mathbf{q},+}^{(x)} & 0 \\ 0 & E_{\mathbf{q},-}^{(x)} \end{pmatrix},$$

and we can write

$$(x_{\mathbf{q}} \quad x_{-\mathbf{q}})\,\mathcal{U}_x\mathcal{U}_x^{\dagger}\begin{pmatrix} A_{\mathbf{q}} & B \\ B & A_{\mathbf{q}} \end{pmatrix}\mathcal{U}_x\mathcal{U}_x^{\dagger}\begin{pmatrix} x_{\mathbf{q}} \\ x_{-\mathbf{q}} \end{pmatrix} = (\alpha_{\mathbf{q}} \quad \beta_{\mathbf{q}})\begin{pmatrix} E_{\mathbf{q},+}^{(x)} & 0 \\ 0 & E_{\mathbf{q},-}^{(x)} \end{pmatrix}\begin{pmatrix} \alpha_{\mathbf{q}} \\ \beta_{\mathbf{q}} \end{pmatrix}, \qquad 2.5.3\text{-}4$$

where $(x_{\mathbf{q}} \quad x_{-\mathbf{q}})\,\mathcal{U}_x = (\alpha_{\mathbf{q}} \quad \beta_{\mathbf{q}})$ and $\mathcal{U}_x^{\dagger}\begin{pmatrix} x_{\mathbf{q}} \\ x_{-\mathbf{q}} \end{pmatrix} = \begin{pmatrix} \alpha_{\mathbf{q}} \\ \beta_{\mathbf{q}} \end{pmatrix}$.

Similarly, the unitary matrix $\mathcal{U}_y$ is made of eigenvectors of $\begin{pmatrix} A_{\mathbf{q}} & -B \\ -B & A_{\mathbf{q}} \end{pmatrix}$, then

$$\mathcal{U}_y^{\dagger}\begin{pmatrix} A_{\mathbf{q}} & -B \\ -B & A_{\mathbf{q}} \end{pmatrix}\mathcal{U}_y = \begin{pmatrix} E_{\mathbf{q},+}^{(y)} & 0 \\ 0 & E_{\mathbf{q},-}^{(y)} \end{pmatrix},$$

$$(y_{\mathbf{q}} \quad y_{-\mathbf{q}})\,\mathcal{U}_y\mathcal{U}_y^{\dagger}\begin{pmatrix} A_{\mathbf{q}} & -B \\ -B & A_{\mathbf{q}} \end{pmatrix}\mathcal{U}_y\mathcal{U}_y^{\dagger}\begin{pmatrix} y_{\mathbf{q}} \\ y_{-\mathbf{q}} \end{pmatrix} = (\xi_{\mathbf{q}} \quad \zeta_{\mathbf{q}})\begin{pmatrix} E_{\mathbf{q},+}^{(y)} & 0 \\ 0 & E_{\mathbf{q},-}^{(y)} \end{pmatrix}\begin{pmatrix} \xi_{\mathbf{q}} \\ \zeta_{\mathbf{q}} \end{pmatrix}, \qquad 2.5.3\text{-}5$$

where $(y_{\mathbf{q}} \quad y_{-\mathbf{q}})\,\mathcal{U}_y = (\xi_{\mathbf{q}} \quad \zeta_{\mathbf{q}})$ and $\mathcal{U}_y^{\dagger}\begin{pmatrix} y_{\mathbf{q}} \\ y_{-\mathbf{q}} \end{pmatrix} = \begin{pmatrix} \xi_{\mathbf{q}} \\ \zeta_{\mathbf{q}} \end{pmatrix}$.

Our next step is explicitly the unitary transformations to find $\mathcal{U}_x$ and $\mathcal{U}_y$. The eigenvalue equation associated with $\mathcal{U}_x$

$$\begin{pmatrix} A_{\mathbf{q}} & B \\ B & A_{\mathbf{q}} \end{pmatrix}\begin{pmatrix} u_{\pm}^{(x)} \\ v_{\pm}^{(x)} \end{pmatrix} = E_{\mathbf{q},\pm}^{(x)}\begin{pmatrix} u_{\pm}^{(x)} \\ v_{\pm}^{(x)} \end{pmatrix}, \qquad 2.5.3\text{-}6$$

a non-trivial solution to these equations exists when

$$\det\begin{pmatrix} A_{\mathbf{q}} - E^{(x)}_{\mathbf{q},\pm} & B \\ B & A_{\mathbf{q}} - E^{(x)}_{\mathbf{q},\pm} \end{pmatrix} = 0,$$

$$E^{(x)}_{\mathbf{q},\pm} = A_{\mathbf{q}} \pm B.$$

For $E^{(x)}_{\mathbf{q},+}$ we obtain

$$\begin{pmatrix} A_{\mathbf{q}} & B \\ B & A_{\mathbf{q}} \end{pmatrix}\begin{pmatrix} u^{(x)}_{+} \\ v^{(x)}_{+} \end{pmatrix} = \left(A_{\mathbf{q}} + B\right)\begin{pmatrix} u^{(x)}_{+} \\ v^{(x)}_{+} \end{pmatrix},$$

So, the components of the eigenvector are

$$u^{(x)}_{+} = \frac{1}{\sqrt{2}}, \qquad v^{(x)}_{+} = \frac{1}{\sqrt{2}},$$

where we used the normalization condition $u^{(x)2}_{+} + v^{(x)2}_{+} = 1$.

We can do the same for $E^{(x)}_{\mathbf{q},-}$, and we get

$$u^{(x)}_{-} = \frac{1}{\sqrt{2}}, \qquad v^{(x)}_{-} = -\frac{1}{\sqrt{2}},$$

Hence,

$$\mathcal{U}_x = \frac{1}{\sqrt{2}}\begin{pmatrix} 1 & 1 \\ 1 & -1 \end{pmatrix},$$

$$\begin{pmatrix} x_{\mathbf{q}} \\ x_{-\mathbf{q}} \end{pmatrix} = \frac{1}{\sqrt{2}}\begin{pmatrix} 1 & 1 \\ 1 & -1 \end{pmatrix}\begin{pmatrix} \alpha_{\mathbf{q}} \\ \beta_{\mathbf{q}} \end{pmatrix}, \qquad \begin{pmatrix} \alpha_{\mathbf{q}} \\ \beta_{\mathbf{q}} \end{pmatrix} = \frac{1}{\sqrt{2}}\begin{pmatrix} 1 & 1 \\ 1 & -1 \end{pmatrix}\begin{pmatrix} x_{\mathbf{q}} \\ x_{-\mathbf{q}} \end{pmatrix}, \qquad \text{2.5.3-7}$$

and

$$\int dx_{\mathbf{q}} dx_{-\mathbf{q}} = \int d\alpha_{\mathbf{q}} d\beta_{\mathbf{q}}.$$

In addition, for the y-contribution, the eigenvalue equation associated with $\mathcal{U}_y$.

$$\begin{pmatrix} A_{\mathbf{q}} & -B \\ -B & A_{\mathbf{q}} \end{pmatrix}\begin{pmatrix} u^{(y)}_{\pm} \\ v^{(y)}_{\pm} \end{pmatrix} = E^{(y)}_{\mathbf{q},\pm}\begin{pmatrix} u^{(y)}_{\pm} \\ v^{(y)}_{\pm} \end{pmatrix}, \qquad \text{2.5.3-8}$$

The correspondent non-trivial solution to these equations exists when

$$\det\begin{pmatrix} A_{\mathbf{q}} - E^{(y)}_{\mathbf{q},\pm} & -B \\ -B & A_{\mathbf{q}} - E^{(y)}_{\mathbf{q},\pm} \end{pmatrix} = 0,$$

and then

$$E^{(y)}_{\mathbf{q},\pm} = A_{\mathbf{q}} \pm B,$$

$$u^{(y)}_{+} = -v^{(y)}_{+} = \frac{1}{\sqrt{2}}, \qquad u^{(y)}_{-} = v^{(y)}_{-} = \frac{1}{\sqrt{2}},$$

Hence,

$$\mathcal{U}_y = \frac{1}{\sqrt{2}}\begin{pmatrix} 1 & 1 \\ -1 & 1 \end{pmatrix},$$

$$\begin{pmatrix} y_{\mathbf{q}} \\ y_{-\mathbf{q}} \end{pmatrix} = \frac{1}{\sqrt{2}}\begin{pmatrix} 1 & 1 \\ -1 & 1 \end{pmatrix}\begin{pmatrix} \xi_{\mathbf{q}} \\ \zeta_{\mathbf{q}} \end{pmatrix}, \qquad \begin{pmatrix} \xi_{\mathbf{q}} \\ \zeta_{\mathbf{q}} \end{pmatrix} = \frac{1}{\sqrt{2}}\begin{pmatrix} 1 & -1 \\ 1 & 1 \end{pmatrix}\begin{pmatrix} y_{\mathbf{q}} \\ y_{-\mathbf{q}} \end{pmatrix}, \qquad 2.5.3\text{-}9$$

and

$$\int dy_{\mathbf{q}} dy_{-\mathbf{q}} = \int d\xi_{\mathbf{q}} d\zeta_{\mathbf{q}}.$$

Using the new variables $\alpha_{\mathbf{q}}, \beta_{\mathbf{q}}, \xi_{\mathbf{q}}, \zeta_{\mathbf{q}}$ one can rewrite the fluctuation Hamiltonian as

$$\mathcal{H} = \sum_{\mathbf{q},q_x \geq 0}\left[\begin{pmatrix} \alpha_{\mathbf{q}} & \beta_{\mathbf{q}} \end{pmatrix}\begin{pmatrix} A_{\mathbf{q}} + B & 0 \\ 0 & A_{\mathbf{q}} - B \end{pmatrix}\begin{pmatrix} \alpha_{\mathbf{q}} \\ \beta_{\mathbf{q}} \end{pmatrix} + \begin{pmatrix} \xi_{\mathbf{q}} & \zeta_{\mathbf{q}} \end{pmatrix}\begin{pmatrix} A_{\mathbf{q}} + B & 0 \\ 0 & A_{\mathbf{q}} - B \end{pmatrix}\begin{pmatrix} \xi_{\mathbf{q}} \\ \zeta_{\mathbf{q}} \end{pmatrix}\right], \qquad 2.5.3\text{-}10$$

and the fluctuation contribution for the partition function becomes

$$\mathcal{Z}_{Fluc} = \int \prod_{\mathbf{q},q_x \geq 0} \left(d\alpha_{\mathbf{q}} d\beta_{\mathbf{q}}\, d\xi_{\mathbf{q}} d\zeta_{\mathbf{q}}\right) \exp\left\{-\frac{\mathcal{H}[\alpha_{\mathbf{q}}, \beta_{\mathbf{q}}, \xi_{\mathbf{q}}, \zeta_{\mathbf{q}}]}{T}\right\}. \qquad 2.5.3\text{-}11$$

So, the fluctuation contribution for free energy is given by

$$\mathcal{F}_{Fluc} = -T \ln \mathcal{Z}_{Fluc}, \qquad 2.5.3\text{-}12$$

writing explicitly, we get

$$\mathcal{F}_{Fluc}$$

$$= -T\ln\int\prod_{\mathbf{q},q_x\geq 0}\left(d\alpha_{\mathbf{q}}d\beta_{\mathbf{q}}\,d\xi_{\mathbf{q}}d\zeta_{\mathbf{q}}\right)\exp\left\{-\frac{1}{T}\sum_{\mathbf{q},q_x\geq 0}\left[(\alpha_{\mathbf{q}}\quad\beta_{\mathbf{q}})\begin{pmatrix}A_{\mathbf{q}}+B & 0\\ 0 & A_{\mathbf{q}}-B\end{pmatrix}\begin{pmatrix}\alpha_{\mathbf{q}}\\ \beta_{\mathbf{q}}\end{pmatrix}\right.\right.$$

$$\left.\left.+\,(\xi_{\mathbf{q}}\quad\zeta_{\mathbf{q}})\begin{pmatrix}A_{\mathbf{q}}+B & 0\\ 0 & A_{\mathbf{q}}-B\end{pmatrix}\begin{pmatrix}\xi_{\mathbf{q}}\\ \zeta_{\mathbf{q}}\end{pmatrix}\right]\right\},$$

$$= -T\ln\int\prod_{\mathbf{q},q_x\geq 0}\left(d\alpha_{\mathbf{q}}d\beta_{\mathbf{q}}\,d\xi_{\mathbf{q}}d\zeta_{\mathbf{q}}\right)\exp\left\{-\frac{1}{T}\sum_{\mathbf{q},q_x\geq 0}\left[\left(A_{\mathbf{q}}+B\right)\alpha_{\mathbf{q}}^2+\left(A_{\mathbf{q}}-B\right)\beta_{\mathbf{q}}^2\right.\right.$$

$$\left.\left.+\left(A_{\mathbf{q}}+B\right)\xi_{\mathbf{q}}^2+\left(A_{\mathbf{q}}-B\right)\zeta_{\mathbf{q}}^2\right]\right\}.$$

That is a Gaussian integral with the following solution

$$\mathcal{F}_{Fluc} = -T\ln\left(\prod_{\mathbf{q},q_x\geq 0}\sqrt{\frac{\pi T}{A_{\mathbf{q}}+B}}\sqrt{\frac{\pi T}{A_{\mathbf{q}}-B}}\sqrt{\frac{\pi T}{A_{\mathbf{q}}+B}}\sqrt{\frac{\pi T}{A_{\mathbf{q}}-B}}\right)$$

$$\mathcal{F}_{Fluc} = -T\sum_{\mathbf{q},q_x\geq 0}\left(\ln\frac{\pi T}{A_{\mathbf{q}}+B}+\ln\frac{\pi T}{A_q-B}\right).$$

And finally, we arrive at the expression given in the book by Larkin and Varlamov[104]:

$$\mathcal{F}_{Fluc} = -\frac{T}{2}\sum_{\mathbf{q}}\left(\ln\frac{\pi T}{A_{\mathbf{q}}+B}+\ln\frac{\pi T}{A_q-B}\right), \qquad 2.5.3\text{-}13$$

$$A_{\mathbf{q}}+B = a+3b\psi_0^2+\sum_j K^{(j)}\,\mathrm{q}_j^2, \qquad A_{\mathbf{q}}-B = a+b\psi_0^2+\sum_j K^{(j)}\,\mathrm{q}_j^2.$$

Some remarks due the eq. 2.5.3-13, this expression holds both for $T > T_{c0}$ and $T \leq T_{c0}$, and for $T \leq T_{c0}$ the second term in this equation is divergent at $\mathbf{q} \to 0$, i.e., the Goldstone mode appears in the system, this term is related to the phase fluctuations. We can also notice that $\frac{\pi T}{A_{\mathbf{q}}+B}$ and $\frac{\pi T}{A_{\mathbf{q}}-B}$ are not dimensionless because in the introduction of $d\left(\mathrm{Re}\eta_{\mathbf{q}}\right)$, and $d\left(\mathrm{Im}\eta_{\mathbf{q}}\right)$, we introduce a dimension quantity under ln. We can also notice that if we can multiply $d\left(\mathrm{Re}\eta_{\mathbf{q}}\right)$ and $d\left(\mathrm{Im}\eta_{\mathbf{q}}\right)$ by arbitrary factor it will not contribute to the fluctuation heat capacity and the Ginzburg number.

2.5.4 Ginzburg number, Ginzburg-Levanyuk parameter, and the fluctuation heat capacity

From the fluctuation free energy now, it is possible to calculate the fluctuation for the heat capacity. This fluctuation contribution is divergent at T_{co}, mean field critical temperature, while the mean field contribution is regular. The temperature $T^* < T_{co}$, at the heat capacity is equal to the mean field contribution, is called the Ginzburg-Levanyuk Temperature. The Ginzburg Number is defined as

$$Gi = 1 - \frac{T^*}{T_{co}}, \qquad \textit{2.5.4-1}$$

it measures the temperature interval below T_{co}, where the fluctuations are important.

The procedure to calculate Gi employs only the contribution from the temperature dependence of $A_{\mathbf{q}} = a + 2b\psi_0^2 + K\mathbf{q}^2$. The fluctuation contribution of free energy $A_{\mathbf{q}}$ appears in two terms $\frac{\pi T}{A_{\mathbf{q}}+B}$ and $\frac{\pi T}{A_{\mathbf{q}}-B}$.

The first one at $T < T_{co}$, we have

$$\frac{\pi T}{2|a| + \sum_j K^{(j)}\,\mathrm{q}_j^2},$$

and the second one

$$\frac{\pi T}{\sum_j K^{(j)}\,\mathrm{q}_j^2},$$

this term is not dependent on the parameter a. We should keep in mind the infrared and ultraviolet cut-offs here (temperature independent).

Thus, the divergent (critical) part of the fluctuation heat capacity is related to

$$\mathcal{F}_{Fluc}^{(crit)} = -\frac{T_{c0}}{2}\sum_{\mathbf{q}} \ln \frac{\pi T_{c0}}{2|a| + \sum_j K^{(j)}\,\mathrm{q}_j^2}. \qquad \textit{2.5.4-2}$$

So, in order to calculate the heat capacity, we need to calculate the entropy first

$$S_{Fluc}^{(crit)} = -\frac{\partial \mathcal{F}_{Fluc}^{(crit)}}{\partial T},$$

$$S_{Fluc}^{(crit)} = \frac{T_{c0}}{2}\sum_{\mathbf{q}}\frac{\partial}{\partial T}\left[-\left(\ln 2|a| + \sum_{j} K^{(j)}\,\mathrm{q}_j^2\right)\right],$$

$$S_{Fluc}^{(crit)} = -\frac{T_{c0}}{2}\sum_{\mathbf{q}}\frac{1}{2|a| + \sum_j K^{(j)}\,\mathrm{q}_j^2}2\frac{\partial|a|}{\partial T},$$

$$S_{Fluc}^{(crit)} = T_{c0}\alpha\sum_{\mathbf{q}}\frac{1}{2|a| + \sum_j K^{(j)}\,\mathrm{q}_j^2}, \qquad 2.5.4\text{-}3$$

where $|a| = \alpha(T_{c0} - T)$.

Then we have everything to calculate the fluctuation contribution to the heat capacity, from statistical mechanics we obtain that

$$C_{v,Fluc}^{(crit)} = k_B T_{c0}\frac{\partial S_{Fluc}^{(crit)}}{\partial T},$$

$$C_{v,Fluc}^{(crit)} = k_B T_{c0}^2 2\alpha^2\sum_{\mathbf{q}}\frac{1}{\left(2|a| + \sum_j K^{(j)}\,\mathrm{q}_j^2\right)^2},$$

$$C_{v,Fluc}^{(crit)} = 2k_B T_{c0}^2\alpha^2\sum_{\mathbf{q}}\frac{1}{\left(2|a| + \sum_j K^{(j)}\,\mathrm{q}_j^2\right)^2}. \qquad 2.5.4\text{-}4$$

It is important to note that integral (sum) in $C_{v,Fluc}^{(crit)}$ is not divergent for $T < T_{c0}$ without any cut-offs, so the cut-offs do not contribute at this stage and can be ignored.

It is instructive to consider the formula for $C_{v,Fluc}^{(crit)}$ in the particular isotropic case with $K^{(j)} = K$. So, it is convenient to write the Eq. 2.5.4-4 in function of the coherence lengths, and we have $\xi = \sqrt{\frac{K}{|a|}}$, the Ginzburg-Landau coherence length that $\xi \rightarrow \infty(T \rightarrow T_{co})$, and the zero temperature coherence length $\xi_0 = \sqrt{\frac{K}{\alpha T_{co}}}$, that ξ_0 is finite at $T \rightarrow T_{co}$. Where $\xi_0 \sim \xi_{BCS}$, ξ_{BCS} is the BCS coherence length or the cooper-pair size for the isotropic case.

Then, one finds

$$C_{v,Fluc}^{(crit)} = \frac{2k_B T_{c0}^2\alpha^2}{4K^2}\sum_{\mathbf{q}}\frac{1}{\left(\frac{|a|}{K} + \frac{\mathbf{q}^2}{2}\right)^2},$$

$$C_{v,Fluc}^{(crit)} = \frac{k_B}{2\xi_0^4}\sum_{\mathbf{q}}\frac{1}{\left(\xi^{-2}+\frac{\mathbf{q}^2}{2}\right)^2}. \qquad 2.5.4\text{-}5$$

And as $\xi^{-2} \to 0$ we have $C_{v,Fluc}^{(crit)} \to \infty (T \to T_{co})$. So, the critical behavior is due to the divergence related to ξ, or due to the fact that $|a| \to 0$ for $T \to T_{co}$. This is why the dependence of $|a|$ on the temperature is decisive in the fluctuation in the free energy.

Further, we perform the calculations for the general case of an anisotropic system, from the discrete to continuous variables by standard procedure

$$\sum_{\mathbf{q}} \to L^D \int \frac{d^D\mathbf{q}}{(2\pi)^D},$$

So, Eq.2.5.4-4 becomes

$$C_{v,Fluc}^{(crit)} = 2k_B T_{c0}^2 \alpha^2 L^D \int \frac{d^D\mathbf{q}}{(2\pi)^D}\frac{1}{\left(2|a| + \sum_j K^{(j)}\,\mathrm{q}_j^2\right)^2},$$

Changing the variables $\mathrm{q}_j\sqrt{K^{(j)}} \to \mathrm{p}_j$

$$C_{v,Fluc}^{(crit)} = 2k_B T_{c0}^2 \alpha^2 \frac{L^D}{\prod_{j=1}^D K^{(j)}} \int \frac{d^D\mathbf{p}}{(2\pi)^D}\frac{1}{(2|a| + \mathbf{p}^2)^2},$$

and, making a new changing of variables $\frac{\mathbf{p}}{\sqrt{|a|}} \to \mathbf{m}$ that means $d^D\mathbf{p} = \left(\sqrt{|a|}\right)^D d^D\mathbf{m}$

$$C_{v,Fluc}^{(crit)} = 2k_B T_{c0}^2 \alpha^2 \frac{L^D |a|^{D/2}}{\prod_{j=1}^D K^{(j)}\,|a|^2} \int \frac{d^D\mathbf{m}}{(2\pi)^D}\frac{1}{(2 + \mathbf{m}^2)^2},$$

as we know $|a| = \alpha T_{c0}\tau$, where $\tau = 1 - T/T_{c0}$, then we can write

$$C_{v,Fluc}^{(crit)} = \frac{L^D}{\tau^{2-D/2}} 2k_B \frac{T_{c0}^{D/2}\alpha^{D/2}}{\prod_{j=1}^D K^{(j)}} \int \frac{d^D\mathbf{m}}{(2\pi)^D}\frac{1}{(2 + \mathbf{m}^2)^2},$$

as we have $\frac{\alpha^{D/2} T_{c0}^{D/2}}{\prod_{j=1}^D K^{(j)}} = \frac{1}{\prod_{j=1}^D \xi_0^{(j)}}$, $\xi_0^{(j)} = \sqrt{\frac{K^{(j)}}{\alpha T_{co}}}$ where $\xi_0^{(j)}$ is the direction-dependent zero temperature coherence length.

Thus, finally we can obtain the critical fluctuation to the heat capacity as

$$c_{v,Fluc}^{(crit)} = \frac{2k_B L^D}{\tau^{2-D/2}} \frac{1}{\prod_{j=1}^D \xi_0^{(j)}} \int \frac{d^D\mathbf{m}}{(2\pi)^D}\frac{1}{(2 + \mathbf{m}^2)^2}. \qquad 2.5.4\text{-}6$$

With this result one can see that

$$C_{v,Fluc}^{(crit)} \propto \begin{cases} D=3 \rightarrow \dfrac{1}{\tau^{1/2}} \dfrac{1}{\xi_0^{(1)}} \dfrac{1}{\xi_0^{(2)}} \dfrac{1}{\xi_0^{(3)}}\ ; \\ D=2 \rightarrow \dfrac{1}{\tau} \dfrac{1}{\xi_0^{(1)}} \dfrac{1}{\xi_0^{(2)}}\ ; \\ D=1 \rightarrow \dfrac{1}{\tau^{3/2}} \dfrac{1}{\xi_0^{(1)}}. \end{cases} \quad 2.5.4\text{-}7$$

We can see that the divergence of heat capacity is more pronounced in lower dimensions. This divergence is connected with the Goldstone mode and sensitive to the presence of strong phase fluctuations, which are beyond the Gaussian picture of the present analysis.

The results of integral of the Eq. 2.5.4-6 are given by

$$\int \frac{d^D \mathbf{m}}{(2\pi)^D} \frac{1}{(2+\mathbf{m}^2)^2} = \begin{cases} D=3 \rightarrow \dfrac{1}{8\pi\sqrt{2}}; \\ D=2 \rightarrow \dfrac{1}{8\pi}; \\ D=1 \rightarrow \dfrac{1}{16\sqrt{2}}. \end{cases}$$

Then, we arrive at

$$C_{v,Fluc}^{(crit)} = \begin{cases} D=3 \rightarrow \dfrac{L^3 k_B}{4\pi\sqrt{2}} \dfrac{1}{\tau^{1/2}\xi_0^{(1)}} \dfrac{1}{\xi_0^{(1)}\xi_0^{(2)}\xi_0^{(3)}}\ ; \\ D=2 \rightarrow \dfrac{L^2 k_B}{4\pi} \dfrac{1}{\tau\xi_0^{(1)}\xi_0^{(2)}}; \\ D=1 \rightarrow \dfrac{L k_B}{8\sqrt{2}} \dfrac{1}{\tau^{3/2}\xi_0^{(1)}}. \end{cases} \quad 2.5.4\text{-}8$$

Recall that the phase fluctuations affect the divergence of $C_{v,Fluc}^{(crit)}$.

2.5.5 Ginzburg Number

Finally, to calculate the Ginzburg number from fluctuation heat capacity, we need to find the mean-field contribution to C_v. The mean field contribution for free energy is

$$\mathcal{F}_{m.f.} = -\frac{a^2}{2b}L^D. \tag{2.5.5-1}$$

For Entropy

$$S_{m.f.} = -\frac{\partial \mathcal{F}_{m.f.}}{\partial T} = -L^D\frac{|a|\alpha}{b}. \tag{2.5.5-2}$$

So, the mean-field contribution for heat capacity (taken in the leading order τ)

$$C_{v,m.f.} = k_B T_{c0}\frac{\partial S_{m.f.}}{\partial T}$$

$$C_{v,m.f.} = L^D k_B \frac{T_{c0}\alpha^2}{b}. \tag{2.5.5-3}$$

Now, we have everything at our disposal to calculate Gi from the equation

$$C_{v,m.f.} = C_{v,Fluc}^{(crit)}(\tau = Gi), \tag{2.5.5-4}$$

$$L^D k_B \frac{T_{c0}\alpha^2}{b} \sim \frac{L^D}{\tau^{2-D/2}}\frac{k_B}{\xi_0^D}.$$

However, before performing the calculations for different dimensions with the proper numerical coefficients involved, let us derive a useful approximation for Gi, neglecting numerical factors and anisotropy. Usually such formula is given in terms of the jump in the mean-field capacity per unit of volume at $T = T_{c0}$, i.e.

$$\Delta C = k_B\frac{T_{c0}\alpha^2}{b}. \tag{2.5.5-5}$$

Then,

$$\Delta C \sim k_B \left.\frac{1}{\xi_0^D \tau^{(4-D)/2}}\right|_{\tau=Gi},$$

$$Gi \sim \frac{1}{\left(\frac{\Delta C}{k_B}\xi_0^D\right)^{2/(4-D)}}. \tag{2.5.5-6}$$

The zero-temperature coherence length ξ_0 plays an important role in the estimation of the fluctuation impact, when ξ_0 decreases Gi increases together with the impact of fluctuations. This increase of Gi is dependent on the dimension of the system, D, i.e.

$$C_{v,Fluc}^{(crit)} \sim \begin{cases} D = 3 \rightarrow \dfrac{1}{\xi_0^6}\,; \\ D = 2 \rightarrow \dfrac{1}{\xi_0^2}\,; \\ D = 1 \rightarrow \dfrac{1}{\xi_0}. \end{cases} \qquad 2.5.5\text{-}7$$

Now, let us proceed to detailed calculations of Gi in the general anisotropic case

1. $D = 3; \tau = Gi$:

$$L^3 k_B \frac{T_{c0}\alpha^2}{b} = \frac{L^3 k_B}{4\pi\sqrt{2}} \frac{1}{Gi^{1/2}\xi_0^{(1)}\xi_0^{(2)}\xi_0^{(3)}},$$

$$Gi^{1/2} = \frac{b}{T_{c0}\alpha^2} \frac{1}{4\pi\sqrt{2}} \frac{\alpha^{3/2}T_{c0}^{3/2}}{\sqrt{K^{(1)}}\sqrt{K^{(2)}}\sqrt{K^{(3)}}},$$

To have an idea about the value of Gi, we consider the particular anisotropic case of a single band superconductor with a standard deep band in the clean limit

$$Gi = \frac{1}{32\pi^2} \frac{T_{c0}b^2}{\alpha K^3}. \qquad 2.5.5\text{-}8$$

$$b = N(0)\frac{7\zeta(3)}{8\pi^2 T_{c0}^2}, \qquad K = N(0)\frac{\hbar^2 v_F^2}{6}\frac{7\zeta(3)}{8\pi^2 T_{c0}^2},$$

$$\alpha = \frac{N(0)}{T_{c0}}, \qquad N(0)|_{D=3} = \frac{mk_F}{2\pi^2\hbar^2}.$$

So, Eq. 2.5.5-8 becomes

$$Gi = \frac{27\pi^4}{14\,\zeta(3)} \frac{T_{c0}^4}{\left(\frac{\hbar^2 k_F^2}{m}\right)^4},$$

$$Gi = \frac{27\pi^4}{14\,\zeta(3)}\left(\frac{T_{c0}}{E_F}\right)^4 \sim 10^2\left(\frac{T_{c0}}{E_F}\right)^4.$$

To have an idea about the value of Gi, for aluminum for example

$$T_{c0} = 1.2K \rightarrow T_{c0} = 1.2K \cdot 0.086183\frac{MeV}{K} \cong 0.1\,MeV,$$

$E_F \cong 10\,000\ MeV,$

$Gi \cong 10^{-18}.$

This value is typical of elemental superconductors. For a shallow band Gi increases significantly and can be of order 1, huge fluctuations. The reason is a drop in E_F, or a corresponding drop in ξ_0. Shallow bands have extremely slow charge carries so that characteristic velocity in the stiffness K is nearly to zero, K is decreased as compared to the case of a deep band, and so is ξ_0.

2. $D = 2; \tau = Gi$:

$$L^2 k_B \frac{T_{c0}\alpha^2}{b} = \frac{L^2 k_B}{4\pi} \frac{1}{Gi\xi_0^{(1)}\xi_0^{(2)}},$$

$$Gi = \frac{1}{4\pi} \frac{b}{\alpha^2 T_{c0}} \frac{\alpha T_{c0}}{\sqrt{K^{(1)}}\sqrt{K^{(2)}}},$$

For a single band isotropic superconductor with a standard deep band in the clean limit,

$$Gi = \frac{1}{4\pi} \frac{b}{\alpha K}. \qquad 2.5.5\text{-}9$$

$$b = N(0)\frac{7\zeta(3)}{8\pi^2 T_{c0}^2}, \qquad K = N(0)\frac{\hbar^2 v_F^2}{4}\frac{7\zeta(3)}{8\pi^2 T_{c0}^2},$$

$$\alpha = \frac{N(0)}{T_{c0}}, \qquad N(0)|_{D=2} = \frac{m}{2\pi\hbar^2}.$$

Eq.2.5.5-9 becomes

$$Gi = 2\frac{T_{c0}}{\frac{m}{\hbar^2}\hbar^2 v_F^2} = 2\frac{T_{c0}}{\frac{\hbar^2 k_F^2}{m}},$$

$$Gi = \frac{T_{c0}}{E_F}.$$

Using again the values for aluminum

$T_{c0} \cong 0.1\ MeV,$

$E_F \cong 10\,000\ MeV,$

$Gi \cong 10^{-5}.$

That is significantly larger than for $D = 3$.

3. $D = 1; \tau = Gi$:

$$Lk_B \frac{T_{c0}\alpha^2}{b} = \frac{Lk_B}{8\sqrt{2}} \frac{1}{Gi^{3/2}\xi_0^{(1)}},$$

$$Gi^{3/2} = \frac{1}{8\sqrt{2}} \frac{\alpha^{1/2}T_{c0}^{1/2}}{\sqrt{K^{(1)}}} \frac{b}{\alpha^2 T_{c0}},$$

$$Gi^{3/2} = \frac{1}{8\sqrt{2}} \frac{b}{\sqrt{K^{(1)}}\alpha^{3/2}T_{c0}^{1/2}},$$

$$Gi = \left(\frac{1}{128} \frac{b^2}{K^{(1)}T_{c0}\alpha^3}\right)^{1/3}. \qquad \text{2.5.5-10}$$

A single band isotropic superconductor with a standard deep band in the clean limit

$$b = N(0)\frac{7\zeta(3)}{8\pi^2 T_{c0}^2}, \qquad K = N(0)\frac{\hbar^2 v_F^2}{2}\frac{7\zeta(3)}{8\pi^2 T_{c0}^2},$$

$$\alpha = \frac{N(0)}{T_{c0}}, \qquad N(0)|_{D=2} = \frac{m}{2\pi\hbar^2}.$$

Eq.2.5.5-10 becomes

$$Gi = \left(\frac{1}{128}\frac{7\zeta(3)}{8\pi^2}2\pi^2\right)^{1/3}\left(\frac{T_{c0}}{E_F}\right)^0,$$

$$Gi \propto \left(\frac{T_{c0}}{E_F}\right)^0 \sim 1.$$

From this result, we can see that, superconductive fluctuations are extremely pronounced in the case $D = 1$ and corresponding Gi does not depend on microscopic parameters.

So, we can obtain the general relation for the Ginzburg number at $D = 3, 2, 1$ as

$$Gi \propto \left(\frac{T_{c0}}{E_F}\right)^{\frac{2(D-1)}{4-D}}. \qquad \text{2.5.5-11}$$

Notice that Eq. 2.5.5-11 is considered for $D = 3, 2, 1$. However, it is an important remark that Gi becomes infinitely small at $D = 4$. This reflects the fact that fluctuations are negligible in the Ginzburg-Landau theory for $D \geq 4$.

2.5.6 Isotropizing an anisotropic Ginzburg-Landau theory and Gi for the initial anisotropic and eventual isotropic models

Here we return to the free energy functional of the Ginzburg-Landau theory.

$$\mathcal{F} = \int_{L^D} d^D\boldsymbol{r}\left[a|\psi(\boldsymbol{r})|^2 + \frac{b}{2}|\psi(\boldsymbol{r})|^4 + K^{(x)}|\partial_x\psi(\boldsymbol{r})|^2 + K^{(y)}\left|\partial_y\psi(\boldsymbol{r})\right|^2 + K^{(z)}|\partial_z\psi(\boldsymbol{r})|^2\right],$$

taken in the general anisotropic case. The model can be isotropic for $D = 3$ by the coordinate transformation

$$\tilde{x} = \frac{x}{\sqrt{\alpha^{(x)}}}, \qquad \tilde{y} = \frac{y}{\sqrt{\alpha^{(y)}}}, \qquad \tilde{z} = \frac{z}{\sqrt{\alpha^{(z)}}},$$

with

$$\alpha^{(x)} = \frac{K^{(x)}}{K}, \qquad \alpha^{(y)} = \frac{K^{(y)}}{K}, \qquad \alpha^{(z)} = \frac{K^{(z)}}{K},$$

and

$$K = \sqrt[3]{K^{(x)}K^{(y)}K^{(z)}}.$$

Notice that

$$\alpha^{(x)}\alpha^{(y)}\alpha^{(z)} = 1,$$

and so, $(D = 3)$

$$d^3\boldsymbol{r} = d^3\tilde{\boldsymbol{r}},$$

which means

$$\mathcal{F} = \int_{L^3} d^3\tilde{\boldsymbol{r}}\left[a|\psi|^2 + \frac{b}{2}|\psi|^4 + K\left|\tilde{\boldsymbol{\nabla}}\psi\right|^2\right],$$

where $\tilde{\boldsymbol{\nabla}} = \left(\partial_{\tilde{x}}, \partial_{\tilde{y}}, \partial_{\tilde{z}}\right)$.

In principle, one could invoke the transformation such that $\alpha^{(i)} = \frac{K^{(i)}}{\tilde{K}}, \tilde{K} \neq \sqrt[3]{K^{(x)}K^{(y)}K^{(z)}}$. However, in this case an extra factor will appear in $\mathcal{F}$ because $d^D\boldsymbol{r} \neq d^D\tilde{\boldsymbol{r}}$. This factor should be taken in account during the calculations of the fluctuation impact.

Under the choice of the coordinate transformation, we can easily find that the outcoming isotropic model yields at $D = 3$

$$Gi_{out} = \frac{1}{32\pi^2}\frac{T_{c0}b^2}{\alpha K^3},$$

which is the same as Gi of the initial anisotropic model

$$Gi_{out} = Gi_{in} = \frac{1}{32\pi^2}\frac{T_{c0}b^2}{\alpha K^{(x)}K^{(y)}K^{(z)}}.$$

The critical temperature is also the same in both models. We note the transformation yields the only solution of the equations

$$\frac{K^{(x)}}{\alpha^{(x)}} = \frac{K^{(y)}}{\alpha^{(y)}} = \frac{K^{(x)}}{\alpha^{(z)}}, \qquad \alpha^{(x)}\alpha^{(y)}\alpha^{(z)} = 1.$$

The same we can do for $D = 2$, the isotropic transformation reads

$$\tilde{x} = \frac{x}{\sqrt{\alpha^{(x)}}}, \qquad \tilde{y} = \frac{y}{\sqrt{\alpha^{(y)}}}.$$

with

$$\alpha^{(x)} = \frac{K^{(x)}}{K}, \qquad \alpha^{(y)} = \frac{K^{(y)}}{K}, \qquad K = \sqrt{K^{(x)}K^{(y)}}.$$

Here

$$\alpha^{(x)}\alpha^{(y)} = 1, \qquad d^2\boldsymbol{r} = d^2\tilde{\boldsymbol{r}}.$$

Finally

$$Gi_{out} = \frac{1}{4\pi}\frac{b}{\alpha K}, \qquad Gi_{in} = \frac{1}{4\pi}\frac{b}{\alpha\sqrt{K^{(x)}K^{(y)}}}.$$

So, $Gi_{out} = Gi_{in}$.

2.5.7 General form of the Gaussian "Hamiltonian" and fluctuation-field average

To proceed with our formalism, we need to generalize the fluctuation "Hamiltonian". In a similar way as we obtained before, but in this case, we can also have contributions of terms like $|\eta|^4$ approximated (a kind of mean field approach) by $\propto \langle|\eta|^2\rangle|\eta|^2$, in further considerations of the fluctuation-driven shift in T_c. Sometimes, such high-power terms are called "fluctuations interactions", just following the interpretation of the nonlinear term in the Ginzburg-Landau equation, notice that, this interpretation is based on the similarity of the Ginzburg-Landau equation with a nonlinear Schrödinger equation, in fact, this interpretation is rather conditional.

So, using the definition $\eta_{\mathbf{q}} = x_{\mathbf{q}} + iy_{\mathbf{q}}$, for the Fourier component of the field $\eta(\boldsymbol{r})$, the general fluctuation "Hamiltonian", in the Gaussian approximation reads

$$\mathcal{H} = \sum_{\mathbf{q}} \left[\varepsilon_+ \left(x_{\mathbf{q}}^2 + y_{\mathbf{q}}^2\right) + \varepsilon_- \left(x_{\mathbf{q}} x_{-\mathbf{q}} - y_{\mathbf{q}} y_{-\mathbf{q}}\right)\right], \qquad 2.5.7\text{-}1$$

And after performing the diagonalization procedure, as we have done before, we obtain

$$\mathcal{H} = \sum_{\mathbf{q}, q_x \geq 0} \left[\varepsilon_{1,\mathbf{q}} \left(\alpha_{\mathbf{q}}^2 + \xi_{\mathbf{q}}^2\right) + \varepsilon_{2,\mathbf{q}} \left(\beta_{\mathbf{q}}^2 + \zeta_{\mathbf{q}}^2\right)\right], \qquad 2.5.7\text{-}2$$

$$\varepsilon_{1,\mathbf{q}} = \varepsilon_+ + \varepsilon_-, \qquad \varepsilon_{2,\mathbf{q}} = \varepsilon_+ - \varepsilon_-,$$

$$\alpha_{\mathbf{q}} = \frac{1}{\sqrt{2}}\left(x_{\mathbf{q}} + x_{-\mathbf{q}}\right), \qquad \beta_{\mathbf{q}} = \frac{1}{\sqrt{2}}\left(x_{\mathbf{q}} - x_{-\mathbf{q}}\right),$$

$$\xi_{\mathbf{q}} = \frac{1}{\sqrt{2}}\left(y_{\mathbf{q}} + y_{-\mathbf{q}}\right), \qquad \zeta_{\mathbf{q}} = \frac{1}{\sqrt{2}}\left(y_{\mathbf{q}} - y_{-\mathbf{q}}\right).$$

$$\alpha_{\mathbf{q}} = \alpha_{-\mathbf{q}}, \qquad \beta_{\mathbf{q}} = \beta_{-\mathbf{q}}, \qquad \xi_{\mathbf{q}} = \xi_{-\mathbf{q}}, \qquad \zeta_{\mathbf{q}} = \zeta_{-\mathbf{q}}$$

$$\varepsilon_+(\mathbf{q}) = \frac{\varepsilon_{1,\mathbf{q}} + \varepsilon_{2,\mathbf{q}}}{2}, \qquad \varepsilon_-(\mathbf{q}) = \frac{\varepsilon_{1,\mathbf{q}} - \varepsilon_{2,\mathbf{q}}}{2},$$

$$x_{\mathbf{q}} = \frac{1}{\sqrt{2}}\left(\alpha_{\mathbf{q}} + \beta_{\mathbf{q}}\right), \qquad x_{-\mathbf{q}} = \frac{1}{\sqrt{2}}\left(\alpha_{\mathbf{q}} - \beta_{\mathbf{q}}\right),$$

$$y_{\mathbf{q}} = \frac{1}{\sqrt{2}}\left(\xi_{\mathbf{q}} + \zeta_{\mathbf{q}}\right), \qquad y_{-\mathbf{q}} = \frac{1}{\sqrt{2}}\left(-\xi_{\mathbf{q}} + \zeta_{\mathbf{q}}\right),$$

and

$$\mathcal{F}_{Fluc} = -\frac{T}{2}\sum_{\mathbf{q}}\left(\ln\frac{\pi T}{\varepsilon_{1,\mathbf{q}}} + \ln\frac{\pi T}{\varepsilon_{2,\mathbf{q}}}\right). \quad 2.5.7\text{-}3$$

Notice that, the functional integration here can be done only over the set $\mathbf{q}_x$, as $\alpha_{\mathbf{q}} = \alpha_{-\mathbf{q}}$, $\beta_{\mathbf{q}} = \beta_{-\mathbf{q}}$, $\xi_{\mathbf{q}} = \xi_{-\mathbf{q}}$, $\zeta_{\mathbf{q}} = \zeta_{-\mathbf{q}}$. The choice of $\mathbf{q}_x$ is not mandatory, we can adopt $\mathbf{q}_y \geq 0$, $\mathbf{q}_z \geq 0$.

It is also important to note that $\varepsilon_{2,\mathbf{q}}$ does not appear in the problem when only the real fluctuation fields are included: $\varepsilon_{2,\mathbf{q}}$ is related to phase fluctuations of the order parameter and, so, to the Goldstone mode, this come from the fact that $x_{\mathbf{q}} = x_{-\mathbf{q}}$ and $y_{\mathbf{q}} = y_{-\mathbf{q}}$ for real fluctuations.

Then, we can use this framework to calculate the average of the fluctuation fields. For $\langle\eta(\boldsymbol{r})\rangle$, we have

$$\langle\eta(\boldsymbol{r})\rangle = \frac{\int \mathrm{D}[\eta]\eta(\boldsymbol{r})e^{-\mathcal{H}[\eta]}}{\int \mathrm{D}[\eta]e^{-\mathcal{H}[\eta]}},$$

as

$$\eta(\boldsymbol{r}) = \frac{1}{L^{D/2}}\sum_{\mathbf{q}} e^{i\mathbf{q}\cdot\boldsymbol{r}}\eta_{\mathbf{q}},$$

becomes

$$\langle\eta(\boldsymbol{r})\rangle = \frac{1}{L^{D/2}}\sum_{\mathbf{q}} e^{i\mathbf{q}\cdot\boldsymbol{r}}\langle\eta_{\mathbf{q}}\rangle,$$

with

$$\langle\eta_{\mathbf{q}}\rangle = \frac{\int \mathrm{D}[\eta]\eta_{\mathbf{q}}e^{-\mathcal{H}[\eta]}}{\int \mathrm{D}[\eta]e^{-\mathcal{H}[\eta]}}.$$

As $\eta_{\mathbf{q}} = x_{\mathbf{q}} + iy_{\mathbf{q}}$ and $\eta_{\mathbf{q}}^* = x_{\mathbf{q}} - iy_{\mathbf{q}}$, we have

$$\langle\eta_{\mathbf{q}}\rangle = \langle x_{\mathbf{q}}\rangle + i\langle y_{\mathbf{q}}\rangle,$$

and

$$\langle x_{\mathbf{q}}\rangle = \frac{\int \mathrm{D}[\eta]x_{\mathbf{q}}e^{-\mathcal{H}[\eta]}}{\int \mathrm{D}[\eta]e^{-\mathcal{H}[\eta]}}, \qquad \langle y_{\mathbf{q}}\rangle = \frac{\int \mathrm{D}[\eta]y_{\mathbf{q}}e^{-\mathcal{H}[\eta]}}{\int \mathrm{D}[\eta]e^{-\mathcal{H}[\eta]}}.$$

Whereas

$$\langle \eta_{\mathbf{q}}^{*} \rangle = \langle x_{\mathbf{q}} \rangle - i\langle y_{\mathbf{q}} \rangle,$$

Then,

$$\langle x_{\mathbf{q}} \rangle = \frac{\int \prod_{\mathbf{k},k_x\geq 0} d\alpha_{\mathbf{k}} d\beta_{\mathbf{k}}\, d\xi_{\mathbf{k}} d\zeta_{\mathbf{k}} x_{\mathbf{q}} \exp\left\{-\frac{1}{T}\sum_{\mathbf{k},k_x\geq 0}\left[\varepsilon_{1,\mathbf{k}}(\alpha_{\mathbf{k}}^2+\xi_{\mathbf{k}}^2)+\varepsilon_{2,\mathbf{k}}(\beta_{\mathbf{k}}^2+\zeta_{\mathbf{k}}^2)\right]\right\}}{\int \prod_{\mathbf{k},k_x\geq 0} d\alpha_{\mathbf{k}} d\beta_{\mathbf{k}}\, d\xi_{\mathbf{k}} d\zeta_{\mathbf{k}} \exp\left\{-\frac{1}{T}\sum_{\mathbf{k}}\left[\varepsilon_{1,\mathbf{k}}(\alpha_{\mathbf{k}}^2+\xi_{\mathbf{k}}^2)+\varepsilon_{2,\mathbf{k}}(\beta_{\mathbf{k}}^2+\zeta_{\mathbf{k}}^2)\right]\right\}},$$

$$\langle x_{\mathbf{q}} \rangle = \frac{\int d\alpha_{\mathbf{q}} d\beta_{\mathbf{q}}\, d\xi_{\mathbf{q}} d\zeta_{\mathbf{q}} \frac{(\alpha_{\mathbf{q}}+\beta_{\mathbf{q}})}{\sqrt{2}} \exp\left\{-\frac{1}{T}\left[\varepsilon_{1,\mathbf{q}}(\alpha_{\mathbf{q}}^2+\xi_{\mathbf{q}}^2)+\varepsilon_{2,\mathbf{q}}(\beta_{\mathbf{q}}^2+\zeta_{\mathbf{q}}^2)\right]\right\}}{\int d\alpha_{\mathbf{q}} d\beta_{\mathbf{q}}\, d\xi_{\mathbf{q}} d\zeta_{\mathbf{q}} \exp\left\{-\frac{1}{T}\left[\varepsilon_{1,\mathbf{q}}(\alpha_{\mathbf{q}}^2+\xi_{\mathbf{q}}^2)+\varepsilon_{2,\mathbf{q}}(\beta_{\mathbf{q}}^2+\zeta_{\mathbf{q}}^2)\right]\right\}},$$

$$\langle x_{\mathbf{q}} \rangle = \frac{\int d\alpha_{\mathbf{q}} d\beta_{\mathbf{q}} \frac{(\alpha_{\mathbf{q}}+\beta_{\mathbf{q}})}{\sqrt{2}} \exp\left[-\frac{1}{T}\left(\varepsilon_{1,\mathbf{q}}\alpha_{\mathbf{q}}^2+\varepsilon_{2,\mathbf{q}}\beta_{\mathbf{q}}^2\right)\right]}{\int d\alpha_{\mathbf{q}} d\beta_{\mathbf{q}} \exp\left[-\frac{1}{T}\left(\varepsilon_{1,\mathbf{q}}\alpha_{\mathbf{q}}^2+\varepsilon_{2,\mathbf{q}}\beta_{\mathbf{q}}^2\right)\right]} = 0.$$

In turn,

$$\langle y_{\mathbf{q}} \rangle = \frac{\int \prod_{\mathbf{k},k_x\geq 0} d\alpha_{\mathbf{k}} d\beta_{\mathbf{k}}\, d\xi_{\mathbf{k}} d\zeta_{\mathbf{k}} y_{\mathbf{q}} \exp\left\{-\frac{1}{T}\sum_{\mathbf{k},k_x\geq 0}\left[\varepsilon_{1,\mathbf{k}}(\alpha_{\mathbf{k}}^2+\xi_{\mathbf{k}}^2)+\varepsilon_{2,\mathbf{k}}(\beta_{\mathbf{k}}^2+\zeta_{\mathbf{k}}^2)\right]\right\}}{\int \prod_{\mathbf{k},k_x\geq 0} d\alpha_{\mathbf{k}} d\beta_{\mathbf{k}}\, d\xi_{\mathbf{k}} d\zeta_{\mathbf{k}} \exp\left\{-\frac{1}{T}\sum_{\mathbf{k}}\left[\varepsilon_{1,\mathbf{k}}(\alpha_{\mathbf{k}}^2+\xi_{\mathbf{k}}^2)+\varepsilon_{2,\mathbf{k}}(\beta_{\mathbf{k}}^2+\zeta_{\mathbf{k}}^2)\right]\right\}},$$

$$\langle y_{\mathbf{q}} \rangle = \frac{\int d\alpha_{\mathbf{q}} d\beta_{\mathbf{q}}\, d\xi_{\mathbf{q}} d\zeta_{\mathbf{q}} \frac{(\xi_{\mathbf{q}}+\zeta_{\mathbf{q}})}{\sqrt{2}} \exp\left\{-\frac{1}{T}\left[\varepsilon_{1,\mathbf{q}}(\alpha_{\mathbf{q}}^2+\xi_{\mathbf{q}}^2)+\varepsilon_{2,\mathbf{q}}(\beta_{\mathbf{q}}^2+\zeta_{\mathbf{q}}^2)\right]\right\}}{\int d\alpha_{\mathbf{q}} d\beta_{\mathbf{q}}\, d\xi_{\mathbf{q}} d\zeta_{\mathbf{q}} \exp\left\{-\frac{1}{T}\left[\varepsilon_{1,\mathbf{q}}(\alpha_{\mathbf{q}}^2+\xi_{\mathbf{q}}^2)+\varepsilon_{2,\mathbf{q}}(\beta_{\mathbf{q}}^2+\zeta_{\mathbf{q}}^2)\right]\right\}},$$

$$\langle y_{\mathbf{q}} \rangle = \frac{\int d\xi_{\mathbf{q}} d\zeta_{\mathbf{q}} \frac{(\xi_{\mathbf{q}}+\zeta_{\mathbf{q}})}{\sqrt{2}} \exp\left[-\frac{1}{T}\left(\varepsilon_{1,\mathbf{q}}\xi_{\mathbf{q}}^2+\varepsilon_{2,\mathbf{q}}\zeta_{\mathbf{q}}^2\right)\right]}{\int d\xi_{\mathbf{q}} d\zeta_{\mathbf{q}} \exp\left[-\frac{1}{T}\left(\varepsilon_{1,\mathbf{q}}\xi_{\mathbf{q}}^2+\varepsilon_{2,\mathbf{q}}\zeta_{\mathbf{q}}^2\right)\right]} = 0.$$

Thus, we conclude that

$$\langle \eta_{\mathbf{q}} \rangle = \langle \eta_{\mathbf{q}}^{*} \rangle = 0,$$

and

$$\langle \eta(\boldsymbol{r}) \rangle = \langle \eta^{*}(\boldsymbol{r}) \rangle = 0.$$

Obviously,

$$\langle \boldsymbol{\nabla}\eta(\boldsymbol{r}) \rangle = \langle \boldsymbol{\nabla}\eta^{*}(\boldsymbol{r}) \rangle = 0$$

Now, we investigate the pair averages, and first we consider $\langle|\eta^2(\boldsymbol{r})|\rangle$, but in order to do this calculation we need to rewrite the product $\eta(\boldsymbol{r})\eta^*(\boldsymbol{r})$ in terms of the variables with $q_x \geq 0$

$$\eta(\boldsymbol{r}) = \frac{1}{L^{D/2}}\sum_{\mathbf{q}} e^{i\mathbf{q}\cdot\boldsymbol{r}}\eta_{\mathbf{q}} = \frac{1}{L^{D/2}}\sum_{\mathbf{q}} e^{i\mathbf{q}\cdot\boldsymbol{r}}\left(x_{\mathbf{q}} + iy_{\mathbf{q}}\right),$$

as we can do the change $\mathbf{q} \to -\mathbf{q}$

$$\eta(\boldsymbol{r}) = \frac{1}{2L^{D/2}}\sum_{\mathbf{q}} e^{i\mathbf{q}\cdot\boldsymbol{r}}\left(x_{\mathbf{q}} + iy_{\mathbf{q}}\right) + e^{i-\mathbf{q}\cdot\boldsymbol{r}}\left(x_{-\mathbf{q}} + iy_{-\mathbf{q}}\right),$$

$$\eta(\boldsymbol{r}) = \frac{1}{L^{D/2}}\sum_{\mathbf{q},q_x\geq 0} \left[e^{i\mathbf{q}\cdot\boldsymbol{r}}\left(x_{\mathbf{q}} + iy_{\mathbf{q}}\right) + e^{i-\mathbf{q}\cdot\boldsymbol{r}}\left(x_{-\mathbf{q}} + iy_{-\mathbf{q}}\right)\right],$$

$$\eta(\boldsymbol{r}) = \frac{1}{L^{D/2}}\sum_{\mathbf{q},q_x\geq 0} \left\{e^{i\mathbf{q}\cdot\boldsymbol{r}}\left[\frac{\left(\alpha_{\mathbf{q}} + \beta_{\mathbf{q}}\right)}{\sqrt{2}} + i\frac{\left(\xi_{\mathbf{q}} + \zeta_{\mathbf{q}}\right)}{\sqrt{2}}\right] + e^{i-\mathbf{q}\cdot\boldsymbol{r}}\left[\frac{\left(\alpha_{\mathbf{q}} - \beta_{\mathbf{q}}\right)}{\sqrt{2}} + i\frac{\left(-\xi_{\mathbf{q}} + \zeta_{\mathbf{q}}\right)}{\sqrt{2}}\right]\right\},$$

$$\eta(\boldsymbol{r}) = \frac{1}{L^{D/2}}\sum_{\mathbf{q},q_x\geq 0} \left\{\frac{e^{i\mathbf{q}\cdot\boldsymbol{r}}}{\sqrt{2}}\left[\left(\alpha_{\mathbf{q}} + \beta_{\mathbf{q}}\right) + i\left(\xi_{\mathbf{q}} + \zeta_{\mathbf{q}}\right)\right] + \frac{e^{i-\mathbf{q}\cdot\boldsymbol{r}}}{\sqrt{2}}\left[\left(\alpha_{\mathbf{q}} - \beta_{\mathbf{q}}\right) + i\left(-\xi_{\mathbf{q}} + \zeta_{\mathbf{q}}\right)\right]\right\}.$$

For the complex conjugate

$$\eta^*(\boldsymbol{r}) = \frac{1}{L^{D/2}}\sum_{\mathbf{q}',q'_x\geq 0} \left\{\frac{e^{-i\mathbf{q}'\cdot\boldsymbol{r}}}{\sqrt{2}}\left[\left(\alpha_{\mathbf{q}'} + \beta_{\mathbf{q}'}\right) - i\left(\xi_{\mathbf{q}'} + \zeta_{\mathbf{q}'}\right)\right] + \frac{e^{i\mathbf{q}'\cdot\boldsymbol{r}}}{\sqrt{2}}\left[\left(\alpha_{\mathbf{q}'} - \beta_{\mathbf{q}'}\right) + i\left(\xi_{\mathbf{q}'} - \zeta_{\mathbf{q}'}\right)\right]\right\}.$$

Considering only the terms with $\mathbf{q} = \mathbf{q}'$, other terms do not contribute, we obtain

$$|\eta^2(\boldsymbol{r})| = \frac{1}{L^D}\sum_{\mathbf{q},q_x\geq 0}\left(\frac{\alpha_{\mathbf{q}}^2}{2} + \frac{\alpha_{\mathbf{q}}^2 e^{i2\mathbf{q}\cdot\boldsymbol{r}}}{2} + \frac{\alpha_{\mathbf{q}}^2 e^{-i2\mathbf{q}\cdot\boldsymbol{r}}}{2} + \frac{\alpha_{\mathbf{q}}^2}{2} + \frac{\beta_{\mathbf{q}}^2}{2} - \frac{\beta_{\mathbf{q}}^2 e^{i2\mathbf{q}\cdot\boldsymbol{r}}}{2} - \frac{\beta_{\mathbf{q}}^2 e^{-i2\mathbf{q}\cdot\boldsymbol{r}}}{2} + \frac{\beta_{\mathbf{q}}^2}{2} + \frac{\xi_{\mathbf{q}}^2}{2} - \frac{\xi_{\mathbf{q}}^2 e^{i2\mathbf{q}\cdot\boldsymbol{r}}}{2} - \frac{\xi_{\mathbf{q}}^2 e^{-i2\mathbf{q}\cdot\boldsymbol{r}}}{2} + \frac{\xi_{\mathbf{q}}^2}{2} + \frac{\zeta_{\mathbf{q}}^2}{2} + \frac{\zeta_{\mathbf{q}}^2 e^{i2\mathbf{q}\cdot\boldsymbol{r}}}{2} + \frac{\zeta_{\mathbf{q}}^2 e^{-i2\mathbf{q}\cdot\boldsymbol{r}}}{2} + \frac{\zeta_{\mathbf{q}}^2}{2}\right).$$

Calculating the average, of each term

$$\langle\alpha_{\mathbf{q}}^2\rangle = \frac{\int d\alpha_{\mathbf{q}}\alpha_{\mathbf{q}}^2 e^{-\mathcal{H}}}{\int d\alpha_{\mathbf{q}} e^{-\mathcal{H}}} = \frac{\int d\alpha_{\mathbf{q}}\alpha_{\mathbf{q}}^2 \exp\left(-\frac{1}{T}\varepsilon_{1,\mathbf{q}}\alpha_{\mathbf{q}}^2\right)}{\int d\alpha_{\mathbf{q}} \exp\left(-\frac{1}{T}\varepsilon_{1,\mathbf{q}}\alpha_{\mathbf{q}}^2\right)} = \frac{\Gamma\left(\frac{3}{2}\right)}{2\left(\frac{\varepsilon_{1,\mathbf{q}}}{T}\right)^{\frac{3}{2}}}\frac{2\left(\frac{\varepsilon_{1,\mathbf{q}}}{T}\right)^{1/2}}{\Gamma\left(\frac{1}{2}\right)} = \frac{1}{2}\frac{T}{\varepsilon_{1,\mathbf{q}}}.$$

$$\langle\beta_{\mathbf{q}}^2\rangle=\frac{\int d\beta_{\mathbf{q}}\beta_{\mathbf{q}}^2e^{-\mathcal{H}}}{\int d\beta_{\mathbf{q}}e^{-\mathcal{H}}}=\frac{\int d\beta_{\mathbf{q}}\beta_{\mathbf{q}}^2\exp\left(-\frac{1}{T}\varepsilon_{2,\mathbf{q}}\beta_{\mathbf{q}}^2\right)}{\int d\beta_{\mathbf{q}}\exp\left(-\frac{1}{T}\varepsilon_{2,\mathbf{q}}\alpha_{\mathbf{q}}^2\right)}=\frac{\Gamma\left(\frac{3}{2}\right)}{2\left(\frac{\varepsilon_{2,\mathbf{q}}}{T}\right)^{\frac{3}{2}}}\frac{2\left(\frac{\varepsilon_{2,\mathbf{q}}}{T}\right)^{1/2}}{\Gamma\left(\frac{1}{2}\right)}=\frac{1}{2}\frac{T}{\varepsilon_{2,\mathbf{q}}}.$$

The same we can do for $\langle\xi_{\mathbf{q}}^2\rangle$ and $\langle\zeta_{\mathbf{q}}^2\rangle$, that read

$$\langle\xi_{\mathbf{q}}^2\rangle=\frac{1}{2}\frac{T}{\varepsilon_{1,\mathbf{q}}},\qquad\qquad \langle\zeta_{\mathbf{q}}^2\rangle=\frac{1}{2}\frac{T}{\varepsilon_{2,\mathbf{q}}}.$$

And, now we can calculate the average

$$\langle|\eta^2(\boldsymbol{r})|\rangle=\frac{1}{L^D}\sum_{\mathbf{q},q_x\geq 0}\left(\langle\alpha_{\mathbf{q}}^2\rangle+\langle\beta_{\mathbf{q}}^2\rangle+\langle\xi_{\mathbf{q}}^2\rangle+\langle\zeta_{\mathbf{q}}^2\rangle\right),$$

So, as we can see $\langle\alpha_{\mathbf{q}}^2\rangle=\langle\xi_{\mathbf{q}}^2\rangle$ and $\langle\beta_{\mathbf{q}}^2\rangle=\langle\zeta_{\mathbf{q}}^2\rangle$, and $\langle|\eta^2(\boldsymbol{r})|\rangle$ writes

$$\langle|\eta^2(\boldsymbol{r})|\rangle=\frac{2}{L^D}\sum_{\mathbf{q},q_x\geq 0}\left(\langle\alpha_{\mathbf{q}}^2\rangle+\langle\beta_{\mathbf{q}}^2\rangle\right),$$

$$\langle|\eta^2(\boldsymbol{r})|\rangle=\frac{1}{L^D}\sum_{\mathbf{q}}\left(\langle\alpha_{\mathbf{q}}^2\rangle+\langle\beta_{\mathbf{q}}^2\rangle\right),$$

$$\langle|\eta^2(\boldsymbol{r})|\rangle=\frac{1}{2L^D}\sum_{\mathbf{q}}\left(\frac{T}{\varepsilon_{1,\mathbf{q}}}+\frac{T}{\varepsilon_{2,\mathbf{q}}}\right). \qquad 2.5.7\text{-}4$$

The same procedure we can do for $\langle\eta^2(\boldsymbol{r})\rangle$, using the previous results for $\eta(\boldsymbol{r})$ in terms of the diagonal variables $\alpha_{\mathbf{q}}$, $\beta_{\mathbf{q}}$, $\xi_{\mathbf{q}}$ and $\zeta_{\mathbf{q}}$

$$\begin{aligned}\langle\eta^2(\boldsymbol{r})\rangle=\frac{1}{L^D}\sum_{\mathbf{q},q_x\geq 0}\Bigg(&\frac{\langle\alpha_{\mathbf{q}}^2\rangle}{2}+\frac{\langle\alpha_{\mathbf{q}}^2\rangle e^{i2\mathbf{q}\cdot\boldsymbol{r}}}{2}+\frac{\langle\alpha_{\mathbf{q}}^2\rangle e^{-i2\mathbf{q}\cdot\boldsymbol{r}}}{2}+\frac{\langle\alpha_{\mathbf{q}}^2\rangle}{2}+\frac{\langle\beta_{\mathbf{q}}^2\rangle e^{i2\mathbf{q}\cdot\boldsymbol{r}}}{2}-\frac{\langle\beta_{\mathbf{q}}^2\rangle}{2}\\&+\frac{\langle\beta_{\mathbf{q}}^2\rangle e^{-i2\mathbf{q}\cdot\boldsymbol{r}}}{2}-\frac{\langle\beta_{\mathbf{q}}^2\rangle}{2}-\frac{\langle\xi_{\mathbf{q}}^2\rangle e^{i2\mathbf{q}\cdot\boldsymbol{r}}}{2}+\frac{\langle\xi_{\mathbf{q}}^2\rangle}{2}-\frac{\langle\xi_{\mathbf{q}}^2\rangle e^{-i2\mathbf{q}\cdot\boldsymbol{r}}}{2}+\frac{\langle\xi_{\mathbf{q}}^2\rangle}{2}-\frac{\langle\zeta_{\mathbf{q}}^2\rangle e^{i2\mathbf{q}\cdot\boldsymbol{r}}}{2}\\&-\frac{\langle\zeta_{\mathbf{q}}^2\rangle}{2}-\frac{\langle\zeta_{\mathbf{q}}^2\rangle e^{-i2\mathbf{q}\cdot\boldsymbol{r}}}{2}-\frac{\langle\zeta_{\mathbf{q}}^2\rangle}{2}\Bigg),\end{aligned}$$

as we can see $\langle\alpha_{\mathbf{q}}^2\rangle=\langle\xi_{\mathbf{q}}^2\rangle$ and $\langle\beta_{\mathbf{q}}^2\rangle=\langle\zeta_{\mathbf{q}}^2\rangle$

$$\langle\eta^2(\boldsymbol{r})\rangle=\frac{1}{L^D}\sum_{\mathbf{q},q_x\geq 0}\left(\langle\alpha_{\mathbf{q}}^2\rangle+\langle\xi_{\mathbf{q}}^2\rangle-\langle\beta_{\mathbf{q}}^2\rangle-\langle\zeta_{\mathbf{q}}^2\rangle\right),$$

Finally

$$\langle \eta^2(\boldsymbol{r}) \rangle = \frac{1}{2L^D} \sum_{\mathbf{q}} \left(\frac{T}{\varepsilon_{1,\mathbf{q}}} - \frac{T}{\varepsilon_{2,\mathbf{q}}} \right). \qquad 2.5.7\text{-}5$$

When $\varepsilon_{1,\mathbf{q}} = \varepsilon_{2,\mathbf{q}}$ (above the critical temperature, where there is no averaged condensate), we have $\langle \eta^2(\boldsymbol{r}) \rangle = 0$, while $\langle |\eta^2(\boldsymbol{r})| \rangle \neq 0$. Generally, $|\langle \eta^2 \rangle| \ll \langle |\eta^2| \rangle$, which is justified by the presence of significant oscillations of η^2 due to the phase variations. This, in particular, dictates the random phase approximation, according which any average including different numbers of η and η^* is nearly zero due to oscillations caused by phase variations.

2.5.8 Fluctuation- Shifted critical temperature

In this section, from the formalism of the Gaussian fluctuations we will calculate how the critical temperature is shifted from the mean field temperature, T_{c0}. As is usual, the critical temperature is found by the Ginzburg-Landau equation, by the temperature dependence in a. So, our starting point is the Ginzburg-Landau equation

$$a\psi(\boldsymbol{r}) + b\psi(\boldsymbol{r})|\psi(\boldsymbol{r})|^2 - \sum_j K^{(j)}\, \partial_j^2 \psi(\boldsymbol{r}) = 0, \qquad 2.5.8\text{-}1$$

Suppose that order parameter is given by its averaged value plus a fluctuation field. $\psi = \psi_0 + \eta$ and $\psi_0 = \langle \psi \rangle$. So, the GL equation becomes

$$a(\psi_0 + \eta) + b(\psi_0 + \eta)|\psi_0 + \eta|^2 - \sum_j K^{(j)}\, \partial_j^2 (\psi_0 + \eta) = 0,$$

$$a(\psi_0 + \eta) + b(\psi_0 + \eta)^2(\psi_0 + \eta)^* - \sum_j K^{(j)}\, \partial_j^2 (\psi_0 + \eta) = 0,$$

$$a(\psi_0 + \eta) + b(\psi_0^2 + \eta^2 + 2\psi_0\eta)^2(\psi_0^* + \eta^*) - \sum_j K^{(j)}\, \partial_j^2 (\psi_0 + \eta) = 0,$$

$$a\psi_0 + a\eta + b\psi_0|\psi_0|^2 + b\psi_0^2\eta^* + b\eta^2\psi_0^* + b\eta|\eta|^2 + 2b\eta|\psi_0|^2 + 2b\psi_0|\eta|^2 - \sum_j K^{(j)}\, \partial_j^2 \psi_0 - \sum_j K^{(j)}\, \partial_j^2 \eta = 0,$$

Collecting the similar terms

$$\underbrace{a\psi_0 + b\psi_0|\psi_0|^2 - \sum_j K^{(j)}\,\partial_j^2\psi_0}_{\text{no fluctuation terms}} + \underbrace{a\eta + b\psi_0^2\eta^* + 2b\eta|\psi_0|^2 - \sum_j K^{(j)}\,\partial_j^2\eta}_{\text{linear in }\eta}$$

$$+\underbrace{b\eta^2\psi_0^* + b\eta|\eta|^2 + 2b\psi_0|\eta|^2}_{\text{non-linear in }\eta} = 0$$

Averaging above equation over η, knowing that $\langle\eta\rangle = \langle\eta^*\rangle = \langle\boldsymbol{\nabla}^2\eta\rangle = 0$, and the non-linear terms gives a contribution if they are normal (not anomalous) from the random phase approximation, i.e. $\langle\eta^2\rangle = \langle\eta|\eta|^2\rangle = 0$, $\langle|\eta|^2\rangle \neq 0$.

We obtain the following

$$a\psi_0 + b\psi_0|\psi_0|^2 + 2b\psi_0\langle|\eta|^2\rangle - \sum_j K^{(j)}\,\partial_j^2\psi_0 = 0,$$

$$(a + 2b\langle|\eta|^2\rangle)\psi_0 + b|\psi_0|^2\psi_0 - \sum_j K^{(j)}\,\partial_j^2\psi_0 = 0. \qquad 2.5.8\text{-}2$$

We can see that; this equation is a GL equation for ψ_0. The solution of ψ_0 depends on the average $\langle|\eta|^2\rangle$, the shape of the resulting equation dictates that $\psi_0 \to 0$ when $T \to T_c$.

So, calculate at $T = T_c$, T_c is given by,

$$\alpha(T_c - T_{c0}) + 2b\langle|\eta|^2\rangle_{T_c} = 0.$$

Then, the shifted value at T_c reads

$$T_c = T_{c0} - \frac{2b}{\alpha}\langle|\eta|^2\rangle_{T_c}. \qquad 2.5.8\text{-}3$$

The equation for the fluctuation field can be represented in the form

$$(a + 2b|\psi_0|^2)\eta + b\psi_0^2\eta^* + b\psi_0^*\eta^2 + (2b|\eta|^2 - 2b\langle|\eta|^2\rangle)\psi + b\eta|\eta|^2 - \sum_j K^{(j)}\,\partial_j^2\eta = 0,$$

To get the related Gaussian functional, one needs to approximate (linearize) the terms $b\psi_0^*\eta^2$, $(2b|\eta|^2 - 2b\langle|\eta|^2\rangle)\psi$, $b\eta|\eta|^2$. However, to calculate Eq. 2.5.8-3, we need to use $T = T_c$ so that $\psi_0 = 0$. In this case the equation for the fluctuation becomes

$$a\eta + b\eta|\eta|^2 - \sum_j K^{(j)}\,\partial_j^2\eta = 0. \qquad 2.5.8\text{-}4$$

Nonlinear term in η is not simply ignored in the GL equation, but is approximated to the mean-field recipe, if the product of two "operators" obeys the relation

$$\langle AB\rangle \approx \langle A\rangle \cdot \langle B\rangle,$$

then, we use the mean field approximation

$$AB = \langle A\rangle B + \langle B\rangle A - \langle A\rangle\langle B\rangle,$$

if not $AB \approx \langle AB\rangle$.

For three "operators" we have

$$ABC \cong \langle A\rangle BC + A\langle BC\rangle - \langle A\rangle\langle BC\rangle + \langle B\rangle AC + B\langle AC\rangle - \langle B\rangle\langle AC\rangle + \langle C\rangle AB + C\langle AB\rangle - \langle C\rangle\langle AB\rangle,$$

or $ABC \cong \langle ABC\rangle$, respectively

$|\eta|^2 \cong \langle|\eta|^2\rangle$,

$\eta^2 \cong \eta\langle\eta\rangle + \langle\eta\rangle\eta - \langle\eta\rangle^2$,

$$\eta|\eta|^2 = \eta\eta\eta^* \cong \langle\eta\rangle\eta\eta^* + \eta\langle\eta\eta^*\rangle - \langle\eta\rangle\langle\eta\eta^*\rangle + \langle\eta\rangle\eta\eta^* + \eta\langle\eta\eta^*\rangle - \langle\eta\rangle\langle\eta\eta^*\rangle + \langle\eta^*\rangle\eta^2 + \eta^*\langle\eta^2\rangle - \langle\eta^*\rangle\langle\eta^2\rangle \cong 2\eta\langle|\eta|^2\rangle,$$

where we keep in mind that $\langle\eta\rangle = \langle\eta^2\rangle = 0$, but $\langle|\eta|^2\rangle \neq 0$. This construction for $\eta|\eta|^2$ looks a bit tricky, however its justification is also in the final result for the shift of the critical temperature, that is known from the renormalization group analysis.

So, Eq. 2.5.8-4 becomes

$$(a + 2b\langle|\eta|^2\rangle)\eta - \sum_j K^{(j)}\,\partial_j^2\eta = 0.$$

We obtain

$$\varepsilon_+ = a + 2b\langle|\eta|^2\rangle - \sum_j K^{(j)}\,q_j^2, \qquad \varepsilon_- = 0,$$

and

$$\varepsilon_{1,\mathbf{q}} = \varepsilon_{2,\mathbf{q}} = a + 2b\langle|\eta|^2\rangle + \sum_j K^{(j)}\,q_j^2.$$

So, one finds

$$\langle|\eta^2|\rangle_{T_c} = \frac{1}{L^D}\sum_{\mathbf{q}} \frac{T_c}{a + 2b\langle|\eta^2|\rangle_{T_c} + \sum_j K^{(j)}\, q_j^2}.$$

Finally, writing in it as a function of continuous variables

$$\langle|\eta^2|\rangle_{T_c} = \int \frac{\mathrm{d}^D\mathbf{q}}{(2\pi)^D} \frac{T_c}{a + 2b\langle|\eta^2|\rangle_{T_c} + K\mathbf{q}^2}, \qquad 2.5.8\text{-}5$$

where $K = \sqrt[3]{K^{(x)}K^{(y)}K^{(z)}}$ for 3D, $K = \sqrt{K^{(x)}K^{(y)}}$ for 2D. As seen, we write $\langle|\eta^2|\rangle_{T_c}$ in terms of the isotropic model.

As $a + 2b\langle|\eta|^2\rangle_{T_c} = 0$, at $T = T_c$

$$\langle|\eta^2|\rangle_{T_c} = \int_{\Lambda_0}^{\Lambda_\infty} \frac{\mathrm{d}^D\mathbf{q}}{(2\pi)^D} \frac{T_c}{K\mathbf{q}^2}, \qquad 2.5.8\text{-}6$$

where the cutoffs are estimated as

$$\Lambda_0 = \frac{c_0}{\xi(Gi)}, \qquad \Lambda_\infty = \frac{c_\infty}{\xi_0},$$

Justified by renormalization group analysis. Here $\xi(Gi)$ is the Ginzburg-Landau length calculated at the Ginzburg-Levanyuk temperature. For $\mathbf{q} > \frac{c_\infty}{\xi_0}$ should not contribute as ξ_0 is the minimal lenght in the Ginzburg-Landau theory. $\mathbf{q} < \frac{c_0}{\xi(Gi)}$ should not make contribution as $\xi(Gi)$ is an upper limit of the coherence radius in the system. The divergence at small momenta appears at T_c.

2.5.9 T_c Shifted by fluctuations

To proceed further, we perform the calculations of the shifted temperature in the case for 3, 2 and 1 spatial dimension

1. $D = 3$:

$$\langle|\eta^2|\rangle_{T_c} = \int_{\Lambda_0}^{\Lambda_\infty} \frac{d^3\mathbf{q}}{(2\pi)^3} \frac{T_c}{K\mathbf{q}^2},$$

$$= \frac{T_c}{2\pi^2 K}\left(\frac{c_\infty}{\xi_0} - \frac{c_0}{\xi(Gi)}\right),$$

as $\xi(Gi) = \xi_0/\sqrt{Gi}$ we obtain

$$\langle|\eta^2|\rangle_{T_c} = \frac{T_c}{2\pi^2 K}\frac{c_\infty}{\xi_0}\left(1 - \frac{c_0}{c_\infty}\sqrt{Gi}\right). \quad \text{2.5.9-1}$$

Inserting in Eq. 2.5.8-3

$$T_{c0} - T_c = \frac{2b}{\alpha}\langle|\eta|^2\rangle_{T_c},$$

$$\frac{T_{c0} - T_c}{T_c} = \frac{2b}{\alpha}\frac{1}{2\pi^2 K}\frac{c_\infty}{\xi_0}\left(1 - \frac{c_0}{c_\infty}\sqrt{Gi}\right).$$

As from Eq.2.5.5-8, $Gi = \frac{1}{32\pi^2}\frac{T_{c0}b^2}{\alpha K^3}$ and $\xi_0 = \sqrt{K/\alpha T_{c0}}$, we get

$$\frac{T_{c0} - T_c}{T_c} = \frac{2b}{\alpha}\frac{1}{2\pi^2 K}\sqrt{\frac{\alpha T_{c0}}{K}}\, c_\infty\left(1 - \frac{c_0}{c_\infty}\sqrt{Gi}\right),$$

$$\frac{T_{c0} - T_c}{T_c} = \frac{c_\infty}{\pi^2}\sqrt{32\pi^2 Gi}\left(1 - \frac{c_0}{c_\infty}\sqrt{Gi}\right). \quad \text{2.5.9-2}$$

For $Gi \ll 1$ we can keep only the leading order contribution in $\sqrt{Gi}$, i.e.,

$$\frac{T_{c0} - T_c}{T_c} = \frac{c_\infty}{\pi^2}\sqrt{32\pi^2 Gi},$$

which recovers the known result of the renormalization group at $c_\infty = \sqrt{2}$,

$$\frac{T_{c0} - T_c}{T_c} = \frac{8}{\pi}\sqrt{Gi}. \quad \text{2.5.9-3}$$

2. $D = 2$:

$$\langle|\eta^2|\rangle_{T_c} = \int_{\Lambda_0}^{\Lambda_\infty} \frac{\mathrm{d}^2\mathbf{q}}{(2\pi)^2}\frac{T_c}{K\mathbf{q^2}},$$

$$\langle|\eta^2|\rangle_{T_c} = \frac{T_c}{2\pi K}\ln\left(\frac{\Lambda_\infty}{\Lambda_0}\right) = \frac{T_c}{2\pi K}\ln\left(\frac{\mathrm{c}_\infty}{\mathrm{c}_0}\frac{\xi_0}{\xi(Gi)}\right),$$

as $\xi(Gi) = \xi_0/\sqrt{Gi}$

$$\langle|\eta^2|\rangle_{T_c} = \frac{T_c}{2\pi K}\ln\left(\frac{\mathrm{c}_\infty}{\mathrm{c}_0\sqrt{Gi}}\right), \quad 2.5.9\text{-}4$$

Inserting in Eq. 2.5.8-3

$$T_{c0} - T_c = \frac{2b}{\alpha}\langle|\eta|^2\rangle_{T_c}.$$

$$\frac{T_{c0} - T_c}{T_c} = \frac{2b}{\alpha}\frac{1}{2\pi K}\ln\left(\frac{\mathrm{c}_\infty}{\mathrm{c}_0\sqrt{Gi}}\right),$$

As from Eq. 2.5.5-9, $Gi = \frac{1}{4\pi}\frac{b}{\alpha K}$, we get

$$\frac{T_{c0} - T_c}{T_c} = 4Gi\ln\left(\frac{\mathrm{c}_\infty}{\mathrm{c}_0}\frac{1}{\sqrt{Gi}}\right). \quad 2.5.9\text{-}5$$

Using $\mathrm{c}_\infty/\mathrm{c}_0 = 1/2$, we recover the renormalization group result

$$\frac{T_{c0} - T_c}{T_c} = 2Gi\ln\left(\frac{1}{4Gi}\right). \quad 2.5.9\text{-}6$$

Here the two leading terms are available $-2Gi\ln Gi$ and $-2Gi\ln 4$.

3. $D = 1$:

Our previous calculations of Gi for one dimension produced the result $Gi{\sim}1$, meaning the failure of the perturbation scheme based on the Gaussian fluctuations. For illustration we will calculate the shift of the critical temperature due to the fluctuations for $D = 1$.

$$\langle|\eta^2|\rangle_{T_c} = \int_{\Lambda_0}^{\Lambda_\infty} \frac{\mathrm{d}\mathbf{q}}{2\pi}\frac{T_c}{K\mathbf{q^2}},$$

$$\langle|\eta^2|\rangle_{T_c} = \frac{T_c}{2\pi K}\left(\frac{\xi(Gi)}{\mathrm{c}_0} - \frac{\xi_0}{\mathrm{c}_\infty}\right),$$

$$\langle|\eta^2|\rangle_{T_c} = \frac{T_c}{2\pi K}\frac{\xi_0}{c_\infty}\left(\frac{c_\infty}{c_0}\frac{1}{\sqrt{Gi}} - 1\right). \qquad 2.5.9\text{-}7$$

Inserting in Eq. 2.5.8-3 and $\xi_0 = \sqrt{K/\alpha T_{c0}}$

$$T_{c0} - T_c = \frac{2b}{\alpha}\langle|\eta|^2\rangle_{T_c},$$

$$\frac{T_{c0} - T_c}{T_c} = \frac{2b}{\alpha}\frac{1}{2\pi K}\sqrt{\frac{K}{\alpha T_{c0}}}\frac{1}{c_\infty}\left(\frac{c_\infty}{c_0}\frac{1}{\sqrt{Gi}} - 1\right),$$

$$\frac{T_{c0} - T_c}{T_c} = \frac{b}{\alpha\pi K}\sqrt{\frac{K}{\alpha T_{c0}}}\frac{1}{c_\infty}\left(\frac{c_\infty}{c_0}\frac{1}{\sqrt{Gi}} - 1\right).$$

As from Eq. 2.5.5-10, $Gi = \left(\frac{1}{128}\frac{b^2}{KT_{c0}\alpha^3}\right)^{1/3} \sim 1$, we get

$$\frac{T_{c0} - T_c}{T_c} = \frac{1}{c_\infty \pi}\sqrt{128 Gi^3}\left(\frac{c_\infty}{c_0}\frac{1}{\sqrt{Gi}} - 1\right). \qquad 2.5.9\text{-}8$$

$$\frac{T_{c0} - T_c}{T_c} = \underbrace{Gi}_{\sim 1}\left(\underbrace{\frac{\sqrt{128}}{\pi c_0}}_{\sim 1} - \underbrace{\frac{\sqrt{128}}{\pi c_\infty}\sqrt{Gi}}_{\sim 1}\right).$$

which is certainly beyond the perturbation theory, fluctuations are huge, and we cannot invoke any framework based on the gaussian picture of fluctuation.

3 EGL FORMALISM FOR MULTIBAND SUPERCONDUCTORS

3.1 FORMALISM

The GL theory distinguishes ideally diamagnetic type I and type II, where the paramagnetic contribution results in the mixed state with an Abrikosov lattice of single-quantum vortices. The boundary between types I and II, in the GL picture, is the temperature-independent line $\kappa = \kappa_0 = 1/\sqrt{2}$, in the κ-T plane [75], [76], [44]. However, this picture is valid only in the limit $T \to T_c$, while below T_c there is a finite temperature-dependent interval of κ's, separating types I and II. Thus, there is a finite domain of the crossover between types I and II in κ-Tplane [61], [51], [52], [60], [81], which is referred as intertype (IT) domain. Inside this domain, the system exhibits a nonstandard field dependence on the magnetization [77]-[80] with unconventional configurations of the mixed state [65], [85], [88], governed by long-range attraction of vortices [80], [81], [60], and many-vortices interactions [63].

In this work, we employed the M-band extension of the two-band BCS model introduced in [1], [2], with the s-wave pairing in all contributing bands and the Josephson like, Cooper-pair transfer between the bands (tunneling from one band to another), a system in the clean limit and that all available bands have a parabolic single-particle energy dispersion and spherical Fermi surfaces. The pairing is controlled by the symmetric real coupling matrix $\check{g}$, with the elements $g_{\nu\nu'}$.

To describe the finite IT domain, we should go beyond the GL theory. Solving microscopic equations for a nonuniform problem with an external magnetic field is a time consuming and rather involved task. However, to reach the objective of our sturdy, it is enough to use a perturbative expansion of these equations in $\tau = 1 - T/T_c$ to one order beyond the GL theory, i.e., the extended GL approach [35]. Here, we generalize the EGL formalism, developed previously for single- and two-band superconductors, to the case of an arbitrary number of contributing bands [35].

3.2 MULTIBAND NEUMANN-TEWORDT FUNCTIONAL

First of all, to construct our formalism we start with constructing a multiband Neumann-Tewordt functional [92], [93]. The NT functional is obtained from the microscopic expression for the condensate free energy by accounting for higher powers and higher gradients of the band-dependent gap functions $\Delta_\nu = \Delta_\nu(\boldsymbol{x})$, as compared to the GL functional. Only the terms giving the GL theory and its leading corrections are taken into account. The general expression for the free energy density of M-band s-wave superconductor, relative to the normal state at zero field, is given by [36], [35].

$$f = \frac{\mathbf{B}^2}{8\pi} + \vec{\Delta}^\dagger \breve{g}^{-1} \vec{\Delta} + \sum_{\nu=1}^{M} f_\nu[\Delta_\nu], \quad 3.2\text{-}1$$

where $\mathbf{B}$ denotes the magnetic field, the vector $\vec{\Delta}^T = (\Delta_1, \Delta_2, \dots, \Delta_M)$ comprises the band order parameters $\Delta_\nu = \Delta_\nu(\boldsymbol{x})$, and the functional $f_\nu[\Delta_\nu]$ reads

$$f_\nu = -\sum_{n=0}^{\infty} \frac{1}{n+1} \int \prod_{j=1}^{2n+1} d^3\boldsymbol{y}_j \, K_{\nu,2n+1}(\boldsymbol{x}, \{\boldsymbol{y}\}_{2n+1}) \times \Delta_\nu^*(\boldsymbol{x}) \Delta_\nu(\boldsymbol{y}_1) \dots \Delta_\nu^*(\boldsymbol{y}_{2n}) \Delta_\nu(\boldsymbol{y}_{2n+1}), \quad 3.2\text{-}2$$

with $\{\boldsymbol{y}\}_{2n+1} = \{\boldsymbol{y}_1, \dots, \boldsymbol{y}_{2n+1}\}$. The integral kernel in Eq. (3.2-2) is given by (m is odd)

$$K_{\nu,m}(\boldsymbol{x}, \{\boldsymbol{y}\}_m) = -T \sum_{\omega} \mathcal{G}_{\nu,\omega}^{(B)}(\boldsymbol{x}, \boldsymbol{y}_1) \bar{\mathcal{G}}_{\nu,\omega}^{(B)}(\boldsymbol{y}_1, \boldsymbol{y}_2) \dots \times \mathcal{G}_{\nu,\omega}^{(B)}(\boldsymbol{y}_{m-1}, \boldsymbol{y}_m) \bar{\mathcal{G}}_{\nu,\omega}^{(B)}(\boldsymbol{y}_m, \boldsymbol{x}), \quad 3.2\text{-}3$$

where ω is the fermionic Matsubara frequency, $\mathcal{G}_{\nu,\omega}^{(B)}(\boldsymbol{x}, \boldsymbol{y})$ is the Fourier transform of the normal Green function calculated in the presence of the magnetic field and $\bar{\mathcal{G}}_{\nu,\omega}^{(B)}(\boldsymbol{x}, \boldsymbol{y}) = -\mathcal{G}_{\nu,-\omega}^{(B)}(\boldsymbol{y}, \boldsymbol{x})$. For $\mathcal{G}_{\nu,\omega}^{(B)}(\boldsymbol{x}, \boldsymbol{y})$ we employ the standard approximation enough to derive the extended GL theory

$$\mathcal{G}_{\nu,\omega}^{(B)}(\boldsymbol{x}, \boldsymbol{y}) = \exp\left[i \frac{e}{\hbar c} \int_{\boldsymbol{y}}^{\boldsymbol{x}} \mathbf{A}(\boldsymbol{z}) \cdot d\boldsymbol{z} \right] \mathcal{G}_{\nu,\omega}^{(0)}(\boldsymbol{x}, \boldsymbol{y}), \quad 3.2\text{-}4$$

where the integral in the exponent is taken along the trajectory of a charge carrier in a magnetic field with the vector potential $\mathbf{A}$. The Green function for zero magnetic field is written as

$$\mathcal{G}^{(0)}_{\nu,\omega}(\boldsymbol{x},\boldsymbol{y}) = \int \frac{d^3\boldsymbol{k}}{(2\pi)^3}\frac{\exp[i\boldsymbol{k}\cdot(\boldsymbol{x}-\boldsymbol{y})]}{i\hbar\omega - \xi_\nu(\boldsymbol{k})}, \qquad 3.2\text{-}5$$

where the band-dependent single-particle energy dispersion reads

$$\xi_\nu(\boldsymbol{k}) = \xi_\nu(0) + \frac{\hbar^2\boldsymbol{k}^2}{2m_\nu} - \mu, \qquad 3.2\text{-}6$$

with m_ν the band effective mass, $\xi_\nu(0)$ the band lower energy and μ the chemical potential.

We invoke the gradient expansion for the gap functions and the vector potential in order to obtain a partial differential equation structure

$$\begin{aligned} \Delta_\nu(\boldsymbol{y}) &= \Delta_\nu(\boldsymbol{x}) + \big((\boldsymbol{y}-\boldsymbol{x})\cdot\boldsymbol{\nabla}_{\vec{x}}\big)\Delta_\nu(\boldsymbol{x}) + \cdots, \\ \mathbf{A}(\boldsymbol{y}) &= \mathbf{A}(\boldsymbol{x}) + \big((\boldsymbol{y}-\boldsymbol{x})\cdot\boldsymbol{\nabla}_{\vec{x}}\big)\mathbf{A}(\boldsymbol{x}) + \cdots. \end{aligned} \qquad 3.2\text{-}7$$

So, it is possible to represent the non-local integrals in the functional f_ν as a series in powers of Δ_ν, its gradients and field spatial derivatives. The series is infinite so that a truncation procedure is needed. For example, to get the GL formalism, the standard Gor'kov truncation is employed [94]. To incorporate the leading corrections to the GL formalism, one needs to go beyond the Gor'kov truncation and obtain a multiband generalization of the Neumann-Tewordt functional [92][93][35]. As the form of f_ν is not sensitive to the number of contributing bands, one can utilize the previous results for the two-band case [35][61]. Then, the multiband Neumann-Tewordt functional reads

$$\begin{aligned} f = \frac{\mathbf{B}^2}{8\pi} &+ \vec{\Delta}^\dagger \check{g}^{-1}\vec{\Delta} \\ &+ \sum_{\nu=1}^{M}\Bigg\{\left[\mathcal{A}_\nu + a_\nu\left(\tau + \frac{\tau^2}{2}\right)\right]|\Delta_\nu|^2 + \frac{b_\nu}{2}(1+2\tau)|\Delta_\nu|^4 - \frac{c_\nu}{3}|\Delta_\nu|^6 \\ &+ K_\nu(1+2\tau)|\mathbf{D}\Delta_\nu|^2 - Q_\nu\left(|\mathbf{D}^2\Delta_\nu|^2 + \frac{1}{3}\mathrm{rot}\mathbf{B}\cdot\boldsymbol{i}_\nu + \frac{4e^2}{\hbar^2c^2}\mathbf{B}^2|\Delta_\nu|^2\right) \\ &- \frac{L_\nu}{2}\left[8|\Delta_\nu|^2|\mathbf{D}\Delta_\nu|^2 + \left(\Delta_\nu^{*2}(\mathbf{D}\Delta_\nu)^2 + \text{c.c.}\right)\right]\Bigg\}, \end{aligned} \qquad 3.2\text{-}8$$

where $\mathbf{D} = \boldsymbol{\nabla} - \mathrm{i}\frac{2e}{\hbar c}\mathbf{A}$, $\boldsymbol{i}_\nu = \frac{2e}{\hbar\, c}[\Delta_\nu \mathbf{D}^* \Delta_\nu^* - \Delta_\nu^* \mathbf{D} \Delta_\nu]$ and the band dependent coefficients are given by

$$\mathcal{A}_\nu = N_\nu \ln\left(\frac{2^\Gamma \hbar\omega_c}{\pi T_c}\right), \qquad a_\nu = -N_\nu, \qquad b_\nu = N_\nu \frac{7\zeta(3)}{8\pi^2 T_c^2}, \qquad c_\nu = N_\nu \frac{93\zeta(5)}{128\pi^4 T_c^4},$$

$$K_\nu = \frac{b_\nu}{6}\hbar^2 v_\nu^2, \qquad Q_\nu = \frac{c_\nu}{30}\hbar^4 v_\nu^4, \qquad L_\nu = \frac{c_\nu}{9}\hbar^2 v_\nu^2,$$

where ω_c is the cut-off frequency, N_ν is the band DOS, v_ν denotes the band Fermi velocity, T_c is in the energy units, $\zeta(\cdots)$ the Riemann zeta-function and Γ the Euler constant.

At first sight the Neumann-Tewordt approach is a natural and straightforward extension of the GL theory. The initial motivation of its derivation was to construct a formalism that goes beyond the GL theory but preserves, to some practical extent, useful relative simplicity of the GL formalism, especially in the case of spatially nonuniform problems with an external magnetic field. However, highly nonlinear equations for the stationary solution of the Neumann-Tewordt extension of the GL theory are, in fact, not easier than the exact microscopic equations, see, e.g., Eq. (3) in Ref. [95]. Furthermore, it was demonstrated that the Neumann-Tewordt functional can lead to unphysical results [95] such as weakly damped oscillations of the order parameter for a single-vortex solution. This problem is related to the fact that the Neumann-Tewordt free energy is not bound from below, as the coefficients c_ν, Q_ν, and L_ν are positive.

It was suggested for the single-band case (see Ref. [95] and references therein) that to remedy the problem, the Neumann-Tewordt functional should be restructured by applying the perturbative τ-expansion. The point is that the stationary solution for the order parameter within the Neumann-Tewordt approach contains all odd powers of $\tau^{1/2}$ while the truncation of the infinite series in Eq.(3.2-3) does not distort only the two lowest orders τ (the GL term) and $\tau^{3/2}$ (the leading correction to the GL term). Incomplete (distorted) higher-order terms in τ cause the problem and should be removed by using the τ-expansion. When removing these terms, the unphysical results disappear[95]. A similar situation should be, of course, expected in the multiband case, for the functional given by Eq. (3.2-8).

3.3 EXTENDED GINZBURG-LANDAU THEORY AND τ-EXPANSION

In order to obtain a consistent extension of the GL theory for multiband superconductors, as mentioned above, the Neumann-Tewordt functional [92], [93] should be restructured by applying the perturbative expansion in powers of τ and keeping only the lowest and next-to-lowest order contributions to the band order parameters (and also to the field), eliminating higher-order contributions. For single-band superconductors such eliminating procedure can be found in Refs. [95] and [61]. For two-band superconductors the extended GL theory has been developed in Ref. [61]. Here we generalize the consideration of this theory and investigate the τ-expansion of the functional given by Eq. (3.2-8) for an arbitrary number of contributing bands M.

When employing the τ-expansion, the band order parameters and fields are sought as series in τ given by [61]

$$\Delta_\nu = \tau^{1/2}\left(\Delta_\nu^{(0)} + \tau\Delta_\nu^{(1)} + \cdots\right),$$

$$\mathbf{A} = \tau^{1/2}\left(\mathbf{A}^{(0)} + \tau\mathbf{A}^{(1)} + \cdots\right),$$

$$\mathbf{B} = \tau\left(\mathbf{B}^{(0)} + \tau\mathbf{B}^{(1)} + \cdots\right). \quad 3.3\text{-}1$$

To obtain explicitly the τ-dependence of spatial derivatives, one needs to apply the spatial coordinate scaling $\boldsymbol{x}' = \tau^{1/2}\boldsymbol{x}$. Below the prime is suppressed for simplicity, unless it causes any confusion. Notice that to get the stationary solution in the two lowest orders in τ, one also needs to operate with $\Delta_\nu^{(2)}$ but only in intermediate expressions

Inserting Eq. (3.3-1) in Eq. (3.2-8), one obtains

$$f = \tau^2\left[\tau^{-1}f^{(-1)} + f^{(0)} + \tau f^{(1)} + \cdots\right], \quad 3.3\text{-}2$$

The two lowest orders in the band gap functions and the field produce three lowest orders in the free energy but, as is shown below, the contribution $f^{(-1)}$ is zero for the stationary point. In Eq. (3.3-2) we have

$$f^{(-1)} = \vec{\Delta}^{(0)\dagger}\check{L}\vec{\Delta}^{(0)}, \quad 3.3\text{-}3$$

where $\vec{\Delta}^{(0)T} = \left(\Delta_1^{(0)},\ \Delta_2^{(0)},\ \ldots\right)$ and the matrix $\check{L}$ has the elements

$$L_{\nu\nu'} = g_{\nu\nu'}^{-1} - \mathcal{A}_\nu\delta_{\nu\nu'}, \quad 3.3\text{-}4$$

with $g^{-1}_{\nu\nu'}$ the matrix element of $\breve{g}^{-1}$ and $\delta_{\nu\nu'}$ the discrete delta-function. The contribution $f^{(0)}$ is of the form

$$f^{(0)} = \frac{\mathbf{B}^{(0)2}}{8\pi} + \left(\vec{\Delta}^{(0)\dagger}\breve{L}\vec{\Delta}^{(0)} + c.c.\right) + \sum_{\nu=1}^{M} f_\nu^{(0)}, \quad 3.3\text{-}5$$

where $f_\nu^{(0)}$ is given by

$$f_\nu^{(0)} = a_\nu\left|\Delta_\nu^{(0)}\right|^2 + \frac{b_\nu}{2}\left|\Delta_\nu^{(0)}\right|^4 + K_\nu\left|\mathbf{D}^{(0)}\Delta_\nu^{(0)}\right|^2, \quad 3.3\text{-}6$$

with $\mathbf{D}^{(0)} = \boldsymbol{\nabla} - \mathrm{i}\frac{2e}{\hbar c}\mathbf{A}^{(0)}$. Finally, for the highest-order term in Eq. (3.3-2) we obtain

$$f^{(1)} = \frac{\left(\mathbf{B}^{(0)}\cdot\mathbf{B}^{(1)}\right)}{4\pi} + \left(\vec{\Delta}^{(0)\dagger}\breve{L}\vec{\Delta}^{(2)} + c.c.\right) + \vec{\Delta}^{(1)\dagger}\breve{L}\vec{\Delta}^{(1)} + \sum_{\nu=1}^{M} f_\nu^{(1)}, \quad 3.3\text{-}7$$

where,

$$\begin{aligned} f_\nu^{(1)} = &\left(a_\nu + b_\nu\left|\Delta_\nu^{(0)}\right|^2\right)\left(\Delta_\nu^{(0)*}\Delta_\nu^{(1)} + c.c.\right) + \frac{a_\nu}{2}\left|\Delta_\nu^{(0)}\right|^2 + b_\nu\left|\Delta_\nu^{(0)}\right|^4 \\ &- \frac{c_\nu}{3}\left|\Delta_\nu^{(0)}\right|^6 + 2K_\nu\left|\mathbf{D}^{(0)}\Delta_\nu^{(0)}\right|^2 \\ &+ K_\nu\left[\left(\mathbf{D}^{(0)}\Delta_\nu^{(0)}\cdot\mathbf{D}^{(0)*}\Delta_\nu^{*(1)} + c.c.\right) - \mathbf{A}^{(1)}\cdot\boldsymbol{i}_\nu^{(0)}\right] \\ &- Q_\nu\left\{\left|\mathbf{D}^{(0)2}\Delta_\nu^{(0)}\right|^2 + \frac{1}{3}\left(\boldsymbol{\nabla}\times\mathbf{B}^{(0)}\cdot\boldsymbol{i}_\nu^{(0)}\right) + \frac{4e^2}{\hbar^2 c^2}\mathbf{B}^{(0)2}\left|\Delta_\nu^{(0)}\right|^2\right\} \\ &- \frac{L_\nu}{2}\left\{8\left|\Delta_\nu^{(0)}\right|^2\left|\mathbf{D}^{(0)}\Delta_\nu^{(0)}\right|^2 + \left[\Delta_\nu^{(0)2}\left(\mathbf{D}^{(0)*}\Delta_\nu^{(0)*}\right)^2 + c.c.\right]\right\}, \end{aligned} \quad 3.3\text{-}8$$

and $\boldsymbol{i}_\nu^{(0)} = \mathrm{i}\frac{2e}{\hbar c}\left[\Delta_\nu^{(0)}\mathbf{D}^{(0)*}\Delta_\nu^{(0)*} - \Delta_\nu^{(0)*}\mathbf{D}^{(0)}\Delta_\nu^{(0)}\right]$ is the lowest-order term in the τ-expansion of the current, $\boldsymbol{i}_\nu$.

To calculate the boundaries of the IT domain, the free energy at the stationary point is needed. The equation for the stationary solution of the extended GL formalism is obtained by calculating the functional derivatives of the free energy $\mathcal{F}$ with the density given by Eq. (3.3-2). As the latter is a series in τ, the stationary solution is specified by a set of equations associated with different order contributions in τ. So, taking the lowest order in Eq. (3.3-2) the corresponding equation for the stationary solution reads

$$\frac{\delta \mathcal{F}^{(-1)}}{\delta \vec{\Delta}^{(0)\dagger}} = \check{L}\vec{\Delta}^{(0)} = 0, \qquad 3.3\text{-}9$$

where $\mathcal{F}^{(-1)}$ is the contribution to the free-energy corresponding to $f^{(-1)}$. This equation has a nontrivial solution for $\vec{\Delta}^{(0)}$ only when

$$\det \check{L} = 0, \qquad 3.3\text{-}10$$

As $\check{L}$ includes $\mathcal{A}_\nu$ and, hence, depends on T_c, Eq. (3.3-10) gives zeros of an M degree polynomial function of a single indeterminate $\ln\left(\frac{2^\gamma \hbar\omega_c}{\pi T_c}\right)$. The minimal zero of this polynomial should be chosen, to get the maximal critical temperature. Once T_c is determined, it is convenient to introduce the eigenvalues and eigenvectors of $\check{L}$ as

$$\check{L}\vec{\epsilon} = 0, \qquad 3.3\text{-}11$$

for the zero eigenvalue and

$$\check{L}\vec{\eta}_i = \Lambda_i \vec{\eta}_i, \qquad 3.3\text{-}12$$

for the nonzero eigenvalues $\Lambda_i \neq 0$. As the matrix $\check{L}$ is real and symmetric, the vectors $\vec{\epsilon}$ and $\vec{\eta}_i$ can be chosen such that $\vec{\epsilon}^\dagger\vec{\epsilon} = 1$, $\vec{\epsilon}^\dagger\vec{\eta}_i = 0$ and $\vec{\eta}_i^\dagger\vec{\eta}_j = \delta_{ij}$. We note that in principle, the zero eigenvalue can be degenerate, and, in this case, there exist more than one corresponding eigenvectors. This occurs when the superconducting system of interest has a symmetry, additional to $U(1)$ and the superconducting properties in the GL domain are governed by a multi-component order parameter, see details in Refs. [61] and [68]. For our investigation, however, it is enough to consider the standard nondegenerate formalism (all eigenvalues are nondegenerate). Then, from Eqs. (3.3-9) and (3.3-11) one obtains

$$\vec{\Delta}^{(0)} = \Psi(\boldsymbol{x})\vec{\epsilon}, \qquad 3.3\text{-}13$$

where $\Psi(\boldsymbol{x})$ is a single-component Landau order parameter of the M band superconductor being discussed. Here we recall that the number of the Landau order parameter components is determined by the dimension of the irreducible representation of the corresponding symmetry group [75] (rather than by the number of the available bands). Equation (3.3-9) assures that spatial profiles of all band condensates are controlled by the same position dependent function $\Psi(\boldsymbol{x})$ ($\vec{\epsilon}$ does not depend on $\boldsymbol{x}$ but it does not give any information about Ψ. To get an equation for Ψ, one needs to address the next order contribution to the free energy.

The next-to-lowest order term in Eq. (3.3-2) yields two equations for the stationary solution. The first one is given by

$$\frac{\delta \mathcal{F}^{(0)}}{\delta \vec{\Delta}^{(0)\dagger}} = \check{L}\vec{\Delta}^{(1)} + \vec{W}\left[\vec{\Delta}^{(0)}\right] = 0, \qquad 3.3\text{-}14$$

where $\mathcal{F}^{(0)}$ is the contribution to the free-energy corresponding to $f^{(0)}$ and the components of $\vec{W}\left[\vec{\Delta}^{(0)}\right]$ are

$$W_\nu = a_\nu \Delta_\nu^{(0)} + b_\nu \Delta_\nu^{(0)} \left|\Delta_\nu^{(0)}\right|^2 - K_\nu \mathbf{D}^{(0)2}\Delta_\nu^{(0)}. \qquad 3.3\text{-}15$$

The second equation is given by

$$\frac{\delta \mathcal{F}^{(0)}}{\delta \mathbf{A}^{(0)}} = \frac{1}{4\pi}\operatorname{rot}\mathbf{B}^{(0)} - \sum_{\nu=1}^{M} K_\nu \boldsymbol{i}_\nu^{(0)} = 0. \qquad 3.3\text{-}16$$

The equation $\frac{\delta \mathcal{F}^{(0)}}{\delta \vec{\Delta}^{(1)\dagger}} = 0$ is the same as Eq. (3.3-9) and $\frac{\delta \mathcal{F}^{(0)}}{\delta \mathbf{A}^{(1)}} = 0$ is trivial because $f^{(0)}$ does not depend of $\mathbf{A}^{(1)}$.

Projecting Eq. (3.3-14) on $\vec{\epsilon}$ and keeping in mind that $\vec{\epsilon}^{\dagger}\check{L} = 0$, we obtain $\vec{\epsilon}^{\dagger}\vec{\mathrm{W}} = 0$, which is written in the explicit form as

$$\sum_{\nu}^{M} \epsilon_\nu^* \left[a_\nu \Delta_\nu^{(0)} + b_\nu \Delta_\nu^{(0)} \left|\Delta_\nu^{(0)}\right|^2 - K_\nu \mathbf{D}^{(0)2}\Delta_\nu^{(0)}\right] = 0, \qquad 3.3\text{-}17$$

where ϵ_ν is the band component of $\vec{\epsilon}$. Taking into account that the stationary solution obeys Eq.(3.3-13), we get $\Delta_\nu^{(0)} = \epsilon_\nu \Psi$, and Eq. (3.3-17) becomes

$$a\Psi + b\Psi|\Psi|^2 - K\mathbf{D}^{(0)2}\Psi = 0, \qquad 3.3\text{-}18$$

which is formally the equation for a single-component GL theory, however, the coefficient a, b and K are averages over the contributing bands

$$a = \sum_{\nu=1}^{M} a_\nu |\epsilon_\nu|^2, \qquad b = \sum_{\nu=1}^{M} b_\nu |\epsilon_\nu|^4, \qquad K = \sum_{\nu=1}^{M} K_\nu |\epsilon_\nu|^2. \qquad 3.3\text{-}19$$

Similarly, using $\Delta_\nu^{(0)} = \epsilon_\nu \Psi$, Eq. (3.3-16) becomes

$$\operatorname{rot}\mathbf{B}^{(0)} = 4\pi K \boldsymbol{i}_\Psi^{(0)}, \qquad 3.3\text{-}20$$

where $\boldsymbol{i}_\Psi^{(0)} = \mathrm{i}\frac{2e}{\hbar c}\left[\Psi \mathbf{D}^{(0)*}\Psi^* - \Psi^* \mathbf{D}^{(0)}\Psi\right]$, is obtained from $\vec{\imath}_\nu^{(0)}$ by substituting $\Delta_\nu^{(0)}$ for Ψ.

Equations (3.3-18) and (3.3-20) are the standard equations for the single-component GL theory. The presence of multiple bands is reflected only in the expressions for the coefficients a, b and K. Each of these coefficients is given by the summation over the M available bands with the band contributions controlled by the components of $\vec{\epsilon}$.

We have investigated only one projection of Eq. (3.3-14). To explore other projections (on $\vec{\eta}_i$, we need to expand $\vec{\Delta}^{(1)}$ as

$$\vec{\Delta}^{(1)} = \Phi\vec{\epsilon} + \sum_{i=1}^{M-1} \Phi_i \vec{\eta}_i, \tag{3.3-21}$$

where we introduce the new position dependent functions $\Phi(\boldsymbol{x})$ and $\Phi_\mathrm{i}(\boldsymbol{x})$ $[\mathrm{i} = 1, \dots, \mathrm{M} - 1]$. So, we can insert Eq. (3.3-21) in Eq. (3.3-14),

$$\check{L}\vec{\Delta}^{(1)} + \vec{W}\big[\vec{\Delta}^{(0)}\big] = 0, \tag{3.3-22}$$

$$\check{L}\left(\Phi\vec{\epsilon} + \sum_{i=1}^{M-1} \Phi_i \vec{\eta}_i\right) + \vec{W}\big[\vec{\Delta}^{(0)}\big] = 0, \tag{3.3-23}$$

$$\sum_{i=1}^{M-1} \Lambda_i \Phi_i \vec{\eta}_i + \vec{W}\big[\vec{\Delta}^{(0)}\big] = 0. \tag{3.3-24}$$

And, projecting Eq. (3.3-24) into $\vec{\eta}_j$, we obtain

$$\vec{\eta}_j^{\dagger}\left\{\sum_{i=1}^{M-1} \Lambda_i \Phi_i \vec{\eta}_i + \vec{W}\big[\vec{\Delta}^{(0)}\big]\right\} = 0,$$

$$\Phi_j = -\frac{1}{\Lambda_j}\left(\alpha_j \Psi + \beta_j \Psi|\Psi|^2 + \Gamma_j \vec{D}^{(0)2}\Psi\right), \tag{3.3-25}$$

where the coefficients α_j, β_j and Γ_j are of the form

$$\alpha_j = \sum_{\nu=1}^{M} a_\nu \eta_{j\nu}^* \epsilon_\nu, \qquad \beta_j = \sum_{\nu=1}^{M} b_\nu \eta_{j\nu}^* \epsilon_\nu |\epsilon_\nu|^2, \qquad \Gamma_j = \sum_{\nu=1}^{M} K_\nu \eta_{j\nu}^* \epsilon_\nu, \tag{3.3-26}$$

and $\eta_{j\nu}$ are the components of $\vec{\eta}_j$. Equations (3.3-21), (3.3-25) and (3.3-26) can be compared with the corresponding expressions for the two-band formalism in Ref. [61]. Here, however, one should keep in mind that the present formalism involves the orthonormal set of the vectors $\vec{\epsilon}$ and $\vec{\eta}_j$ while $\vec{\Delta}^{(1)}$ in Ref. [35] was represented as a linear combination of two explicitly chosen vectors that were not normalized and orthogonal. Therefore, to recover the expression for $\vec{\Delta}^{(1)}$ in Ref. [35]it is not enough to insert $N = 2$ in Eqs. (3.3-21) and (3.3-25). One should also express the vectors defined by Eqs. (3.3-11) and (3.3-12) in terms of those of Ref. [35].

Thus, considering the two lowest order contributions to the free energy makes it possible to derive the equations for $\vec{\Delta}^{(0)}$ and $\mathbf{B}^{(0)}\left[\mathbf{A}^{(0)}\right]$ and also algebraic expressions for the $M-1$ functions Φ_i that determine the second term in Eq. (3.3-21) for $\vec{\Delta}^{(1)}$. To find the remaining part of $\vec{\Delta}^{(1)}$, involving Φ and $\mathbf{A}^{(1)}$, one needs to investigate functional derivatives of the free-energy term corresponding to $f^{(1)}$. However, it is shown below that Φ and $\mathbf{A}^{(1)}$ do not contribute to the boundaries of the IT domain in the next-to-lowest order in τ (and, of course, in the lowest order as well). Therefore, the equations for Φ and $\mathbf{A}^{(1)}$ are beyond the scope of the present study.

3.4 FREE ENERGY AT THE STATIONARY POINT AND THERMODYNAMIC CRITICAL FIELD

To pursue our goal, the Eqs. (3.3-9), (3.3-14) and (3.3-16) [and the related ones (3.3-18), (3.3-20) and (3.3-25)] are necessary to find the free energy density for the stationary solution, and, in addition, to obtain the thermodynamic critical field which is also used in calculations of the IT domain. When inserting the stationary solution, the free energy density reads

$$f_{st} = \tau^2\left[f_{st}^{(0)} + \tau f_{st}^{(1)} + \cdots\right], \qquad 3.4\text{-}1$$

where the term of the order τ^{-1} is absent by the virtue of Eq. (3.3-9). The lowest order term in Eq. (3.4-1) is given by

$$f_{st}^{(0)} = \frac{\mathbf{B}^{(0)2}}{8\pi} + a|\Psi|^2 + \frac{b}{2}|\Psi|^4 + K\left|\mathbf{D}^{(0)}\Psi\right|^2, \qquad 3.4\text{-}2$$

where it is considered that $\vec{\Delta}^{(0)\dagger}\check{L}\vec{\Delta}^{(1)} = 0$,which follows from Eq. (3.3-9).

To simplify the expression for $f_{st}^{(1)}$, we first rearrange the terms in $f^{(1)}$ that include $\Delta_\nu^{(1)}$ and $\Delta_\nu^{*(1)}$. As the free energy is needed rather than the free-energy density,

we can utilize the substitution

$$-\Delta_\nu^{*(1)}\mathbf{D}^{(0)2}\Delta_\nu^{(0)} \rightarrow \mathbf{D}^{(0)}\Delta_\nu^{(0)} \cdot \mathbf{D}^{(0)*}\Delta_\nu^{(1)*}, \qquad 3.4\text{-}3$$

which is correct up to a vanishing surface integral in the free energy. Based on Eq. (3.4-3), the sum of the terms involving $\Delta_\nu^{(1)}$ and $\Delta_\nu^{*(1)}$ can be represented for the stationary solution as

$$\vec{\Delta}^{(1)\dagger}\breve{L}\vec{\Delta}^{(1)}+\sum_{\nu=1}^{M}\left[\left(a_\nu+b_\nu\left|\Delta_\nu^{(0)}\right|^2\right)\left(\Delta_\nu^{(1)*}\Delta_\nu^{(0)}+c.c.\right)\right.$$
$$\left.+K_\nu\left(\mathbf{D}^{(0)}\Delta_\nu^{(0)}\cdot\mathbf{D}^{(0)*}\Delta_\nu^{*(1)}+c.c.\right)\right]=$$

$$\vec{\Delta}^{(1)\dagger}\breve{L}\vec{\Delta}^{(1)}+\sum_{\nu=1}^{M}\left[\left(a_\nu+b_\nu\left|\Delta_\nu^{(0)}\right|^2\right)\left(\Delta_\nu^{(1)*}\Delta_\nu^{(0)}+c.c.\right)\right.$$
$$\left.-K_\nu\left(\Delta_\nu^{*(1)}\mathbf{D}^{(0)2}\Delta_\nu^{(0)}+c.c.\right)\right]=$$

$$\vec{\Delta}^{(1)\dagger}\breve{L}\vec{\Delta}^{(1)}+\vec{\Delta}^{(1)\dagger}\vec{W}+\vec{W}^{\dagger}\vec{\Delta}^{(1)}=-\vec{\Delta}^{(1)\dagger}\breve{L}\vec{\Delta}^{(1)},\qquad 3.4\text{-}4$$

where Eq. (3.3-14) was considered to find the relation. Using Eqs. (3.3-17) and (3.3-24), we obtain

$$\vec{\Delta}^{(1)\dagger}\breve{L}\vec{\Delta}^{(1)}=\vec{\Delta}^{(1)\dagger}\breve{L}\left(\Phi\vec{\epsilon}+\sum_{j=1}^{M-1}\Phi_j\vec{\eta}_j\right),$$

$$\vec{\Delta}^{(1)\dagger}\breve{L}\vec{\Delta}^{(1)}=\left(\Phi\vec{\epsilon}+\sum_{i=1}^{M-1}\Phi_i\vec{\eta}_i\right)^{\dagger}\left(\sum_{j=1}^{M-1}\Phi_j\Lambda_j\vec{\eta}_j\right),$$

$$\vec{\Delta}^{(1)\dagger}\breve{L}\vec{\Delta}^{(1)}=\sum_{i=1}^{M-1}\Lambda_i|\Phi_i|^2,$$

and

$$\mathbf{D}^{(0)2}\Psi=-\frac{a}{K}\Psi-\frac{b}{K}\Psi|\Psi|^2,$$

so,

$$\Phi_j=-\frac{1}{\Lambda_j}\left[\alpha_j\Psi+\beta_j\Psi|\Psi|^2-\Gamma_j\left(\frac{a}{K}\Psi+\frac{b}{K}\Psi|\Psi|^2\right)\right],$$

$$\Phi_j=-\frac{1}{\Lambda_j}\left[\left(\alpha_j-\Gamma_j\frac{a}{K}\right)\Psi+\left(\beta_j-\Gamma_j\frac{b}{K}\right)\Psi|\Psi|^2\right],$$

$$\Phi_j=-\frac{1}{\Lambda_j}\left[a\left(\frac{\alpha_j}{a}-\frac{\Gamma_j}{K}\right)\Psi+b\left(\frac{\beta_j}{b}-\frac{\Gamma_j}{K}\right)\Psi|\Psi|^2\right],$$

finally, we obtain

$$\vec{\Delta}^{(1)\dagger}\check{L}\vec{\Delta}^{(1)} = |\Psi|^2 \sum_{i=1}^{M-1} \frac{a^2|\bar{\alpha}_i|^2}{\Lambda_i} + |\Psi|^6 \sum_{i=1}^{M-1} \frac{b^2|\bar{\beta}_i|^2}{\Lambda_i} + |\Psi|^4 \sum_{i=1}^{M-1} \frac{ab(\bar{\alpha}_i^*\bar{\beta}_i + c.c.)}{\Lambda_i}, \quad 3.4\text{-}5$$

where the dimensionless parameters $\bar{\alpha}_i$ and $\bar{\beta}_i$ are defined as

$$\bar{\alpha}_i = \frac{\alpha_i}{a} - \frac{\Gamma_i}{K}, \qquad \bar{\beta}_i = \frac{\beta_i}{b} - \frac{\Gamma_i}{K}. \quad 3.4\text{-}6$$

Then, $f^{(1)}$ given by Eqs. (3.3-7) and (3.3-8), can be represented for the stationary solution in the form

$$\begin{aligned} f_{st}^{(1)} = &\frac{\mathbf{B}^{(0)}\cdot\mathbf{B}^{(1)} - \mathbf{A}^{(1)}\cdot \operatorname{rot}\mathbf{B}^{(0)}}{4\pi} + \left(\frac{a}{2} - \sum_{i=1}^{M-1}\frac{a^2|\bar{\alpha}_i|^2}{\Lambda_i}\right)|\Psi|^2 \\ &+ \left(b - \sum_{i=1}^{M-1}\frac{ab(\bar{\alpha}_i^*\bar{\beta}_i + c.c.)}{\Lambda_i}\right)|\Psi|^4 - \left(\frac{c}{3} + \sum_{i=1}^{M-1}\frac{b^2|\bar{\beta}_i|^2}{\Lambda_i}\right)|\Psi|^6 \\ &+ 2K\left|\mathbf{D}^{(0)}\Psi\right|^2 \\ &- Q\left[\left|\mathbf{D}^{(0)2}\Psi\right|^2 + \frac{1}{3}\operatorname{rot}\mathbf{B}^{(0)}\cdot \boldsymbol{i}_\Psi^{(0)} + \frac{4e^2\mathbf{B}^{(0)2}}{\hbar^2 c^2}|\Psi|^2\right] \\ &- \frac{L}{2}\left\{8|\Psi|^2\left|\mathbf{D}^{(0)}\Psi\right|^2 + \left[\Psi^2\left(\mathbf{D}^{(0)*}\Psi^*\right)^2 + c.c.\right]\right\}, \end{aligned} \quad 3.4\text{-}7$$

where

$$Q = \sum_{\nu=1}^{M} Q_\nu|\epsilon_\nu|^2, \qquad L = \sum_{\nu=1}^{M} L_\nu|\epsilon_\nu|^4, \qquad c = \sum_{\nu=1}^{M} c_\nu|\epsilon_\nu|^6. \quad 3.4\text{-}8$$

Now we have everything at our disposal to find the thermodynamic critical field H_c in the lowest and next-to-lowest orders in τ. According to the well-known definition of H_c, we have

$$\frac{H_c^2}{8\pi} = -f_{st,0}, \quad 3.4\text{-}9$$

where $f_{st,0}$ is the value of the free energy density for the spatially uniform stationary solution $\Psi = \Psi_0 = \sqrt{\frac{-a}{b}}$.

Following Eq. (3.4-1), the τ -expansion of H_c is obtained in the form

$$H_c = \tau\left[H_c^{(0)} + \tau H_c^{(1)} + \cdots\right], \qquad 3.4\text{-}10$$

Using (3.4-1), (3.4-2), (3.4-7), and (3.4-10), one finds

$$H_c^{(0)} = \sqrt{\frac{4\pi a^2}{b}}, \qquad 3.4\text{-}11$$

and

$$f_{st,0}^{(1)} = \frac{-a}{b}\left(\frac{a}{2} - \sum_{i=1}^{M-1}\frac{a^2|\bar{\alpha}_i|^2}{\Lambda_i}\right) + \left(\frac{-a}{b}\right)^2\left(b - \sum_{i=1}^{M-1}\frac{ab\left(\bar{\alpha}_i^*\bar{\beta}_i + c.c.\right)}{\Lambda_i}\right) - ab3\left(\frac{c}{3} + \sum_{i=1}^{M-1}\frac{b^2\left|\bar{\beta}_i\right|^2}{\Lambda_i}\right),$$

$$f_{st,0}^{(1)} = \frac{a^2}{b}\left[\left(-\frac{1}{2} + \sum_{i=1}^{M-1}\frac{a|\bar{\alpha}_i|^2}{\Lambda_i}\right) + \left(1 - \sum_{i=1}^{M-1}\frac{a\left(\bar{\alpha}_i^*\bar{\beta}_i + c.c.\right)}{\Lambda_i}\right) + \frac{a}{b^2}\left(\frac{c}{3} + \sum_{i=1}^{M-1}\frac{b^2\left|\bar{\beta}_i\right|^2}{\Lambda_i}\right)\right],$$

$$f_{st,0}^{(1)} = \frac{a^2}{b}\left\{\left(\frac{1}{2} + \frac{ca}{3b^2}\right) + \left[\sum_{i=1}^{M-1}\frac{a}{\Lambda_i}\left(|\bar{\alpha}_i|^2 + \left(\bar{\alpha}_i^*\bar{\beta}_i + c.c.\right) + \left|\bar{\beta}_i\right|^2\right)\right]\right\},$$

$$f_{st,0}^{(1)} = \frac{a^2}{b}\left\{\left(\frac{1}{2} + \frac{ca}{3b^2}\right) + \left[\sum_{i=1}^{M-1}\frac{a}{\Lambda_i}\left(|\bar{\alpha}_i|^2 + \left|\bar{\beta}_i\right|^2 + \left(\bar{\alpha}_i^*\bar{\beta}_i + c.c.\right)\right)\right]\right\},$$

$$f_{st,0}^{(1)} = \frac{a^2}{b}\left[\left(\frac{1}{2} + \frac{ca}{3b^2}\right) + \sum_{i=1}^{M-1}\frac{a}{\Lambda_i}\left|\bar{\alpha}_i - \bar{\beta}_i\right|^2\right].$$

Now we can calculate $H_c^{(1)}$

$$H_c = \sqrt{-8\pi\tau^2\left[f_{st,0}^{(0)} + \tau f_{st,0}^{(1)} + \cdots\right]},$$

$$H_c = \sqrt{-8\pi\tau^2 f_{st,0}^{(0)}\left[1 + \tau\frac{f_{st,0}^{(1)}}{f_{st,0}^{(0)}} + \cdots\right]},$$

as the second term is small, we can expand the square root, and the critical field can be written as

$$H_c = H_c^{(0)}\tau\left(1+\tau\frac{1}{2}\frac{f_{st,0}^{(1)}}{f_{st,0}^{(0)}}\right).$$

So, $H_c^{(1)}$ reads

$$H_c^{(1)} = \frac{H_c^{(0)}}{2}\frac{f_{st,0}^{(1)}}{f_{st,0}^{(0)}},$$

$$\frac{H_c^{(1)}}{H_c^{(0)}} = \frac{\frac{a^2}{b}\left[\left(\frac{1}{2}+\frac{ca}{3b^2}\right)+\sum_{i=1}^{M-1}\frac{a}{\Lambda_i}\left|\bar{\alpha}_i-\bar{\beta}_i\right|^2\right]}{-\frac{a^2}{b}},$$

$$\frac{H_c^{(1)}}{H_c^{(0)}} = -\frac{1}{2}-\frac{ca}{3b^2}-\sum_{i=1}^{M-1}\frac{a}{\Lambda_i}\left|\bar{\alpha}_i-\bar{\beta}_i\right|^2. \qquad 3.4\text{-}12$$

Comparing Eq. (3.4-11) with the corresponding result for the two-band case [35], one finds that $H_c^{(0)}$ is formally the same as that of the two-band system (but a and b are now averages over M contributing bands). As for Eq. (3.4-12), the third term in the left-hand side has a different form as compared to its counterpart in the two-band expression for $H_c^{(0)}$ in Ref. [35]. The reason is the same as mentioned in the discussion after Eq. (3.3-26). Namely, the orthonormal set of vectors defined by Eqs. (3.3-11) and (3.3-12) is used in the present study while the two-band formalism of [35] involved two linearly independent vectors that were not orthonormal. The latter was given by explicit analytical expressions, which was convenient for solving two-band equations.

3.5 GIBBS FREE ENERGY DIFFERENCE

As is known from textbooks, only spatially uniform distribution of the condensate can appear in bulk type-I superconductors. For a sufficiently low applied field **H**, such a system is in the Meissner state with a nonzero position-independent condensate density. When the applied field amplitude **H** exceeds the thermodynamic critical field H_c, the system undergoes an abrupt transition to the zero-condensate solution (normal state). Switching from type I to type II occurs when a spatially inhomogeneous condensate-field configuration becomes more thermodynamically favorable at the thermodynamic critical field than the spatially uniform condensate. As the system is under an external magnetic field, the thermodynamic potential in charge is the Gibbs free energy. Thus, investigating the switching between superconductivity types I and II, one needs to compare the Gibbs free energy of a uniform and nonuniform condensate solutions at $H = H_c$, i.e., to calculate the corresponding Gibbs free energy difference. The Gibbs free energy density for a superconductor in an external magnetic field $H = H_c$, is given by $g = f_{st} - \frac{H_c B}{4\pi}$. For the uniform solution we have $B = 0$ and $f_{st,0} = -\frac{H_c^2}{8\pi}$ and so $g_0 = -\frac{H_c^2}{8\pi}$. Therefore, the density of the Gibbs free energy difference $g_\Delta = g - g_0$ is given by

$$g_\Delta = f_{st} - \frac{H_c B}{4\pi} + \frac{H_c^2}{8\pi}, \qquad 3.5\text{-}1$$

where $B = |\mathbf{B}|$.

To proceed further and find the τ-expansion for g_Δ, it is convenient to introduce the dimensionless quantities

$$\tilde{\boldsymbol{x}} = \frac{\boldsymbol{x}}{\lambda_L\sqrt{2}}, \qquad \tilde{\mathbf{A}} = \kappa\frac{\mathbf{A}}{\lambda_L H_c^{(0)}}, \qquad \tilde{\mathbf{B}} = \kappa\sqrt{2}\frac{\mathbf{B}}{H_c^{(0)}},$$

$$\tilde{\Psi} = \frac{\Psi}{\Psi_0}, \qquad \tilde{g}_\Delta = \frac{4\pi g_\Delta}{H_c^{(0)2}}, \qquad \tilde{G}_\Delta = \frac{4\pi G_\Delta}{H_c^{(0)2}\left(\lambda_L\sqrt{2}\right)^3}, \qquad 3.5\text{-}2$$

where G_Δ is the Gibbs free energy difference and

$$\lambda_L = -\frac{\hbar c}{e}\sqrt{-\frac{b}{32\pi K a}}, \qquad \kappa = \frac{\lambda_L}{\varepsilon_{GL}} = \lambda_L\sqrt{-\frac{a}{K}}. \qquad 3.5\text{-}3$$

Here we recall that to get the τ-expansion of the microscopic formalism in the explicit form, we have previously introduced the scaled spatial coordinates $\boldsymbol{x}' = \tau^{1/2}\boldsymbol{x}$, suppressing the prime for convenience. Therefore, the expressions for the GL coherence length ε_{GL} and the magnetic London penetration depth λ_L given by Eq. (3.5-3), should be divided by $\tau^{1/2}$ to obtain the standard definitions of these characteristic lengths. Below we use the GL equations for the dimensionless order parameter and magnetic field.

First, we must find $\mathbf{D}^{(0)}$ in dimensionless quantities

$$\mathbf{D}^{(0)} = \boldsymbol{\nabla} - \mathrm{i}\frac{2e}{\hbar \mathrm{c}}\mathbf{A}^{(0)} = \frac{\widetilde{\boldsymbol{\nabla}}}{\lambda_L\sqrt{2}} - \mathrm{i}\frac{2e}{\hbar \mathrm{c}}\frac{\lambda_L H_c^{(0)}\widetilde{\mathbf{A}}^{(0)}}{\kappa} = \frac{\widetilde{\boldsymbol{\nabla}}}{\lambda_L\sqrt{2}} - \mathrm{i}\frac{2e}{\hbar \mathrm{c}}\frac{\lambda_L H_c^{(0)}\widetilde{\mathbf{A}}^{(0)}}{\lambda_L\sqrt{-\frac{a}{K}}},$$

$$\mathbf{D}^{(0)} = \frac{1}{\lambda_L\sqrt{2}}\left[\widetilde{\boldsymbol{\nabla}} - \mathrm{i}\frac{2e}{\hbar \mathrm{c}}\sqrt{2}\frac{\left(-\frac{\hbar \mathrm{c}}{e}\sqrt{-\frac{b}{32\pi K a}}\right)\left(\sqrt{\frac{4\pi a^2}{b}}\right)\widetilde{\mathbf{A}}^{(0)}}{\sqrt{-\frac{a}{K}}}\right],$$

$$\mathbf{D}^{(0)} = \frac{1}{\lambda_L\sqrt{2}}\left(\widetilde{\boldsymbol{\nabla}} + \mathrm{i}\widetilde{\mathbf{A}}^{(0)}\right) = \frac{1}{\lambda_L\sqrt{2}}\widetilde{\mathbf{D}}^{(0)}.$$

Now, we can rewrite the first GL equation

$$a\Psi + b\Psi|\Psi|^2 - K\mathbf{D}^{(0)2}\Psi = 0,$$

$$a\Psi_0\widetilde{\Psi} + b\Psi_0|\Psi_0|^2\widetilde{\Psi}\left|\widetilde{\Psi}\right|^2 - \frac{\Psi_0}{2\lambda_L^2}K\widetilde{\mathbf{D}}^{(0)2}\widetilde{\Psi} = 0,$$

$$a\widetilde{\Psi} - \frac{a}{b}b\widetilde{\Psi}\left|\widetilde{\Psi}\right|^2 + \frac{1}{2\left(\kappa^2\frac{K}{a}\right)}K\widetilde{\mathbf{D}}^{(0)2}\widetilde{\Psi} = 0,$$

$$\widetilde{\Psi} - \widetilde{\Psi}\left|\widetilde{\Psi}\right|^2 + \frac{1}{2\kappa^2}\widetilde{\mathbf{D}}^{(0)2}\widetilde{\Psi} = 0.$$

The second GL equation

$$\mathrm{rot}\,\mathbf{B}^{(0)} = 4\pi \mathrm{i}K\boldsymbol{i}_\Psi^{(0)} = 4\pi \mathrm{i}K\frac{2e}{\hbar \mathrm{c}}\left[\Psi\mathbf{D}^{(0)*}\Psi^* - \Psi^*\mathbf{D}^{(0)}\Psi\right],$$

$$\frac{1}{\lambda_L\sqrt{2}}\frac{H_c^{(0)}}{\kappa\sqrt{2}}\widetilde{\mathrm{rot}}\,\widetilde{\mathbf{B}}^{(0)} = 4\pi \mathrm{i}K\frac{2e}{\hbar \mathrm{c}}|\Psi_0|^2\frac{1}{\lambda_L\sqrt{2}}\left[\widetilde{\Psi}\widetilde{\mathbf{D}}^{(0)*}\widetilde{\Psi}^* - \widetilde{\Psi}^*\widetilde{\mathbf{D}}^{(0)}\widetilde{\Psi}\right],$$

$$\widetilde{\mathrm{rot}}\,\widetilde{\mathbf{B}}^{(0)} = 4\pi \mathrm{i}K\frac{2e}{\hbar\,\mathrm{c}}\frac{\kappa\sqrt{2}}{H_c^{(0)}}|\Psi_0|^2\left[\widetilde{\Psi}\widetilde{\mathbf{D}}^{(0)*}\widetilde{\Psi}^* - \widetilde{\Psi}^*\widetilde{\mathbf{D}}^{(0)}\widetilde{\Psi}\right],$$

$$\widetilde{\mathrm{rot}}\,\widetilde{\mathbf{B}}^{(0)} = 4\pi \mathrm{i}K\frac{2e}{\hbar\,\mathrm{c}}\sqrt{2}\frac{\left(-\frac{\hbar \mathrm{c}}{e}\sqrt{-\frac{b}{32\pi K a}}\right)\sqrt{-\frac{a}{K}}}{H_c^{(0)}}|\Psi_0|^2\left[\widetilde{\Psi}\widetilde{\mathbf{D}}^{(0)*}\widetilde{\Psi}^* - \widetilde{\Psi}^*\widetilde{\mathbf{D}}^{(0)}\widetilde{\Psi}\right],$$

$$\tilde{\mathrm{rot}}\,\tilde{\mathbf{B}}^{(0)} = -8\pi i\frac{\sqrt{\frac{b}{16\pi}}}{\sqrt{\frac{4\pi a^2}{b}}}\left(\frac{-a}{b}\right)\left[\tilde{\Psi}\tilde{\mathbf{D}}^{(0)*}\tilde{\Psi}^* - \tilde{\Psi}^*\tilde{\mathbf{D}}^{(0)}\tilde{\Psi}\right],$$

$$\tilde{\mathrm{rot}}\,\tilde{\mathbf{B}}^{(0)} = \mathrm{i}\left[\tilde{\Psi}\tilde{\mathbf{D}}^{(0)*}\tilde{\Psi}^* - \tilde{\Psi}^*\tilde{\mathbf{D}}^{(0)}\tilde{\Psi}\right].$$

So, the GL equations for the dimensionless order parameter and magnetic field reads

$$\tilde{\Psi}\left(1-\left|\tilde{\Psi}\right|^2\right)+\frac{1}{2\kappa^2}\tilde{\mathbf{D}}^{(0)2}\tilde{\Psi}=0, \qquad \tilde{\mathrm{rot}}\,\tilde{\mathbf{B}}^{(0)}=\tilde{\boldsymbol{\imath}}_{\tilde{\Psi}}^{(0)}, \tag{3.5-4}$$

where $\tilde{\mathbf{D}}^{(0)}=\tilde{\boldsymbol{\nabla}}+\mathrm{i}\tilde{\mathbf{A}}^{(0)}$, $\tilde{\boldsymbol{\imath}}_{\tilde{\Psi}}^{(0)}=\mathrm{i}\left[\tilde{\Psi}\tilde{\mathbf{D}}^{(0)*}\tilde{\Psi}^*-\tilde{\Psi}^*\tilde{\mathbf{D}}^{(0)}\tilde{\Psi}\right]$, and the vector differential operators are associated with the dimensionless radius vector $\tilde{\boldsymbol{x}}$.

Based on Eqs. (3.3-1), (3.4-1), and (3.4-2), the τ-expansion for g_Δ is obtained in the form

$$g_\Delta=\tau^2\left[g_\Delta^{(0)}+\tau g_\Delta^{(1)}+\cdots\right], \tag{3.5-5}$$

where

$$g_\Delta^{(0)}=\frac{B^{(0)2}}{8\pi}+a|\Psi|^2+\frac{b}{2}|\Psi|^4+K\left|\mathbf{D}^{(0)}\Psi\right|^2-\frac{H_c^{(0)}B^{(0)}}{4\pi}+\frac{H_c^{(0)2}}{8\pi}$$
$$=\frac{H_c^{(0)2}}{8\pi}\left(\frac{B^{(0)}}{H_c^{(0)}}-1\right)^2+a|\Psi|^2+\frac{b}{2}|\Psi|^4+K\left|\mathbf{D}^{(0)}\Psi\right|^2,$$

$$\tilde{g}_\Delta^{(0)}=\frac{4\pi}{H_c^{(0)2}}\left[\frac{H_c^{(0)2}}{8\pi}\left(\frac{\tilde{B}^{(0)}H_c^{(0)}}{\kappa\sqrt{2}H_c^{(0)}}-1\right)^2+a\left(\frac{-a}{b}\right)\left|\tilde{\Psi}\right|^2+\frac{b}{2}\left(\frac{-a}{b}\right)^2\left|\tilde{\Psi}\right|^4\right.$$
$$\left.+K\left(\frac{-a}{b}\right)\left(\frac{1}{\lambda_L\sqrt{2}}\right)^2\left|\tilde{\mathbf{D}}^{(0)}\tilde{\Psi}\right|^2\right],$$

$$\tilde{g}_\Delta^{(0)}=\frac{4\pi}{H_c^{(0)2}}\left[\frac{H_c^{(0)2}}{8\pi}\left(\frac{\tilde{B}^{(0)}H_c^{(0)}}{\kappa\sqrt{2}H_c^{(0)}}-1\right)^2-\frac{a^2}{b}\left|\tilde{\Psi}\right|^2+\frac{a^2}{2b}\left|\tilde{\Psi}\right|^4-\frac{a^2}{2b}\frac{K}{a\lambda_L^2}\left|\tilde{\mathbf{D}}^{(0)}\tilde{\Psi}\right|^2\right],$$

here and in the results below the tilde is suppressed for brevity

$$g_\Delta^{(0)}=\frac{1}{2}\left(\frac{B^{(0)}}{\kappa\sqrt{2}}-1\right)^2-|\Psi|^2+\frac{1}{2}|\Psi|^4-\frac{\left|\mathbf{D}^{(0)}\Psi\right|^2}{2\kappa^2}, \tag{3.5-6}$$

with $B^{(0)}=\left|\mathbf{B}^{(0)}\right|$.

Before the next derivation, we need to rearrange Eq. (3.4-7) by inserting

$$\mathbf{A}^{(1)} \cdot \operatorname{rot} \mathbf{B}^{(0)} = \mathbf{A}^{(1)} \cdot \operatorname{rot}\left[\mathbf{B}^{(0)} - \mathbf{H}_c^{(0)}\right],$$

and then performing the substitution

$$\mathbf{A}^{(1)} \cdot \operatorname{rot} \mathbf{B}^{(0)} \rightarrow \mathbf{B}^{(1)} \cdot \left[\mathbf{B}^{(0)} - \mathbf{H}_c^{(0)}\right]. \qquad 3.5\text{-}7$$

According to Gauss's theorem, this substitution results in an additional surface integral in G_Δ that vanishes because $\mathbf{B}^{(0)}$ approaches $\mathbf{H}_c^{(0)}$ at infinity. Then,

$$\begin{aligned} g_\Delta^{(1)} = {} & \frac{B^{(0)}B^{(1)} - B^{(1)}\left[B^{(0)} - H_c^{(0)}\right]}{4\pi} - \frac{\left[H_c^{(0)}B^{(1)} + H_c^{(1)}B^{(0)}\right]}{4\pi} + \frac{H_c^{(1)}H_c^{(0)}}{4\pi} \\ & + \left(\frac{a}{2} - \sum_{i=1}^{M-1} \frac{a^2|\bar{\alpha}_i|^2}{\Lambda_i}\right)|\Psi|^2 + \left(b - \sum_{i=1}^{M-1} \frac{ab\left(\bar{\alpha}_i^*\bar{\beta}_i + c.c.\right)}{\Lambda_i}\right)|\Psi|^4 \\ & - \left(\frac{c}{3} + \sum_{i=1}^{M-1} \frac{b^2\left|\bar{\beta}_i\right|^2}{\Lambda_i}\right)|\Psi|^6 + 2K\left|\mathbf{D}^{(0)}\Psi\right|^2 \\ & - Q\left[\left|\mathbf{D}^{(0)2}\Psi\right|^2 + \frac{1}{3}\operatorname{rot}\mathbf{B}^{(0)} \cdot \boldsymbol{i}_\Psi^{(0)} + \frac{4e^2\mathbf{B}^{(0)2}}{\hbar^2 c^2}|\Psi|^2\right] \\ & - \frac{L}{2}\left\{8|\Psi|^2\left|\mathbf{D}^{(0)}\Psi\right|^2 + \left[\Psi^2\left(\mathbf{D}^{(0)*}\Psi^*\right)^2 + c.c.\right]\right\}, \end{aligned}$$

$$\begin{aligned} g_\Delta^{(1)} = {} & \frac{-H_c^{(1)}\left[B^{(0)} - H_c^{(0)}\right]}{4\pi} + \left(\frac{a}{2} - \sum_{i=1}^{M-1} \frac{a^2|\bar{\alpha}_i|^2}{\Lambda_i}\right)|\Psi|^2 + \left(b - \sum_{i=1}^{M-1} \frac{ab\left(\bar{\alpha}_i^*\bar{\beta}_i + c.c.\right)}{\Lambda_i}\right)|\Psi|^4 \\ & - \left(\frac{c}{3} + \sum_{i=1}^{M-1} \frac{b^2\left|\bar{\beta}_i\right|^2}{\Lambda_i}\right)|\Psi|^6 + 2K\left|\mathbf{D}^{(0)}\Psi\right|^2 \\ & - Q\left[\left|\mathbf{D}^{(0)2}\Psi\right|^2 + \frac{1}{3}\operatorname{rot}\mathbf{B}^{(0)} \cdot \vec{i}_\Psi^{(0)} + \frac{4e^2\mathbf{B}^{(0)2}}{\hbar^2 c^2}|\Psi|^2\right] \\ & - \frac{L}{2}\left\{8|\Psi|^2\left|\mathbf{D}^{(0)}\Psi\right|^2 + \left[\Psi^2\left(\mathbf{D}^{(0)*}\Psi^*\right)^2 + c.c.\right]\right\}. \end{aligned}$$

Now, we will write each part of this equation in terms of dimensionless parameters

1. $\frac{-H_c^{(1)}\left[B^{(0)}-H_c^{(0)}\right]}{4\pi}$:

$$\frac{-H_c^{(1)}\left[B^{(0)}-H_c^{(0)}\right]}{4\pi}=\frac{-H_c^{(0)2}}{4\pi}\left[\frac{H_c^{(1)}}{H_c^{(0)}}\right]\left[\frac{B^{(0)}}{H_c^{(0)}}-1\right]$$

$$=\frac{H_c^{(0)2}}{4\pi}\left(\frac{\tilde{B}^{(0)}}{\kappa\sqrt{2}}-1\right)\left[\frac{1}{2}+\frac{ca}{3b^2}+\sum_{i=1}^{M-1}\frac{a}{\Lambda_i}\left|\bar{\alpha}_i-\bar{\beta}_i\right|^2\right].$$

2. $\left(\frac{a}{2}-\sum_{i=1}^{M-1}\frac{a^2|\bar{\alpha}_i|^2}{\Lambda_i}\right)|\Psi|^2+\left(b-\sum_{i=1}^{M-1}\frac{ab\left(\bar{\alpha}_i^*\bar{\beta}_i+c.c.\right)}{\Lambda_i}\right)|\Psi|^4-\left(\frac{c}{3}+\sum_{i=1}^{M-1}\frac{b^2\left|\bar{\beta}_i\right|^2}{\Lambda_i}\right)|\Psi|^6+$ $2K\left|\mathbf{D}^{(0)}\Psi\right|^2$:

$$\left(\frac{a}{2}-\sum_{i=1}^{M-1}\frac{a^2|\bar{\alpha}_i|^2}{\Lambda_i}\right)\left(\frac{-a}{b}\right)\left|\tilde{\Psi}\right|^2+\left(b-\sum_{i=1}^{M-1}\frac{ab\left(\bar{\alpha}_i^*\bar{\beta}_i+c.c.\right)}{\Lambda_i}\right)\left(\frac{-a}{b}\right)^2\left|\tilde{\Psi}\right|^4$$
$$-\left(\frac{c}{3}+\sum_{i=1}^{M-1}\frac{b^2\left|\bar{\beta}_i\right|^2}{\Lambda_i}\right)\left(\frac{-a}{b}\right)^3\left|\tilde{\Psi}\right|^6+2K\left(\frac{-a}{b}\right)\left(\frac{1}{\lambda_L\sqrt{2}}\right)^2\left|\tilde{\mathbf{D}}^{(0)}\tilde{\Psi}\right|^2$$

$$=-\frac{a^2}{b}\left(\frac{1}{2}-\sum_{i=1}^{M-1}\frac{a|\bar{\alpha}_i|^2}{\Lambda_i}\right)\left|\tilde{\Psi}\right|^2+\frac{a^2}{b}\left(1-\sum_{i=1}^{M-1}\frac{a\left(\bar{\alpha}_i^*\bar{\beta}_i+c.c.\right)}{\Lambda_i}\right)\left|\tilde{\Psi}\right|^4$$
$$+\frac{a^2}{b}\left(\frac{ac}{3b^2}+\sum_{i=1}^{M-1}\frac{a\left|\bar{\beta}_i\right|^2}{\Lambda_i}\right)\left|\tilde{\Psi}\right|^6+\frac{a^2}{b}\frac{\left|\tilde{\mathbf{D}}^{(0)}\tilde{\Psi}\right|^2}{\kappa^2},$$

$$=\frac{H_c^{(0)2}}{4\pi}\left[-\left(\frac{1}{2}-\sum_{i=1}^{M-1}\frac{a|\bar{\alpha}_i|^2}{\Lambda_i}\right)\left|\tilde{\Psi}\right|^2+\left(1-\sum_{i=1}^{M-1}\frac{a\left(\bar{\alpha}_i^*\bar{\beta}_i+c.c.\right)}{\Lambda_i}\right)\left|\tilde{\Psi}\right|^4\right.$$
$$\left.+\left(\frac{ca}{3b^2}+\sum_{i=1}^{M-1}\frac{a\left|\bar{\beta}_i\right|^2}{\Lambda_i}\right)\left|\tilde{\Psi}\right|^6+\frac{\left|\tilde{\mathbf{D}}^{(0)}\tilde{\Psi}\right|^2}{\kappa^2}\right].$$

3. $-Q\left[\left|\mathbf{D}^{(0)2}\Psi\right|^2+\frac{1}{3}\operatorname{rot}\mathbf{B}^{(0)}\cdot\boldsymbol{i}_\Psi^{(0)}+\frac{4e^2\mathbf{B}^{(0)2}}{\hbar^2c^2}|\Psi|^2\right]$:

$$-Q\left[\left(\frac{-a}{b}\right)\left(\frac{1}{\lambda_L\sqrt{2}}\right)^4\left|\tilde{\mathbf{D}}^{(0)2}\tilde{\Psi}\right|^2+\frac{1}{3}\frac{1}{\lambda_L\sqrt{2}}\frac{H_c^{(0)}}{\kappa\sqrt{2}}4\pi K\frac{2e}{\hbar c}\left(\frac{-a}{b}\right)\frac{1}{\lambda_L\sqrt{2}}\operatorname{r\tilde{o}t}\tilde{\mathbf{B}}^{(0)}\cdot\tilde{\boldsymbol{i}}_{\tilde{\Psi}}^{(0)}\right.$$
$$\left.+\left(\frac{-a}{b}\right)\left(\frac{H_c^{(0)}}{\kappa\sqrt{2}}\right)^2\frac{4e^2}{\hbar^2c^2}\tilde{\mathbf{B}}^{(0)2}\left|\tilde{\Psi}\right|^2\right]$$
$$=\frac{H_c^{(0)2}}{4\pi}Q\left[\frac{1}{4a\lambda_L^4}\left|\tilde{\mathbf{D}}^{(0)2}\tilde{\Psi}\right|^2-\frac{1}{4K\lambda_L^2\kappa^2}\frac{1}{3}\operatorname{r\tilde{o}t}\tilde{\mathbf{B}}^{(0)}\cdot\tilde{\boldsymbol{i}}_{\tilde{\Psi}}^{(0)}+\frac{a}{b}\frac{8\pi}{\kappa^2}\frac{e^2}{\hbar^2c^2}\tilde{\mathbf{B}}^{(0)2}\left|\tilde{\Psi}\right|^2\right],$$
$$=\frac{H_c^{(0)2}}{4\pi}Q\left[\frac{1}{4a\kappa^4\varepsilon_{GL}^4}\left|\tilde{\mathbf{D}}^{(0)2}\tilde{\Psi}\right|^2-\frac{1}{4K\kappa^4\varepsilon_{GL}^2}\frac{1}{3}\operatorname{r\tilde{o}t}\tilde{\mathbf{B}}^{(0)}\cdot\tilde{\boldsymbol{i}}_{\tilde{\Psi}}^{(0)}-\frac{1}{4\lambda_L^2K\kappa^2}\tilde{\mathbf{B}}^{(0)2}\left|\tilde{\Psi}\right|^2\right],$$
$$=\frac{H_c^{(0)2}}{4\pi}\frac{Qa}{K^2}\frac{1}{4\kappa^4}\left[\left|\tilde{\mathbf{D}}^{(0)2}\tilde{\Psi}\right|^2+\frac{1}{3}\operatorname{r\tilde{o}t}\tilde{\mathbf{B}}^{(0)}\cdot\tilde{\boldsymbol{i}}_{\tilde{\Psi}}^{(0)}+\tilde{\mathbf{B}}^{(0)2}\left|\tilde{\Psi}\right|^2\right].$$

4. $-\frac{L}{2}\left\{8|\Psi|^2\left|\vec{D}^{(0)}\Psi\right|^2+\left[\Psi^2\left(\vec{D}^{(0)*}\Psi^*\right)^2+c.c.\right]\right\}$:

$$-\frac{L}{2}\left\{8\left(\frac{-a}{b}\right)\left(\frac{1}{\lambda_L\sqrt{2}}\right)^2\left|\tilde{\Psi}\right|^2\left|\tilde{\mathbf{D}}^{(0)}\tilde{\Psi}\right|^2+\left(\frac{-a}{b}\right)^2\left(\frac{1}{\lambda_L\sqrt{2}}\right)^2\left[\tilde{\Psi}^2\left(\tilde{\mathbf{D}}^{(0)*}\tilde{\Psi}^*\right)^2+c.c.\right]\right\}$$
$$=-\frac{H_c^{(0)2}}{4\pi}\frac{L}{4b\lambda_L^2}\left\{8\left|\tilde{\Psi}\right|^2\left|\tilde{\mathbf{D}}^{(0)}\tilde{\Psi}\right|^2+\left[\tilde{\Psi}^2\left(\tilde{\mathbf{D}}^{(0)*}\tilde{\Psi}^*\right)^2+c.c.\right]\right\},$$
$$=-\frac{H_c^{(0)2}}{4\pi}\frac{L}{4b\kappa^2\varepsilon_{GL}^2}\left\{8\left|\tilde{\Psi}\right|^2\left|\tilde{\mathbf{D}}^{(0)}\tilde{\Psi}\right|^2+\left[\tilde{\Psi}^2\left(\tilde{\mathbf{D}}^{(0)*}\tilde{\Psi}^*\right)^2+c.c.\right]\right\},$$
$$=\frac{H_c^{(0)2}}{4\pi}\frac{La}{Kb}\frac{1}{4\kappa^2}\left\{8\left|\tilde{\Psi}\right|^2\left|\tilde{\mathbf{D}}^{(0)}\tilde{\Psi}\right|^2+\left[\tilde{\Psi}^2\left(\tilde{\mathbf{D}}^{(0)*}\tilde{\Psi}^*\right)^2+c.c.\right]\right\}.$$

So, the next-to-lowest order correction of Gibbs free energy in dimensionless quantities where the tilde is suppressed for brevity is written as

$$g_\Delta^{(1)}=\left(\frac{B^{(0)}}{\kappa\sqrt{2}}-1\right)\left[\frac{1}{2}+\bar{c}+\sum_{i=1}^{M-1}\frac{\left|\bar{\alpha}_i-\bar{\beta}_i\right|^2}{\bar{\Lambda}_i}\right]-\left(\frac{1}{2}-\sum_{i=1}^{M-1}\frac{|\bar{\alpha}_i|^2}{\bar{\Lambda}_i}\right)|\Psi|^2$$
$$+\left(1-\sum_{i=1}^{M-1}\frac{\bar{\alpha}_i^*\bar{\beta}_i+c.c.}{\bar{\Lambda}_i}\right)|\Psi|^4+\left(\bar{c}+\sum_{i=1}^{M-1}\frac{\left|\bar{\beta}_i\right|^2}{\bar{\Lambda}_i}\right)|\Psi|^6+\frac{\left|\mathbf{D}^{(0)}\Psi\right|^2}{\kappa^2}\qquad 3.5\text{-}8$$
$$+\frac{\bar{Q}}{4\kappa^4}\left[\left|\mathbf{D}^{(0)2}\Psi\right|^2+\frac{1}{3}\operatorname{rot}\mathbf{B}^{(0)}\cdot\boldsymbol{i}_\Psi^{(0)}+\mathbf{B}^{(0)2}|\Psi|^2\right]$$
$$+\frac{\bar{L}}{4\kappa^2}\left\{8|\Psi|^2\left|\mathbf{D}^{(0)}\Psi\right|^2+\left[\Psi^2\left(\mathbf{D}^{(0)*}\Psi^*\right)^2+c.c.\right]\right\},$$

with the dimensionless parameters

$$\bar{c} = \frac{ca}{3b^2}, \qquad \bar{Q} = \frac{Qa}{K^2}, \qquad \bar{L} = \frac{La}{Kb}, \qquad \bar{\Lambda}_i = \frac{\Lambda_i}{a}. \tag{3.5-9}$$

When utilizing Eq. (3.5-7), we find that the next-to-lowest order correction to the magnetic field does not appear in the Gibbs free energy difference. In addition, one notes that the contribution $g_\Delta^{(0)}$ is not sensitive to the number of available bands. However, $g_\Delta^{(1)}$ depends explicitly on M, which is the basis for the main conclusions of the present study.

3.6 BOGOMOLNYI SELF-DUALITY AND INTERTYPE DOMAIN

As is discussed in Sec.3.1, the IT domain is located on the $\kappa - T$ plane near $\kappa = \kappa_0$ so that it is convenient to expand the Gibbs free energy difference G_Δ, integration of $g_\Delta^{(0)}$, in powers of $\delta\kappa = \kappa - \kappa_0$. Keeping only terms up to order $\tau \sim \delta\kappa$, we obtain

$$G_\Delta = \tau^2 \left[G_\Delta^{(0)}\Big|_{\kappa=\kappa_0} + \delta\kappa \frac{dG_\Delta^{(0)}}{d\kappa}\Big|_{\kappa=\kappa_0} + \tau G_\Delta^{(1)}\Big|_{\kappa=\kappa_0} \right], \tag{3.6-1}$$

where the derivative of $G_\Delta^{(0)}$ with respect to κ is not dependent on the number of contributing bands ($g_\Delta^{(0)}$ is not sensitive to M, as is mentioned above) and, so, we simply quote the two-band result of Ref. [35]

$$\frac{dG_\Delta^{(0)}}{d\kappa}\Big|_{\kappa=\kappa_0} = -\int d^3\boldsymbol{x} \left[\sqrt{2} B^{(0)} \left(B^{(0)} - 1 \right) + 2\sqrt{2} \left| \mathbf{D}^{(0)} \Psi \right|^2 \right], \tag{3.6-2}$$

where we recall that $\kappa_0 = 1/\sqrt{2}$.

A significant advantage of using the expansion in $\delta\kappa$ is related to the special property of the GL theory at $\kappa = \kappa_0$. This property is called the Bogomolnyi self-duality [57], or the matching between the magnetic-field and condensate spatial profiles given by [35], [57]

$$B^{(0)} = 1 - |\Psi|^2. \tag{3.6-3}$$

This local relation between the order parameter and magnetic field amplitude is consistent with the GL equations (3.5-4) when [35], [57]

$$D_-^{(0)} \Psi = 0, \tag{3.6-4}$$

where $D_{\pm}^{(0)} = D_x^{(0)} \pm \mathrm{i}D_y^{(0)}$, with $D_{x,y}^{(0)}$ the x- and y-components of $\mathbf{D}^{(0)}$. Here $\mathbf{B}^{(0)}$ is assumed to be along the z-direction so that Ψ is not dependent on z and $\mathbf{D}^{(0)2} = D_+^{(0)}D_-^{(0)} + B^{(0)}$. Equations (3.6-3) and (3.6-4) are usually called the Bogomolnyi equations [57] (they are also known as the Sarma solution [44]). Using Eqs. (3.5-4) and (3.6-3) and also the substitution $\left|\mathbf{D}^{(0)}\Psi\right|^2 \to \Psi^*\mathbf{D}^{(0)2}\Psi$ (producing a zero surface integral), we find

$$G_\Delta^{(0)}\Big|_{\kappa=\kappa_0} = \int d^3\boldsymbol{x}\left[\frac{1}{2}\left(B^{(0)} - 1\right)^2 - |\Psi|^2 + \frac{1}{2}|\Psi|^4 - \Psi^*\mathbf{D}^{(0)2}\Psi\right],$$

$$G_\Delta^{(0)}\Big|_{\kappa=\kappa_0} = \int d^3\boldsymbol{x}\left[\frac{1}{2}|\Psi|^4 - |\Psi|^2 + \frac{1}{2}|\Psi|^4 - \Psi^*\mathbf{D}^{(0)2}\Psi\right],$$

$$G_\Delta^{(0)}\Big|_{\kappa=\kappa_0} = -\int d^3\boldsymbol{x}\,\Psi^*\left[\Psi(1 - |\Psi|^2) + \mathbf{D}^{(0)2}\Psi\right] = 0,$$

so,

$$G_\Delta^{(0)}\Big|_{\kappa=\kappa_0} = \int d^3\boldsymbol{x}\left(|\Psi|^4 - |\Psi|^2 - \Psi^*\mathbf{D}^{(0)2}\Psi\right) = 0. \qquad 3.6\text{-}5$$

This result is valid for any stationary solution of the GL formalism at $\kappa = \kappa_0$ and reflects another benchmark property of the Bogomolnyi self-duality: at the thermodynamic critical field all possible GL solutions are degenerate (there is an infinite number of GL self-dual configurations, including very exotic patterns, see Appendix C in Ref. [35]). Above H_c the normal state $\Psi = 0$ is stable while below H_c the Meissner state $\Psi = 1$ is favourable. Thus, the mixed state appears only at the single point $H = H_c$ and all exotic self-dual patterns of the field and condensate are locked at this point. However, corrections to the GL formalism break the Bogomolnyi degeneracy and successive self-dual patterns determine the properties of the IT mixed state.

Similarly, to the procedure used to obtain Eq. (3.6-5), we rewrite Eq. (3.6-2) as

$$\frac{dG_\Delta^{(0)}}{d\kappa}\bigg|_{\kappa=\kappa_0} = -\sqrt{2}\int d^3\boldsymbol{x}\left[(1 - |\Psi|^2)|\Psi|^2 + 2\left(\Psi^*\mathbf{D}^{(0)2}\Psi\right)\right],$$

$$\frac{dG_\Delta^{(0)}}{d\kappa}\bigg|_{\kappa=\kappa_0} = -\sqrt{2}\int d^3\boldsymbol{x}\left[(1 - |\Psi|^2)|\Psi|^2 + 2\left(\Psi^*\mathbf{D}^{(0)2}\Psi\right)\right],$$

$$\frac{dG_\Delta^{(0)}}{d\kappa}\bigg|_{\kappa=\kappa_0} = -\sqrt{2}\int d^3\boldsymbol{x}\,[|\Psi|^2 - |\Psi|^4 + 2(|\Psi|^4 - |\Psi|^2)],$$

$$\left.\frac{dG_{\Delta}^{(0)}}{d\kappa}\right|_{\kappa=\kappa_0} = -\sqrt{2}\int d^3\boldsymbol{x}\,(|\Psi|^4 - |\Psi|^2),$$

so,

$$\left.\frac{dG_{\Delta}^{(0)}}{d\kappa}\right|_{\kappa=\kappa_0} = \int d^3\boldsymbol{x}\,|\Psi|^2(|\Psi|^2 - 1). \qquad 3.6\text{-}6$$

The terms contributing to $G_{\Delta}^{(1)}$ and containing $\vec{D}^{(0)}$ can be rewritten by applying Gauss's theorem with vanishing surface integrals and using Eqs. (3.5-4), (3.6-3), and Eq. (3.6-4). We also have $\left(\mathbf{D}^{(0)}\Psi\right)^2 = \left(\mathbf{D}^{(0)*}\Psi^*\right)^2 = 0$ resulting from $D_x^{(0)}\Psi = \mathrm{i}D_y^{(0)}\Psi$, see Eq. (3.6-4). Notice that at the same time $\left|\mathbf{D}^{(0)}\Psi\right|^2 \neq 0$, as is seen from Eq. (3.6-5).

1. $\left|\mathbf{D}^{(0)}\Psi\right|^2 \rightarrow\ |\Psi|^2(1 - |\Psi|^2)$.

2. $\left|\mathbf{D}^{(0)2}\Psi\right|^2$:

$$\int d^3\boldsymbol{x}\left|\mathbf{D}^{(0)2}\Psi\right|^2 = \int d^3\boldsymbol{x}\,|\Psi(|\Psi|^2 - 1)|^2,$$

$$\int d^3\boldsymbol{x}\left|\mathbf{D}^{(0)2}\Psi\right|^2 = \int d^3\boldsymbol{x}\,(|\Psi|^6 + |\Psi|^2 - 2|\Psi|^4),$$

$$\int d^3\boldsymbol{x}\left|\mathbf{D}^{(0)2}\Psi\right|^2 = \int d^3\boldsymbol{x}\,[|\Psi|^2(1 - |\Psi|^2) - |\Psi|^4(1 - |\Psi|^2)].$$

3. $|\Psi|^2\left|\mathbf{D}^{(0)}\Psi\right|^2$:

$$\int d^3\boldsymbol{x}\,|\Psi|^2\left|\mathbf{D}^{(0)}\Psi\right|^2 = \int d^3\boldsymbol{x}\sum_j |\Psi|^2 D_j^{(0)}\Psi D_j^{(0)*}\Psi^*,$$

$$\int d^3\boldsymbol{x}\,|\Psi|^2\left|\mathbf{D}^{(0)}\Psi\right|^2 = \int d^3\boldsymbol{x}\sum_j |\Psi|^2 D_j^{(0)}\Psi \mathrm{e}^{\mathrm{i}\theta}\partial_j\left(\mathrm{e}^{-\mathrm{i}\theta}\Psi^*\right),$$

where $D_j^{(0)}$ is the component of $\mathbf{D}^{(0)}$ given by Eq. (3.5-4), ∂_j is the component of $\boldsymbol{\nabla}$, and θ is defined so that $\boldsymbol{\nabla}\theta = \mathbf{A}^{(0)}$. Then, we obtain

$$\int d^3\vec{x}\,|\Psi|^2\left|\mathbf{D}^{(0)}\Psi\right|^2 = \int d^3\boldsymbol{x}\sum_j\left[\partial_j\left(|\Psi|^2 D_j^{(0)}\Psi\Psi^*\right) - \Psi^*\mathrm{e}^{-\mathrm{i}\theta}\partial_j\left(\mathrm{e}^{\mathrm{i}\theta}|\Psi|^2 D_j^{(0)}\Psi\right)\right]$$

where the first term yields, by virtue of Gauss's theorem, a vanishing surface integral (Ψ is zero at infinity).

Hence,

$$\int d^3\boldsymbol{x}\,|\Psi|^2\left|\mathbf{D}^{(0)}\Psi\right|^2$$

$$= -\int d^3\boldsymbol{x}\sum_j\left[\Psi^* D_j^{(0)}\Psi\partial_j|\Psi|^2 + \Psi^*|\Psi|^2\mathrm{e}^{-\mathrm{i}\theta}\partial_j\left(\mathrm{e}^{\mathrm{i}\theta}D_j^{(0)}\Psi\right)\right],$$

$$= -\int d^3\boldsymbol{x}\sum_j\left[\Psi^* D_j^{(0)}\Psi\partial_j|\Psi|^2 + \Psi^*|\Psi|^2 D_j^{(0)2}\Psi\right],$$

$$= -\int d^3\boldsymbol{x}\sum_j\left[\Psi^* D_j^{(0)}\Psi\partial_j\left(\mathrm{e}^{\mathrm{i}\theta}\mathrm{e}^{-\mathrm{i}\theta}\Psi\Psi^*\right) + \Psi^*|\Psi|^2 D_j^{(0)2}\Psi\right],$$

$$= -\int d^3\boldsymbol{x}\sum_j\left[\Psi^{*2} D_j^{(0)}\Psi\mathrm{e}^{-\mathrm{i}\theta}\partial_j\left(\mathrm{e}^{\mathrm{i}\theta}\Psi\right) + \Psi^*\Psi D_j^{(0)}\Psi\mathrm{e}^{\mathrm{i}\theta}\partial_j\left(\mathrm{e}^{-\mathrm{i}\theta}\Psi^*\right)\right.$$
$$\left. + \Psi^*|\Psi|^2 D_j^{(0)2}\Psi\right],$$

$$= -\int d^3\boldsymbol{x}\left[\Psi^{*2}\left(\mathbf{D}^{(0)}\Psi\right)^2 + |\Psi|^2\left|\mathbf{D}^{(0)}\Psi\right|^2 + \Psi^*|\Psi|^2\mathbf{D}^{(0)}\Psi\right].$$

Here the first term is equal to zero because $D_x^{(0)}\Psi = \mathrm{i}D_y^{(0)}\Psi$, as is seen from Eq. (3.6-4).

$$\int d^3\boldsymbol{x}\,|\Psi|^2\left|\mathbf{D}^{(0)}\Psi\right|^2 = -\int d^3\boldsymbol{x}\left[|\Psi|^2\left|\mathbf{D}^{(0)}\Psi\right|^2 + \Psi^*|\Psi|^2\mathbf{D}^{(0)}\Psi\right].$$

Then, we obtain

$$2\int d^3\boldsymbol{x}\,|\Psi|^2\left|\mathbf{D}^{(0)}\Psi\right|^2 = -\int d^3\boldsymbol{x}\,\Psi^*|\Psi|^2\mathbf{D}^{(0)}\Psi.$$

Now, using the scaled GL equations (3.5-4), we conclude that

$$\int d^3\boldsymbol{x}\left|\mathbf{D}^{(0)2}\Psi\right|^2 = -\frac{1}{2}\int d^3\boldsymbol{x}\,|\Psi|^2(|\Psi|^4 - |\Psi|^2),$$

$$\int d^3\boldsymbol{x}\left|\mathbf{D}^{(0)2}\Psi\right|^2 = \frac{1}{2}\int d^3\boldsymbol{x}\,|\Psi|^4(1 - |\Psi|^2).$$

4. $\mathrm{rot}\,\mathbf{B}^{(0)}\cdot\boldsymbol{i}_\Psi^{(0)}$:

$$\int d^3\boldsymbol{x}\,\mathrm{rot}\,\mathbf{B}^{(0)}\cdot\boldsymbol{i}_\Psi^{(0)} = \int d^3\boldsymbol{x}\,\boldsymbol{i}_\Psi^{(0)2}$$

$$= \int d^3\boldsymbol{x}\,(-1)\left(\Psi\mathbf{D}^{(0)*}\Psi^* - \Psi^*\mathbf{D}^{(0)}\Psi\right)^2,$$

$$= -\int d^3\boldsymbol{x}\left[\Psi^2\left(\mathbf{D}^{(0)*}\Psi^*\right)^2 + \Psi^{*2}\left(\mathbf{D}^{(0)}\Psi\right)^2 - 2|\Psi|^2\left|\mathbf{D}^{(0)}\Psi\right|^2\right].$$

Here the first and second terms are equal to zero because $D_x^{(0)}\Psi = \mathrm{i}D_y^{(0)}\Psi \to \left(\mathbf{D}^{(0)}\Psi\right)^2 = \left(\mathbf{D}^{(0)*}\Psi^*\right)^2 = 0$, as is seen from Eq. (3.6-4).

$$\int d^3\boldsymbol{x}\,\mathrm{rot}\,\mathbf{B}^{(0)}\cdot\boldsymbol{i}_\Psi^{(0)} = 2\int d^3\boldsymbol{x}\,|\Psi|^2\left|\mathbf{D}^{(0)}\Psi\right|^2,$$

$$\int d^3\boldsymbol{x}\,\mathrm{rot}\,\mathbf{B}^{(0)}\cdot\boldsymbol{i}_\Psi^{(0)} = \int d^3\boldsymbol{x}\,|\Psi|^4(1-|\Psi|^2).$$

Now, we can rewrite the terms contributing to $G_\Delta^{(1)}$ and containing $\mathbf{D}^{(0)}$ by using the following substitutions:

$$\left|\mathbf{D}^{(0)}\Psi\right|^2 \to |\Psi|^2(1-|\Psi|^2),$$

$$\left|\mathbf{D}^{(0)2}\Psi\right|^2 \to |\Psi|^2(1-|\Psi|^2) - |\Psi|^4(1-|\Psi|^2),$$

$$|\Psi|^2\left|\mathbf{D}^{(0)}\Psi\right|^2 \to \frac{1}{2}|\Psi|^4(1-|\Psi|^2),$$

$$\mathrm{rot}\,\mathbf{B}^{(0)}\cdot\boldsymbol{i}_\Psi^{(0)} \to |\Psi|^4(1-|\Psi|^2), \qquad 3.6\text{-}7$$

Then, $G_\Delta^{(1)}$ reads

$$\begin{aligned} G_\Delta^{(1)}\Big|_{\kappa=\kappa_0} = \int d^3\boldsymbol{x}\Bigg\{&-|\Psi|^2\left[\frac{1}{2}+\bar{c}+\sum_{i=1}^{M-1}\frac{|\bar{\alpha}_i-\bar{\beta}_i|^2}{\bar{\Lambda}_i}\right]-\left(\frac{1}{2}-\sum_{i=1}^{M-1}\frac{|\bar{\alpha}_i|^2}{\bar{\Lambda}_i}\right)|\Psi|^2 \\ &+\left(1-\sum_{i=1}^{M-1}\frac{\bar{\alpha}_i^*\bar{\beta}_i+c.c.}{\bar{\Lambda}_i}\right)|\Psi|^4+\left(\bar{c}+\sum_{i=1}^{M-1}\frac{|\bar{\beta}_i|^2}{\bar{\Lambda}_i}\right)|\Psi|^6+2|\Psi|^2(1-|\Psi|^2) \\ &+\bar{Q}\left\{[|\Psi|^2(1-|\Psi|^2)-|\Psi|^4(1-|\Psi|^2)]+\frac{1}{3}|\Psi|^4(1-|\Psi|^2)+|\Psi|^2(1-|\Psi|^2)^2\right\} \\ &+2\bar{L}|\Psi|^4(1-|\Psi|^2)\Bigg\}, \end{aligned}$$

$$\begin{aligned} G_\Delta^{(1)}\Big|_{\kappa=\kappa_0} = \int d^3\boldsymbol{x}\Bigg\{&|\Psi|^2(1-|\Psi|^2)+\bar{c}(|\Psi|^6-|\Psi|^2)+\left[(|\Psi|^2-|\Psi|^4)\sum_{i=1}^{M-1}\frac{\bar{\alpha}_i^*\bar{\beta}_i+c.c.}{\bar{\Lambda}_i}\right] \\ &+(|\Psi|^6-|\Psi|^2)\left(\sum_{i=1}^{M-1}\frac{|\bar{\beta}_i|^2}{\bar{\Lambda}_i}\right) \\ &+\bar{Q}\left\{|\Psi|^2(1-|\Psi|^2)-\frac{2}{3}|\Psi|^4(1-|\Psi|^2)+|\Psi|^2+|\Psi|^6-2|\Psi|^4\right\} \\ &+2\bar{L}|\Psi|^4(1-|\Psi|^2)\Bigg\}. \end{aligned}$$

So,

$$G_{\Delta}^{(1)}\Big|_{\kappa=\kappa_0} = \int d^3\boldsymbol{x}\Bigg\{|\Psi|^2(1-|\Psi|^2) - \bar{c}[|\Psi|^4(1-|\Psi|^2) + |\Psi|^2(1-|\Psi|^2)] + \left[|\Psi|^2(1-|\Psi|^2)\sum_{i=1}^{M-1}\frac{\bar{\alpha}_i^*\bar{\beta}_i + c.c.}{\bar{\Lambda}_i}\right] - [|\Psi|^4(1-|\Psi|^2) + |\Psi|^2(1-|\Psi|^2)]\left(\sum_{i=1}^{M-1}\frac{|\bar{\beta}_i|^2}{\bar{\Lambda}_i}\right) + \bar{Q}\left[2|\Psi|^2(1-|\Psi|^2) - \frac{5}{3}|\Psi|^4(1-|\Psi|^2)\right] + 2\bar{L}|\Psi|^4(1-|\Psi|^2)\Bigg\}. \quad 3.6\text{-}8$$

Then, it follows from Eqs. (3.6-6) and (3.6-8) that G_{Δ} can be expressed in terms of the two integrals defined by

$$I = \int d^3\boldsymbol{x}\,|\Psi|^2(1-|\Psi|^2), \qquad \mathcal{J} = \int d^3\boldsymbol{x}\,|\Psi|^4(1-|\Psi|^2). \quad 3.6\text{-}9$$

Utilizing Eqs. (3.6-5), (3.6-6), (3.6-8), and (3.6-9), we can rewrite G_{Δ} given by Eq. (3.6-1) in the form

$$G_{\Delta} = \tau^2\left[-\sqrt{2}I\delta\kappa + \tau(\mathcal{A}I + \mathcal{B}\mathcal{J})\right], \quad 3.6\text{-}10$$

where the coefficients $\mathcal{A}$ and $\mathcal{B}$ read

$$\mathcal{A} = 1 - \bar{c} + 2\bar{Q} + \sum_{i=1}^{M-1}\frac{\bar{\alpha}_i^*\bar{\beta}_i + \bar{\alpha}_i\bar{\beta}_i^* - |\bar{\beta}_i|^2}{\bar{\Lambda}_i},$$

$$\mathcal{B} = 2\bar{L} - \bar{c} - \frac{5}{3}\bar{Q} - \sum_{i=1}^{M-1}\frac{|\bar{\beta}_i|^2}{\bar{\Lambda}_i}, \quad 3.6\text{-}11$$

with the dimensionless parameters $\bar{c}$, $\bar{L}$, $\bar{Q}$, $\bar{\alpha}_i$, $\bar{\beta}_i$ and $\bar{\Lambda}_i$ given by Eqs. (3.4-8) and (3.5-9).

Now we have everything at our disposal to determine the boundaries of the IT domain on the $\kappa - T$ plane. This domain with the general remark that the superconductivity types are related to the way the magnetic field penetrates the bulk superconductor and produces a nonuniform configuration of the flux/condensate, is found when the Gibbs free energy difference becomes smaller than that of the Meissner state at the thermodynamic critical field H_c, and this flux/condensate in question can appear. The appearance/disappearance marks the mixed state and separates the domains[35], the onset of this nonuniform state is found from the equation

$$G_{\Delta}(\kappa, T) = 0, \tag{3.6-12}$$

that yields the corresponding GL critical parameter $\kappa^*(T)$, referred to as simply a critical parameter. On the $\kappa - T$ plane $\kappa^*(T)$ separates domains with and without the flux/condensate configuration of interest.

Using Eq. (3.6-12) into Eq. (3.6-10), and $\delta\kappa^* = \kappa^* - \kappa_0$, one obtains the general expression for critical parameters up to the leading correction

$$\sqrt{2}\mathcal{I}\delta\kappa^* = \tau(\mathcal{A}\mathcal{I} + \mathcal{B}\mathcal{J}),$$

$$\delta\kappa^* = \frac{\tau}{\sqrt{2}}(\mathcal{A} + \mathcal{B}\mathcal{J}/\mathcal{I}). \tag{3.6-13}$$

We obtain

$$\kappa^* = \kappa_0[1 + \tau(\mathcal{A} + \mathcal{B}\mathcal{J}/\mathcal{I})]. \tag{3.6-14}$$

The lower boundary $\kappa^*_{\min}(T)$ marks the appearance/disappearance of the mixed state. The condensate vanishes at H_{c2} and so the Gibbs free energies of the normal and condensate states become equal. At the same time the normal and Meissner states have the same Gibbs free energy at H_c. Therefore, when type I separation of the IT domain approaches the, $\Psi \to 0$. Using this information and considering that $\mathcal{J}/\mathcal{I} \to 0$ for $\Psi \to 0$, from Eq. (3.6-10) we find

$$\kappa^*_{\min} = \kappa_0(1 + \tau\mathcal{A}). \tag{3.6-15}$$

The upper boundary $\kappa^*_{\max}(T)$ separates type-II and IT regimes and is determined by zero long-range interaction between superconducting vortices [35]: this interaction is repulsive in type II whereas it is attractive inside the IT domain. To calculate $\kappa^*_{\max}(T)$, one solves the Bogomolnyi equations for the case of two vortices at a distance R apart and finds the asymptote of Ψ at $R \to \infty$. The position dependent part of this asymptote is plugged into Eq. (3.6-12). As the Gibbs free energy of the normal state is not dependent on R, this procedure yields the long-range asymptote of the Gibbs free energy of two vortices or, in other words, their long-range interaction potential. The scaled GL equations (3.5-4) and, in turn, the Bogomolnyi equations are not sensitive to the number of contributing bands M, we can adopt the long-range asymptote of the two-vortex solution Ψ found previously in the two-band case [35], which yields $\mathcal{J}/\mathcal{I} = 2$. Then, we get

$$\kappa^*_{\max} = \kappa_0\big(1 + \tau(\mathcal{A} + 2\mathcal{B})\big). \qquad 3.6\text{-}16$$

Equations (3.6-15) and (3.6-16) are generalization of the expressions for the boundaries of the IT domain obtained previously for the two-band case [35]. As is already mentioned above, within the two-band formalism, $\vec{\Delta}^{(0)}$ and $\vec{\Delta}^{(1)}$ were represented as linear combinations of two explicitly chosen vectors[61] and the IT boundaries were expressed in terms of their components [35]. In the case of $\mathrm{M} > 2$, the extended GL formalism is obtained in a more compact form when $\vec{\Delta}^{(0)}$ and $\vec{\Delta}^{(1)}$ are written as linear combinations of the eigenvectors of the matrix $\check{L}$ [see Eq. (3.3-4)]. Then, to use Eqs.(3.6-15) and (3.6-16), one needs first to solve Eqs. (3.3-11) and (3.3-12) to determine the eigenvalues and eigenvectors of $\check{L}$.

In the next chapter we will investigate how the IT domain boundaries given by Eqs. (3.6-15) and (3.6-16) are sensitive to the number of contributing bands M for multiband systems with degenerate gaps. Analyzing Eqs. (3.3-19), (3.3-26), (3.4-6), (3.4-8), (3.5-9), and (3.6-11), one finds that $\kappa^*_{\min}$ and $\kappa^*_{\max}$ depend on the following microscopic parameters: the dimensionless couplings $\lambda_{\nu\nu'} = g_{\nu\nu'}N$ (with $N = \sum_\nu N_\nu$ the total DOS), the relative band DOSs $n_\nu = N_\nu/N$, and the band velocities ratios v_ν/v_1 (here the Fermi velocity of band 1 can be replaced by another band characteristic velocity). Since $T_c \propto \hbar c$, the cut-off frequency ω_c does not contribute to $\kappa^*_{\min}$ and $\kappa^*_{\max}$.

For two-band models available in the literature (see Ref. [35] and references therein) the intraband couplings λ_{11}, λ_{22} are usually in the range 0.2-0.7 (they are larger for MgB_2), the interband coupling λ_{12} is typically much smaller than the intraband ones, and the relative band DOSs n_1 and n_2 are usually close quantities. Thus, we can expect in general that $0.2 \lesssim \lambda_{\nu\nu'} \lesssim 0.7$, $\lambda_{\nu\neq\nu'} \ll \lambda_{\nu\nu}$ and $n_\nu \approx n_{\nu'}$.

To have an idea about the ratio v_ν/v_1, we can invoke available results of the first principle calculations for multiband superconductors. For example, the averaged Fermi velocity in the a-b plane of MgB_2 is estimated[99] as $v_\sigma^{(a-b)} = 4.4 \times 10^5 m/s$ and $v_\pi^{(a-b)} = 5.35 \times 10^5 m/s$ for σ and π bands, respectively. One sees that $v_\sigma^{(a-b)}$ is about 20% smaller than $v_\pi^{(a-b)}$. However, for the c-direction one obtains[99] that $v_\sigma^c = 7 \times 10^4 m/s$ is by an order of magnitude smaller than that $v_\pi^c = 7 \times 10^5 m/s$. In addition, ARPES measurements can be also employed. For instance, these measurements demonstrate that there exist three contributing bands in iron chalcogenide $FeSe_{0.35}Te_{0.65}$ and the maximal ratio of the band Fermi velocities is about 4, see Ref. [100] and discussion in Ref. [101]

3.7 RESULTS AND CONCLUSIONS

As is mentioned in the Introduction, it is usually assumed that the number of the energy gaps in the excitation spectrum determines the number of contributing bands in a superconducting model designed to capture essential physics in the multiband system of interest. The results given in the below demonstrate that this common expectation is an oversimplification and the magnetic properties of multiband systems with the same excitation gaps but with different numbers of bands can be significantly different.

For illustration, we first consider a two-band superconductor with degenerate excitation gaps and compare the boundaries of the IT domain for such a system with those for a single-band superconductor. The excitation gaps are calculated from the BCS equations

$$\Delta_\nu = \sum_{\nu'} \lambda_{\nu\nu'}\, n_{\nu'} \int_{-\hbar\omega_c}^{\hbar\omega_c} \frac{\Delta_{\nu'}}{2E_{\nu'}} [1 - 2f(E_{\nu'})], \qquad 3.7\text{-}1$$

with $E_\nu = \sqrt{\varepsilon^2 + |\Delta_\nu|^2}$ and $f(E_{\nu'})$ the fermi function. In the two-band case we choose

$$\lambda_{11} = \lambda_{22} = 0.3, \qquad \lambda_{12} = 0.05, \qquad n_1 = n_2. \qquad 3.7\text{-}2$$

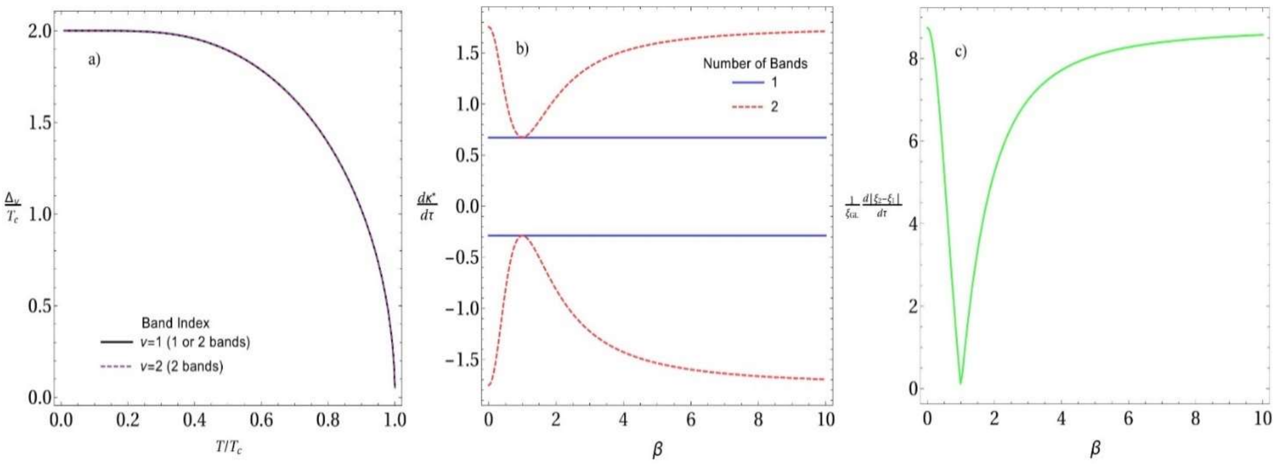

Figure 3.7-1 "Reference-[131]", The two-band system with the couplings and relative DOSs given by Eq. (3.7-2) versus the single-band system with the coupling $\lambda = 0.35$: (a) The single temperature dependent gap for both systems; (b) The τ-derivatives of the IT boundaries κ^*_{max} (two upper lines) and κ^*_{min} (two lower lines) versus the band Fermi velocities ratio $\beta = v_2/v_1$ for the two-band (dotted) and single-band (solid) cases, the single-band results are material independent quantities 0.67 and 0.29, see Ref. [35]; (c) The derivative $d|\xi_2 - \xi_1|/d\tau$ versus β, where $|\xi_2 - \xi_1|$ is the absolute value of the difference of the band healings lengths ξ_2 and ξ_1 for the two-band system in question.

The results of Δ_1 and Δ_2 (in units of T_c, Δ_ν in units of T_c does not depend on $\hbar\omega_c$), are given by the solid and dotted lines and merge into one curve (degenerate), as seen from Figure 3.7-1 a). To get the same excitation gap for the single-band case, one needs to adopt the dimensionless coupling 0.35, which is the sum of λ_{11} and λ_{12} given by Eq. (3.7-2), see Figure 3.7-1 a). Thus, the excitation spectra of the chosen two-band and single-band systems exhibit the same single energy gap. Notice that there are infinite combinations of parameters resulting in a single excitation energy gap in the two-band case: one simply needs to use $\lambda_{11}n_1 = \lambda_{22}n_2$. However, our qualitative conclusions are not sensitive to a particular choice of the couplings and DOSs.

In Figure 3.7-1 b) the derivatives $d\kappa^*/d\tau$ for $\kappa^*_{\rm min}$ and $\kappa^*_{\rm max}$ are shown versus the ratio $\beta = v_2/v_1$ for the single-gap system with two bands (dotted lines). The same quantities for the single-band system are universal material-independent constants [35] given by the solid lines. One sees that the boundaries of the IT domain of the two-band system are sensitive to the velocity ratio β and, in general, differ significantly from the single-band boundaries. We arrive at the conclusion that the superconducting magnetic properties depend on features of a Fermi surface with multiple band Fermi sheets, irrespective of the appearance of a multigap structure in the excitation spectrum.

To gain deeper understanding, it is of importance to emphasize that the IT domain boundaries of the both systems in Figure 3.7-1 b) coincide at $\beta = 1$. To clarify this point, we utilize the formalism of Ref. [101] and calculate the derivative $d|\xi_2 - \xi_1|/d\tau$, where $|\xi_2 - \xi_1|$ is the absolute value of the difference of the band healings lengths ξ_2 and ξ_1 for the two-band system in question. To the next-to-lowest order in τ, we have $\xi_\nu = \xi_\nu^{(0)} + \tau\xi_\nu^{(0)}$, with $\xi_\nu^{(0)} = \xi_{GL}$, see Refs. [61][101][102][103]. [Due to using the scaling transformation $\vec{x}' = \tau^{1/2}\vec{x}$, this healing-length expression should be multiplied by $\tau^{-1/2}$ to return to the standard definition]. Therefore, taken to one order beyond the GL theory, $d|\xi_2 - \xi_1|/d\tau$, is equal to $\left|\xi_2^{(1)} - \xi_1^{(1)}\right|$ and is not τ-dependent. The result is given in Figure 3.7-1 c) [in units of the GL coherence length $\xi_{\rm GL}$] and one sees that ξ_2 and ξ_1 coincide at $\beta = 1$. As is seen, when the band condensates are controlled by the same characteristic length, we find no difference in the superconducting magnetic properties as compared to the single-band case. Thus, the most promising regime of searching for non-single-condensate superconducting magnetic effects is the one with diverse and competing lengths of multiple contributing condensates.

For another illustration we compare the boundaries of the IT domain calculated for the two- and four-band systems with two different energy gaps in the excitation spectrum. Now the dimensionless couplings and relative DOSs are chosen as, the two-band system

$$\lambda_{11} = 0.175, \qquad \lambda_{22} = 0.125, \qquad \lambda_{12} = 0.05, \qquad n_1 = n_2, \qquad 3.7\text{-}3$$

and for the four-band one

$$\lambda_{11} = \lambda_{22} = 0.3, \qquad \lambda_{33} = \lambda_{44} = 0.2, \qquad \lambda_{\nu\nu'} = 0.05, \qquad n_\nu = n_{\nu'}, \qquad 3.7\text{-}4$$

Two energy gaps obtained from Eqs. (3.7-3) and (3.7-4) are shown in Figure 3.7-2 a). As in the previous illustration, there again exist infinite variants the couplings and DOSs. From Eq. 3.7-1 we can see that, the excitation gaps become degenerate when the quantity

$$\Delta_\nu = \sum_{\nu'=1}^{M} \lambda_{\nu\nu'} n_{\nu'}, \qquad 3.7\text{-}5$$

assumes the same value for several bands.

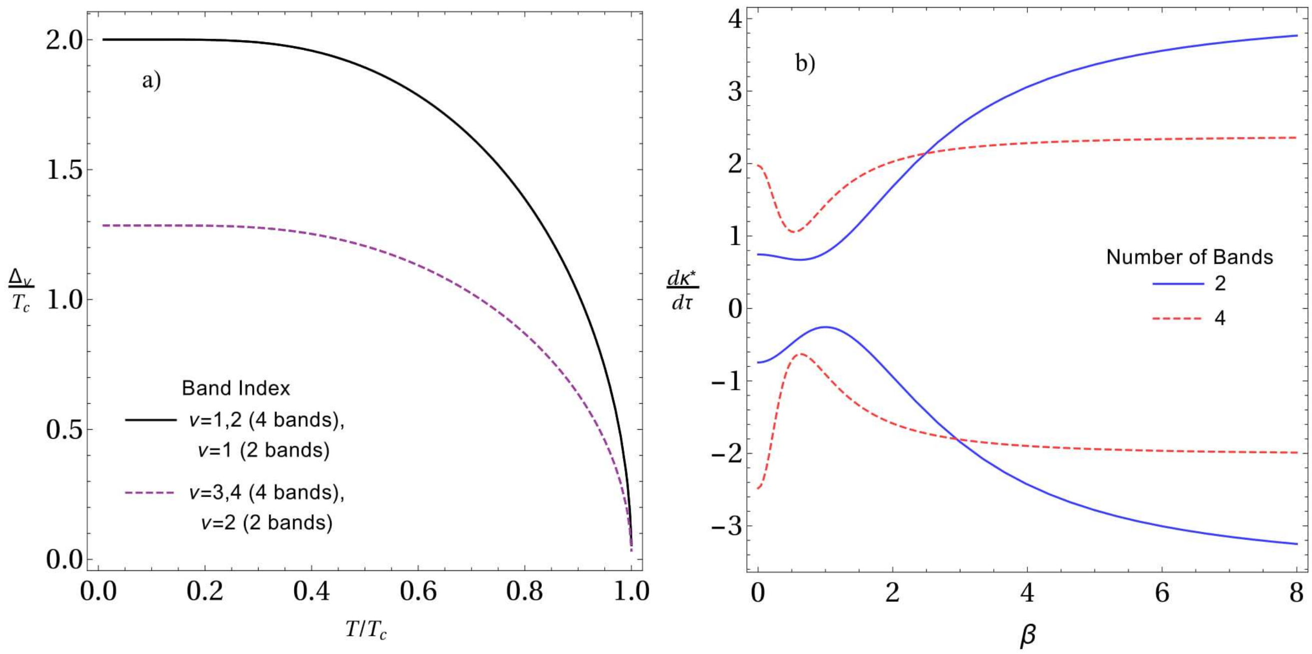

Figure 3.7-2 "Reference-[131]", The four-band system with the couplings and relative DOSs given by Eq. (3.7-4) versus the two-band system with $\lambda_{\nu\nu'}$ and n_ν given by Eq. (3.7-3): (a) The two temperature dependent gaps for both systems; (b) The τ-derivatives of the IT boundaries κ^*_{max} (two upper lines) and κ^*_{min} (two lower lines) versus β for the two-band (dotted) and single-band (solid) cases, where $\beta = v_2/v_1$ for the two-band case and $v_2/v_1 = v_3/v_1 = \beta$ and $v_4/v_1 = 2\beta$ for the four-band

For example, to get $\Delta_1^{(4b)} = \Delta_2^{(4b)} = \Delta_1^{(2b)}$, we can use $\sum_{\nu'=1}^{4} \lambda_{\nu\nu'}^{(4b)} n_{\nu'}^{(4b)}\Big|_{\nu=1,2} = \sum_{\nu'=1}^{2} \lambda_{\nu\nu'}^{(2b)} n_{\nu'}^{(2b)}$, similar expression with obvious alterations is needed to obtain $\Delta_3^{(4b)} = \Delta_4^{(4b)} = \Delta_2^{(2b)}$. We note again, however, that a particular choice of the couplings and DOSs does not influence our qualitative results.

The IT domain boundaries (their τ-derivatives) for the two-band system with two distinguished gaps governed by Eq. (3.7-3) are shown in Figure 3.7-2 b) versus $\beta = v_2/v_1$ (solid lines). One can see that in general, the corresponding IT domain is significantly different from the two-band IT domain shown in Figure 3.7-1 b). However, the two-band IT boundaries in Figure 3.7-2 b) are still close to the single-band ones in vicinity of $\beta = 1$, recall that $d\kappa^*_{\max}/d\tau$ and $d\kappa^*_{min}/d\tau$ in the single-band case are universal material-independent constants 0.67 and 0.29, respectively. Close to $\beta = 1$ the healing lengths ξ_2 and ξ_1 are nearly the same and the two-band system exhibits a nearly single-band superconducting magnetic response despite the presence of two excitation gaps. We again observe that the presence/absence of diverse characteristic lengths of multiple condensates coexisting in one material is more important for the superconducting magnetic properties than the presence/absence of multiple gaps in the excitation spectrum.

The quantities $d\kappa^*_{\max}/d\tau$ and $d\kappa^*_{min}/d\tau$ for the four-band system with two excitation gaps controlled by Eq. (3.7-4) are given by dotted lines in Figure 3.7-2 b). Here we use the parametrization of the band Fermi velocities as $v_2/v_1 = v_3/v_1 = \beta$ and $v_4/v_1 = 2\beta$. The adopted parametrization is not crucial: our study demonstrates that the IT domain boundaries for the four-band system are always very sensitive to the choice of the band Fermi velocities and in general different from the IT boundaries for the single- and two-band systems. In particular, we can see that the IT domain for the four-band case is always larger than the IT domain for the single-band system [c.f. Figure 3.7-2 b)]. More complex results are obtained when comparing the two- and four-band cases. The two-band and four-band lines corresponding to $d\kappa^*_{\max}/d\tau$ intersect at $\beta \approx 2.5$ while the corresponding lines for $d\kappa^*_{mi}\ /d\tau$ cross each other at the larger value $\beta \approx 3$. One sees that the IT domain boundaries for the four-band case are close to those for the two-band case at $\beta \approx$ 2.5-3. However, at $\beta \approx$ 6-8 the size of the IT domain is notably larger for the two-band case whereas the four-band IT domain is more pronounced for $\beta < 2$. Thus, the number of bands always matters, regardless the presence/absence of degenerate excitation gaps.

We have demonstrated that the superconducting magnetic properties are sensitive to the number of contributing bands even for degenerate excitation gaps. We have compared single-band results for the boundaries of the IT domain with those for the two-band case with degenerate superconducting gaps. In addition, the IT domain boundaries have been calculated for a four-band system with two excitation gaps and compared with the corresponding boundaries of a two-band case with the same two gaps in the excitation spectrum. We have found that nontrivial competition between diverse characteristic lengths of different contributing band condensates can result in non-single-condensate magnetic response even when the excitation spectrum of a superconductor exhibits a single energy gap. At the same time, we have observed that a superconductor can demonstrate a nearly single-condensate magnetic response in the presence of multiple excitation gaps. Characteristic lengths of multiple condensates are directly related to the complex Fermi surface made of different band Fermi sheets. The set of diverse and competing coherence lengths and the multigap energy structure of the excitation spectrum are both results of a complex Fermi surface with multiple Fermi sheets associated with different contributing bands. However, interference between different band condensates is not directly related to multiple excitation gaps. Thus, multiband superconductors are not the same as multigap ones.

Our analysis has been performed within the EGL approach that considers the leading corrections to the GL theory in the perturbative expansion of the microscopic equations in $\tau = 1 - T/T_c$. This formalism, previously constructed for single- and two-band systems, has been extended in the present work to the case of an arbitrary number of contributing bands. Its advantage is that it allows one to clearly distinguish various effects appearing due to the multiband structure in different types of superconducting characteristics. It particular, it reveals solid correlations between changes in the IT domain with the competition of multiple characteristic lengths of the contributing condensates.

4 MULTIBAND MATERIAL WITH A QUASI-1D BAND AS A HIGH TEMPERATURE SUPERCONDUCTOR

It is a common knowledge that superconductivity in 1D systems is suppressed due to fluctuations of the order parameter. The superconducting state can still be achieved when several 1D structures (parallel chains of molecules or atoms) are coupled one to another, creating a weakly coupled matrix. Earlier theoretical studies demonstrated that such quasi-1D materials can superconduct [105]–[110] but the fluctuations significantly reduce the critical temperature T_c [105]. These predictions were confirmed by observations of the low-temperature superconductivity in Bechgaard salts-organic quasi-1D superconductors [111], [112]. Subsequent theoretical analysis revealed that in some situations the critical temperature in quasi-1D systems can be enhanced rather than suppressed. In particular, this was calculated for weakly interacting stripes formed due to a particular transformation of the antiferromagnetic insulator [109], [110] and the enhancement is achieved under subtle balance of different physical mechanisms.

The interest in quasi-1D superconductors has been recently boosted by the discovery of Cr_2As_3-chain based quasi-1D materials [113]–[116]. Results of the first principle calculations of the electronic band structure of those compounds led to a conclusion that these quasi-1D superconductors are multiband materials with some of the contributing bands being quasi-1D ([116], [117]), multiband quasi-1D superconductors. In particular, there are two quasi-1D Fermi surface sheets coexisting with one 3D sheet in $K_2Cr_3As_3$ [13] and also in $KCr_3As_3H_x$ [12]. Furthermore, it was demonstrated that in $KCr_3As_3H_x$ the Fermi level is lifted by changing the H-intercalation [116], which gives rise to alterations in topology of the Fermi surface manifested in Lifshitz transitions. It is expected that proximity to a Lifshitz transition has a profound effect on the superconducting properties. For example, the mean field calculations reveal a considerable increase in the critical temperature when the chemical potential approaches the edge of a quasi-1D band [119]–[122]). However, the fluctuations, being already strong due to quasi-1D effects, severely increase due to the Bose-like character of the pairing in this regime. This can rule out any expectations based on the mean-field arguments.

On the other side, the interband coupling between condensates in different bands can reduce the fluctuations due to the multiband screening mechanism [118]. However, this mechanism was previously investigated only for quasi-2D bands and it is not clear how effective it is for quasi-1D superconductors. In the present thesis, motivated by recent experiments with multiband quasi-1D superconductors, we investigate a two-band system with coupled quasi-1D and 3D condensates. The goal of this work is to demonstrate that under a fairly general assumptions on the microscopic details, this system is a robust mean-field superconductor. This result opens promising prospects to engineer quasi-1D superconducting materials with higher critical temperatures.

4.1 QUASI-1D BAND

It is known that the GL theory in the vicinity of the mean-field critical temperature T_{c0} is obtained from the BCS microscopic formalism via the Gor'kov derivation. Below, for the reader convenience, we outline this derivation, specifying important features of the quasi-1D band in the vicinity of the Lifshitz transition (shallow quasi-1D band). The initial step of the Gor'kov procedure is the integral equation for the superconducting order parameter $\Delta(\boldsymbol{x}) = g\langle\psi_\uparrow(\boldsymbol{x})\psi_\downarrow(\boldsymbol{x})\rangle$ (g is the Gor'kov coupling) in terms of the normal-state temperature Green functions $\mathcal{G}_\omega^{(0)}$ and $\bar{\mathcal{G}}_\omega^{(0)}$, i.e.,

$$\frac{\Delta(\boldsymbol{x})}{g} = \int d^3\boldsymbol{y}\, K_a(\boldsymbol{x},\boldsymbol{y})\Delta(\boldsymbol{y}) + \int\left(\prod_{i=1}^{3} d^3\boldsymbol{y}_i\right) K_b(\boldsymbol{x},\boldsymbol{y}_1,\boldsymbol{y}_2,\boldsymbol{y}_3)\Delta(\boldsymbol{y}_1)\Delta^*(\boldsymbol{y}_2)\Delta(\boldsymbol{y}_3), \qquad 4.1\text{-}1$$

where the kernels are given by

$$K_a(\boldsymbol{x},\boldsymbol{y}) = -T\sum_\omega e^{-i\omega 0^+}\, \mathcal{G}_\omega^{(0)}(\boldsymbol{x},\boldsymbol{y})\bar{\mathcal{G}}_\omega^{(0)}(\boldsymbol{y},\boldsymbol{x}),$$

$$K_b(\boldsymbol{x},\boldsymbol{y}_1,\boldsymbol{y}_2,\boldsymbol{y}_3) = -T\sum_\omega e^{-i\omega 0^+}\, \mathcal{G}_\omega^{(0)}(\boldsymbol{x},\boldsymbol{y}_1)\bar{\mathcal{G}}_\omega^{(0)}(\boldsymbol{y}_1,\boldsymbol{y}_2)\mathcal{G}_\omega^{(0)}(\boldsymbol{y}_2,\boldsymbol{y}_3)\bar{\mathcal{G}}_\omega^{(0)}(\boldsymbol{y}_3,\boldsymbol{x}). \qquad 4.1\text{-}2$$

The normal-state temperature Green functions are expressed as

$$\mathcal{G}_\omega^{(0)}(\boldsymbol{x},\boldsymbol{y}) = \int \frac{d^3\boldsymbol{k}}{(2\pi)^3}\frac{\exp[i\boldsymbol{k}\cdot(\boldsymbol{x}-\boldsymbol{y})]}{i\hbar\omega - \xi_{\boldsymbol{k}}}, \qquad 4.1\text{-}3$$

and $\bar{\mathcal{G}}_{\omega}^{(0)}(\boldsymbol{y},\boldsymbol{x}) = -\mathcal{G}_{-\omega}^{(0)}(\boldsymbol{x},\boldsymbol{y})$. The integral kernels involve, as usual, the summation over the fermionic Matsubara frequencies $\omega_n = \frac{\pi T(2n+1)}{\hbar}$ (here the Boltzmann constant k_B is set to 1). The magnetic field is zero in the present consideration. The quasi-1D Fermi surface is modelled in such a way that the dispersion relation has very large effective electronic masses in two directions, say, $m_y, m_z \gg m_x$. Then the related single-particle energy becomes

$$\xi_k = \sum_i^3 \frac{\hbar^2 k_i^2}{2m_{\mathrm{i}}} - \mu \approx \frac{\hbar^2 k_x^2}{2m_{\mathrm{x}}} - \mu, \qquad 4.1\text{-}4$$

with μ the chemical potential (the Fermi level) and m_{x} set to the free electron mass m.

Considering only the linear contribution to the gap equation given by Eq. (3.7-1) and making its expansion

$$\int d^3\boldsymbol{y}\, K_a(\boldsymbol{x},\boldsymbol{y})\Delta(\boldsymbol{y}) = \int d^3\boldsymbol{z}\, K_a(\boldsymbol{x},\boldsymbol{x}+\boldsymbol{z})\Delta(\boldsymbol{x}+\boldsymbol{z}),$$

$$\int d^3\boldsymbol{z}\, K_a(\boldsymbol{x},\boldsymbol{x}+\boldsymbol{z})\Delta(\boldsymbol{x}+\boldsymbol{z})$$
$$\cong \int d^3\boldsymbol{z}\, K_a(\boldsymbol{x},\boldsymbol{x}+\boldsymbol{z}) \left[\Delta(\boldsymbol{x}) + \underbrace{\frac{\boldsymbol{z}\cdot\boldsymbol{\nabla}}{1!}\Delta(\boldsymbol{x})}_{0} + \frac{(\boldsymbol{z}\cdot\boldsymbol{\nabla})^2}{2!}\Delta(\boldsymbol{x}) + \cdots\right],$$
$$\cong \int d^3\boldsymbol{z}\, K_a(\boldsymbol{x},\boldsymbol{x}+\boldsymbol{z}) \left[\Delta(\boldsymbol{x}) + \frac{(\boldsymbol{z}\cdot\boldsymbol{\nabla})^2}{2!}\Delta(\boldsymbol{x}) + \cdots\right],$$

$$\int d^3\boldsymbol{z}\, K_a(\boldsymbol{x},\boldsymbol{x}+\boldsymbol{z})\Delta(\boldsymbol{x}+\boldsymbol{z})$$
$$\cong \int d^3\boldsymbol{z}\, K_a(\boldsymbol{x},\boldsymbol{x}+\boldsymbol{z})\Delta(\boldsymbol{x}) + \int d^3\boldsymbol{z}\, K_a(\boldsymbol{x},\boldsymbol{x}+\boldsymbol{z})\frac{(\boldsymbol{z}\cdot\boldsymbol{\nabla})^2}{2!}\Delta(\boldsymbol{x}) + \cdots. \qquad 4.1\text{-}5$$

Now, we deal with the local term $\int d^3\boldsymbol{z}\, K_a(\boldsymbol{x},\boldsymbol{x}+\boldsymbol{z})\Delta(\boldsymbol{x}) = a_{1s}\Delta(\boldsymbol{x})$

$$a_{1s} = -T\int d^3\boldsymbol{z} \sum_{\omega} e^{-i\omega 0^+}\, \mathcal{G}_{\omega}^{(0)}(\boldsymbol{x},\boldsymbol{x}+\boldsymbol{z})\bar{\mathcal{G}}_{\omega}^{(0)}(\boldsymbol{x}+\boldsymbol{z},\boldsymbol{x}),$$

$$a_{1s} = -T\int d^3\boldsymbol{z} \sum_{\omega} e^{-i\omega 0^+} \int \frac{d^3\boldsymbol{k}}{(2\pi)^3}\frac{\exp[-i\boldsymbol{k}\cdot\boldsymbol{z}]}{i\hbar\omega - \xi_{\boldsymbol{k}}} \int \frac{d^3\boldsymbol{q}}{(2\pi)^3}\frac{\exp[i\boldsymbol{q}\cdot\boldsymbol{z}]}{i\hbar\omega + \xi_{\boldsymbol{k}'}},$$

$$a_{1s} = -T\sum_{\omega} e^{-i\omega 0^+} \int\int d^3\boldsymbol{k}'\, \delta(\boldsymbol{k}-\boldsymbol{q})\frac{d^3\boldsymbol{k}}{(2\pi)^3}\frac{1}{i\hbar\omega - \xi_{\boldsymbol{k}}}\frac{1}{i\hbar\omega + \xi_{\boldsymbol{k}'}},$$

$$a_{1s} = -T\sum_{\omega} e^{-i\omega\ +}\int \frac{d^3\boldsymbol{k}}{(2\pi)^3}\frac{1}{i\hbar\omega - \xi_{\boldsymbol{k}}}\frac{1}{i\hbar\omega + \xi_{\boldsymbol{k}}},$$

$$a_{1s} = -T\sum_{\omega} e^{-i\omega 0^+}\int \frac{d^3\boldsymbol{k}}{(2\pi)^3}\frac{1}{2\xi_{\boldsymbol{k}}}\left(\frac{1}{i\hbar\omega - \xi_{\boldsymbol{k}}} - \frac{1}{i\hbar\omega + \xi_{\boldsymbol{k}}}\right),$$

$$a_{1s} = -T\int \frac{d^3\boldsymbol{k}}{(2\pi)^3}\frac{1}{2\xi_{\boldsymbol{k}}}\left(\sum_{\omega}\frac{e^{-i\omega 0^+}}{i\hbar\omega - \xi_{\boldsymbol{k}}} - \sum_{\omega}\frac{e^{-i\omega 0^+}}{i\hbar\omega + \xi_{\boldsymbol{k}}}\right),$$

$$a_{1s} = -T\int \frac{d^3\boldsymbol{k}}{(2\pi)^3}\frac{1}{2\xi_{\boldsymbol{k}}}\left(-\frac{1}{T}\frac{1}{e^{-\frac{1}{\mathrm{T}}\xi_{\boldsymbol{k}}} + 1} + \frac{1}{T}\frac{1}{e^{\frac{1}{\mathrm{T}}\xi_{\boldsymbol{k}}} + 1}\right),$$

$$a_{1s} = \int \frac{d^3\boldsymbol{k}}{(2\pi)^3}\frac{1}{2\xi_{\boldsymbol{k}}}\left(\frac{1}{e^{-\frac{1}{\mathrm{T}}\xi_{\boldsymbol{k}}} + 1} - \frac{1}{e^{\frac{1}{\mathrm{T}}\xi_{\boldsymbol{k}}} + 1}\right),$$

$$a_{1s} = \int \frac{d^3\boldsymbol{k}}{(2\pi)^3}\frac{1}{2\xi_{\boldsymbol{k}}}\tanh\left(\frac{\xi_{\boldsymbol{k}}}{2\mathrm{T}}\right). \qquad 4.1\text{-}6$$

Introducing the dimensionless coupling λ_s that is defined as

$$\lambda_s = gN_s = g\sigma^{(yz)}\sqrt{\frac{m}{32\pi^2\hbar^3\omega_c}} = g\frac{\sigma^{(yz)}}{4\pi\hbar v_s}. \qquad 4.1\text{-}7$$

Here $\sigma^{(yz)}$ is given by

$$\sigma^{(yz)} = \int \frac{dk_y}{2\pi}\frac{dk_z}{2\pi} \sim \left(a_y a_z\right)^{-1}, \qquad 4.1\text{-}8$$

and introduced to account for the states in y and z directions. It is proportional to the inverse product of the lattice parameters a_y and a_z. The auxiliary quantity N_s is the effective DOS in the quasi-1D band at the energy $\hbar\omega_c$, and we also introduce the effective band velocity v_s that is determined by the cutoff energy ($\hbar\omega_c$), where ω_c is the cut-off frequency, as $v_s = \sqrt{\frac{2\hbar\omega_c}{m}}$.

So, from this considerations and eq. 4.1-4, eq. 4.1-6 becomes

$$a_{1s} = \sigma^{(yz)}\int \frac{dk_x}{2\pi}\frac{1}{2\xi_{\boldsymbol{k}}}\tanh\left(\frac{\xi_{\boldsymbol{k}}}{2\mathrm{T}}\right),$$

changing to the energy space, $dk_x = \sqrt{\frac{m}{2\hbar^2}}\frac{d\xi}{\sqrt{\xi+\mu}}$,

$$a_{1s} = \frac{\sigma^{(yz)}}{4\pi}\sqrt{\frac{m}{2\hbar^2}}\int_{-\mu}^{\hbar\omega_c}\frac{d\xi}{\sqrt{\xi+\mu}}\frac{1}{\xi}\tanh\left(\frac{\xi}{2T}\right).$$

Normalizing the energies in function of the cutoffs $\hbar\omega_c$, $\bar{\xi} = \frac{\xi}{\hbar\omega_c}$, $\bar{\mu} = \frac{\mu}{\hbar\omega_c}$ and temperature $\bar{T} = \frac{T}{\hbar\omega_c}$, and changing to the normalized variables

$$a_{1s} = \sigma^{(yz)}\sqrt{\frac{m}{32\pi^2\hbar^3\omega_c}}\int_{-\bar{\mu}}^{1}\frac{d\bar{\xi}}{\sqrt{\bar{\xi}+\bar{\mu}}}\frac{1}{\bar{\xi}}\tanh\left(\frac{\bar{\xi}}{2\bar{T}}\right),$$

$$a_{1s} = N_s\int_{-\bar{\mu}}^{1}\frac{d\bar{\xi}}{\sqrt{\bar{\xi}+\bar{\mu}}}\frac{1}{\bar{\xi}}\tanh\left(\frac{\bar{\xi}}{2\bar{T}}\right), \qquad \textit{4.1-9}$$

As

$$a_{1s} = \mathcal{A}_s - a_s[\tau + \mathcal{O}(\tau^2)].$$

Where $\tau = 1 - T/T_c$, one obtains

$$\mathcal{A}_s = N_s\int_{-\bar{\mu}}^{1}\frac{d\bar{\xi}}{\sqrt{\bar{\xi}+\bar{\mu}}}\frac{1}{\bar{\xi}}\tanh\left(\frac{\bar{\xi}}{2\bar{T}_{c0}}\right), \qquad \textit{4.1-10}$$

$$a_s = -\frac{N_s}{2\bar{T}_{c0}}\int_{-\bar{\mu}}^{1}\frac{d\bar{\xi}}{\sqrt{\bar{\xi}+\bar{\mu}}}\text{sech}^2\left(\frac{\bar{\xi}}{2\bar{T}_{c0}}\right). \qquad \textit{4.1-11}$$

From eq. 4.1-10, we can find $\bar{T}_{c0}$ due to the fact that $\mathcal{A}_s = 1$.

Now, we will solve the square-gradient term $\int d^3\boldsymbol{z}\, K_a(\boldsymbol{x},\boldsymbol{x}+\boldsymbol{z})\frac{(\boldsymbol{z}\cdot\boldsymbol{\nabla})^2}{2!}\Delta(\boldsymbol{x})$,

$$\int d^3\boldsymbol{z}\, K_a(\boldsymbol{x},\boldsymbol{x}+\boldsymbol{z})\frac{(\boldsymbol{z}\cdot\boldsymbol{\nabla})^2}{2!}\Delta(\boldsymbol{x}) = \sum_n\int d^3\boldsymbol{z}\, K_a(\boldsymbol{x},\boldsymbol{x}+\boldsymbol{z})\frac{z_n^2\nabla_n^2}{2}\Delta(\boldsymbol{x})$$

$$= \sum_n\left[\int d^3\boldsymbol{z}\, K_a(\boldsymbol{x},\boldsymbol{x}+\boldsymbol{z})\frac{z_n^2}{2}\right]\nabla_n^2\Delta(\boldsymbol{x}).$$

Solving this term first

$$a_{2s}^{(n)} = \int d^3\boldsymbol{z}\, K_a(\boldsymbol{x},\boldsymbol{x}+\boldsymbol{z})\frac{z_n^2}{2},$$

$$a_{2s}^{(n)} = -\frac{T}{2}\int d^3\boldsymbol{z}\sum_\omega e^{-i\omega 0^+}\,\mathcal{G}_\omega^{(0)}(\boldsymbol{z})z_n\bar{\mathcal{G}}_\omega^{(0)}(-\boldsymbol{z})(-z_n)(-1),$$

$$a_{2s}^{(n)} = \frac{T}{2}\int d^3\boldsymbol{z}\sum_{\omega} e^{-\mathrm{i}\omega 0^+}\, \mathcal{G}_{\omega}^{(0)}(\boldsymbol{z}) z_n \bar{\mathcal{G}}_{\omega}^{(0)}(-\boldsymbol{z})(-z_n). \qquad 4.1\text{-}12$$

And the relations

$$\frac{1}{i\hbar\omega - \xi_{\boldsymbol{k}}} = \int d^3\boldsymbol{z}\, \mathcal{G}_{\omega}^{(0)}(\boldsymbol{z}) e^{-i\boldsymbol{k}\cdot\boldsymbol{z}}, \qquad -\frac{1}{i}\partial_{k_n}\frac{1}{i\hbar\omega - \xi_{\boldsymbol{k}}} = \int d^3\boldsymbol{z}\, z_n \mathcal{G}_{\omega}^{(0)}(\boldsymbol{z}) e^{-i\boldsymbol{k}\cdot\boldsymbol{z}},$$

$$\frac{1}{i\hbar\omega + \xi_{\boldsymbol{k}}} = \int d^3\boldsymbol{z}\, \bar{\mathcal{G}}_{\omega}^{(0)}(\boldsymbol{z}) e^{-i\boldsymbol{k}\cdot\boldsymbol{z}}, \qquad -\frac{1}{i}\partial_{k_n}\frac{1}{i\hbar\omega + \xi_{\boldsymbol{k}}} = \int d^3\boldsymbol{z}\, z_n \bar{\mathcal{G}}_{\omega}^{(0)}(\boldsymbol{z}) e^{-i\boldsymbol{k}\cdot\boldsymbol{z}},$$

$$-\frac{1}{i}\partial_{k_n}\frac{1}{i\hbar\omega + \xi_{\boldsymbol{k}}} = \int d^3\boldsymbol{z}\, (-z_n) \bar{\mathcal{G}}_{\omega}^{(0)}(-\boldsymbol{z}) e^{i\boldsymbol{k}\cdot\boldsymbol{z}}.$$

So,

$$z_n \mathcal{G}_{\omega}^{(0)}(\boldsymbol{z}) = \int \frac{d^3\boldsymbol{k}}{(2\pi)^3} e^{i\boldsymbol{k}\cdot\boldsymbol{z}}\left(-\frac{1}{i}\right)\partial_{k_n}\frac{1}{i\hbar\omega - \xi_{\boldsymbol{k}}},$$

$$(-z_n)\bar{\mathcal{G}}_{\omega}^{(0)}(-\boldsymbol{z}) = \int \frac{d^3\boldsymbol{k}}{(2\pi)^3} e^{-i\boldsymbol{k}\cdot\boldsymbol{z}}\left(-\frac{1}{i}\right)\partial_{k_n}\frac{1}{i\hbar\omega + \xi_{\boldsymbol{k}}}.$$

Then, eq. 4.1-12 becomes

$$a_{2s}^{(n)} = \frac{T}{2}\int d^3\boldsymbol{z}\sum_{\omega} e^{-\mathrm{i}\omega 0^+}\int \frac{d^3\boldsymbol{k}}{(2\pi)^3} e^{i\boldsymbol{k}\cdot\boldsymbol{z}}\left(-\frac{1}{i}\right)\partial_{k_n}\frac{1}{i\hbar\omega - \xi_{\boldsymbol{k}}}\int \frac{d^3\boldsymbol{q}}{(2\pi)^3} e^{-i\boldsymbol{q}\cdot\boldsymbol{z}}\left(-\frac{1}{i}\right)\partial_{q_n}\frac{1}{i\hbar\omega + \xi_{\boldsymbol{q}}},$$

So, one obtains

$$a_{2s}^{(n)} = -\frac{T}{2}\sum_{\omega} e^{-\mathrm{i}\omega 0^+}\int \frac{d^3\boldsymbol{k}}{(2\pi)^3}\partial_{k_n}\frac{1}{i\hbar\omega - \xi_{\boldsymbol{k}}}\partial_{k_n}\frac{1}{i\hbar\omega + \xi_{\boldsymbol{k}}}. \qquad 4.1\text{-}13$$

Solving this equation, and $\partial_{k_n}\frac{1}{i\hbar\omega - \xi_{\boldsymbol{k}}} = 0$ in y and z direction.

$$a_{2s}^{(x)} = -\frac{T}{2}\sum_{\omega}\int \frac{d^3\boldsymbol{k}}{(2\pi)^3}\frac{1}{(i\hbar\omega - \xi_{\boldsymbol{k}})^2}\frac{\hbar^2}{m}k_x\frac{(-1)}{(i\hbar\omega + \xi_{\boldsymbol{k}})^2}\frac{\hbar^2}{m}k_x,$$

$$a_{2s}^{(x)} = \frac{T}{2}\frac{\hbar^2}{m}\sum_{\omega}\int \frac{d^3\boldsymbol{k}}{(2\pi)^3}\frac{1}{(i\hbar\omega - \xi_{\boldsymbol{k}})^2}\frac{1}{(i\hbar\omega + \xi_{\boldsymbol{k}})^2}\frac{\hbar^2}{m}k_x^2,$$

$$a_{2s}^{(x)} = \frac{T}{2}\frac{\hbar^2}{m}\sum_{\omega} e^{-\mathrm{i}\omega 0^+}\int \frac{d^3\boldsymbol{k}}{(2\pi)^3}\frac{1}{(\hbar^2\omega^2 + \xi_{\boldsymbol{k}}^2)^2}2(\xi_{\boldsymbol{k}} + \mu),$$

changing to the energy space, $dk_x = \sqrt{\frac{m}{2\hbar^2}}\frac{d\xi}{\sqrt{\xi+\mu}}$, and using $\sigma^{(yz)} = \int \frac{dk_y}{2\pi}\frac{dk_z}{2\pi}$,

$$a_{2s}^{(x)} = T\frac{\hbar^2}{m}\sqrt{\frac{m}{2\hbar^2}}\sigma^{(yz)}\sum_{\omega}\int_{-\mu}^{\hbar\omega_c}\frac{d\xi}{2\pi\sqrt{\xi+\mu}}\frac{(\xi+\mu)}{(\hbar^2\omega^2+\xi^2)^2}, \qquad 4.1\text{-}14$$

and here we use the tabled infinite summation over fermionic Matsubara frequencies($\eta = -1$)

$$\sum_{\omega}\frac{1}{(\hbar^2\omega^2+\xi^2)^2} = -\frac{\eta}{2T\xi^2}\left(c_\eta(0,\xi) + n'_\eta(\xi)\right),$$

where

$$c_\eta(a,\mathrm{b}) = \frac{\sinh(b/T)}{2b(\cosh(a/T) - \eta\cosh(b/T))}.$$

Then,

$$c_F(0,\xi) = \frac{1}{2\xi}\tanh\left(\frac{\xi}{2T}\right).$$

And

$$n_\eta(\xi) = \frac{1}{e^{\xi/\mathrm{T}} - \eta}.$$

For fermions

$$n_F(\xi) = \frac{1}{2}\left[1 - \tanh\left(\frac{\xi}{2T}\right)\right].$$

So,

$$n'_F(\xi) = -\frac{\mathrm{sech}^2\left(\frac{\xi}{2T}\right)}{4T}.$$

Finally, one obtains the infinite summation over fermionic Matsubara frequencies

$$\sum_{\omega}\frac{1}{(\hbar^2\omega^2+\xi^2)^2} = \frac{1}{2\xi^2 T}\left[\frac{1}{2\xi}\tanh\left(\frac{\xi}{2T}\right) - \frac{1}{4T}\mathrm{sech}^2\left(\frac{\xi}{2T}\right)\right],$$

$$\sum_{\omega}\frac{1}{(\hbar^2\omega^2+\xi^2)^2} = \frac{\left[T\sinh\left(\frac{\xi}{T}\right) - \xi\right]\mathrm{sech}^2\left(\frac{\xi}{2T}\right)}{8\xi^3 T^2}. \qquad 4.1\text{-}15$$

Then using this equation in 4.1-14, reads

$$a_{2s}^{(x)} = T\frac{\hbar^2}{2\pi m}\sqrt{\frac{m}{2\hbar^2}}\sigma^{(yz)}\int_{-\mu}^{\hbar\omega_c} d\xi\sqrt{\xi+\mu}\frac{\left[T\sinh\left(\frac{\xi}{T}\right)-\xi\right]\mathrm{sech}^2\left(\frac{\xi}{2T}\right)}{8\xi^3T^2}.$$

Normalizing the energies in function of the cutoffs and changing to the normalized variables

$$a_{2s}^{(x)} = \frac{1}{16\pi\hbar\omega_c}\sqrt{\frac{\hbar^2}{2m\hbar\omega_c}}\sigma^{(yz)}\int_{-\bar{\mu}}^{1} d\bar{\xi}\frac{\sqrt{\bar{\xi}+\bar{\mu}}}{\bar{\xi}^3}\left[\sinh\left(\frac{\bar{\xi}}{\bar{\mathrm{T}}}\right)-\frac{\bar{\xi}}{\bar{\mathrm{T}}}\right]\mathrm{sech}^2\left(\frac{\bar{\xi}}{2\bar{\mathrm{T}}}\right),$$

using $\sigma^{(yz)} = N_s 4\pi\hbar v_s$ and $v_s = \sqrt{\frac{2\hbar\omega_c}{m}}$,

$$a_{2s}^{(x)} = \frac{1}{16\pi\omega_c}\frac{v_s}{\sqrt{2\hbar\omega_c}}\sqrt{\frac{1}{2\hbar\omega_c}}N_s 4\pi\hbar v_s\int_{-\bar{\mu}}^{1} d\bar{\xi}\frac{\sqrt{\bar{\xi}+\bar{\mu}}}{\bar{\xi}^3}\left[\sinh\left(\frac{\bar{\xi}}{\bar{\mathrm{T}}}\right)-\frac{\bar{\xi}}{\bar{\mathrm{T}}}\right]\mathrm{sech}^2\left(\frac{\bar{\xi}}{2\bar{\mathrm{T}}}\right),$$

$$a_{2s} = \hbar^2 v_s^2\frac{N_s}{8\hbar^2\omega_c^2}\int_{-\bar{\mu}}^{1} d\bar{\xi}\frac{\sqrt{\bar{\xi}+\bar{\mu}}}{\bar{\xi}^3}\left[\sinh\left(\frac{\bar{\xi}}{\bar{\mathrm{T}}}\right)-\frac{\bar{\xi}}{\bar{\mathrm{T}}}\right]\mathrm{sech}^2\left(\frac{\bar{\xi}}{2\bar{\mathrm{T}}}\right).$$

Thus, we obtain

$$\int d^3\boldsymbol{z}\, K_a(\boldsymbol{x},\boldsymbol{x}+\boldsymbol{z})\frac{(\boldsymbol{z}\cdot\boldsymbol{\nabla})^2}{2!}\Delta(\boldsymbol{x}) = \sum_n\left[\int d^3\boldsymbol{z}\, K_a(\boldsymbol{x},\boldsymbol{x}+\boldsymbol{z})\frac{z_n^2}{2}\right]\nabla_n^2\Delta(\boldsymbol{x}),$$

$$\sum_n a_{2s}^{(n)}\nabla_n^2\Delta(\boldsymbol{x}) = a_{2s}^{(x)}\nabla_x^2\Delta(\boldsymbol{x}),$$

$$a_{2s}^{(x)} = K_s^{(x)}[1+\mathcal{O}(\tau)].$$

So,

$$K_s^{(x)} = \hbar^2 v_s^2\frac{N_s}{8\hbar^2\omega_c^2}\int_{-\bar{\mu}}^{1} d\bar{\xi}\frac{\sqrt{\bar{\xi}+\bar{\mu}}}{\bar{\xi}^3}\left[\sinh\left(\frac{\bar{\xi}}{\bar{T}_{c0}}\right)-\frac{\bar{\xi}}{\bar{T}_{c0}}\right]\mathrm{sech}^2\left(\frac{\bar{\xi}}{2\bar{T}_{c0}}\right). \quad \text{4.1-16}$$

and the stiffnesses of the gap parameter along the other orthogonal directions is zero.

Now we will deal with the last term given by the cubic contribution from Eq. (3.7-1). It is enough to consider only the zero-order contribution of the gap in the Taylor expansion on the coordinates (i.e. it becomes independent of the gap) and thus the integral becomes

$$\int\left(\prod_{i=1}^{3} d^3\boldsymbol{y}_i\right) K_b(\boldsymbol{x},\boldsymbol{y}_1,\boldsymbol{y}_2,\boldsymbol{y}_3)\Delta(\boldsymbol{y}_1)\Delta^*(\boldsymbol{y}_2)\Delta(\boldsymbol{y}_3)$$

$$= -T\sum_{\omega}\int\left(\prod_{i=1}^{3} d^3\boldsymbol{y}_i\right)\mathcal{G}_\omega^{(0)}(\boldsymbol{x},\boldsymbol{y}_1)\bar{\mathcal{G}}_\omega^{(0)}(\boldsymbol{y}_1,\boldsymbol{y}_2)\mathcal{G}_\omega^{(0)}(\boldsymbol{y}_2,\boldsymbol{y}_3)\bar{\mathcal{G}}_\omega^{(0)}(\boldsymbol{y}_3,\boldsymbol{x})\Delta(\boldsymbol{y}_1)\Delta^*(\boldsymbol{y}_2)\Delta(\boldsymbol{y}_3),$$

$$= -T\sum_{\omega}\int\left(\prod_{i=1}^{3} d^3\boldsymbol{z}_i\right)\mathcal{G}_\omega^{(0)}(-\boldsymbol{z}_1)\bar{\mathcal{G}}_\omega^{(0)}(\boldsymbol{z}_1-\boldsymbol{z}_2)\mathcal{G}_\omega^{(0)}(\boldsymbol{z}_2-\boldsymbol{z}_3)\bar{\mathcal{G}}_\omega^{(0)}(\boldsymbol{z}_3)\Delta(\boldsymbol{x}+\boldsymbol{y}_1)\Delta^*(\boldsymbol{x} + \boldsymbol{y}_2)\Delta(\boldsymbol{x}+\boldsymbol{y}_3),$$

with $\boldsymbol{z}_1 = \boldsymbol{y}_1 - \boldsymbol{x}$, $\boldsymbol{z}_2 = \boldsymbol{y}_2 - \boldsymbol{x}$, $\boldsymbol{z}_3 = \boldsymbol{y}_3 - \boldsymbol{x}$.

$$\int\left(\prod_{i=1}^{3} d^3\boldsymbol{y}_i\right) K_b(\boldsymbol{x},\boldsymbol{y}_1,\boldsymbol{y}_2,\boldsymbol{y}_3)\Delta(\boldsymbol{y}_1)\Delta^*(\boldsymbol{y}_2)\Delta(\boldsymbol{y}_3)$$

$$= -T\sum_{\omega}\int\left(\prod_{i=1}^{3} d^3\boldsymbol{z}_i\right)\mathcal{G}_\omega^{(0)}(-\boldsymbol{z}_1)\bar{\mathcal{G}}_\omega^{(0)}(\boldsymbol{z}_1-\boldsymbol{z}_2)\mathcal{G}_\omega^{(0)}(\boldsymbol{z}_2-\boldsymbol{z}_3)\bar{\mathcal{G}}_\omega^{(0)}(\boldsymbol{z}_3)\Delta(\boldsymbol{x} + \cdots)(\boldsymbol{x}+\cdots)\Delta^*(\boldsymbol{x}+\cdots)\Delta(\boldsymbol{x}+\cdots),$$

$$= -T\sum_{\omega}\int\left(\prod_{i=1}^{3} d^3\boldsymbol{z}_i\right)\mathcal{G}_\omega^{(0)}(-\boldsymbol{z}_1)\bar{\mathcal{G}}_\omega^{(0)}(\boldsymbol{z}_1-\boldsymbol{z}_2)\mathcal{G}_\omega^{(0)}(\boldsymbol{z}_2-\boldsymbol{z}_3)\bar{\mathcal{G}}_\omega^{(0)}(\boldsymbol{z}_3)|\Delta(\boldsymbol{x})|^2\Delta(\boldsymbol{x}).$$

Then,

$$b_{1s} = -T\sum_{\omega}\int\left(\prod_{i=1}^{3} d^3\boldsymbol{z}_i\right)\mathcal{G}_\omega^{(0)}(-\boldsymbol{z}_1)\bar{\mathcal{G}}_\omega^{(0)}(\boldsymbol{z}_1-\boldsymbol{z}_2)\mathcal{G}_\omega^{(0)}(\boldsymbol{z}_2-\boldsymbol{z}_3)\bar{\mathcal{G}}_\omega^{(0)}(\boldsymbol{z}_3), \qquad 4.1\text{-}17$$

$$b_{1s} = -T\sum_{\omega}\int\left(\prod_{i=1}^{3} d^3\boldsymbol{z}_i\frac{d^3\boldsymbol{k}_i}{(2\pi)^3}\right)\frac{d^3\boldsymbol{k}}{(2\pi)^3}\frac{e^{i\boldsymbol{k}\cdot(-\boldsymbol{z}_1)}}{i\hbar\omega-\xi_{\boldsymbol{k}}}\frac{e^{i\boldsymbol{k}_1\cdot(\boldsymbol{z}_1-\boldsymbol{z}_2)}}{i\hbar\omega+\xi_{\boldsymbol{k}_1}}\frac{e^{i\boldsymbol{k}_2\cdot(\boldsymbol{z}_2-\boldsymbol{z}_3)}}{i\hbar\omega-\xi_{\boldsymbol{k}_2}}\frac{e^{i\boldsymbol{k}_3\cdot\boldsymbol{z}_3}}{i\hbar\omega+\xi_{\boldsymbol{k}_3}},$$

$$b_{1s} = -T\sum_{\omega}\int\left(\prod_{i=1}^{3} d^3\boldsymbol{k}_i\right)\frac{d^3\boldsymbol{k}}{(2\pi)^3}\delta(\boldsymbol{k}-\boldsymbol{k}_1)\delta(\boldsymbol{k}_1-\boldsymbol{k}_2)\delta(\boldsymbol{k}_2 - \boldsymbol{k}_3)\frac{1}{i\hbar\omega-\xi_{\boldsymbol{k}}}\frac{1}{i\hbar\omega+\xi_{\boldsymbol{k}_1}}\frac{1}{i\hbar\omega-\xi_{\boldsymbol{k}_2}}\frac{1}{i\hbar\omega+\xi_{\boldsymbol{k}_3}},$$

$$b_{1s} = -T\sum_{\omega}\int\frac{d^3\boldsymbol{k}}{(2\pi)^3}\frac{1}{(\hbar^2\omega^2+\xi_{\boldsymbol{k}}^2)^2},$$

changing to the energy space, $dk_x = \sqrt{\frac{m}{2\hbar^2}}\frac{d\xi}{\sqrt{\xi+\mu}}$, and using $\sigma^{(yz)} = \int \frac{dk_y}{2\pi}\frac{dk_z}{2\pi}$

$$b_{1s} = -T\sqrt{\frac{m}{2\hbar^2}}\sigma^{(yz)}\sum_{\omega}\int_{-\mu}^{\hbar\omega_c}\frac{d\xi}{2\pi\sqrt{\xi+\mu}}\frac{1}{(\hbar^2\omega^2+\xi^2)^2}.$$

And using Eq. 4.1-15, we obtain

$$b_{1s} = -T\sqrt{\frac{m}{2\hbar^2}}\sigma^{(yz)}\int_{-\mu}^{\hbar\omega_c}\frac{d\xi}{2\pi\sqrt{\xi+\mu}}\frac{\left[T\sinh\left(\frac{\xi}{T}\right)-\xi\right]\operatorname{sech}^2\left(\frac{\xi}{2T}\right)}{8\xi^3T^2},$$

changing to the normalized variables

$$b_{1s} = -\sqrt{\frac{m}{2\hbar^3\omega_c}}\frac{\sigma^{(yz)}}{16\pi(\hbar\omega_c)^2}\int_{-\bar{\mu}}^{1}d\bar{\xi}\frac{\operatorname{sech}^2\left(\frac{\bar{\xi}}{2\bar{T}}\right)}{\bar{\xi}^3\sqrt{\bar{\xi}+\bar{\mu}}}\left[\sinh\left(\frac{\bar{\xi}}{\bar{T}}\right)-\frac{\bar{\xi}}{\bar{T}}\right].$$

As, $\sigma^{(yz)} = N_s\sqrt{\frac{32\ \ ^2\hbar^3\omega_c}{m}}$

$$b_{1s} = -\sqrt{\frac{m}{2\hbar^3\omega_c}}\frac{N_s}{16\pi(\hbar\omega_c)^2}\sqrt{\frac{32\pi^2\hbar^3\omega_c}{m}}\int_{-\bar{\mu}}^{1}d\bar{\xi}\frac{\operatorname{sech}^2\left(\frac{\bar{\xi}}{2\bar{T}}\right)}{\bar{\xi}^3\sqrt{\bar{\xi}+\bar{\mu}}}\left[\sinh\left(\frac{\bar{\xi}}{\bar{T}}\right)-\frac{\bar{\xi}}{\bar{T}}\right],$$

$$b_{1s} = -\frac{N_s}{4\hbar^2\omega_c^2}\int_{-\bar{\mu}}^{1}d\bar{\xi}\frac{\operatorname{sech}^2\left(\frac{\bar{\xi}}{2\bar{T}}\right)}{\bar{\xi}^3\sqrt{\bar{\xi}+\bar{\mu}}}\left[\sinh\left(\frac{\bar{\xi}}{\bar{T}}\right)-\frac{\bar{\xi}}{\bar{T}}\right].$$

Finally

$$\int\left(\prod_{i=1}^{3}d^3\boldsymbol{y}_i\right)K_b(\boldsymbol{x},\boldsymbol{y}_1,\boldsymbol{y}_2,\boldsymbol{y}_3)\Delta(\boldsymbol{y}_1)\Delta^*(\boldsymbol{y}_2)\Delta(\boldsymbol{y}_3) = b_{1s}|\Delta(\boldsymbol{x})|^2\Delta(\boldsymbol{x}),$$

$$b_{1s} = -b_s[1+\mathcal{O}(\tau)],$$

$$b_s = \frac{N_s}{4\hbar^2\omega_c^2}\int_{-\bar{\mu}}^{1}d\bar{\xi}\frac{\operatorname{sech}^2\left(\frac{\bar{\xi}}{2\bar{T}_{c0}}\right)}{\bar{\xi}^3\sqrt{\bar{\xi}+\bar{\mu}}}\left[\sinh\left(\frac{\bar{\xi}}{\bar{T}_{c0}}\right)-\frac{\bar{\xi}}{\bar{T}_{c0}}\right]. \quad \text{4.1-18}$$

4.2 TWO-BAND SUPERCONDUCTOR WITH A QUASI-1D AND 3D BAND

We consider a two-band superconductor with the s-wave pairing in quasi-1D and 3D bands, with their partial condensates coupled by the Josephson-like Cooper pairs transfer. To describe this system, we adopt a standard two-band generalization of the BCS model given in Refs. [1], [2]. The intra- and interband pairing is determined by the real matrix $\breve{g}$ of the coupling constants $g_{\nu\nu'} = g_{\nu'\nu}$ ($\nu = 1{,}2$). For simplicity we assume the parabolic momentum dispersion of the single-particle energy in both bands. For the same reason the Fermi surface of the 3D band ($\nu = 1$) is taken spherically symmetric. The principal axis of the quasi-1D band ($\nu = 2$) is chosen parallel to the x-axis, while in the y - and z directions the energy dispersion is degenerate. We assume the effective finite integral of the density of states (DOS) for both these directions. The single-particle energy in both bands, shifted by the chemical potential μ, are thus given by

$$\xi_{\boldsymbol{k}}^{(1)} = \xi_0 + \frac{\hbar^2 \boldsymbol{k}^2}{2m_1} - \mu, \qquad \xi_{\boldsymbol{k}}^{(1)} = \frac{\hbar^2 k_x^2}{2m_2} - \mu, \qquad 4.2\text{-}1$$

where $m_{1,2}$ are the effective masses and $\boldsymbol{k} = (k_x + k_y + k_z)$. The energy and μ are measured relative to the the bottom of the quasi-1D band. The lowest energy of the 3D band is thus negative $\xi_0 < 0$ and we adopt also that $|\xi_0| \gg 0$. Our study is focused on the superconducting state near the Lifshitz point $\mu = 0$. The system is considered in the clean limit (the role of impurities is negligible). In what follows we set $k_B = 1$ for the Boltzmann constant.

Following Refs. [1], [2], the mean-field Hamiltonian of the two-band superconductors is written as

$$\mathcal{H} = \int d^3\boldsymbol{r} \left\{ \sum_{\nu=1,2} \sum_{\sigma} \left[\hat{\psi}_{\nu\sigma}^{\dagger}(\boldsymbol{r}) T_\nu(\boldsymbol{r}) \hat{\psi}_{\nu\sigma}(\boldsymbol{r}) + \hat{\psi}_{\nu\uparrow}^{\dagger}(\boldsymbol{r}) \hat{\psi}_{\nu\downarrow}^{\dagger}(\boldsymbol{r}) \Delta_\nu(\boldsymbol{r}) + \text{h.c.} \right] + \left(\vec{\Delta}, \breve{g}^{-1}\vec{\Delta}\right) \right\}, \qquad 4.2\text{-}2$$

where $\hat{\psi}_{\nu\sigma}^{\dagger}(\boldsymbol{r})$ and $\hat{\psi}_{\nu\sigma}(\boldsymbol{r})$ are the field operators for the carriers in band ν, $T_\nu(\boldsymbol{r})$ is the single-particle Hamiltonian with the single-particle energies given by Eq. 4.2-1, and $\Delta_\nu(\boldsymbol{r})$ is the superconducting gap function for band ν. We also use vector notations $\vec{\Delta} = (\Delta_1, \Delta_2)$, where $(.,.)$ denotes the scalar product in the band vector space, and $\breve{g}^{-1}$ is the inverse of the coupling matrix. The band dependent superconducting gap functions satisfy the self-consistency condition, known as the matrix gap equation,

$$\vec{\Delta} = \breve{g}\vec{R}, \quad 4.2\text{-}3$$

where components of $\vec{R}$ are the anomalous Green functions $R_\nu = \langle \hat{\psi}_{\nu\uparrow}(\boldsymbol{r}), \hat{\psi}_{\nu\downarrow}(\boldsymbol{r}) \rangle$.

The model based on Eqs. 4.2-2 and 4.2-3 is used to calculate the mean-field critical temperature T_{c0} and then the fluctuation-shifted T_c. T_{c0} is obtained by solving the linearized variant of the gap equation 4.2-3. The fluctuations are investigated by using the expansion for the free energy functional for the two-band system with respect to the band superconducting gap functions, which essentially gives the two-band Ginzburg-Landau (GL) free energy functional.

Assuming T_{c0} is known, one expands the r.h.s. of Eq. 4.2-3 with respect to Δ_ν. The lowest order terms of this expansion are given by [21–27]

$$R_\nu[\Delta_\nu] = (\mathcal{A}_\nu - a_\nu)\Delta_\nu - b_\nu \Delta_\nu |\Delta_\nu|^2 + \sum_{i=x,y,z} K_\nu^{(i)} \nabla_i^2 \Delta_\nu, \quad 4.2\text{-}4$$

where the coefficients $\mathcal{A}_\nu$, a_ν, b_ν, and $K_\nu^{(i)}$ are to be calculated using the microscopic model for each band, and external fields are assumed to be zero.

For the 3D band, $\nu = 1$, with the spherically symmetric Fermi surface, one obtains the standard result

$$\mathcal{A}_1 = N_1 \ln\left(\frac{2^\gamma \hbar\omega_c}{\pi T_{c0}}\right), \qquad a_1 = -\tau N_1, \qquad b_1 = N_1 \frac{7\zeta(3)}{8\pi^2 T_{c_0}^2},$$

$$K_1^{(x)} = K_1^{(y)} = K_1^{(z)} = \frac{\hbar^2 v_1^2}{6} b_1, \quad 4.2\text{-}5$$

where $\tau = 1 - T/T_{c0}$, ω_c is the energy cutoff (assumed to be the same for both bands), γ is the Euler constant, $\zeta(x)$ is the Riemann zeta function, the DOS of the 3D band at the Fermi energy is $N_1 = m_1 k_F / 2\pi^2\hbar^2$ and the 3D band Fermi velocity $v_1 = \hbar k_F / m_1$ is determined by the corresponding Fermi wavenumber $k_F = \sqrt{2m_1(\mu - \xi_0)}/\hbar$.

For the quasi-1D band near the Lifshitz transition, at $|\mu| < \hbar\omega_c$, the expressions for the coefficients are given by the integrals to be evaluated numerically, i.e.

$$\mathcal{A}_2 = N_2 \int_{-\bar{\mu}}^{1} \frac{d\bar{\xi}}{\sqrt{\bar{\xi}+\bar{\mu}}} \frac{1}{\bar{\xi}} \tanh\left(\frac{\bar{\xi}}{2\bar{T}_{c0}}\right),$$

$$a_2 = -\frac{N_2}{2\bar{T}_{c0}} \int_{-\bar{\mu}}^{1} \frac{d\bar{\xi}}{\sqrt{\bar{\xi}+\bar{\mu}}} \operatorname{sech}^2\left(\frac{\bar{\xi}}{2\bar{T}_{c0}}\right),$$

$$b_2 = \frac{N_2}{4\hbar^2\omega_c^2} \int_{-\bar{\mu}}^{1} d\bar{\xi} \frac{\operatorname{sech}^2\left(\frac{\bar{\xi}}{2\bar{T}_{c0}}\right)}{\bar{\xi}^3\sqrt{\bar{\xi}+\bar{\mu}}} \left[\sinh\left(\frac{\bar{\xi}}{\bar{T}_{c0}}\right) - \frac{\bar{\xi}}{\bar{T}_{c0}}\right],$$

$$K_2^{(x,y)} = 0$$

$$K_2^{(z)} = \hbar^2 v_s^2 \frac{N_2}{8\hbar^2\omega_c^2} \int_{-\bar{\mu}}^{1} d\bar{\xi} \frac{\sqrt{\bar{\xi}+\bar{\mu}}}{\bar{\xi}^3} \left[\sinh\left(\frac{\bar{\xi}}{\bar{T}_{c0}}\right) - \frac{\bar{\xi}}{\bar{T}_{c0}}\right] \operatorname{sech}^2\left(\frac{\bar{\xi}}{2\bar{T}_{c0}}\right), \quad 4.2\text{-}6$$

where we use the scaled quantities $\bar{T}_{c0} = T_{c0}/\hbar\omega_c$ and $\bar{\mu} = \mu/\hbar\omega_c$, and the effective band velocity v_2 is determined by the cutoff energy as $v_2 = \sqrt{2\hbar\omega_c/m_2}$ (independent of μ). The effective DOS of the quasi-1D band is given by $N_2 = \sigma^{(xy)}/4\pi\hbar v_s$, where the factor $\sigma^{(xy)}$ accounts for the contribution to DOS by the x, y dimensions.

The mean-field critical temperature T_{c0} is obtained by solving the linearized gap equation which reads as (see Eqs. 4.2-3 and 4.2-4)

$$\check{L}\vec{\Delta} = 0, \qquad \check{L} = \check{g}^{-1} - \begin{pmatrix} \mathcal{A}_1 & 0 \\ 0 & \mathcal{A}_2 \end{pmatrix}. \quad 4.2\text{-}7$$

This is the matrix equation with the solution in the form

$$\vec{\Delta} = \psi(\boldsymbol{r})\vec{\eta}, \quad 4.2\text{-}8$$

where $\vec{\eta}$ is an eigenvector of $\check{L}$ corresponding to its zero eigenvalue while $\psi(\boldsymbol{r})$ is a coordinate dependent GL parameter of the system [133]. A non-trivial solution to Eq. 4.2-7 exists only when the determinant of $\check{L}$ is zero, which gives the equation

$$(g_{22} - G\mathcal{A}_1)(g_{11} - G\mathcal{A}_2) - g_{12}^2 = 0, \quad 4.2\text{-}9$$

with $G = g_{11}g_{22} - g_{12}^2$. Of the two solutions to Eq. 4.2-9, one chooses the maximal T_{c0}. The corresponding eigenvector $\vec{\eta}$ can be adopted in the form

$$\vec{\eta} = \begin{pmatrix} S \\ 1 \end{pmatrix}, \qquad S = \frac{g_{11} - G\mathcal{A}_2}{g_{12}}, \quad 4.2\text{-}10$$

Notice that this choice is unique up to the normalization factor which is absorbed by $\psi(\boldsymbol{r})$.

The actual critical temperature T_c is lower than its mean field value T_{c0} due to fluctuations [104]. The fluctuation-induced correction to T_{c0} is obtained by using the standard Gibbs distribution $\exp(-\mathcal{F}/T)$, where the free energy functional writes as (see e.g. [123], [124])

$$\mathcal{F} = \int d^3\boldsymbol{r}\left[\sum_{\nu=1,2} f_\nu + \left(\vec{\Delta}, \check{L}\vec{\Delta}\right)\right], \quad 4.2\text{-}11$$

with

$$f_\nu = a_\nu|\Delta_\nu|^2 + \frac{b_\nu}{2}|\Delta_\nu|^4 + \sum_{i=x,y,z} K_\nu^{(i)}|\nabla_\nu^2\Delta_\nu|^2. \quad 4.2\text{-}12$$

The stationary solution of this functional satisfies the gap equation 4.2-3. The fluctuation corrections are obtained by assuming the standard Gibbs distribution $\exp(-\mathcal{F}/\mathrm{T})$, with the free energy $\mathcal{F}$ given by Eqs. 4.2-11, 4.2-12.

The calculations are simplified by representing $\vec{\Delta}$ as a linear combination of the contributions proportional to $\vec{\eta}$ and to the orthogonal vector $\vec{\xi} = (1, -S)^T$ as

$$\vec{\Delta}(\boldsymbol{r}) = \psi(\boldsymbol{r})\vec{\eta} + \varphi(\boldsymbol{r})\vec{\xi}, \quad 4.2\text{-}13$$

where $\varphi(\boldsymbol{r})$ is the second spatial mode. The free energy functional is then expressed using ψ and φ as

$$\mathcal{F} = \int d^3\boldsymbol{r}\left(f_\psi + f_\varphi + f_{\psi\varphi}\right). \quad 4.2\text{-}14$$

Here contributionsf_ψ and f_φ have the same structure as given by Eq. 4.2-12, where Δ_ν is replaced by $\psi(\boldsymbol{r})$ and $\varphi(\boldsymbol{r})$, respectively, and a set of coefficients $\{a_\nu, b_\nu, K_\nu\}$ is changed to $\{a_\psi, b_\psi, K_\psi\}$ and $\{a_\varphi, b_\varphi, K_\varphi\}$. The contribution $f_{\psi\varphi}$ represents the coupling between the two modes $\psi(\boldsymbol{r})$ and $\varphi(\boldsymbol{r})$.

Coefficients in f_ψ one obtained as

$$a_\psi = S^2 a_1 + a_2, \qquad b_\psi = S^4 b_1 + b_2,$$

$$K_\psi^{(i)} = S^2 K_1^{(i)} + K_2^{(i)}, \quad 4.2\text{-}15$$

whereas the coefficients in f_φ are given by

$$a_\varphi = a_1 + S^2 a_2, \qquad b_\varphi = b_1 + S^4 b_2,$$

$$K_\varphi^{(i)} = K_1^{(i)} + S^2 K_2^{(i)}, \tag{4.2-16}$$

with

$$\alpha_\varphi^{(0)} = \frac{(1+S^2)^2}{SGg_{12}}, \tag{4.2-17}$$

Here $\alpha_\varphi^{(0)} \neq 0$ since S is real. This means that only f_ψ represents the critical fluctuations in the vicinity of the superconducting transition because $\alpha_\varphi \to 0$ in the limit $T \to T_{c0}$. The contribution f_φ describes non-critical fluctuations and can be safely omitted [125]. Thus, the fluctuations are determined by the GL functional f_ψ, with the single component order parameter $\psi(\boldsymbol{r})$. Due to the presence of the quasi-1D band, this functional is anisotropic with $K_\psi^{(x,y)} \neq K_\psi^{(z)}$.

With this simplification we can apply the known results for the fluctuation-driven shift of the critical temperature in the single-component GL theory. Using the renormalization group approach, performed in the section 2.5.9, we obtain that the actual 3D critical temperature is related to the mean-field one by

$$\frac{T_{c0} - T_c}{T_c} = \frac{8}{\pi}\sqrt{Gi}, \tag{4.2-18}$$

where Gi is the Ginzburg number (Ginzburg-Levanyuk parameter). For the 3D anisotropic GL functional it reads

$$Gi = \frac{1}{32\pi^2}\frac{T_{c0} b_\psi^2}{a'_\psi K_\psi^{(x)} K_\psi^{(y)} K_\psi^{(z)}}, \tag{4.2-19}$$

with $a'_\psi = da_\psi/dT$. Using Eq. 4.2-15, this above expression can be rearranged as

$$Gi = Gi_{3D}\frac{(b_2/b_1 + S^4)^2}{(a_2/a_1 + S^2)\left(K_2^{(z)}/K_1^{(z)} + S^2\right)S^4}, \tag{4.2-20}$$

where Gi_{3D} is the Ginzburg number of the uncoupled (standalone) 3D band, given by Eq. 4.2-19 with the substitution $\left\{a_\psi,\ b_\psi,\ K_\psi^{(i)}\right\} \to \left\{a_1,\ b_1,\ K_1^{(x)}\right\}$.

4.3 RESULTS AND CONCLUSIONS

Using the obtained expressions, we can now calculate both the mean-field T_{c0} and fluctuation-shifted T_c critical temperatures. Essential parameters of the model are the three coupling constants $g_{\nu\nu'}$ and the band DOSs N_ν, while the cutoff $\hbar\omega_c$ sets the energy scale. It is convenient to introduce the dimensionless coupling constants $\lambda_{\nu\nu'} = g_{\nu\nu'}\sqrt{N_\nu N_{\nu'}}$. The parameter S, which controls Eqs. (4.2-18)-(4.2-20) and also T_{c0}, depends on λ_{11}, λ_{22}, λ_{12} as well as on the ratio N_2/N_1. In the calculations we assume $\lambda_{22} = 0.2$ and $\lambda_{11} = 0.18$, which is in the range of typical values of the dimensionless couplings in conventional weak-coupling superconductors [126]. We also take $N_2/N_1 = 1$ for simplicity. Finally, we need also to specify N_1 which defines Gi_{3D}. We follow a different path and use an estimate $Gi_{3D} = 10^{-10}$ by taking into account that the Ginzburg number of most 3D superconductors is in the range 10^{-6}-10^{-1} [127], being $Gi_{3D} \approx (T_{c1}/E_F)^4$ with T_{c1} the critical temperature of the standalone band 1 and $E_F = \hbar^2 k_F^2/2m_1$ (for the stable 3D condensate $T_{c1} \ll E_F$). Notice, that our results are not sensitive to a particular choice of the microscopic parameters unless the dimensionless intraband coupling of the 3D band is significantly larger than that of the quasi-1D band and the two-band system approaches a routine 3D superconductor.

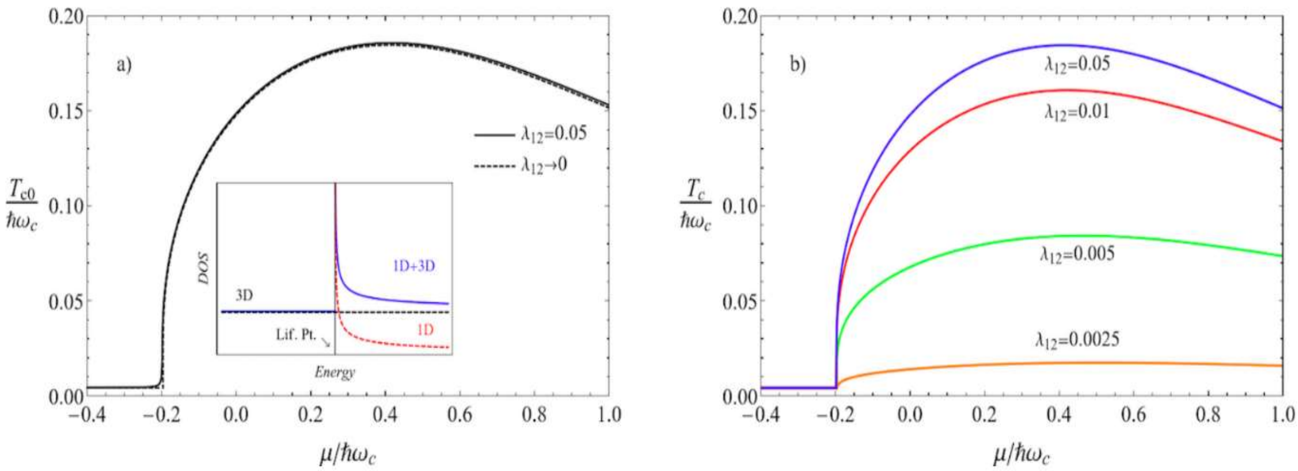

Figure 4.3-1 "Reference-[132]", a) The mean-field critical temperature T_{c0} versus the chemical potential μ, calculated for $\lambda_{12} = 0.05$ and $\lambda_{12} \to 0$; the insert demonstrates the energy dependent DOSs with the van Hove singularity of the quasi-1D DOS at the Lifshitz point $\mu = 0$. b) The fluctuation-shifted critical temperatures Tc as a function of μ, calculated for selected values of the dimensionless pair-exchange coupling constant $\lambda_{12} = 0.001$, $\lambda_{12} = 0.025$, $\lambda_{12} = 0.005$, $\lambda_{12} = 0.05$ at the Ginzburg number $Gi_{3D} = 10^{-10}$ of the uncoupled 3D band.

Numerical results for T_{c0} and T_c versus the chemical potential μ, calculated for several values of the dimensionless pair-exchange coupling λ_{12}, are shown in Figure 4.3-1. One sees from a) that when μ is sufficiently below zero, the quasi-1D band does not contribute and T_{c0} is determined by the uncoupled band 1. In the vicinity of the Lifshitz transition at $\mu = 0$, T_{c0} rises sharply. At larger μ, T_{c0} decreases, approaching the critical temperature of the decouple 3D band again. As is well known, the reason for this sharp rise is the increase in the energy-dependent quasi-1D DOS that has the van Hove singularity at the band edge, as illustrated in the inset in Fig. 1 a). It is remarkable that T_{c0} is almost insensitive to the pair-exchange coupling as long as $\lambda_{12} \ll \lambda_{11}$. Consequently, in the vicinity of the Lifshitz transition, the superconducting properties of the two-band system on the mean field level are fully determined by the quasi-1D band.

In contrast, the fluctuation-induced shift of the critical temperature strongly depends on the pair-exchange coupling. In the limit $\lambda_{12} \to 0$ the fluctuations suppress the superconductivity. However, this suppression ceases rapidly with increasing the pair-exchange coupling. Figure 4.3-1 b) demonstrates that the presence of even a vanishingly small coupling, $\lambda_{12} \ll \lambda_{\nu\nu'}$, is enough to quench the fluctuations and to eliminate the shift. In particular, T_c approaches T_{c0} already at $\lambda_{12} \cong 0.01$ and at $\lambda_{12} \cong 0.05$ the two critical temperatures are practically indistinguishable.

Concluding, our calculations demonstrate that coupling to a stable 3D condensate "screens" out the severe thermal fluctuations of the quasi-1D superconducting condensate. This coupling gives rise to a single critical mode that controls the thermal fluctuations of the condensate gap functions $\Delta_1(\boldsymbol{r})$ and $\Delta_2(\boldsymbol{r})$. In other words, "light" excitations of the quasi-1D condensate are always accompanied by "heavy" excitations of the stable 3D condensate. Therefore, such a two-band system becomes a robust mean-field superconductor. The superconductivity enhancement, based on the interaction between a quasi-1D condensate near the Lifshitz point and a BCS-like condensate, is general and does not depend on the model details. Thus, it opens a possibility for a significant amplification (up to orders of magnitude) of the critical temperature by tuning the Lifshitz transition. Notice that in addition to the chemical engineering, Lifshitz transitions can be tuned by an appropriate doping of multiband superconducting compounds, as e.g. reported in [129].

Finally, we note that although our results are obtained for the model with the s-wave pairing, one can expect that the fluctuations screening mechanism, based on the coupling of multiple condensates, applies also to materials with the d-wave symmetry and even to the case of the triplet pairing, having the multicomponent order parameter. In this regard we note that first theoretical calculations of the possible pairing symmetry in quasi-1D multiband superconductors $A_2Cr_3As_3$ (with $A = K, Rb, Sc$) are in favor of the triplet pairing [128]. A detailed analysis of the fluctuations for the triplet pairing requires a separate investigation.

5 CONCLUSIONS

These remarkable phenomena related to multiple coupled condensates addressed during the doctorate brought good results, ending with a published article and another one in the submission process.

a) **Intertype magnetic response of multiband superconductors with degenerate excitation gaps.**

In the first problem addressed by the thesis, we were able to demonstrate that the presence of multiple competing lengths, each connected with corresponding partial condensate, is a more fundamental feature of a multiband superconductor for its magnetic properties than the presence of multiple gaps in the excitation spectrum. This is illustrated by considering boundaries of the IT domain in the phase diagram of the superconducting magnetic response. For example, our results have revealed that a superconductor can have many gaps in the excitation spectrum while exhibiting standard magnetic properties of a single-band material. There is also a reverse situation, when a superconductor has a single energy gap in the excitation spectrum but multiple competing characteristic lengths of contributing band condensates, which results in notable changes of the superconducting magnetic properties in the IT regime as compared to the single-band case.

Generally, our analysis shows that the multi-condensate physics can appear irrespective of the presence/absence of multiple spectral gaps. Two superconductors with different numbers of the contributing bands but with the same energy gaps in their excitation spectra (some of the spectral gaps are degenerate) can exhibit different magnetic properties sensitive to the spatial scales of the band condensates. This discrepancy between different manifestations of multiple bands in superconducting materials must be taken into account in analysis of experimental data and, generally, in studies of multiband superconductors.

In addition, given the significant advances in chemical engineering of various materials, including multiband superconductors, it is of great importance to search for systems that enrich our knowledge of and understanding the physics of the materials. Multiband superconductors with degenerate excitation gaps can be a good example of such systems, clearly demonstrating that ‘multiband’ can be dramatically different from ‘multigap’. Our analysis has been performed within the EGL approach that considers the leading corrections to the GL theory in the perturbative expansion of the microscopic equations in $\tau = 1 - T/T_c$. This formalism, previously constructed for single- and two-band systems, has been extended in the present work to the case of an arbitrary number of contributing bands. Its advantage is that it allows one to clearly distinguish various effects appearing due to the multiband structure in different types of superconducting characteristics. It particular, it reveals solid correlations between changes in the IT domain with the competition of multiple characteristic lengths of the contributing condensates.

b) **Multiband material with a quasi-1D band as a robust high-temperature superconductor.**

In the second problem addressed in the thesis, we were able to demonstrate that the coupling to a stable 3D condensate "screens" large fluctuations of a Q1D condensate by means of two mechanisms. First, the resulting GL free energy functional becomes the 3D anisotropic one, which makes it possible to employ the result of the 3D renormalization group for T_c. Second, the pair-exchange coupling creates a single critical mode that controls the fluctuations of both $\Delta_1(\mathbf{r})$ and $\Delta_2(\mathbf{r})$. Physically, one can be said that "light" excitations of the Q1D condensate are always accompanied by "heavy" excitations of the stable 3D condensate, reducing the amplitude of the fluctuations. Mathematically, the characteristic length of this critical mode is the sum of length Q1D and length 3D, both multiplied by corresponding weighing factors. As the length of the 3D stable condensate is large, the resulting length is also large, suppressing fluctuations so that the two bands system becomes a robust mean-field superconductor, even in the vicinity of the Lifshitz transition.

Our results are obtained for the model with s-wave pairing, however, one can be expected that the fluctuation screening, based on the coupling of multiple condensates, also applies to materials with d-wave symmetry of even for the case of the triplets pairing, having the multicomponent order parameter. A detailed analysis of the superconducting fluctuations for the triplet pair requires further investigation. We also observed that the specific values of the increase in T_c can be influenced by smoothing the van Hove singularity. It occurs because the Q1D Fermi sheet is often curved due to dispersions in the direction perpendicular to the main axis of the Q1D band.

Finally, although this work studies the effect of thermal fluctuations on T_c, a similar suppression of quantum fluctuations can be expected at low temperatures, near the upper critical field. Thus, the superconductivity enhancement, based on the interaction between a Q1D condensate near the Lifshitz point and a BCS-like 3D condensate, is a generic phenomenon that opens a possibility for a significant critical temperature amplification by adjusting the Lifshitz transition.

REFERENCES

[1] H. Suhl, B. T. Matthias, and L. R. Walker, Phys. Rev. Lett. **3**, 552 (1959).

[2] V.A. Moskalenko, Phys. Met. Metallogr. **8**, 25 (1959) [Fiz. Met. Metalloved. **8**, 503 (1959)].

[3] P. L. Richards and M. Tinkham, Phys. Rev. Lett. **1**, 318 (1958).

[4] D. M. Ginsberg, P. L. Richards, and M. Tinkham, Phys. Rev. Lett. **3**, 337 (1959).

[5] P. C. Canfield and G. W. Crabtree, Phys. Today **56**, 34 (2003).

[6] P. Szabó, P. Samuely, J. Kačmarčík, T. Klein, J. Marcus, D. Fruchart, S. Miraglia, C. Marcenat, and A. G. M. Jansen, Phys. Rev. Lett. **87**, 137005 (2001).

[7] M. Iavarone, G. Karapetrov, A. E. Koshelev, W. K. Kwok, G. W. Crabtree, D. G. Hinks, W. N. Kang, Eun-Mi Choi, Hyun Jung Kim, Hyeong-Jin Kim, and S. I. Lee, Phys. Rev. Lett. **89**, 187 (2002).

[8] J. Paglione and R. L. Greene, Nat. Phys. **6**, 645 (2010).

[9] M. V. Mazziotti1, A. Valletta, G. Campi, D. Innocenti, A. Perali, and A. Bianconi, Eur. Phys. Lett. **118**, 37003 (2017) .

[10] S. Deng, L. Viola, and G. Ortiz, Phys. Rev. Lett. **108**, 036803 (2012).

[11] S. Deng, G. Ortiz, and L. Viola, Phys. Rev. B **87**, 205414 (2013).

[12] İ. N. Askerzade, A. Gencer, and N Güçlü, Supercond. Sci. Technol. **15**, L13 (2002).

[13] A. A. Golubov, J. Kortus, O. V. Dolgov, O. Jepsen, Y. Kong, O. K. Andersen, B. J. Gibson, K. Ahn and R. K. Kremer, J. Phys.: Condens. Matter **14**, 1353 (2002).

[14] A. Gurevich, Phys. Rev. B **67**, 184515 (2003).

[15] A. E. Koshelev and A. A. Golubov, Phys. Rev. Lett. **92**, 107008 (2004).

[16] J. Kortus, I. I. Mazin, K. D. Belashchenko, V. P. Antropov, and L. L. Boyer, Phys. Rev. Lett. **86**, 4656 (2001).

[17] J. M. An and W. E. Pickett, Phys. Rev. Lett. **86**, 4366 (2001).

[18] M. Seul and R. Wolfe, Phys. Rev. A **46**, 7519 (1992).

[19] M. Seul and D. Andelman, Science **267**, 476 (1995).

[20] J. Maclennan and M. Seul, Phys. Rev. Lett. **69**, 2082 (1992).

[21] N. Stoop, R. Lagrange, D. Terwagne, P. M. Reis, and J. Dunkel, Nature Mat. **14**, 337 (2015).

[22] S. L. Keller and H. M. McConnell, Phys. Rev. Lett. **82**, 1602 (1993).

[23] I. S. Aranson and L. S. Tsimring, Rev. Mod. Phys. **78**, 641 (2006).

[24] V. Moshchalkov, M. Menghini, T. Nishio, Q. H. Chen, A. V. Silhanek, V. H. Dao, L. F. Chibotaru, N. D. Zhigadlo, and J. Karpinski, Phys. Rev. Lett. **102**, 117001 (2009).

[25] P. J. Curran, W. M. Desoky, M. V. Milošević, A. Chaves, J.-B. Laloë, J. S. Moodera, and S. J. Bending, Sci. Rep. **5**, 15569 (2015).

[26] E. Babaev, Phys. Rev. Lett. **89**, 067001 (2002).

[27] J. C. Piña, C. C. de Souza Silva, and M. V. Milošević, Phys. Rev. B {\bf 86}, 024512 (2012).

[28] S. Z. Lin and L. N. Bulaevskii, Phys. Rev. Lett. **110**, 087003 (2013).

[29] S. Z. Lin and C. Reichhardt, Phys. Rev. B **87**, 100508 (2013).

[30] R. M. da Silva, M. V. Milošević, D. Domínguez, F. M. Peeters, and J. Albino Aguiar, Appl. Phys. Lett. **105**, 232601 (2014).

[31] S. Z. Lin, J. Phys.: Condens. Matter **26**, 493203 (2014).

[32] Y. Tanaka, Phys. Rev. Lett. **88**, 017002 (2001).

[33] Y. Tanaka, J. Phys. Soc. Jpn. **70**, 2844 (2001).

[34] R. M. da Silva, M. V. Milošević, A. A. Shanenko, F. M. Peeters, and J. Albino Aguiar, Sci. Rep. **5**, 12695 (2015).

[35] A. Vagov, A. A. Shanenko, M. V. Milošević, V. M. Axt, V. M. Vinokur, J. Albino Aguiar, and F. M. Peeters, Phys. Rev. B **93**, 174503 (2016).

[36] S. Wolf, A. Vagov, A. A. Shanenko, V. M. Axt, A. Perali, and J. A. Aguiar, Phys. Rev. B **95**, 094521 (2017).

[37] L. Komendová, Yajiang Chen, A. A. Shanenko, M. V. Milošević, and F. M. Peeters, Phys. Rev. Lett. **108**, 207002 (2012).

[38] L. Salasnich, A. A. Shanenko, A. Vagov, J. Albino Aguiar, A. Perali, arXiv:1810.3321, Feb 2019.

[39] H. K. Onnes, Commun. Phys. Lab. Univ. Leiden, n. 119, 120, 122, 124 (1911); H.K. Onnes, Akad. Van Wetenschappen (Amsterdam) 14, 113 (1911).

[40] W. Meissner and R. Ochsenfeld, Naturwissenschaften **21**, 787 (1933)

[41] F. London and H. London, Proceedings of the Royal Society (London) A **149**, 71 (1935); F. London and H. London, Physica **2**, 341 (1935).

[42] V. L. Ginzburg and L. Landau, Zhurnal Eksperimental'noi I Teoreticheskoi Fiziki **20**, 1064 (1950)

[43] L. Landau. On the theory of phase transitions. Zh. Eksp. Teor. Fiz., 7:19–32, 1937. [Cited at page(s) 12]

[44] P. G. de Gennes, Superconductivity of Metals and Alloys(Benjamin, New York, 1966).

[45] J. Bardeen, L. N. Cooper, and J. R. Schrieffer, Phys. Rev. **108**, 1175 (1957).

[46] L. P. Gor'kov, Sov. Phys.–JETP **36**, 1364 (1959) [Zh. Eksp. Teor. Fiz. **36**, 1918 (1959)].

[47] J.-F. Ge, Z.-L. Liu, C. Liu, C.-L. Gao, D. Qian, Q.-K. Xue, Y. Liu, and J.-F. Jia, Nat. Materials **14**, 285 (2015).

[48] I. Bozovic and C. Ahn, Nat. Physics **10**, 892 (2014).

[49] E. M. Lifshitz and L. P. Pitaevskii, *Statistical Physics*, Part 2, *Landau and Lifshitz Course of Theoretical Physics* (Pergamon, Oxford, 1980), Vol. 9.

[50] Ketterson, J. B. and Song, S. N. Superconductivity (Univ. Press, Cambridge, 1999).

[51] J. Auer and H. Ullmaier, Phys. Rev. B **7**, 136 (1973).

[52] H. W. Weber, E. Seidl, M. Botlo, C. Laa, E. Mayerhofer, F. M Sauerzopf, R.M. Schalk, and H. P. Wiesingerh, Physica C **161**, 272 (1989).

[53] A. E. Jacobs, Phys. Rev. Lett. **26**, 629 (1971).

[54] A. E. Jacobs, Phys. Rev. B **4**, 3016 (1971).

[55] A. E. Jacobs, Phys. Rev. B **4**, 3022 (1971).

[56] E. B. Bogomolnyi and A. I. Vainstein, Sov. J. Nucl. Phys. **23**, 588 (1976).

[57] E. B. Bogomolnyi, Sov. J. Nucl. Phys. **24**, 449 (1976).

[58] E. J. Weinberg, Phys. Rev. D **19**, 3008 (1978).

[59] Y. N. Ovchinnikov, Sov. Phys. JETP **88**, 398 (1999) [Zh. Eksp. Teor. Fiz. **115**, 726 (1999), in Russian].

[60] I. Luk'yanchuk, Phys. Rev. B **63**, 174504 (2001).

[61] A. A. Shanenko, M. V. Milošević, F. M. Peeters, and A. V. Vagov, ´ Phys. Rev. Lett. **106**, 047005 (2011); A. Vagov, A. A. Shanenko, Milošević, V. M. Axt, and F. M. Peeters, Phys. Rev. B **86**, 144514 (2012); A. Vagov, A.A. Shanenko, M.V. Milošević, V.M. Axt, and F.M. Peeters, Phys. Rev. B **85**, 014502 (2012); N.V. Orlova, A.A. Shanenko, M.V. Milošević, F.M. Peeters, A. Vagov and V. M. Axt, Phys. Rev. B **87**, 134510 (2013).

[62] W. Y. Córdoba-Camacho, R. M. da Silva, A. Vagov, A. A. Shanenko, and J. Albino Aguiar, Phys. Rev. B **94**, 054511 (2016).

[63] S. Wolf, A. Vagov, A. A. Shanenko, V. M. Axt, A. Perali, and J. Albino Aguiar, Phys. Rev. B **95**, 094521 (2017).

[64] A. Vagov, A. A. Shanenko, M. V. Milošević, V. M. Axt, V. M. Vinokur, & F. M. Peeters, arXiv:1311.5624 (2013).

[65] A. A. Shanenko, A. Vagov, M.V. Milošević, V.M. Axt, and F.M. Peeters, Europhys. Lett. **102**, 27003 (2013).

[66] D. M. Eagles, Phys. Rev. **186**, 456 (1969).

[67] A. A. Shanenko, M. D. Croitoru, A. Vagov, V. M. Axt, A. Perali, and F. M. Peeters, Phys. Rev. A **86**, 033612 (2012).

[68] M. Sigrist and K. Ueda, Rev. Mod. Phys. **63** 239 (1991).

[69] P. C. Canfield and G. W. Crabtree, Phys. Today **56**(3), 34 (2003).

[70] Y. Kamihara, T. Watanabe, M. Hirano, and H. Hosono, J. Am. Chem. Soc. **130**, 3296 (2008).

[71] M. Rotter, M. Tegel, and D. Johrendt, Phys. Rev. Lett. **101**, 107006 (2008).

[72] J. Paglione and R. L. Greene, Nat. Phys. **6**, 645 (2010); M. L. Teague, G. K. Drayna, G. P. Lockhart, P. Cheng, B. Shen, H. H. Wen, and N. C. Yeh, Phys. Rev. Lett. **106**, 087004 (2011).

[73] C. P. Jr. Poole, "Superconductivity" (Elsevier, 2007), 2 ed.

[74] M. Tinkham, "Introduction to superconductivity" (Dover Publications, 2004), 2 ed.

[75] E. M. Lifshitz and L. P. Pitaevskii, "Statistical Physics, Part 2, Landau and Lifshitz Course of Theoretical Physics, Volume 9" (Oxford, Pergamon, 1980).

[76] J. B. Ketterson and S. N. Song, "Superconductivity" (Univ. Press, Cambridge, 1999).

[77] U. Krägeloh, Phys. Lett. A **28**, 657 (1969).

[78] U. Essmann, Physica **55**, 83 (1971).

[79] D. R. Aston, L. W. Dubeck, and F. Rothwarf, Phys. Rev. **3**, 2231 (1971).

[80] A. E. Jacobs, Phys. Rev. B **4**, 3029 (1971).

[81] U. Klein, J. Low Temp. Phys. **69**, 1 (1987).

[82] E. H. Brandt, Rep. Prog. Phys. **58**, 1465 (1995).

[83] M. Laver, E. M. Forgan, S. P. Brown, D. Charalambous, D. Fort, C. Bowell, S. Ramos, R. J. Lycett, D. K. Christen, J. Kohlbrecher, C. D. Dewhurst, and R. Cubitt, Phys. Rev. Lett. **96**, 167002 (2006).

[84] M. Laver, C. J. Bowell, E. M. Forgan, A. B. Abrahamsen, D. Fort, C. D. Dewhurst, S. Mühlbauer, D. K. Christen, J. Kohlbrecher, R. Cubitt, and S. Ramos, Phys. Rev. B **79**, 014518 (2009).

[85] S. Mühlbauer, C. Pfleiderer, P. Böni, M. Laver, E. M. Forgan, D. Fort, U. Keiderling, and G. Behr, Phys. Rev. Lett. **102**, 136408 (2009).

[86] E. H. Brandt and M. P. Das, J. Supercond. Nov. Magn. **24**, 57 (2011).

[87] A. Pautrat and A. Brûlet, J. Phys.: Condens. Matter **26**, 232201 (2014).

[88] T. Reimann, S. Mühlbauer, M. Schulz, B. Betz, A. Kaestner, V. Pipich, P. Böni, and C. Grünzweig, Nat. Comm. **6**, 8813 (2015).

[89] Y. Wang, R. Lortz, Y. Paderno, V. Filippov, S. Abe, U. Tutsch, and A. Junod, Phys. Rev. B **72**, 024548 (2005).

[90] J.-Y. Ge, V. N. Gladilin, N. E. Sluchanko, A. Lyashenko, V. B. Filipov, J. O. Indekeu, and V. V. Moshchalkov, New J. Phys. **19**, 093020 (2017).

[91] S. Wolf, A. Vagov, A. A. Shanenko, V. M. Axt, and J. Albino Aguiar, Phys. Rev. B **96**, 144515 (2017).

[92] L. Neumann and L. Tewordt, Z. Phys. **180**, 55 (1966).

[93] L. Neumann and L. Tewordt, Z. Phys. **191**, 73 (1966).

[94] A. L. Fetter and J. D. Walecka, " Quantum Theory of Many-Particle Systems" (Dover, New York, 2003).

[95] A. E. Jacobs, Phys. Lett. A **38**, 153 (1972).

[96] M. Houzet and A. Buzdin, Phys. Rev. B **63**, 184521 (2001).

[97] M. Houzet and V. P. Mineev, Phys. Rev. B **76**, 224508 (2007).

[98] M. Sigrist and K. Ueda, Rev. Mod. Phys. **63**, 239 (1991).

[99] A. Brinkman, A. A. Golubov, H. Rogalla, O. V. Dolgov, J. Kortus, Y. Kong, O. Jepsen, and O. K. Andersen, Phys. Rev. B **65**, 180517(R) (2002).

[100] Y. Lubashevsky, E. Lahoud, K. Chashka, D. Podolsky, and A. Kanigel, Nat. Phys. **8**, 309 (2012).

[101] Tiago T. Saraiva, C. C. de Souza Silva, J. Albino Aguiar, and A. A. Shanenko, Phys. Rev. B **96**, 134521 (2017).

[102] V. G. Kogan and J. Schmalian, Phys. Rev. B **83**, 054515 (2011).

[103] B. T. Geilikman, R. O. Zaitsev, and V. Z. Kresin, Sov. Phys. Solid State **9**, 642 (1967).

[104] A. Larkin and A. Varlamov, Theory of Fluctuations in Superconductors (Oxford, Oxford University Press, 2005).

[105] K. B. Efetov and A. I. Larkin, Sov. Phys.-JETP **39**, 1129 (1974).

[106] L. P. Gor'kov L. P. and I. E. Dzyaloshinskii I. E., Sov. Phys. JETP **40**, 198 (1975).

[107] R. A. Klemm and H. Gutfreund, Phys. Rev. B **14**, 1086 (1976).

[108] H. J. Schulz and C. Bourbonnais , Phys. Rev. B **27**, 5856 (1983).

[109] S. A. Kivelson, E. Fradkin, and V. J. Emery, Nature **393**, 550 (1998).

[110] E. Arrigoni, E. Fradkin, and S. A. Kivelson, Phys. Rev. B **69**, 214519 (2004).

[111] D. J´erome, A. Mazaud, M. Ribault, and K. Bechgaard, Phys. Lett. France **41**, 95 (1980).

[112] D. J´erome, Historical Approach to Organic Superconductivity, The Physics of Organic Superconductors and Conductors, Springer Series in Materials Science, ed. A. Lebed, v. 110, Bollinger Series (Springer, Berlin, 2008)

[113] J.-K Bao, J-Y. Liu, C.-W. Ma, Z.-H. Meng, Z.-T. Tang, Y.-L. Sun, H.-F. Zhai, H. Jiang, H. Bai, C.-M Feng, Z.- A. Xu, and G.-H. Cao, Phys. Rev. X **5**, 011013 (2015).

[114] Z.-T. Tang, J.-K. Bao, Y. Liu, Y.-L. Sun, A. Ablimit, H.-F. Zhai, H. Jiang, C.-M. Feng, Z.-A. Xu, and G.- H. Cao, Phys. Rev. B **91**, 020506 (2015).

[115] Z.-T. Tang, J.-K. Bao, Z. Wang, H. Bai, H. Jiang, Y. Liu, H.-F. Zhai, C.-M. Feng, Z.-A. Xu, and G.-H. Cao, Sci. China Mater. **58**, 16 (2015).

[116] S.-Q. Wu, C. Cao, and G.-H. Cao, Phys. Rev. B **100**, 155108 (2019).

[117] H. Jiang, G. Cao, and C. Cao, Scientific Reports **5**, 16054 (2015).

[118] L. Salasnich, A. A. Shanenko, A. Vagov, J. Albino Aguiar, and A. Perali, Phys. Rev. B **100**, 064510 (2019).

[119] A. Bianconi, A. Valletta, A. Perali, N. L. Saini, Solid State Commun. **102**, 369 (1997).

[120] A. A. Shanenko and M. D. Croitoru, Phys. Rev. B **73**, 012510 (2006).

[121] A. A. Shanenko, M. D. Croitoru, R. G. Mints, and F. M. Peeters, Phys. Rev. Lett. **99**, 067007 (2007).

[122] M. V. Mazziotti, A. Valletta, G. Campi, D. Innocenti, A. Perali, and A. Bianconi, EPL **118**, 37003 (2017).

[123] I. N. Askerzade, A. Gencer, and N. Güclü , Supercond. Sci. Technol. 15, L13 (2002).

[124] M. E. Zhitomirsky and V.-H. Dao, Phys. Rev. B **69**, 054508 (2004).

[125] L. Salasnich, A. A. Shanenko, A. Vagov, J. Albino Aguiar, and A. Perali, Phys. Rev. B **100**, 064510 (2019)

[126] A. L. Fetter and J. D. Walecka, Quantum Theory of Many-Particle Systems (New York, Dover, 2003).

[127] J. B. Ketterson and S. N. Song Superconductivity (Univ. Press, Cambridge, 1999).

[128] X. Wu, F. Yang, C. Le, H. Fan, and J. Hu, Phys. Rev. B **92**, 104511 (2015).

[129] S.-Q. Wu, C. Cao, and G.-H. Cao, Phys. Rev. B **100**, 155108 (2019).

[130] Newton, Isaac, and Robert Hooke. *Isaac Newton Letter to Robert Hooke, 1675*.

[131] Paulo J F Cavalcanti *et al* 2020 *J. Phys.: Condens. Matter* **32** 455702.

[132] Saraiva, T. T., Cavalcanti, P. J. F., Vagov, A., Vasenko, A. S., Perali, A., Dell'Anna, L., & Shanenko, A. A. (2020). Physical Review Letters, **125**(21).

APPENDIX A – SCIENTIFIC PUBLICATION PRODUCED DURING THE DOCTORADE

IOP Publishing | Journal of Physics: Condensed Matter
J. Phys.: Condens. Matter 32 (2020) 455702 (13pp) | https://doi.org/10.1088/1361-648X/aba776

Multiband superconductors with degenerate excitation gaps

Paulo J F Cavalcanti[1], Tiago T Saraiva[2], J Albino Aguiar[1], A Vagov[3,4], M D Croitoru[1] and A A Shanenko[1,2,5]

[1] Departamento de Física, Universidade Federal de Pernambuco, Av. Prof. Aníbal Fernandes, s/n, 50740-560, Recife-PE, Brazil
[2] National Research University, Higher School of Economics, Moscow, 101000, Russia
[3] Institute for Theoretical Physics III, University of Bayreuth, Bayreuth 95440, Germany
[4] ITMO University, St. Petersburg, 197101, Russia

E-mail: arkadyshanenko@df.ufpe.br and shanenkoa@gmail.com

Received 15 May 2020, revised 7 July 2020
Accepted for publication 20 July 2020
Published 13 August 2020

Abstract

There is a tacit assumption that multiband superconductors are essentially the same as multigap superconductors. More precisely, it is usually assumed that the number of excitation gaps in the single-particle energy spectrum of a uniform superconductor (i.e. number of peaks in the density of states of the superconducting electrons) determines the number of contributing bands in the corresponding superconducting model. Here we demonstrate that contrary to this widely accepted viewpoint, the superconducting magnetic properties are sensitive to the number of contributing bands even when the spectral gaps are degenerate and cannot be distinguished. In particular, we find that the crossover between superconductivity types I and II—the intertype regime—is strongly affected by the difference between characteristic lengths of multiple contributing condensates. The reason for this is that condensates with diverse characteristic lengths, when coexisting in one system, interfere constructively or destructively, which results in multi-condensate magnetic phenomena regardless of the presence/absence of the multigap spectrum of a superconducting multiband material.

Keywords: multiband superconductors, superconducting properties, superconducting magnetic response

(Some figures may appear in colour only in the online journal)

1. Introduction

The concept of the multiband superconductivity was introduced in 1959 [1, 2] as a possible explanation of a multigap fine structure observed in frequency dependent conductivity of superconducting Pb and Hg, extracted from the infrared absorption spectrum [3]. Despite the long history of the concept and several other experimental results about the multigap character of some superconductors [4, 5], its detailed and unambiguous confirmation was obtained only in 2000s after experiments with MgB_2 (see, e.g., reference [6] and references therein). The observation of two well distinguished energy gaps in the excitation spectrum of MgB_2 [7, 8] [the density of states (DOS) of the superconducting electrons contains two peaks] ignited widespread interest in multiband superconductivity, boosting further experimental and theoretical studies. After a decade of intensive investigations, it became clear that multiple overlapping single-particle bands are present in many superconducting materials, ranging from iron-based [9] to organic high-T_c [10] and even topological superconductors [11, 12]. Recent first principle calculations have demonstrated that the Fermi surface of Pb comprises two Fermi sheets, confirming multiband nature of its superconducting state proposed [1] to explain pioneering experiments in [3].

It is widely assumed that a key marker for the multiband superconductivity is the appearance of multiple energy gaps in the single-particle spectrum of a homogeneous (bulk)

[5] Author to whom any correspondence should be addressed.

superconductor. Then, if the spectrum does not exhibit the multigap structure, the superconducting properties are expected to be those of single-band materials. More generally, it is usually assumed that the *number of spectral gaps determines the number of contributing bands* in a superconducting model that captures the essential physics of interest. A well-known example is MgB_2 which exhibits two spectral gaps associated with π and σ states [6–8]. Accordingly, theoretical models for superconductivity in MgB_2 consider two contributing bands (see, e.g., references [6, 13–19]) despite the fact that the first principle calculations reveal [20, 21] four single-particle bands for MgB_2, see also reference [6]. The two σ bands have different microscopic parameters (diverse Fermi sheets) but degenerate excitation gaps and the same holds for the π bands. A general perception is that the two-band model is sufficient to fully describe the superconducting state with the two spectral gaps.

However, there exists another approach that regards a multiband superconductor as a system governed by a set of *competing characteristic lengths* associated with different bands, see calculations of the healing lengths for different partial condensates in, e.g., references [18, 19, 22–25]. The single-particle spectrum of superconducting electrons is usually measured for bulk superconductors to avoid problems with the interpretation of nonuniform measurements. When the corresponding tunnelling measurements reveal, for example, a single peak in the DOS, it does not mean that the position-dependent gap functions of different contributing condensates are always the same. Their characteristic spatial lengths can be different due to peculiarities of the Fermi surface.

For clean systems (under consideration in the present work) such difference appears due to the presence of the band-dependent Fermi velocities. It is well-known that the Fermi velocity affects the condensate length in the single-band case. Similarly, the band-dependent Fermi velocities have an effect on the lengths of the partial condensates in multiband materials. However, here the physics is more complicated because of the interaction between the condensates. There is complex competition of the interband interactions with the disparity of the band Fermi velocities, and it becomes even more nontrivial in the presence of magnetic effects. In general, the disparity of the Fermi velocities increases the difference between the condensate lengths while the interband interactions support the so-called 'lengths-locking' regime (see the details of the 'lengths-locking' regime in [25]). Thus, the appearance of multiple characteristic lengths and the existence of many excitation gaps are both consequences of multiple sheets of the Fermi surface, interpreted as separate single-particle bands. However, these features appear on different levels of the theory—the system can have multiple energy gaps in the excitation spectrum but a single condensate length and, vice versa, a multiband superconductor can have multiple condensate lengths but a single spectral gap.

As is well known, the competition of different length-scales can lead to non-trivial physical consequences, e.g., to the spontaneous pattern formation [26]. Examples of systems with spontaneous patterns are well-known in the literature and include magnetic films [26, 27], liquid crystals [28], multilayer soft tissues [29], lipid monolayers [30], granular media [31] etc. A possibility of symmetry breaking patterns of vortices (labyrinth and stripes) induced by the presence of two condensate components with significantly different coherence lengths has recently attracted much interest in the context of unusual mixed (Shubnikov) phase configurations observed in MgB_2 (see, e.g., references [32, 33] and references therein). Coupled condensates coexisting in one material with diverse coherence lengths can interfere (interact) constructively or destructively, giving rise to phenomena absent in superconductors with a single-band condensate. In addition to the labyrinths and stripes of vortices mentioned above, other effects can be listed, e.g., chiral solitons [34–36], possible fractional vortices [37–42], hidden criticality [23], unusual oscillations in the current carrying state [43], enhancement of the intertype superconductivity [44, 45], unconventional Shapiro steps in the Josephson junctions [46, 47], the multiband vortex splitting effects [37, 48], a giant paramagnetic Meissner effect [49], multiband screening of superconducting fluctuations [50], gapless states and the related phase dependence of the excitation spectrum due to crossband pairing [51], etc.

In the present work we demonstrate that the crossover between superconductivity types I and II—the intertype (IT) regime (see, e.g., [44, 45])—is strongly affected by the difference between healing lengths of multiple contributing condensates even when the corresponding excitation gaps are degenerate and cannot be distinguished. Our analysis is done by using the formalism of the extended Ginzburg–Landau (EGL) theory [52, 53] generalized to the case of an arbitrary number of contributing bands. Here we consider systems in which the position-dependent gap functions associated with different contributing condensates have the same phases, i.e. there is no frustration related to the broken time-reversal symmetry, see e.g. [54–56]. The case of the gap functions with different phases [54–56] can also be appealing and can provide additional illustrations supporting our present conclusions. However, it requires a different variant of the EGL formalism and separate consideration.

The paper is organized as follows. In section 2 we discuss our formalism based on the τ-expansion of the microscopic equations, with $\tau = 1 - T/T_c$ the proximity to the critical temperature. It goes to one order beyond the standard Ginzburg–Landau (GL) approach, which is sufficient to describe a finite IT domain between types I and II in the phase diagram of the superconducting magnetic response. This formalism is then used in section 3, where boundaries of the IT domain are obtained for different configurations of the multiband structure. Conclusions are given in section 4.

2. Multiband EGL formalism

The EGL formalism is a convenient tool that can be employed when the physics beyond the GL theory is of interest but full microscopic calculations are impractical. A relevant example is the crossover between superconductivity types I and II—the IT regime. It is well known that within the GL theory, the crossover is reduced to a single point—it takes place at the critical GL parameter [57–59] $\kappa = \kappa_0 = 1/\sqrt{2}$ ($\kappa = \lambda_L/\xi_{GL}$, where λ_L and ξ_{GL} are the London magnetic penetration depth and GL coherence length). However, as is known since 70s, this GL-based picture is valid only in the limit $T \to T_c$ (more precisely, in the lowest order in τ). At $T < T_c$ (beyond the lowest order in τ) there is a finite temperature-dependent crossover interval of κ's [60–76], which the GL theory does not capture. In the corresponding finite domain in the κ-T plain (the IT domain), the system has nonstandard field dependence of the magnetization [60–65] with unconventional spatial configurations of the mixed state [44, 61, 69–76], governed by long-range attraction of vortices [60–68] and many-vortex interactions [92]—the so-called intermediate mixed state.

For the derivation of the EGL formalism, we employ the M-band generalization of the two-band BCS model [1, 2] with the s-wave pairing in all contributing bands and the Josephson-like Cooper-pair transfer between the bands. For illustration, we consider a system in the clean limit and assume that all available bands have parabolic single-particle energy dispersions with 3D spherical Fermi surfaces. The pairing is controlled by the symmetric real coupling matrix $\check{g}$, with the elements $g_{\nu\nu'}$. The derivation of the formalism comprises two main steps: (1) the multiband Neumann–Tewordt (NT) functional is obtained from the microscopic model and (2) the τ-expansion is applied to reconstruct the NT functional. We outline main details of these steps, highlighting important differences in comparison with the two-band EGL approach [53]. The obtained formalism is then used in the analysis of the boundaries of the IT domain in the κ–T phase diagram.

2.1. Multiband Neumann–Tewordt functional

The NT functional [77, 78] is obtained from the microscopic expression for the condensate free energy by accounting for higher powers and higher gradients of the band-dependent gap functions $\Delta_\nu = \Delta_\nu(\mathbf{x})$, as compared to the GL functional. (Notice that from here on we use the notion 'gap function' for $\Delta_\nu(\mathbf{x})$ while the excitation or spectral gap is the feature of the single-particle spectrum of the uniform superconductor.) Only the terms giving the GL theory and its leading corrections are taken into account. The general expression for the free energy density of M-band s-wave superconductor (relative to that of the normal state at zero field) can be written as [44, 53]

$$f = \frac{\mathbf{B}^2}{8\pi} + \langle \vec{\Delta}, \check{g}^{-1}\vec{\Delta}\rangle + \sum_{\nu=1}^{M} f_\nu[\Delta_\nu], \tag{1}$$

where $\mathbf{B}$ is the magnetic field, $\vec{\Delta} = (\Delta_1, \Delta_2, \ldots, \Delta_M)$, $\langle \vec{a}, \vec{b}\rangle = \sum_\nu a_\nu^* b_\nu$ denotes the scalar product of vectors $\vec{a}$ and $\vec{b}$ in the band space, and the functional $f_\nu[\Delta_\nu]$ reads

$$f_\nu = -\sum_{n=0}^{\infty} \frac{1}{n+1} \int \prod_{j=1}^{2n+1} \mathrm{d}^3 y_j K_{\nu,2n+1}(\mathbf{x}, \{\mathbf{y}\}_{2n+1}) \times \Delta_\nu^*(\mathbf{x})\Delta_\nu(\mathbf{y}_1)\ldots\Delta_\nu^*(\mathbf{y}_{2n})\Delta_\nu(\mathbf{y}_{2n+1}), \tag{2}$$

with $\{\mathbf{y}\}_{2n+1} = \{\mathbf{y}_1, \ldots, \mathbf{y}_{2n+1}\}$. The integral kernels in equation (2) are given by (m is odd)

$$K_{\nu,m}(\mathbf{x}, \{\mathbf{y}\}_m) = -T\sum_\omega \mathcal{G}^{(B)}_{\nu,\omega}(\mathbf{x}, \mathbf{y}_1)\bar{\mathcal{G}}^{(B)}_{\nu,\omega}(\mathbf{y}_1, \mathbf{y}_2)\ldots \times \mathcal{G}^{(B)}_{\nu,\omega}(\mathbf{y}_{m-1}, \mathbf{y}_m)\bar{\mathcal{G}}^{(B)}_{\nu,\omega}(\mathbf{y}_m, \mathbf{x}), \tag{3}$$

where ω is the fermionic Matsubara frequency, $\mathcal{G}^{(B)}_{\nu,\omega}(\mathbf{x}, \mathbf{y})$ is the Fourier transform of the single-particle Green function calculated in the presence of the magnetic field and $\bar{\mathcal{G}}^{(B)}_{\nu,\omega}(\mathbf{x}, \mathbf{y}) = -\mathcal{G}^{(B)}_{\nu,-\omega}(\mathbf{y}, \mathbf{x})$. For $\mathcal{G}^{(B)}_{\nu,\omega}$ we employ the standard approximation sufficient to derive the extended GL theory

$$\mathcal{G}^{(B)}_{\nu,\omega}(\mathbf{x}, \mathbf{y}) = \exp\left[\mathrm{i}\frac{e}{\hbar c}\int_{\mathbf{y}}^{\mathbf{x}} \mathbf{A}(\mathbf{z})\cdot \mathrm{d}\mathbf{z}\right] \mathcal{G}^{(0)}_{\nu,\omega}(\mathbf{x}, \mathbf{y}), \tag{4}$$

where the integral in the exponent is taken along the classical trajectory of a charge carrier in a magnetic field with the vector potential $\mathbf{A}$. Here the Green function for zero field writes

$$\mathcal{G}^{(0)}_{\nu,\omega}(\mathbf{x}, \mathbf{y}) = \int \frac{\mathrm{d}^3\mathbf{k}}{(2\pi)^3} \frac{\exp[\mathrm{i}\mathbf{k}\cdot(\mathbf{x}-\mathbf{y})]}{\mathrm{i}\hbar\omega - \xi_\nu(\mathbf{k})}, \tag{5}$$

where the band-dependent single-particle energy dispersion reads

$$\xi_\nu(\mathbf{k}) = \xi_\nu(0) + \frac{\hbar^2\mathbf{k}^2}{2m_\nu} - \mu, \tag{6}$$

with m_ν the band effective mass, $\xi_\nu(0)$ the band lower edge, and μ the chemical potential.

To get simpler differential structure of the functional (1), one invokes the gradient expansion for the band gap functions and the vector potential as

$$\Delta_\nu(\mathbf{y}) = \Delta_\nu(\mathbf{x}) + ((\mathbf{y}-\mathbf{x})\cdot\boldsymbol{\nabla}_\mathbf{x})\Delta_\nu(\mathbf{x}) + \ldots,$$
$$\mathbf{A}(\mathbf{y}) = \mathbf{A}(\mathbf{x}) + ((\mathbf{y}-\mathbf{x})\cdot\boldsymbol{\nabla}_\mathbf{x})\mathbf{A}(\mathbf{x}) + \ldots, \tag{7}$$

which makes it possible to represent non-local integrals in f_ν as a series in powers of Δ_ν, its gradients and field spatial derivatives. The series are infinite and therefore a truncation procedure is needed. The GL theory follows from the standard Gor'kov truncation [79]. To incorporate the leading corrections to the GL formalism, one needs to go beyond the Gor'kov approximation. As the form of f_ν is not sensitive to the number of contributing bands, one can apply the truncation procedure to each of the band contributions separately and utilize the previous results derived for the single- and two-band cases, see reference [53]. The resulting multiband NT functional reads

$$f = \frac{\mathbf{B}^2}{8\pi} + \langle \vec{\Delta}, \check{g}^{-1}\vec{\Delta}\rangle + \sum_{\nu=1}^{M}\Bigg\{\left[\mathcal{A}_\nu + a_\nu\left(\tau + \frac{\tau^2}{2}\right)\right]|\Delta_\nu|^2 + \frac{b_\nu}{2}(1+2\tau)|\Delta_\nu|^4 - \frac{c_\nu}{3}|\Delta_\nu|^6 + \mathcal{K}_\nu(1+2\tau)|\mathbf{D}\Delta_\nu|^2 - \mathcal{Q}_\nu\left(|\mathbf{D}^2\Delta_\nu|^2 + \frac{1}{3}\mathrm{rot}\,\mathbf{B}\cdot\mathbf{i}_\nu + \frac{4e^2}{\hbar^2c^2}\mathbf{B}^2|\Delta_\nu|^2\right) - \frac{\mathcal{L}_\nu}{2}\left[8|\Delta_\nu|^2|\mathbf{D}\Delta_\nu|^2 + \left(\Delta_\nu^{*2}(\mathbf{D}\Delta_\nu)^2 + \mathrm{c.c.}\right)\right]\Bigg\}, \tag{8}$$

with $\mathbf{D} = \nabla - \mathrm{i}(2e/\hbar c)\mathbf{A}$ and $\mathbf{i}_\nu = (4e/\hbar c)\,\mathrm{Im}\left[\Delta_\nu^*\mathbf{D}\Delta_\nu\right]$. The band dependent coefficients in equation (8) are

$$\mathcal{A}_\nu = N_\nu \ln\left(\frac{2e^\Gamma \hbar\omega_c}{\pi T_c}\right), \quad a_\nu = -N_\nu, \quad b_\nu = N_\nu \frac{7\zeta(3)}{8\pi^2 T_c^2},$$
$$c_\nu = N_\nu \frac{93\zeta(5)}{128\pi^4 T_c^4}, \quad \mathcal{K}_\nu = \frac{b_\nu}{6}\hbar^2 v_\nu^2, \quad \mathcal{Q}_\nu = \frac{c_\nu}{30}\hbar^4 v_\nu^4,$$
$$\mathcal{L}_\nu = \frac{c_\nu}{9}\hbar^2 v_\nu^2, \tag{9}$$

where ω_c is the cut-off frequency, N_ν is the band DOS, v_ν denotes the band Fermi velocity, T_c is in the energy units, and $\zeta(\ldots)$ and Γ are the Riemann zeta-function and Euler constant.

The NT functional appears as a natural extension of the GL theory. The initial motivation of its derivation was to have an approach beyond the GL theory, which preserves, to some extent, the simplicity of the GL formalism. Such an approach is especially important in the case of spatially nonuniform problems. Unfortunately, the stationary point equations derived from the NT functional are rather complex even for the single-band case and not easier to solve than the original microscopic equations (see, e.g., equation (3) in reference [80]). Furthermore, these equations admit unphysical solutions [80] such as weakly damped oscillations of the condensate near the core of a single vortex state. The roots of this problem lie in the fact that the NT free energy functional is not bound from below because the coefficients c_ν, $\mathcal{Q}_\nu$, and $\mathcal{L}_\nu$ are positive. We also note in passing that a similar functional is commonly used in the analysis of the Fulde–Ferrel–Larkin–Ovchinnikov (FFLO) pairing (see, e.g., references [81–83]), however, in that case the sign of c_ν, $\mathcal{Q}_\nu$ and $\mathcal{L}_\nu$ is changed due the spin–magnetic interaction, which marks the appearance of the stable FFLO regime.

2.2. *Perturbative τ-expansion*

It was suggested for the single-band case (see reference [80] and references therein) that to eliminate the nonphysical solutions, the NT functional should be restructured by applying the perturbative τ-expansion, based on the fact that the fundamental small parameter of the microscopic equations is the proximity to the critical temperature τ. The stationary solution for the order parameter within the NT approach contains all odd powers of $\tau^{1/2}$ while the truncation of the infinite series in equation (3) does not distort only the two lowest orders $\tau^{1/2}$ (the GL term) and $\tau^{3/2}$ (the leading correction to the GL term). Incomplete higher-order terms in τ should be removed by means of the τ-expansion. A similar approach was subsequently applied to the two-band NT functional [53]. Here we generalize it to the case of an arbitrary number of contributing bands M.

Following this approach, we represent the band gap functions and fields in the form of τ-series [52, 53]

$$\Delta_\nu = \tau^{1/2}\left[\Delta_\nu^{(0)} + \tau\Delta_\nu^{(1)} + \ldots\right],$$
$$\mathbf{A} = \tau^{1/2}\left[\mathbf{A}^{(0)} + \tau\mathbf{A}^{(1)} + \ldots\right], \tag{10}$$
$$\mathbf{B} = \tau\left[\mathbf{B}^{(0)} + \tau\mathbf{B}^{(1)} + \ldots\right].$$

One also takes into account divergent condensate and field characteristic lengths $\propto \tau^{-1/2}$ that affect spatial gradients in the NT functional. This is formally done by introducing the spatial scaling as $\mathbf{x} \to \tau^{1/2}\mathbf{x}$ (see discussion after equation (10) in reference [52]). Notice that to get the stationary solution in the two lowest orders in τ, one also needs to operate with $\Delta_\nu^{(2)}$ but only in intermediate expressions.

Inserting equation (10) into equation (8) and applying the scaling $\mathbf{x} \to \tau^{1/2}\mathbf{x}$, one obtains the free energy density as

$$f = \tau^2\left[\tau^{-1}f^{(-1)} + f^{(0)} + \tau f^{(1)} + \ldots\right]. \tag{11}$$

Notice that the two lowest orders in the band gap functions and the field produce three lowest orders in the free energy but, as is shown below, the contribution $f^{(-1)}$ is zero for the stationary point. This contribution reads as

$$f^{(-1)} = \langle \vec{\Delta}^{(0)}, \check{L}\vec{\Delta}^{(0)}\rangle, \tag{12}$$

where the matrix elements of $\check{L}$ are defined as

$$L_{\nu\nu'} = g_{\nu\nu'}^{-1} - \mathcal{A}_\nu\delta_{\nu\nu'}, \tag{13}$$

with $g_{\nu\nu'}^{-1}$ being elements of the inverse coupling matrix $\check{g}^{-1}$ and $\delta_{\nu\nu'}$ denoting the Kronecker symbol. The next-order term $f^{(0)}$ is the GL functional

$$f^{(0)} = \frac{\mathbf{B}^{(0)2}}{8\pi} + \left(\langle \vec{\Delta}^{(0)}, \check{L}\vec{\Delta}^{(1)}\rangle + \mathrm{c.c.}\right) + \sum_{\nu=1}^{M} f_\nu^{(0)}, \tag{14}$$

where $f_\nu^{(0)}$ is given by

$$f_\nu^{(0)} = a_\nu|\Delta_\nu^{(0)}|^2 + \frac{b_\nu}{2}|\Delta_\nu^{(0)}|^4 + \mathcal{K}_\nu|\mathbf{D}^{(0)}\Delta_\nu^{(0)}|^2, \tag{15}$$

and $\mathbf{D}^{(0)} = \nabla - \mathrm{i}(2e/\hbar c)\mathbf{A}^{(0)}$. Finally, the highest-order term in equation (11) is given by

$$f^{(1)} = \frac{\mathbf{B}^{(0)}\cdot\mathbf{B}^{(1)}}{4\pi} + \left(\langle \vec{\Delta}^{(0)}, \check{L}\vec{\Delta}^{(2)}\rangle + \mathrm{c.c.}\right) + \langle \vec{\Delta}^{(1)}, \check{L}\vec{\Delta}^{(1)}\rangle + \sum_{\nu=1}^{M} f_\nu^{(1)}, \tag{16}$$

where

$$\begin{aligned} f_\nu^{(1)} = {} & \left(a_\nu + b_\nu|\Delta_\nu^{(0)}|^2\right)\left(\Delta_\nu^{(0)*}\Delta_\nu^{(1)} + \mathrm{c.c.}\right) + \frac{a_\nu}{2}|\Delta_\nu^{(0)}|^2 \\ & + b_\nu|\Delta_\nu^{(0)}|^4 - \frac{c_\nu}{3}|\Delta_\nu^{(0)}|^6 + 2\mathcal{K}_\nu|\mathbf{D}^{(0)}\Delta_\nu^{(0)}|^2 \\ & + \mathcal{K}_\nu\left[\left(\mathbf{D}^{(0)}\Delta_\nu^{(0)}\cdot\mathbf{D}^{(0)*}\Delta_\nu^{(1)*} + \mathrm{c.c.}\right) - \mathbf{A}^{(1)}\cdot\mathbf{i}_\nu^{(0)}\right] \\ & - \mathcal{Q}_\nu\left(|\mathbf{D}^{(0)2}\Delta_\nu^{(0)}|^2 + \frac{1}{3}\mathrm{rot}\,\mathbf{B}^{(0)}\cdot\mathbf{i}_\nu^{(0)} + \frac{4e^2\mathbf{B}^{(0)2}}{\hbar^2c^2}|\Delta_\nu^{(0)}|^2\right) \\ & - \frac{\mathcal{L}_\nu}{2}\left\{8|\Delta_\nu^{(0)}|^2|\mathbf{D}^{(0)}\Delta_\nu^{(0)}|^2 \right. \\ & \left. + \left[\Delta_\nu^{(0)2}(\mathbf{D}^{(0)*}\Delta_\nu^{(0)*})^2 + \mathrm{c.c.}\right]\right\}, \end{aligned} \tag{17}$$

and $\mathbf{i}_\nu^{(0)}$ is the lowest-order term in the τ-expansion of $\mathbf{i}_\nu$.

The τ-expansion of the NT functional is then used to derive a set of the stationary-point equations for the gap functions and fields contributions—each of the equations correspond to a particular order of the τ-expansion. The equation in the lowest order reads

$$\frac{\delta \mathcal{F}^{(-1)}}{\delta \vec{\Delta}^{(0)\dagger}} = \check{L}\vec{\Delta}^{(0)} = 0, \quad (18)$$

where $\mathcal{F}^{(-1)}$ the free energy contribution obtained by integrating $f^{(-1)}$. This is the linearized gap equation in the multiband BCS theory that determines T_c. It has a nontrivial solution when

$$\det \check{L} = 0. \quad (19)$$

Recalling the definition of $\check{L}$, which includes $\mathcal{A}_\nu$ and, hence, depends on T_c, one sees that equation (19) determines zeros of an M-degree polynomial of the variable $\ln(2e^\Gamma \hbar\omega_c/\pi T_c)$. One should choose the smallest root of this polynomial, which gives the largest T_c. Here we assume that this solution is non-degenerate. This implies that the solution of the gap equation (18) corresponds to a one-dimensional irreducible representation of the system symmetry group. The opposite occurs in a particular case when the superconducting system has a symmetry additional to $U(1)$, which is reflected in a special symmetry of the matrix $\check{L}$ and results in the appearance of multi-component order parameter (see references [55, 84, 85]).

Once T_c is determined, it is convenient to introduce the eigenvalues and eigenvectors of $\check{L}$ as

$$\check{L}\vec{\epsilon} = 0 \quad (20)$$

with the zero eigenvalue and

$$\check{L}\vec{\eta}_i = \Lambda_i \vec{\eta}_i, \quad (21)$$

with nonzero eigenvalues $\Lambda_i \neq 0$. As the matrix $\check{L}$ is real and symmetric, the vectors $\vec{\epsilon}$ and $\vec{\eta}_i$ can be chosen such that they form an orthonormal basis so that $\langle \vec{\epsilon}, \vec{\epsilon} \rangle = 1$, $\langle \vec{\epsilon}, \vec{\eta}_i \rangle = 0$ and $\langle \vec{\eta}_i, \vec{\eta}_j \rangle = \delta_{ij}$. Then a general solution to the gap equation (18) reads in the form

$$\vec{\Delta}^{(0)} = \psi(\mathbf{x})\vec{\epsilon}, \quad (22)$$

where $\psi(\mathbf{x})$ controls the spatial profiles of all band condensates in the lowest order in τ.

The shape of $\psi(\mathbf{x})$ is governed by the stationary point equations associated with the GL functional (14). The first one of those is given by

$$\frac{\delta \mathcal{F}^{(0)}}{\delta \vec{\Delta}^{(0)\dagger}} = \check{L}\vec{\Delta}^{(1)} + \vec{W}[\vec{\Delta}^{(0)}] = 0, \quad (23)$$

where $\mathcal{F}^{(0)}$ is the free-energy term corresponding to $f^{(0)}$ and the components of $\vec{W}$ read

$$W_\nu = a_\nu \Delta_\nu^{(0)} + b_\nu \Delta^{(0)}|\Delta_\nu^{(0)}|^2 - \mathcal{K}_\nu \mathbf{D}^{(0)2}\Delta_\nu^{(0)}. \quad (24)$$

The second (Maxwell) equation is obtained as

$$\frac{\delta \mathcal{F}^{(0)}}{\delta \mathbf{A}^{(0)}} = \frac{1}{4\pi}\text{rot } \mathbf{B}^{(0)} - \sum_{\nu=1}^{M} \mathcal{K}_\nu \mathbf{i}_\nu^{(0)} = 0. \quad (25)$$

Notice that the equation $\delta\mathcal{F}^{(0)}/\delta\vec{\Delta}^{(1)\dagger} = 0$ coincides with equation (18) while $\delta\mathcal{F}^{(0)}/\delta\mathbf{A}^{(1)} = 0$ is an identity relation because $\mathbf{A}^{(1)}$ does not contribute to $f^{(0)}$. By projecting equation (23) onto $\vec{\epsilon}$ and keeping in mind that $\vec{\epsilon}^\dagger \check{L} = 0$, one gets

$$a\psi + b\psi|\psi|^2 - \mathcal{K}\mathbf{D}^{(0)2}\psi = 0, \quad (26)$$

where coefficients a, b and $\mathcal{K}$ are averages over the contributing bands

$$a = \sum_{\nu=1}^{M} a_\nu |\epsilon_\nu|^2, \qquad b = \sum_{\nu=1}^{M} b_\nu |\epsilon_\nu|^4, \qquad \mathcal{K} = \sum_{\nu=1}^{M} \mathcal{K}_\nu |\epsilon_\nu|^2, \quad (27)$$

and ϵ_ν are the components of $\vec{\epsilon}$. Similarly, equation (25) is reduced to

$$\text{rot } \mathbf{B}^{(0)} = 4\pi\mathcal{K}\mathbf{i}_\psi^{(0)}, \quad (28)$$

where $\mathbf{i}_\psi^{(0)}$ is obtained from $\mathbf{i}_\nu^{(0)}$ by substituting ψ for $\Delta_\nu^{(0)}$.

Therefore, the GL equations for the M-band system are given by equations (26) and (28). The corresponding condensate state is described by a single-component order parameter $\psi(\mathbf{x})$, in full agreement with the Landau theory in the case of a non-degenerate solution for T_c, see also references [16, 86, 87]. We note that the number of the components of the order parameter is determined by the dimensionality of the relevant irreducible representation of the corresponding symmetry group [57, 84], not by the number of the bands. The single-component order parameter means that the standard classification of the superconducting magnetic response is applied here: we have types I and II with the IT regime in between. The presence of multiple bands is reflected only in the expressions for the coefficients a, b and $\mathcal{K}$.

Using the eigenvectors of $\check{L}$ as the basis, we represent the next-to-leading contribution to the gap function as

$$\vec{\Delta}^{(1)} = \varphi(\mathbf{x})\vec{\epsilon} + \sum_{i=1}^{M-1} \varphi_i(\mathbf{x})\vec{\eta}_i, \quad (29)$$

with new position-dependent functions φ and φ_i to be found. Inserting equation (29) in equation (23), one obtains the equation

$$\sum_{i=1}^{M-1} \Lambda_i \varphi_i \vec{\eta}_i + \vec{W}[\vec{\Delta}^{(0)}] = 0. \quad (30)$$

Equation (30) is solved by projecting it onto $\vec{\eta}_j$, which yields $M-1$ equations for φ_j, i.e.,

$$\varphi_j = -\frac{1}{\Lambda_j}\left(\alpha_j\psi + \beta_j\psi|\psi|^2 - \Gamma_j\mathbf{D}^{(0)2}\psi\right), \quad (31)$$

where the coefficients α_j, β_j, and Γ_j are of the form

$$\alpha_j = \sum_{\nu=1}^{M} a_\nu \eta_{j\nu}^* \epsilon_\nu, \qquad \beta_j = \sum_{\nu=1}^{M} b_\nu \eta_{j\nu}^* \epsilon_\nu |\epsilon_\nu|^2,$$
$$\Gamma_j = \sum_{\nu=1}^{M} \mathcal{K}_\nu \eta_{j\nu}^* \epsilon_\nu, \quad (32)$$

and $\eta_{j\nu}$ are components of $\vec{\eta}_j$. Equations (29), (31), and (32) generalize the corresponding expressions for the two-band case [53]. One should keep in mind that the present formalism involves the eigenvectors of $\check{L}$ while $\vec{\Delta}^{(1)}$ in reference [53] was represented as a linear combination of other explicitly chosen vectors. Therefore, to recover the expression for $\vec{\Delta}^{(1)}$ in reference [53], one needs to express $\vec{\epsilon}$ and $\vec{\eta}_j$ for $M = 2$ in terms of the vectors used in reference [53].

Thus, $M-1$ functions φ_i, which determine the second term for $\vec{\Delta}^{(1)}$ in equation (29), are found from the simple algebraic expressions (31) when using solutions to the GL equations (26) and (28). To find the first term in equation (29), that depends on φ and the leading correction to the field $\mathbf{A}^{(1)}$, one needs to solve the system of equations resulting from the projection of equation (30) onto the eigenvector $\vec{\epsilon}$ and zero functional derivatives of the free-energy contribution corresponding to $f^{(1)}$. However, as will be shown below, φ and $\mathbf{A}^{(1)}$ do not contribute to the boundaries of the IT domain. We note, however, that φ is necessary to calculate the band healing lengths—this calculation is outlined in the appendix A.

2.3. Free energy at the stationary point and thermodynamic critical field

The stationary free energy density is found by substituting the obtained stationary solutions into the corresponding expressions for the free energy functional, i.e.,

$$f_{st} = \tau^2 \left[f_{st}^{(0)} + \tau f_{st}^{(1)} + \ldots \right], \tag{33}$$

where the term of the order τ is absent by the virtue of equation (18) and the first non-vanishing contribution is the GL free energy

$$f_{st}^{(0)} = \frac{\mathbf{B}^{(0)2}}{8\pi} + a|\psi|^2 + \frac{b}{2}|\psi|^4 + \mathcal{K}|\mathbf{D}^{(0)}\psi|^2, \tag{34}$$

we have also taken into account that $\langle \vec{\Delta}^{(0)}, \check{L}\vec{\Delta}^{(1)} \rangle = 0$, which follows from equation (18).

To find the leading order correction to the stationary GL free energy, we first rearrange the terms in $f^{(1)}$ that include $\Delta_\nu^{(1)}$ and $\Delta_\nu^{(1)*}$. For the stationary solution the sum of these terms in equation (16) can be represented as

$$\langle \vec{\Delta}^{(1)}, \check{L}\vec{\Delta}^{(1)} \rangle + \left(\langle \vec{\Delta}^{(1)}, \vec{W} \rangle + \text{c.c.} \right) = -\langle \vec{\Delta}^{(1)}, \check{L}\vec{\Delta}^{(1)} \rangle, \tag{35}$$

where equation (23) is taken into consideration. Using equations (26) and (31), we further obtain that $\langle \vec{\Delta}^{(1)}, \check{L}\vec{\Delta}^{(1)} \rangle$ can be expressed only in terms of ψ as

$$\langle \vec{\Delta}^{(1)}, \check{L}\vec{\Delta}^{(1)} \rangle = |\psi|^2 \sum_{i=1}^{M-1} \frac{a^2|\bar{\alpha}_i|^2}{\Lambda_i} + 2|\psi|^4 \sum_{i=1}^{M-1} \frac{ab\ \text{Re}[\bar{\alpha}_i^* \bar{\beta}_i]}{\Lambda_i} + |\psi|^6 \sum_{i=1}^{M-1} \frac{b^2|\bar{\beta}_i|^2}{\Lambda_i}, \tag{36}$$

where the dimensionless parameters $\bar{\alpha}_i$ and $\bar{\beta}_i$ are defined by

$$\bar{\alpha}_i = \frac{\alpha_i}{a} - \frac{\Gamma_i}{\mathcal{K}}, \qquad \bar{\beta}_i = \frac{\beta_i}{b} - \frac{\Gamma_i}{\mathcal{K}}. \tag{37}$$

Then, $f^{(1)}$, given by equations (16) and (17), can be represented for the stationary solution in the form

$$\begin{aligned} f_{st}^{(1)} = &\frac{\mathbf{B}^{(0)} \cdot \mathbf{B}^{(1)} - \mathbf{A}^{(1)} \cdot \text{rot}\, \mathbf{B}^{(0)}}{4\pi} + \frac{\gamma_a}{2}|\psi|^2 \\ &+ \gamma_b|\psi|^4 - \frac{\gamma_c}{3}|\psi|^6 + 2\mathcal{K}|\mathbf{D}^{(0)}\psi|^2 \\ &- \mathcal{Q}\left(|\mathbf{D}^{(0)2}\psi|^2 + \frac{1}{3}\text{rot}\, \mathbf{B}^{(0)} \cdot \mathbf{i}_\psi^{(0)} + \frac{4e^2\mathbf{B}^{(0)2}}{\hbar^2 c^2}|\psi|^2 \right) \\ &- \frac{\mathcal{L}}{2}\left\{ 8|\psi|^2|\mathbf{D}^{(0)}\psi|^2 + \text{Re}\left[\psi^2 \left(\mathbf{D}^{(0)*}\psi^* \right)^2 \right] \right\}, \end{aligned} \tag{38}$$

where

$$\mathcal{Q} = \sum_{\nu=1}^{M} \mathcal{Q}_\nu |\epsilon_\nu|^2, \qquad \mathcal{L} = \sum_{\nu=1}^{M} \mathcal{L}_\nu |\epsilon_\nu|^4, \qquad c = \sum_{\nu=1}^{M} c_\nu |\epsilon_\nu|^6. \tag{39}$$

and

$$\gamma_a = a - 2\sum_{i=1}^{M-1} \frac{a^2|\bar{\alpha}_i|^2}{\Lambda_i}, \qquad \gamma_b = b - 2\sum_{i=1}^{M-1} \frac{ab\ \text{Re}[\bar{\alpha}_i^* \bar{\beta}_i]}{\Lambda_i},$$
$$\gamma_c = c + 3\sum_{i=1}^{M-1} \frac{b^2|\bar{\beta}_i|^2}{\Lambda_i}. \tag{40}$$

Using the above result, one can calculate the thermodynamic critical field H_c which is also sought in the form of the τ-expansion

$$H_c = \tau \left[H_c^{(0)} + \tau H_c^{(1)} + \ldots \right]. \tag{41}$$

By virtue of the definition, H_c can be obtained from

$$\frac{H_c^2}{8\pi} = -f_{st,0}, \tag{42}$$

where $f_{st,0}$ is the free energy density of the Meissner state. In the lowest (GL) order, the uniform solution of equation (26) is given by $\psi_0 = \sqrt{|a|/b}$. This yields the corresponding contribution to the thermodynamic critical field as

$$H_c^{(0)} = \sqrt{\frac{4\pi a^2}{b}}, \tag{43}$$

see equations (33), (34), and (41). $H_c^{(0)}$ is formally the same as that for the single- and two-band cases [52, 53] but with the difference that a and b are now averages over M contributing bands. The next-order contribution to H_c is obtained from equations (33), (38), and (41), which gives

$$\frac{H_c^{(1)}}{H_c^{(0)}} = -\frac{1}{2} - \frac{ca}{3b^2} - \sum_{i=1}^{M-1} \frac{a}{\Lambda_i}|\bar{\alpha}_i - \bar{\beta}_i|^2. \tag{44}$$

Here the third term in the left-hand side has a different form as compared to the corresponding expressions for the single- and two-band cases in references [52, 53]. The origin of the differences has been already discussed after equation (32).

2.4. Gibbs free energy difference

A type I superconductor can only have a spatially uniform Meissner condensate state, which undergoes an abrupt transition to the normal state when the amplitude of the applied field $\mathbf{H}$ exceeds H_c. Type II superconductors, in addition to the Meissner phase, develop a nonuniform (mixed) state between the lower H_{c1} and upper H_{c2} critical fields, where $H_{c1} \leqslant H_c \leqslant H_{c2}$. A formal criterion for switching from type I to type II is that at $H = H_c$ the Meissner state becomes less energetically favourable than the mixed state. It is investigated by using the Gibbs free energy so that the switching criterion is obtained as the vanishing difference between the Gibbs free energies of the Meissner and nonuniform states. The Gibbs free energy density for a superconductor at $H = H_c$ is given by $g = f_{st} - H_c B/4\pi$, where $\mathbf{B}$ is directed along the external field $\mathbf{H}$ and found from the stationary-point equations for the corresponding condensate state. For the Meissner state we have $B = 0$ and $g = g_0 = f_{st,0} = -H_c^2/8\pi$. Thus, the density of the Gibbs free energy difference $\mathfrak{g} = g - g_0$ is written as

$$\mathfrak{g} = f_{st} - \frac{H_c B}{4\pi} + \frac{H_c^2}{8\pi}. \tag{45}$$

To calculate $\mathfrak{g}$, it is convenient to the use dimensionless quantities

$$\tilde{\mathbf{x}} = \frac{\mathbf{x}}{\sqrt{2}\lambda}, \qquad \tilde{\mathbf{A}} = \kappa \frac{\mathbf{A}}{\lambda_L H_c^{(0)}}, \qquad \tilde{\mathbf{B}} = \sqrt{2}\kappa \frac{\mathbf{B}}{H_c^{(0)}},$$
$$\tilde{\psi} = \frac{\psi}{\psi_0}, \qquad \tilde{\mathfrak{g}} = \frac{4\pi\mathfrak{g}}{H^{(0)2}}, \qquad \tilde{G} = \frac{4\pi G}{H^{(0)2}(\sqrt{2}\lambda_L)^3}, \tag{46}$$

where G is the integral of $\mathfrak{g}$ and

$$\lambda_L = \frac{\hbar c}{|e|}\sqrt{\frac{b}{32\pi K|a|}}, \qquad \kappa = \frac{\lambda_L}{\xi_{GL}} = \lambda_L\sqrt{\frac{|a|}{K}}. \tag{47}$$

We note that equation (47) differs from the conventional definitions for the GL coherence length ξ_{GL} and London penetration depth λ_L by the absence of the factor $\tau^{-1/2}$. This difference appears due to the scaling $\mathbf{x} \to \tau^{1/2}\mathbf{x}$ used in the derivation of the τ-expansion. Using the dimensionless units, we write the GL equations as

$$\psi - \psi|\psi|^2 + \frac{1}{2\kappa^2}\mathbf{D}^{(0)2}\psi = 0, \qquad \text{rot}\,\mathbf{B}^{(0)} = \mathbf{i}_\psi^{(0)}, \tag{48}$$

$\mathbf{D}^{(0)} = \nabla + \mathrm{i}\mathbf{A}^{(0)}$, $\mathbf{i}_\psi^{(0)} = 2\ \mathrm{Im}\left[\psi\mathbf{D}^{(0)*}\psi^*\right]$ and the spatial gradients are also dimensionless. Hereafter we omit the tilde for brevity.

The τ-expansion for $\mathfrak{g}$ is obtained from equations (33), (34), (38), and (45) in the form

$$\mathfrak{g} = \tau^2\left[\mathfrak{g}^{(0)} + \tau\mathfrak{g}^{(1)} + \ldots\right], \tag{49}$$

where

$$\mathfrak{g}^{(0)} = \frac{1}{2}\left(1 - \frac{B^{(0)}}{\sqrt{2}\kappa}\right)^2 - |\psi|^2 + \frac{1}{2}|\psi|^4 + \frac{|\mathbf{D}^{(0)}\psi|^2}{2\kappa^2} \tag{50}$$

and

$$\mathfrak{g}^{(1)} = \left(1 - \frac{B^{(0)}}{\sqrt{2}\kappa}\right)\left(\frac{\bar{\gamma}_a}{2} - \bar{c}\bar{\gamma}_c - \bar{\gamma}_b\right) - \frac{\bar{\gamma}_a}{2}|\psi|^2 + \bar{\gamma}_b|\psi|^4$$
$$+ \bar{c}\bar{\gamma}_c|\psi|^6 + \frac{|\mathbf{D}^{(0)}\psi|^2}{\kappa^2} + \frac{\bar{\mathcal{Q}}}{4\kappa^4}\left(|\mathbf{D}^{(0)2}\psi|^2 + \frac{\mathbf{i}_\psi^{(0)2}}{3} + \mathbf{B}^{(0)2}|\psi|^2\right)$$
$$+ \frac{\bar{\mathcal{L}}}{4\kappa^2}\left\{8|\psi|^2|\mathbf{D}^{(0)}\psi|^2 + \mathrm{Re}\left[\psi^2\left(\mathbf{D}^{(0)*}\psi^*\right)^2\right]\right\}, \tag{51}$$

where the dimensionless parameters are given by

$$\bar{c} = \frac{ca}{3b^2}, \qquad \bar{\mathcal{Q}} = \frac{\mathcal{Q}a}{K^2}, \qquad \bar{\mathcal{L}} = \frac{\mathcal{L}a}{Kb}, \qquad \bar{\Lambda}_j = \frac{\Lambda_j}{a},$$
$$\bar{\gamma}_a = \frac{\gamma_a}{a}, \qquad \bar{\gamma}_b = \frac{\gamma_b}{b}, \qquad \bar{\gamma}_c = \frac{\gamma_c}{c}. \tag{52}$$

We note that to derive equation (51), we rearrange equation (38) by using the identity $\mathbf{A}^{(1)} \cdot \text{rot}\ \mathbf{B}^{(0)} = \mathbf{A}^{(1)} \cdot \text{rot}\ (\mathbf{B}^{(0)} - \mathbf{H}_c^{(0)})$. It is then integrated by parts, giving $\mathbf{B}^{(1)} \cdot (\mathbf{B}^{(0)} - \mathbf{H}_c^{(0)})$ while surface integrals vanish. This makes sure that the next-to-lowest order contribution to $\mathbf{B}$ does not appear in the Gibbs free energy difference, similarly to φ contributing to $\vec{\Delta}^{(1)}$. Thus, the Gibbs free energy difference, taken in the lowest and next-to-lowest orders in τ depends only on the solution to the GL equations. One also notes that the GL contribution $\mathfrak{g}^{(0)}$ is not sensitive to M which enters only its leading correction $\mathfrak{g}^{(1)}$.

2.5. B point and intertype domain

Integrating equation (49) yields the Gibbs free energy difference G. However, since the goal of our study is superconducting properties in the vicinity of the B point, in addition to the τ-expansion we apply the expansion with respect to $\delta\kappa = \kappa - \kappa_0$, which gives

$$\frac{G}{\tau^{1/2}} = G^{(0)} + \frac{\mathrm{d}G^{(0)}}{\mathrm{d}\kappa}\delta\kappa + G^{(1)}\tau, \tag{53}$$

where only the linear contributions in $\propto \delta\kappa$ and $\propto \tau$ are kept and the expansion coefficients are calculated at $\kappa = \kappa_0$. A significant advantage of this approach is that at κ_0 the GL theory simplifies considerably because the condensate-field configurations become self-dual being related by [88]

$$B^{(0)} = 1 - |\Psi|^2, \tag{54}$$

while the order parameter ψ satisfies the first order differential equation

$$\left(D_x^{(0)} - \mathrm{i}D_y^{(0)}\right)\psi = 0. \tag{55}$$

Here the field is taken along the z-direction so that ψ is not dependent on z and one can use $\mathbf{D}^{(0)2} = D_x^{(0)2} + D_y^{(0)2}$. Equations (54) and (55) are often referred to as the Bogomolnyi equations [88] (in the context of superconductivity they are also known as the Sarma solution [58]). Using these equations, one can demonstrate that the first contribution to the Gibbs free energy difference $G^{(0)}$ vanishes identically for any solution of the GL equations, which is a manifestation of the fact that at $H = H_c$ the self-dual GL theory is infinitely degenerate. The GL theory predicts that at κ_0 the normal state $\psi = 0$

is stable above H_c while below H_c the Meissner state $\psi = 1$ appears. Then, the mixed state appears only at $H = H_c$, hosting a plethora of exotic condensate-field configurations. Corrections to the GL theory break the degeneracy and successive self-dual configurations of the magnetic flux and condensate determine the properties of the IT mixed state.

With the Bogomolnyi equations, the Gibbs free energy difference given by equation (53) is reduced to

$$\frac{G}{\tau^{1/2}L} = -\sqrt{2}\,\mathcal{I}\,\delta\kappa + (\mathcal{I}\mathcal{A} + \mathcal{J}\mathcal{B})\,\tau, \qquad (56)$$

where L is the system size along the direction of the field, $\mathcal{I}$ and $\mathcal{J}$ are given by the integrals

$$\mathcal{I} = \int \mathrm{d}^3\mathbf{x}|\psi|^2\left(1 - |\psi|^2\right), \qquad \mathcal{J} = \int \mathrm{d}^3\mathbf{x}|\psi|^4\left(1 - |\psi|^2\right), \qquad (57)$$

while coefficients $\mathcal{A}$ and $\mathcal{B}$ are given by

$$\mathcal{A} = 2(1 + \bar{\mathcal{Q}}) - \bar{\gamma}_b - \bar{c}\bar{\gamma}_c, \qquad \mathcal{B} = 2\bar{\mathcal{L}} - \frac{5}{3}\bar{\mathcal{Q}} - \bar{c}\bar{\gamma}_c. \qquad (58)$$

Apart from the constants, that depend on M contributing bands, this expression for the Gibbs free energy difference is the same as obtained earlier for single- and two-band superconductors [44].

Now we have everything at our disposal to determine the boundaries of the IT domain on the κ–T plane. Its lower boundary $\kappa^*_{\min}(T)$ separates type I and IT regimes and marks the appearance/disappearance of the mixed state [44]. At this boundary the upper critical field H_{c2} approaches H_c. The condensate vanishes at H_{c2} and so the Gibbs free energies of the normal and condensate states become equal. At the same time the normal and Meissner states have the same Gibbs free energy at H_c. Therefore, the lower boundary of the IT domain is found from the criterion $G = 0$ taken together with the condition $\psi \to 0$. The latter means $\mathcal{J}/\mathcal{I} = 0$ in equation (56). Then one finds

$$\kappa^*_{\min} = \kappa_0(1 + \tau\mathcal{A}). \qquad (59)$$

The upper boundary $\kappa^*_{\max}(T)$ separates type II and IT regimes and is determined by changing the sign of the long range interaction between vortices [44]—it is repulsive in type II and attractive in the IT domain. In order to calculate $\kappa^*_{\max}(T)$, one finds the asymptote of the GL solution for two vortices at large distance between them. The position dependent part of this asymptotic solution is plugged into equation (56), which yields the long-range interaction potential between two vortices. As the scaled GL equations (48) are independent of the number of contributing bands, one can adopt the long-range asymptote of the two-vortex solution ψ found previously in the two-band case [44], which yields $\mathcal{J}/\mathcal{I} = 2$. Then, the upper boundary is obtained as

$$\kappa^*_{\max} = \kappa_0\left[1 + \tau\left(\mathcal{A} + 2\mathcal{B}\right)\right]. \qquad (60)$$

3. Role of multiple bands

3.1. General observations

A transparent structure of all contributions in the EGL formalism makes it possible to obtain important preliminary results before calculating $\kappa^*_{\min}$ and $\kappa^*_{\max}$. The most significant observation is that the multigap structure and the disparity between characteristic lengths of different band condensates appear on different levels of the theory, leading to different physical consequences. Multiple excitation gaps appear in the lowest order in τ of the EGL theory: following equation (22), a multiband superconductor in the GL regime has, in general, multiple excitation gaps while the contributing band condensates are governed by the unique GL coherence length $\xi_{\rm GL}$. Thus, on the level of the GL theory superconducting magnetic properties of a multiband system are the same as those of the single-band superconductor having the only energy gap in the excitation spectrum.

Differences between the condensate characteristic lengths and, thus, between spatial profiles of different band condensates appear only when the corrections to the GL theory are taken into account, i.e., in the next-to-lowest order in τ. Using the EGL approach, one calculates the band condensate healing lengths, to find a band-dependent leading correction to $\xi_{\rm GL}$ as $|\xi_\nu - \xi_{\nu'}| \propto \tau\xi_{\rm GL}$ (see appendix A and reference [24]). Thus, one can expect that phenomena associated with the disparity between the band condensate lengths are notable only at sufficiently low temperatures.

However, an important exception is the vicinity of the B point, i.e., the IT domain between types I and II. Here the GL theory is close to degeneracy and the next-to-lowest corrections in τ (and, thus, the difference between the band condensate lengths) play a crucial role in shaping the superconducting magnetic properties. In this case the mixed state becomes very sensitive to all characteristics of the multiband system, including the number of contributing bands and parameters of multiple Fermi sheets comprising the complex Fermi surface. The multiband structure can, therefore, have a notable effect on the IT domain, justifying the focus of this work.

It is also of significance, that the number of the energy gaps in the excitation spectrum of a uniform multiband superconductor is not always equal to the number of the contributing bands M, which can be seen from the corresponding gap equation

$$\Delta_\nu = \sum_{\nu'=1}^{M} \lambda_{\nu\nu'} n_{\nu'} \int_0^{\hbar\omega_c} \mathrm{d}\varepsilon\, \frac{\Delta_{\nu'}}{E_{\nu'}}\left[1 - 2f(E_{\nu'})\right], \qquad (61)$$

where $E_\nu = \sqrt{\varepsilon^2 + |\Delta_\nu|^2}$ is the single-particle excitation energy, $\lambda_{\nu\nu'} = g_{\nu\nu'}N$ denotes the dimensionless coupling constant, $N = \sum_\nu N_\nu$ is the total single-particle DOS, $n_\nu = N_\nu/N$ is the relative DOS for band ν, $f(E_\nu)$ is the Fermi distribution function. For example, all the excitation gaps $\Delta_\nu = \Delta_\nu(T)$ (i.e., the gap functions for the uniform case) become degenerate when the quantity

$$D_\nu = \sum_{\nu'=1}^{M} \lambda_{\nu\nu'} n_{\nu'} \quad (62)$$

assumes the same value for all contributing bands.

3.2. Microscopic parameters

The IT domain boundaries $\kappa^*_{\min}$ and $\kappa^*_{\max}$ depend on the following microscopic parameters: the dimensionless couplings $\lambda_{\nu\nu'} = g_{\nu\nu'}N$ (with $N = \sum_\nu N_\nu$ the total DOS), the relative band DOSs $n_\nu = N_\nu/N$, and the band velocities ratios v_ν/v_1. Since $T_c \propto \hbar\omega_c$, the cut-off frequency ω_c does not contribute to $\kappa^*_{\min}$ and $\kappa^*_{\max}$.

For the calculations we choose realistic values of the parameters, recalling that in two-band superconductors the intraband dimensionless couplings are typically in the range 0.2–0.7 while the interband coupling is much smaller (see reference [44] and references therein). The relative band DOSs are usually similar for all bands so below we use $n_\nu = 1/M$ for any ν. The range of v_ν/v_1 can be estimated from the first principle calculations as well as from the ARPES measurements. For example, the angle-averaged Fermi velocities in the a–b plane of MgB_2 are calculated from first principles as $v_\sigma^{(a-b)} = 4.4 \times 10^5$ m s^{-1} for the σ states and $v_\pi^{(a-b)} = 5.35 \times 10^5$ m s^{-1} for the π states [89]. However, for the c-direction such calculations yield $v_\sigma^{(c)} = 7 \times 10^4$ m s^{-1} which is by an order of magnitude smaller than $v_\pi^{(c)} = 6 \times 10^5$ m s^{-1}. In addition, ARPES measurements for iron chalcogenide $FeSe_{0.35}Te_{0.65}$ have revealed three contributing bands with the maximal ratio of the band Fermi velocities close to 4 (see reference [90] and discussion in reference [24]).

In order to illustrate the role of the multiband structure in the presence of degenerate gaps, we consider models with one and two spectral gaps. In particular, in figure 1 for the one-band system we use $\lambda = 0.35$ whereas for the two-band system $\lambda_{11} = \lambda_{22} = 0.3$, $\lambda_{12} = 0.05$ ($n_\nu = 1/2$, as mentioned in the previous paragraph). This choice ensures that the both variants exhibit the same single energy gap in the excitation spectrum. In figure 2 we consider multiband superconductors comprising M contributing bands, with $M = 3, 4, 5$. The dimensionless couplings are chosen so that to get the same single excitation gap as in figure 1, namely, we adopt $\lambda_{\nu\neq\nu'} = 0.05$ and $\lambda_{\nu\nu} = 0.35 - 0.05(M-1)$. In this case D_ν given by equation (62) does not depend on ν (with $n_\nu = 1/M$). To consider the two-gap case, we investigate the two- and four-band materials, see figure 3. We take $\lambda_{11} = 0.175$, $\lambda_{22} = 0.125$, $\lambda_{12} = 0.05$ for the two-band system and $\lambda_{11} = \lambda_{22} = 0.3$, $\lambda_{33} = \lambda_{44} = 0.2$ and $\lambda_{\nu\neq\nu'} = 0.05$ for the four-band superconductor; the relative band DOSs for all contributing bands are assumed equal. To illustrate variations in the boundaries of the IT domain, we assume that the relative Fermi velocities depend on the variable parameter β. For the two band system in figures 1 and 3 we use $\beta = v_2/v_1$. For the M-band models in figure 2 we set $\beta = v_2/v_1$ and $v_\nu = v_2$ for $\nu > 2$. Finally, for the four-band model in figure 3 we utilize a more complicated parametrization $\beta = v_2/v_1 = v_3/v_1 = v_4/2v_1$. We stress that our qualitative conclusions do not depend on a particular choice of the microscopic parameters.

3.3. Numerical results for the IT domain boundaries

Using the chosen microscopic parameters, we examine excitation gaps, the boundaries of the IT domain as well as the condensate healing lengths for superconductors with one, two and four bands.

Figure 1 illustrates a comparison between the one- and two-band models. The both models exhibit the same single energy gap in the excitation spectrum, as shown in figure 1(a). However, the difference between them is apparent in figure 1(b) which shows $\mathrm{d}\kappa^*_{\min}/\mathrm{d}\tau$ and $\mathrm{d}\kappa^*_{\max}/\mathrm{d}\tau$ as functions of the Fermi velocities ratio $\beta = v_2/v_1$. The calculation reveals a notable dependence of the IT domain boundaries of the two-band model on β (dotted lines) in comparison with the one-band case, for which the IT boundaries are given by the material-independent constants -0.29 and 0.67, [44] as illustrated by solid lines. The difference between the two cases is maximal in the limits $\beta \ll 1$ and $\beta \gg 1$ but disappears when $\beta = 1$.

To clarify the physical roots of the obtained results, we utilize the formalism of reference [24] (for reader's convenience, outlined in appendix A), and calculate the derivative $\mathrm{d}|\xi_2 - \xi_1|/\mathrm{d}\tau$, where $|\xi_2 - \xi_1|$ is the absolute value of the difference of the band healing lengths ξ_2 and ξ_1 for the two-band system in question. To the next-to-lowest order in τ, we have $\xi_\nu = \xi_\nu^{(0)} + \tau\xi_\nu^{(1)}$, with $\xi_\nu^{(0)} = \xi_{\rm GL}$, see references [24, 53, 86, 87]. (This healing-length expression should be multiplied by $\tau^{-1/2}$ to return to the standard definition.) Therefore, taken to one order beyond the GL theory, $\mathrm{d}|\xi_2 - \xi_1|/\mathrm{d}\tau$ is equal to $|\xi_2^{(1)} - \xi_2^{(1)}|$ and is not τ-dependent. The result is given in figure 1(c) in units of the GL coherence length $\xi_{\rm GL}$. Comparing figures 1(b) and (c) demonstrates that the size of the IT domain closely follows the healing length difference—the domain size grows with increasing the difference. One can thus see that even though the two-band system has a single gap in its excitation spectrum, its magnetic properties are strongly affected by the presence of multiple condensates with different characteristic lengths and, in general, differ significantly from those of the single-band case. The only exception is the case of $\xi_1 = \xi_2$, when the excitation spectra and magnetic properties of the single- and two-band systems become indistinguishable. At this point the quantity $\mathrm{d}|\xi_2 - \xi_1|/\mathrm{d}\tau$ exhibits a pronounced minimum at which the slope of $\mathrm{d}|\xi_2 - \xi_1|/\mathrm{d}\tau$, as a function of β, changes its sign abruptly. Notice that this discontinuity of the derivative with respect to β is not a consequence of any phase transition but appears because the lengths ξ_1 and ξ_2 cross each other at $\beta = 1$.

To gain a further insight, figure 2 demonstrates the boundaries of the IT domain for multiband superconductors with the number of the contributing bands $M = 3, 4, 5$. These multiband superconductors have the only excitation gap being the same as in figure 1. One observes that the IT domain boundaries are sensitive to a particular value of M so that the results are different from those for the one-band and two-band models. This difference is pronounced for $\beta \ll 1$ and $\beta \gg 1$, i.e. when the characteristic lengths of the partial condensates deviate significantly from each other. Due to the choice of the band Fermi velocities, we have two distinguished condensate lengths ξ_1 and ξ_2, the latter is equal to ξ_ν with $\nu > 2$. Similarly

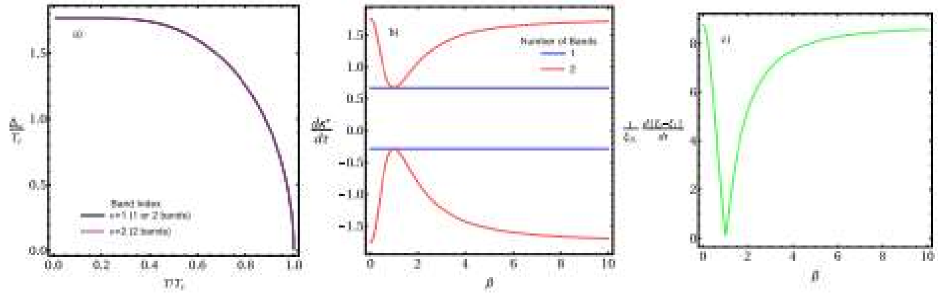

Figure 1. Results for one- and two-band superconductors with the microscopic parameters given in section 3.2, chosen so that both materials have the same excitation gap, degenerate for the two-band system, shown in panel (a) as a function of T (in units of T_c). Panel (b) plots slopes of the IT domain boundaries $\mathrm{d}\kappa^*_{\max}/\mathrm{d}\tau$ (two upper lines) and $\mathrm{d}\kappa^*_{\min}/\mathrm{d}\tau$ (two lower lines) versus $\beta = v_2/v_1$ for the two-band (dotted) and single-band (solid) cases, the single-band results are material independent quantities -0.29 and 0.67. Panel (c) shows the derivative $\mathrm{d}|\xi_2 - \xi_1|/\mathrm{d}\tau$ versus β, where $|\xi_2 - \xi_1|$ is the absolute value of the difference of the band healings lengths ξ_2 and ξ_1 for the two-band system in question.

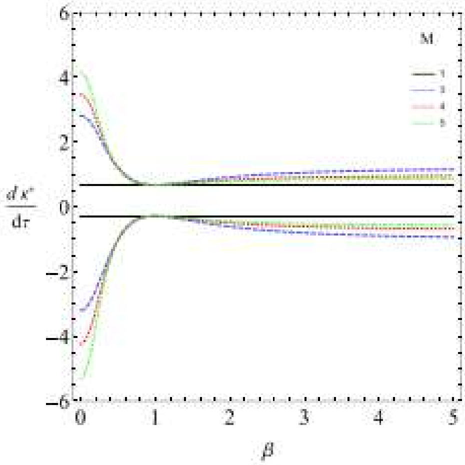

Figure 2. The slopes of the IT domain boundaries $\mathrm{d}\kappa^*_{\max}/\mathrm{d}\tau$ (upper lines) and $\mathrm{d}\kappa^*_{\min}/\mathrm{d}\tau$ (lower lines) for the case of a single spectral gap in the model with the number of bands $M = 3$ (dashed line), $M = 4$ (dotted) and $M = 5$ (dashed-dotted). The microscopic parameters are discussed in section 3.2 and chosen so that all the given materials have the same temperature-dependent gap as in figure 1. The results are versus $\beta = v_2/v_1$, with $v_\nu = v_2$ for $\nu > 2$; the single-band boundaries are the universal constants -0.29 and 0.67 shown as a guide for the eye by the solid line.

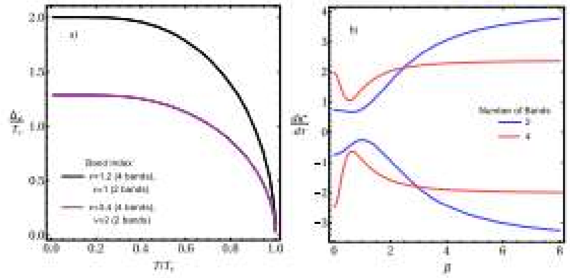

Figure 3. Results for two- and four-band materials, calculated with the microscopic parameters given in section 3.2 and chosen such that both materials have two excitation gaps. Panel (a) shows the gaps versus temperature (in units of T_c). Panel (b) plots slopes of the IT domain boundaries $\mathrm{d}\kappa^*_{\max}/\mathrm{d}\tau$ (two upper lines) and $\mathrm{d}\kappa^*_{\min}/\mathrm{d}\tau$ (two lower lines) as functions of $\beta = v_2/v_1$ (for the two-band case, solid lines) and $\beta = v_2/v_1 = v_3/v_1 = v_4/2v_1$ (for the four-band system, dashed lines).

to figure 1, when $\xi_1 = \xi_2$, i.e. for $\beta = 1$, the IT boundaries of the M-band model approach the boundaries of the IT domain for the one-band model. One sees again that the crossover between types I and II is determined by the number of contributing bands and by the interplay of the related condensate characteristic lengths. Obviously, the IT behavior cannot be captured by the model with the number of bands equal to the number of gaps in the single-particle spectrum of the uniform superconductor.

A further illustration is given in figure 3 which compares results for the two- and four-band systems. The parameters are chosen such that both systems have the same two excitation gaps (see figure 3(a)). In particular, spectral gaps are degenerate for bands 1, 2 and 2, 3 in the four-band case. The IT domain boundaries (their τ-derivatives) for the two-band system are shown in figure 3(b) versus $\beta = v_2/v_1$ by solid lines. One can see that in general, the corresponding IT domain is significantly different from the two-band IT domain shown in figure 1(b), which is a consequence of the two excitation gaps in the present case. However, the two-band IT boundaries in figure 3(b) are still close to the single-band ones in vicinity of $\beta = 1$. Here the difference between the healing lengths ξ_1 and ξ_2 is minimal and the two-band system exhibits a nearly single-band superconducting magnetic response, despite the presence of two excitation gaps. We again observe that the presence/absence of diverse characteristic lengths of multiple condensates coexisting in one material is more essential for the superconducting magnetic properties than the presence/absence of multiple gaps in the excitation spectrum of the uniform superconductor.

The quantities $\mathrm{d}\kappa^*_{\max}/\mathrm{d}\tau$ and $\mathrm{d}\kappa^*_{\min}/\mathrm{d}\tau$ for the four-band system are given by dotted lines in figure 3(b) versus $\beta = v_2/v_1 = v_2/v_1 = v_4/2v_1$. One sees that the IT domain boundaries for the four-band case are close to the two-band IT boundaries at $\beta \sim 3$. For $\beta \gtrsim 3$ the size of the IT domain for the two-band system is notably larger and, on the contrary, for $\beta \lesssim 3$ the IT domain is larger in the four-band case. One also notes that unlike the two-band case the IT domain for the four-band system in figure 3(b) never approaches the single-band result (cf figure 1(b)). In general, one can expect that the larger is the number of competing superconducting condensates with different characteristics, the more significant are the deviations from the single-condensate physics.

4. Conclusions

In this work we have demonstrated that the presence of multiple competing lengths, each connected with corresponding partial condensate, is a more fundamental feature of a multiband superconductor for its magnetic properties than the presence of multiple gaps in the excitation spectrum. This is illustrated by considering boundaries of the IT domain in the phase diagram of the superconducting magnetic response. For example, our results have revealed that a superconductor can have many gaps in the excitation spectrum while exhibiting standard magnetic properties of a single-band material. There is also a reverse situation, when a superconductor has a single energy gap in the excitation spectrum but multiple competing characteristic lengths of contributing band condensates, which results in notable changes of the superconducting magnetic properties in the IT regime as compared to the single-band case. Generally, our analysis shows that the multi-condensate physics can appear irrespective of the presence/absence of multiple spectral gaps. Two superconductors with different numbers of the contributing bands but with the same energy gaps in their excitation spectra (some of the spectral gaps are degenerate) can exhibit different magnetic properties sensitive to the spatial scales of the band condensates. This discrepancy between different manifestations of multiple bands in superconducting materials must be taken into account in analysis of experimental data and, generally, in studies of multiband superconductors. In addition, given the significant advances in chemical engineering of various materials, including multiband superconductors, it is of great importance to search for systems that enrich our knowledge of and understanding the physics of the materials. Multiband superconductors with degenerate excitation gaps can be a good example of such systems, clearly demonstrating that 'multiband' can be dramatically different from 'multigap'.

Our analysis has been performed within the EGL approach that takes into account the leading corrections to the GL theory in the perturbative expansion of the microscopic equations in $\tau = 1 - T/T_c$. This formalism, previously constructed for single- and two-band systems, has been extended in the present work to the case of an arbitrary number of contributing bands. Its advantage is that it allows one to clearly distinguish various effects appearing due to the multiband structure in different types of superconducting characteristics. It particular, it reveals solid correlations between changes in the IT domain with the competition of multiple characteristic lengths of the contributing condensates.

Acknowledgments

This work was supported by Brazilian agencies, Conselho Nacional de Ciência e Tecnologia (CNPq), Grant No. 309374/2016-2 and Fundação de Amparo a Ciência e Tecnologia do Estado de Pernambuco (FACEPE) Grant No. APQ-0936-1.05/15. PJFC thanks CAPES Programa de Doutorado Sanduíche no Exterior, Processo No. 88881.186964/2018-01. TTS and AV acknowledge hospitality of Departamento de Física da Universidade Federal de Pernambuco during their temporary stays in 2018 and support from CNPq Grant No. 400510/2014-6 and FACEPE. MDC acknowledges the Departamento de Física da Universidade Federal de Pernambuco for visiting professor fellowship in 2019, Grant Propesq 05.2018-031782/2018-88.

Appendix A. Leading correction to the GL coherence length

He we employ the EGL approach to calculate the band dependent healing lengths ξ_ν up to the leading corrections to the GL coherence length. The GL theory of multiband superconductors has a single order parameter which yields equal healing lengths for different band condensates. (A multiband superconductor can have more than one order parameter in the GL regime when the solution of the linearized gap equation for T_c is degenerate [55]; this case is not considered here.) However, when one takes into account the leading corrections to GL theory, band healing lengths become different. These corrections have been calculated earlier [24] for the one-band and two-band systems, and we now recall those results and extend them to the case of an arbitrary number of contributing bands.

We consider the condensate that occupies a half space $x > 0$ and is suppressed for $x \leqslant 0$. Each band condensate recovers its bulk value in a distance (measured from the interface $x = 0$) that is called the band healing length ξ_ν. This length is defined from the criterion

$$\frac{\Delta_\nu(\xi_\nu)}{\Delta_\nu(\infty)} = \frac{\Delta_\nu^{(0)}(\xi_\nu^{(0)})}{\Delta_\nu^{(0)}(\infty)}, \tag{A.1}$$

where ξ_ν is given by the τ-expansion

$$\xi_\nu = \xi_\nu^{(0)}\left(1 + \tau\xi_\nu^{(1)}\right), \tag{A.2}$$

and, taken in the lowest order in τ, the band healing length coincides with the GL coherence length $\xi_\nu^{(0)} = \xi_{\rm GL}$. We solve the GL equation (48) without magnetic field and with the boundary conditions $\psi(0) = \psi'(\infty) = 0$, with ψ' the first derivative with respect to x measured in units of $\xi_{\rm GL}$. The well-known solution reads as [91]

$$\psi = \tanh\left(x/\sqrt{2}\right), \tag{A.3}$$

where ψ is given in units of $\psi_0 = \sqrt{|a|/b}$. One sees from equation (22) that ψ controls $\bar{\Delta}^{(0)}$.

The next-to-lowest contribution to Δ_ν is given by equation (29). In this equation φ_j are explicitly expressed via

ψ by equation (31) but φ should be obtained from the stationary equation $\delta\mathcal{F}^{(1)}/\delta\vec{\Delta}^{(0)\dagger}=0$, where $\mathcal{F}^{(1)}$ corresponds to $f^{(1)}$ in equation (11). The projection of this equation onto the eigenvector $\vec{\epsilon}$ yields the equation for φ that can be written as

$$(1-3\psi^2)\varphi+\varphi''=A\psi+B\psi^3+C\psi^5+D\psi\psi'^2, \qquad \text{(A.4)}$$

where φ is in units of ψ_0, φ'' is the second derivative with respect to the scaled variable x, and the coefficients read as

$$\begin{aligned} A &= \frac{3}{2}+\bar{\mathcal{Q}}+\sum_{i=1}^{M-1}\frac{\bar{\alpha}_i^2}{\bar{\Lambda}_i}, \\ B &= 5\bar{\mathcal{L}}-4\bar{\mathcal{Q}}-2\sum_{i=1}^{M-1}\frac{\Gamma_i(\bar{\alpha}_i-\bar{\beta}_i)+2\mathcal{K}\bar{\alpha}_i\bar{\beta}_i}{\mathcal{K}\bar{\Lambda}_i}, \\ C &= 3\bar{c}+3\bar{\mathcal{Q}}-5\bar{\mathcal{L}}+3\sum_{i=1}^{M-1}\frac{\bar{\beta}_i^2}{\bar{\Lambda}_i}, \\ D &= 6\bar{\mathcal{Q}}-5\bar{\mathcal{L}}-6\sum_{i=1}^{M-1}\frac{\Gamma_i\bar{\beta}_i}{\mathcal{K}\bar{\Lambda}_i}, \end{aligned} \qquad \text{(A.5)}$$

where $\mathcal{K}$, Γ_j, $\bar{c}$, $\bar{\mathcal{Q}}$, $\bar{\mathcal{L}}$, $\bar{\alpha}_j$, $\bar{\beta}_j$ and $\bar{\Lambda}_j$ are given by equations (27), (32), (37), and (52). Here we consider that vectors $\vec{\epsilon}$ and $\vec{\eta}_j$ have only real components, i.e., $\alpha_i=\alpha_i^*$, $\beta_i=\beta_i^*$, and $\Gamma_i=\Gamma_i^*$.

The solution of equation (A.4) at $\varphi(0)=\varphi'(\infty)=0$ is obtained as

$$\varphi=-\frac{3(A+B)+5C+D}{6}\tanh\left(\frac{x}{\sqrt{2}}\right)+\frac{2C+D}{6} \times\tanh^3\left(\frac{x}{\sqrt{2}}\right)-\frac{A-C}{2}\frac{x}{\sqrt{2}}\operatorname{sech}^2\left(\frac{x}{\sqrt{2}}\right). \qquad \text{(A.6)}$$

Then, using equations (22), (29), (A.3), and (A.6), one finds

$$\xi_\nu^{(1)}=\frac{A-C}{2}+\sqrt{2}\psi\left(\frac{1}{\sqrt{2}}\right)\left(\frac{2C+D}{6}+\sum_{i=1}^{M-1}\frac{\bar{\beta}_i}{\bar{\Lambda}_i}\frac{\eta_{i\nu}}{\epsilon_\nu}\right). \qquad \text{(A.7)}$$

We note that only the last term in this expression contributes to the difference between the healing lengths of two different bands ν and ν', so that

$$\xi_\nu-\xi_{\nu'}=0.86\,\tau\,\xi_{\mathrm{GL}}\sum_{i=1}^{M-1}\frac{\bar{\beta}_i}{\bar{\Lambda}_i}\left(\frac{\eta_{i\nu}}{\epsilon_\nu}-\frac{\eta_{i\nu'}}{\epsilon_{\nu'}}\right), \qquad \text{(A.8)}$$

with $\psi(1/\sqrt{2})=0.86$.

Let us consider, for illustration, equation (A.7) for the two-band system with degenerate excitation gaps. In this case the eigenvector of the matrix $\check{L}$ with zero eigenvalue satisfies $\epsilon_1=\epsilon_2$. Then, for equal band Fermi velocities the parameter $\bar{\beta}_1=0$ as $\beta_1/b=\Gamma_1/\mathcal{K}$, see the definition of these quantities in section 2.2. Since only $i=1$ contributes to the sum in equation (A.7), we find $\xi_1^{(1)}=\xi_2^{(1)}$. Thus, the healing lengths ξ_1 and ξ_2 are the same (at least up to the leading correction to the GL theory), which is in agreement with the results given in figure 1(c), where the healing length difference drops to zero at $v_2=v_1$. The same conclusion can easily be obtained for $M>2$, when all excitation gaps are degenerate and the bands have the same Fermi velocity.

ORCID iDs

A A Shanenko https://orcid.org/0000-0002-6031-5106

References

[1] Suhl H, Matthias B T and Walker L R 1959 *Phys. Rev. Lett.* **3** 552–4
[2] Moskalenko V A 1959 *Phys. Met. Metallogr.* **8** 25–36
[3] Ginsberg D M, Richards P L and Tinkham M 1959 *Phys. Rev. Lett.* **3** 337–8
[4] Townsend P and Sutton J 1963 *Phys. Rev. Lett.* **11** 154–6
[5] Zavaritskii N V 1965 *Sov. Phys. - JETP* **21** 557–62
[6] Canfield P C and Crabtree G W 2003 *Phys. Today* **56** 34–40
[7] Szabó P, Samuely P, Kačmarčík J, Klein T, Marcus J, Fruchart D, Miraglia S, Marcenat C and Jansen A G M 2001 *Phys. Rev. Lett.* **87** 137005
[8] Iavarone M *et al* 2002 *Phys. Rev. Lett.* **89** 187002
[9] Paglione J and Greene R L 2010 *Nat. Phys.* **6** 645–58
[10] Mazziotti M V, Valletta A, Campi G, Innocenti D, Perali A and Bianconi A 2017 *Europhys. Lett.* **118** 37003
[11] Deng S, Viola L and Ortiz G 2012 *Phys. Rev. Lett.* **108** 036803
[12] Deng S, Ortiz G and Viola L 2013 *Phys. Rev.* B **87** 205414
[13] Askerzade İ N, Gencer A and Güçlü N 2002 *Supercond. Sci. Technol.* **15** L13–6
[14] Golubov A A, Kortus J, Dolgov O V, Jepsen O, Kong Y, Andersen O K, Gibson B J, Ahn K and Kremer R K 2002 *J. Phys.: Condens. Matter.* **14** 1353–60
[15] Gurevich A 2003 *Phys. Rev.* B **67** 184515
[16] Koshelev A E and Golubov A A 2004 *Phys. Rev. Lett.* **92** 107008
[17] Zhitomirsky M E and Dao V-H 2004 *Phys. Rev.* B **69** 054508
[18] Tanaka K, Agterberg D F, Kop J and Eschrig M 2006 *Phys. Rev.* B **73** 220501(R)
[19] Tanaka K, Eschrig M and Agterberg D F 2007 *Phys. Rev.* B **75** 214512
[20] Kortus J, Mazin I I, Belashchenko K D, Antropov V P and Boyer L L 2001 *Phys. Rev. Lett.* **86** 4656
[21] An J M and Pickett W E 2001 *Phys. Rev. Lett.* **86** 4366
[22] Komendová L, Milošević M V, Shanenko A A and Peeters F M 2011 *Phys. Rev.* B **84** 064522
[23] Komendová L, Chen Y, Shanenko A A, Milošević M V and Peeters F M 2012 *Phys. Rev. Lett.* **108** 207002
[24] Saraiva T T, de Souza Silva C C, Aguiar J A and Shanenko A A 2017 *Phys. Rev.* B **96** 134521
[25] Chen Y, Zhu H and Shanenko A A 2020 *Phys. Rev.* B **101** 215510
[26] Seul M and Wolfe R 1992 *Phys. Rev.* A **46** 7519–33
[27] Seul M and Andelman D 1995 *Science* **267** 476–83
[28] Maclennan J and Seul M 1992 *Phys. Rev. Lett.* **69** 2082–5
[29] Stoop N, Lagrange R, Terwagne D, Reis P M and Dunkel J 2015 *Nat. Mater.* **14** 337–42
[30] Keller S L and McConnell H M 1999 *Phys. Rev. Lett.* **82** 1602–5
[31] Aranson I S and Tsimring L S 2006 *Rev. Mod. Phys.* **78** 641–92
[32] Moshchalkov V, Menghini M, Nishio T, Chen Q H, Silhanek A V, Dao V H, Chibotaru L F, Zhigadlo N D and Karpinski J 2009 *Phys. Rev. Lett.* **102** 117001
[33] Curran P J, Desoky W M, Milošević M V, Chaves A, Laloë J-B, Moodera J S and Bending S J 2015 *Sci. Rep.* **5** 15569
[34] Tanaka Y 2001 *Phys. Rev. Lett.* **88** 017002
[35] Tanaka Y 2001 *J. Phys. Soc. Japan* **70** 2844–7
[36] Kuplevakhsky S V, Omelyanchouk A N and Yerin Y S 2011 *J. Low Temp. Phys.* **37** 667–77

[37] Izyumov Y A and Laptev V M 1990 *Phase Transit.* **20** 95–112
[38] Piña J C, de Souza Silva C C and Milošević M V 2012 *Phys. Rev.* B **86** 024512
[39] Lin S Z and Bulaevskii L N 2013 *Phys. Rev. Lett.* **110** 087003
[40] Lin S Z and Reichhardt C 2013 *Phys. Rev.* B **87** 100508
[41] da Silva R M, Milošević M V, Domínguez D, Peeters F M and Aguiar J A 2014 *Appl. Phys. Lett.* **105** 232601
[42] Lin S Z 2014 *J. Phys.: Condens. Matter.* **26** 493203
[43] Fenchenko V N and Yerin Y S 2012 *Physica* C **480** 129–36
[44] Vagov A, Shanenko A A, Milošević M V, Axt V M, Vinokur V M, Aguiar J A and Peeters F M 2016 *Phys. Rev.* B **93** 174503
[45] Wolf S, Vagov A, Shanenko A A, Axt V M, Perali A and Aguiar J A 2017 *Phys. Rev.* B **95** 094521
[46] Lin S Z 2012 *Phys. Rev.* B **86** 014510
[47] Yerin Y S and Omelyanchouk A N 2017 *Low Temp. Phys.* **43** 1013–37
[48] Mosquera Polo A S, da Silva R M, Vagov A, Shanenko A A, Deluque Toro C E and Aguiar J A 2017 *Phys. Rev.* B **96** 054517
[49] da Silva R M, Milošević M V, Shanenko A A, Peeters F M and Aguiar J A 2015 *Sci. Rep.* **5** 12695
[50] Salasnich L, Shanenko A A, Vagov A, Aguiar J A and Perali A 2019 *Phys. Rev.* B **100** 064510
[51] Vargas-Paredes A A, Shanenko A A, Vagov A, Milošević M V and Perali A 2020 *Phys. Rev.* B **101** 094516
[52] Vagov A, Shanenko A A, Milošević M V, Axt V M and Peeters F M 2012 *Phys. Rev.* B **85** 014502
[53] Vagov A, Shanenko A A, Milošević M V, Axt V M and Peeters F M 2012 *Phys. Rev.* B **86** 144514
[54] Stanev V and Tešanović Z 2010 *Phys. Rev.* B **81** 134522
[55] Orlova N V, Shanenko A A, Milošević M V, Peeters F M, Vagov A and Axt V M 2013 *Phys. Rev.* B **87** 134510
[56] Yerin Y, Omelyanchouk A, Drechsler S-L, Efremov D V and van den Brink J 2017 *Phys. Rev.* B **96** 144513
[57] Lifshitz E M and Pitaevskii L P 1980 *Statistical Physics, Part 2* (Landau and Lifshitz Course of Theoretical Physics vol 9) (Oxford: Pergamon)
[58] de Gennes P G 1966 *Superconductivity of Metals and Alloys* (New York: Benjamin)
[59] Ketterson J B and Song S N 1999 *Superconductivity* (Cambridge: Cambridge University Press)
[60] Krägeloh U 1969 *Phys. Lett.* A **28** 657–8
[61] Essmann U 1971 *Physica* **55** 83–93
[62] Aston D R, Dubeck L W and Rothwarf F 1971 *Phys. Rev.* **3** 2231–6
[63] Jacobs A E 1971 *Phys. Rev.* B **4** 3029–34
[64] Auer J and Ullmaier H 1973 *Phys. Rev.* B **7** 136–45
[65] Klein U 1987 *J. Low Temp. Phys.* **69** 1–36
[66] Weber H W, Seidl E, Botlo M, Laa C, Mayerhofer E, Sauerzopf F M, Schalk R M and Wiesingerh H P 1989 *Physica* C **161** 272–86
[67] Brandt E H 1995 *Rep. Prog. Phys.* **58** 1465–594
[68] Luk'yanchuk I 2001 *Phys. Rev.* B **63** 174504
[69] Laver M *et al* 2006 *Phys. Rev. Lett.* **96** 167002
[70] Laver M *et al* 2009 *Phys. Rev.* B **79** 014518
[71] Mühlbauer S, Pfleiderer C, Böni P, Laver M, Forgan E M, Fort D, Keiderling U and Behr G 2009 *Phys. Rev. Lett.* **102** 136408
[72] Brandt E H and Das M P 2011 *J. Supercond. Nov. Magn.* **24** 57–67
[73] Pautrat A and Brûlet A 2014 *J. Phys.: Condens. Matter.* **26** 232201
[74] Reimann T, Mühlbauer S, Schulz M, Betz B, Kaestner A, Pipich V, Böni P and Grünzweig C 2015 *Nat. Commun.* **6** 8813
[75] Wang Y, Lortz R, Paderno Y, Filippov V, Abe S, Tutsch U and Junod A 2005 *Phys. Rev.* B **72** 024548
[76] Ge J Y, Gladilin V N, Sluchanko N E, Lyashchenko A, Filipov V, Indekeu J O and Moshchalkov V V 2017 *New J. Phys.* **19** 093020
[77] Neumann L and Tewordt L 1966 *Z. Phys.* **189** 55–66
[78] Neumann L and Tewordt L 1966 *Z. Phys.* **191** 73–80
[79] Fetter A L and Walecka J D 2003 *Quantum Theory of Many-Particle Systems* (New York: Dover)
[80] Jacobs A E 1972 *Phys. Lett.* A **38** 153
[81] Buzdin A I and Kachkachi H 1997 *Phys. Lett.* A **225** 341–8
[82] Houzet M and Buzdin A 2001 *Phys. Rev.* B **63** 184521
[83] Houzet M and Mineev V P 2007 *Phys. Rev.* B **76** 224508
[84] Sigrist M and Ueda K 1991 *Rev. Mod. Phys.* **63** 239–311
[85] Tanaka Y 2015 *Supercond. Sci. Technol.* **28** 034002
[86] Geilikman B T, Zaitsev R O and Kresin V Z 1967 *Sov. Phys. Solid State* **9** 642–7
[87] Kogan V G and Schmalian J 2011 *Phys. Rev.* B **83** 054515
[88] Bogomolnyi E B 1976 *Sov. J. Nucl. Phys.* **24** 449–54
[89] Brinkman A, Golubov A A, Rogalla H, Dolgov O V, Kortus J, Kong Y, Jepsen O and Andersen O K 2002 *Phys. Rev.* B **65** 180517(R)
[90] Lubashevsky Y, Lahoud E, Chashka K, Podolsky D and Kanigel A 2012 *Nat. Phys.* **8** 309–12
[91] Poole C P, Farach H A, Creswick R J and Prozorov R 2014 *Superconductivity* (Amsterdam: Elsevier)
[92] Wolf S, Vagov A, Shanenko A A, Axt V M and Aguiar J A 2017 *Phys. Rev.* B **96** 144515